HEINI KALLIO

Regulation and Roles of Carbonic Anhydrases IX and XII

ACADEMIC DISSERTATION
To be presented, with the permission of
the board of the Institute of Biomedical Technology
of the University of Tampere,
for public discussion in the Auditorium of Finn-Medi 5,
Biokatu 12, Tampere, on December 2nd, 2011, at 12 o'clock.

UNIVERSITY OF TAMPERE

UNIVERSITY
OF TAMPERE

ACADEMIC DISSERTATION
University of Tampere, Institute of Biomedical Technology
Tampere University Hospital
Tampere Graduate Program in Biomedicine and Biotechnology (TGPBB)
Finland

Supervised by
Professor Seppo Parkkila
University of Tampere
Finland

Reviewed by
Docent Peppi Karppinen
University of Oulu
Finland
Professor Robert McKenna
University of Florida
USA

Distribution
Bookshop TAJU
P.O. Box 617
33014 University of Tampere
Finland

Tel. +358 40 190 9800
Fax +358 3 3551 7685
taju@uta.fi
www.uta.fi/taju
http://granum.uta.fi

Cover design by
Mikko Reinikka

Acta Universitatis Tamperensis 1675
ISBN 978-951-44-8621-0 (print)
ISSN-L 1455-1616
ISSN 1455-1616

Acta Electronica Universitatis Tamperensis 1139
ISBN 978-951-44-8622-7 (pdf)
ISSN 1456-954X
http://acta.uta.fi

Tampereen Yliopistopaino Oy – Juvenes Print
Tampere 2011

There is a crack in everything,
that's how the light gets in.
-Leonard Cohen

CONTENTS

LIST OF ORIGINAL COMMUNICATIONS

This thesis is based on the following original communications, which are referred to in the text by their Roman numerals (I-IV).

I **Kallio H**, Pastoreková S, Pastorek J, Waheed A, Sly WS, Mannisto S, Heikinheimo M, and Parkkila S (2006): Expression of carbonic anhydrases IX and XII during mouse embryonic development. BMC Dev Biol 6:22.

II **Kallio H**, Rodriguez Martinez A, Hilvo M, Hyrskyluoto A, and Parkkila S (2010): Cancer-associated carbonic anhydrases IX and XII: effect of growth factors on gene expression in human cancer cell lines. J Cancer Mol 5:73-78.

III **Kallio H**, Hilvo M, Rodriguez A, Lappalainen EH, Lappalainen AM, and Parkkila S (2010): Global transcriptional response to carbonic anhydrase IX deficiency in the mouse stomach. BMC Genomics 11:397.

IV **Kallio H**, Tolvanen M, Jänis J, Pan P, Laurila E, Kallioniemi A, Kilpinen S, Tuominen VJ, Isola J, Valjakka J, Pastoreková S, Pastorek J, and Parkkila S. Characterization of non-specific cytotoxic cell receptor protein 1: a new member of the lectin-type subfamily of F-box proteins. PLoS ONE, in press.

ABBREVIATIONS

$1,25(OH)_2D3$	1,25-dihydroxyvitamin D3
ACTB	beta-actin
AE	anion exchanger
AP	activator protein
ATF4	activating transcription factor 4
AZA	acetazolamide
B2M	beta-2-microglobulin
CA	carbonic anhydrase
CA9	human carbonic anhydrase 9 (gene or mRNA)
CA12	human carbonic anhydrase 12 (gene or mRNA)
Car9	mouse carbonic anhydrase 9 (gene or mRNA)
CA-RP	carbonic anhydrase-related protein
ccRCC	clear cell renal cell carcinoma
CNS	central nervous system
Cp	crossing point
CRL	crown-rump length
E. coli	*Escherichia coli*
ED	embryonic day
EGF	epidermal growth factor
EGFR	epidermal growth factor receptor
eIF2α	eukaryotic translation initiation factor
ER	estrogen receptor
ERK	extracellular signal-regulated kinase
FBA	Fbox-associated
FBXO	F-box-only
FT-ICR	Fourier transform ion cyclotron resonance
GABA	gamma-aminobutyric acid
GAPDH	glyceraldehyde-3-phosphate dehydrogenase

GIST	gastrointestinal stromal tumor
GPI	glycosylphosphatidylinositol
GST	glutathione S-transferase
HIF	hypoxia-inducible factor
HPRT	hypoxanthine guanine phosphoribosyl transferase
HRE	hypoxia response element
HRP	horseradish peroxidase
IGF-1	insulin-like growth factor 1
JNK	c-Jun N-terminal kinase
MAPK	mitogen-activated protein kinase
MMP	matrix metalloproteinase
NCCRP1	non-specific cytotoxic cell receptor protein 1
PAI	plasminogen activator inhibitor
PAP	peroxidase-antiperoxidase
p.c.	post coitum
PERK	protein kinase RNA-like endoplasmic reticulum kinase
PG	proteoglycan
PHD	HIF prolyl-4-hydroxylase
PI3K	phosphatidylinositol 3-kinase
p.p.	postpartum
PR	protected region
PPYLUC	luciferase
QRT-PCR	quantitative real-time PCR
RAR	retinoic acid receptor
RARE	retinoic acid response element
RCC	renal cell carcinoma
RPTP	receptor-type protein tyrosine phosphatase
SDHA	succinate dehydrogenase complex, subunit A
SDS-PAGE	sodium dodecyl sulfate-polyacrylamide gel electrophoresis
siRNA	small interfering RNA
SP	specificity protein
SRC	steroid receptor coactivator
TGF-α	transforming growth factor-alpha
TGF-β1	transforming growth factor-beta 1

TIMP	tissue inhibitor of metalloproteinase
UBC	ubiquitin C
u-PA	urokinase-type plasminogen activator
UPR	unfolded protein response
VDRE	vitamin D response element
VHL	von Hippel-Lindau

TIIVISTELMÄ

Hiilihappoanhydraasit (CA:t) ovat metalloentsyymejä, jotka katalysoivat reversiibelisti hiilidioksidin hydraatiota bikarbonaatiksi ja protoniksi. CA-entsyymejä tuotetaan monissa kudoksissa, joissa ne osallistuvat useisiin fysiologisiin prosesseihin, kuten pH:n säätelyyn, CO_2:n ja HCO_3^-:n kuljetukseen, elimistössä olevien nesteiden tuotantoon, luun hajotukseen ja aineenvaihduntareaktioihin. Nisäkkäiden CA-entsyymiperhe koostuu 13 aktiivisesta isoentsyymistä, joista CA I, II, III, VII ja XIII sijaitsevat solulimassa, CA IV, IX, XII, XIV ja XV ovat liittyneet solukalvoon, CA VA ja VB ovat mitokondriaalisia ja CA VI on ainoa soluista erittyvä CA-entsyymi.

Tällä työllä oli neljä päätavoitetta. Ensimmäinen tavoite oli löytää CA IX:n ja CA XII:n säätelijöitä, sillä hypoksiaa lukuun ottamatta niiden säätelijät tunnetaan huonosti. Toinen tavoite oli tutkia näiden kahden isoentsyymin ilmentymistä hiiren sikiönkehityksen aikana. Kolmas tavoite oli karakterisoida *Car9*-poistogeenisen hiiren mahalaukussa tapahtuvia koko genomin laajuisia geenien transkriptiotasojen muutoksia. Näillä hiirillä on havaittu mahalaukun epiteelin hyperplasiaa, mutta tähän fenotyyppiin johtavat tarkat mekanismit ovat olleet tuntemattomia. Neljäs tavoite oli tutkia tarkemmin proteiineja, joiden ilmentyminen on muuttunut *Car9*-poistogeenisten hiirten mahalaukun limakalvolla.

Kvantitatiivisella reaalikaikaisella PCR -menetelmällä tehty tutkimuksemme osoitti, että kasvutekijät IGF-1, TGF-α, TGF-β1 ja EGF nostivat CA IX:n ja CA XII:n lähetti-RNA:n (mRNA) tasoja syöpäsolulinjoissa. CA IX:n mRNA:n taso nousi vain yhdessä syöpäsolulinjassa, kun taas CA XII:n mRNA:n taso nousi neljässä syöpäsolulinjassa. Näyttää siis siltä, että CA XII:n ilmentymisen tärkein säätelijä ei ole hypoksia, kuten CA IX:n.

CA IX:n ja CA XII:n ilmentymistä hiiren organogeneesin aikana tutkittiin immunohistokemiallisella värjäyksellä. Molempia isoentsyymejä ilmennettiin useissa kehittyvän hiiren kudoksissa; osa näistä oli sellaisia, jotka eivät ilmennä

kyseisiä proteiineja aikuisella hiirellä. Siksi onkin mahdollista, että CA IX:ää ja CA XII:ta tarvitaan tiettyjen kudosten muodostumiseen.

Car9-poistogeenisyyden aiheuttamia geenien transkriptiotasojen muutoksia hiirten mahalaukuissa tutkittiin cDNA-mikrosirutekniikalla. Analyysi osoitti, että 86 geenin mRNA-taso oli noussut ja 46 geenin laskenut. Näiden geenien joukossa oli sellaisia, jotka ovat mukana kehitykseen liittyvissä prosesseissa, solujen erilaistumisessa ja immuunivasteissa. Nämä tulokset ja muiden tutkijoiden aikaisemmat havainnot viittaavat siihen, että CA IX:n ensisijainen tehtävä mahassa ei liity pH:n säätelyyn tai vaihtoehtoisesti CA IX on korvattavissa tätä toimintoa ajatellen.

cDNA-mikrosirutekniikalla tehty tutkimus osoitti, että *NCCRP1* (non-specific cytotoxic cell receptor protein 1) -geenin mRNA-taso oli noussut tilastollisesti merkitsevästi *Car9*-poistogeenisten hiirten mahalaukussa. Koska kyseinen geeni on huonosti tunnettu, se valittiin jatkoanalyyseihin. Kun *CA9* hiljennettiin syöpäsolulinjassa, ei NCCRP1:n mRNA-taso muuttunut, mikä viittaa siihen, ettei *CA9* säätele suoraan *NCCRP1*:tä. Tutkimus osoitti myös, että NCCRP1 ilmentyy sytosolissa. Bioinformatiikka-analyysit ehdottivat NCCRP1-proteiinin kuuluvan F-box-proteiinien lektiini-tyypin alaperheeseen (FBXO-perhe). Kyseiset proteiinit ovat E3-ubikitiiniligaasikompleksin osia. Koetulostemme mukaan NCCRP1 ei ole solukalvoon kiinnittynyt immuunivasteita välittävä proteiini, kuten on ajateltu aiemmin. Näin ollen *NCCRP1*:n nimi tulisi muuttaa *FBXO50*:ksi.

ABSTRACT

The carbonic anhydrases (CAs) are a family of metalloenzymes that catalyze the reversible hydration of carbon dioxide to bicarbonate and a proton. The CAs are produced in a variety of tissues where they participate in several physiological processes, such as pH regulation, CO_2 and HCO_3^- transport, the production of body fluids, bone resorption, and metabolic processes. The CA family consists of 13 active isozymes in mammals: CA I, II, III, VII, and XIII are cytoplasmic; CA IV, IX, XII, XIV, and XV are anchored to plasma membranes; CA VA and VB are mitochondrial; and CA VI is the only secreted protein.

This study had four specific aims. The first aim was to identify new regulators of CA IX and CA XII. This aim was proposed because, besides hypoxia, the regulation of these proteins is poorly characterized. The second goal was to examine the expression profiles of these isozymes during mouse embryonic development. The third aim was to investigate the whole-genome expression changes that occur in response to CA IX deficiency in the mouse stomach. These mice exhibit gastric hyperplasia, but the exact mechanisms leading to this disturbed cell lineage phenotype remain unknown. The fourth and final goal was to elucidate further the properties of some selected proteins that are dysregulated in the gastric mucosa of *Car9*$^{-/-}$ mice.

Our studies demonstrate that the growth factors IGF-1, TGF-α, TGF-β1, and EGF increase *CA9* and *CA12* mRNA expression in cancer-derived cell lines as determined by quantitative real-time PCR (QRT-PCR). In the case of *CA9*, this effect was observed in only one cell line, whereas *CA12* was elevated by growth factors in four cell lines. Thus, hypoxia may not be the primary regulator of *CA12* in contrast to *CA9*.

Immunohistochemistry was used to study CA IX and CA XII expression during mouse organogenesis. These isozymes were detected in several tissues of which a portion are negative for expression in adult mice. Therefore, it is possible that CA IX and CA XII have specific roles in the assembly of certain tissues.

The changes caused by CA IX deficiency in the mouse stomach were explored using a cDNA microarray, which revealed the induction of 86 genes and the repression of 46 genes. Among the genes with altered regulation were those involved in developmental processes, cell differentiation and immune responses. These data and previous findings by others suggest that the primary role of CA IX in the stomach is not related to pH regulation or, alternatively, that its function in this tissue is compensated for by other CA isozymes.

The microarray data indicated significant upregulation of non-specific cytotoxic cell receptor protein 1 (*Nccrp1*), a poorly characterized gene that was selected for further analyses. Silencing of *CA9* in HeLa cells did not affect *NCCRP1* levels, suggesting that *NCCRP1* is not directly regulated by *CA9* and that its upregulation is secondary to *Car9* gene disruption. Moreover, it was demonstrated that human recombinant NCCRP1 is expressed intracellularly. Bioinformatic analyses revealed that NCCRP1 belongs to the lectin-type subfamily of F-box (FBXO) proteins, which are components of the E3 ubiquitin ligase complex. In conclusion, our data clearly demonstrate that NCCRP1 is not a transmembrane protein responsible for the cytolytic function of nonspecific cytotoxic cells as has been previously suggested. Therefore, the name of *Nccrp1* should be changed to *FBXO50*.

1. INTRODUCTION

Carbonic anhydrases (CAs) (EC 4.2.1.1) are zinc-containing metalloenzymes that catalyze the reversible hydration of carbon dioxide in the following reaction: $CO_2 + H_2O \leftrightarrow H^+ + HCO_3^-$. The importance of CA enzymes is emphasized by the fact that they are found in a wide variety of organisms within the phylogenetic tree (Hewett-Emmett 2000). In mammals, each characterized CA enzyme is a member of the α-CA family. This family consists of 13 active isozymes, 12 of which are expressed and functional in humans (Hilvo et al. 2005). Each isozyme has a characteristic subcellular localization, distribution within the body, enzymatic activity, and affinity for inhibitors.

CA IX is a transmembrane protein with many unique properties compared to the other CA isozymes. CA IX is expressed in only a few normal human tissues, but its ectopic expression is induced in several cancers (Pastorekova and Zavada 2004). Tissue oxygen content has been considered the primary regulatory mechanism of CA IX. This regulatory mechanism is proposed because *CA9* expression in tumor tissues is linked with the hypoxic phenotype mediated by hypoxia-inducible transcription factor 1 (HIF-1) (Wykoff et al. 2000). However, little is known of other possible regulators of CA IX. In addition to the basic CA function, CA IX has been implicated in several other processes. It is the only member of the CA family that contains both a CA domain and a proteoglycan (PG) domain, which has been suggested to participate in cell adhesion (Svastova et al. 2003). The study describing *Car9*$^{-/-}$ mice demonstrated that CA IX deficiency leads to gastric pit cell hyperplasia and a depletion of chief cells (Ortova Gut et al. 2002). Based on this observation, it was concluded that CA IX probably regulates cell proliferation and differentiation. Thus, it appears that the functions of CA IX extend far beyond that of pH regulation.

Similar to CA IX, CA XII is a membrane-associated isozyme. However, CA XII is expressed in a variety of normal tissues, and its expression generally becomes stronger or more widespread in tumors compared to normal tissues. Accordingly,

CA XII does not appear to be as tightly regulated by the hypoxia pathway or as strongly linked to cancer as CA IX (Wykoff et al. 2000, Ivanov et al. 2001). Therefore, it is likely that the regulators of CA XII are mainly undiscovered at present.

This study aims to uncover other factors that regulate CA IX and CA XII in addition to hypoxia. Moreover, the expression patterns of these isozymes during mouse embryonic development is investigated, given that mammalian embryonic and early fetal development occur in a hypoxic environment. Additionally, the specific molecular mechanisms underlying the observed phenotype of CA IX-deficient mice are examined in greater detail. The final aim is to examine further the properties of NCCRP1 protein whose mRNA levels were observed to be significantly upregulated in response to CA IX deficiency in the mouse gastric mucosa.

2. REVIEW OF THE LITERATURE

2.1 The importance of acid-base balance

Almost every biological process is pH-dependent, meaning that a small change in pH can have large effects on the rate of a given process. This property is due to the fact that many biological molecules, such as proteins, amino acids and phosphates, contain chemical groups that can function as weak acids or weak bases that can release or bind H^+ ions, respectively. Thus, a change in pH may affect the protonation state of these groups and, therefore, impact the biological activity and conformation of the molecule. For example, enzymes typically demonstrate maximal catalytic activity at a characteristic pH, which is referred to as the pH optimum. On either side of the optimum pH, catalytic activity often declines sharply. Therefore, biological control of cellular and extracellular fluid pH is highly important for all aspects of metabolism and cellular activities. The organism's first line of defense against changes in internal pH is provided by buffer systems. Three important systems include the bicarbonate, phosphate, and ammonia buffer systems. (Nelson and Cox 2000)

The bicarbonate buffer system is based on the following reactions: $CO_2 + H_2O \leftrightarrow H_2CO_3 \leftrightarrow H^+ + HCO_3^-$. In animals with lungs, the bicarbonate buffer system is an effective physiological buffer at approximately pH 7.4. This property is observed because the H_2CO_3 of blood plasma is in equilibrium with a large reserve capacity of gaseous CO_2 in the air space of the lungs. The dissociation of carbonic acid to form bicarbonate and a proton is a rapid reaction that does not require enzymatic catalysis. Alternatively, the hydration of carbon dioxide occurs too slowly without catalysis. Thus, the carbonic anhydrase enzyme family evolved to catalyze a reaction in which carbon dioxide is hydrated to form a proton and bicarbonate: $CO_2 + H_2O \leftrightarrow H^+ + HCO_3^-$ (Nelson and Cox 2000, Supuran 2008).

2.2 The carbonic anhydrase isozyme family

2.2.1 Historical and general aspects

In the beginning of the 20th century, it was not clear how bicarbonate was transported in the blood and released in the lung capillaries; however, it was known that the transit time of blood through the capillaries was only about 1 s. In the late 1920s, it was realized that blood probably contains a catalyst for this reaction (Henriques 1928, Van Slyke and Hawkins 1930). Some years later, it became evident that the catalyst in blood is, indeed, an enzyme (Meldrum and Roughton 1932, Meldrum and Roughton 1933). The name of this enzyme was reportedly suggested by Philip Eggleton to be "carbonic anhydrase" (Davenport 1984). Nevertheless, it was not until 1960 that the CA enzyme was purified for the first time from bovine erythrocytes (Lindskog 1960).

To date, four evolutionarily unrelated CA gene families have been identified: α, β, γ, and δ (Chegwidden and Carter 2000). The α-CAs are present in animals, plants, algae, and certain eubacteria and viruses (Hewett-Emmett 2000). The β-CAs have been reported in many photosynthetic organisms, including plants and algae, but they are also widespread among invertebrates (Hewett-Emmett 2000, Syrjanen et al. 2010). The γ-CAs are expressed primarily in archaea and some eubacteria, whereas δ-CAs are present in marine diatoms (Hewett-Emmett 2000, Xu et al. 2008). In the active site of α-, γ- and δ-CAs, the zinc atom is coordinated by three histidine residues, whereas in β-CAs it is coordinated by one histidine and two cysteine residues (Cox et al. 2000).

In mammals, 13 enzymatically active α-CAs have been identified. Of these CAs, CA I, II, III, VII, and XIII are cytoplasmic (Lehtonen et al. 2004); CA IV, IX, XII, XIV, and XV are membrane-associated (Pastorekova et al. 1997, Tureci et al. 1998, Parkkila et al. 2001, Hilvo et al. 2005); CA VA and VB are mitochondrial (Fujikawa-Adachi et al. 1999b); and CA VI is the only secreted isozyme (Kivela et al. 1999, Karhumaa et al. 2001b). These enzymes catalyze a simple reaction, specifically, the interconversion between carbon dioxide and the bicarbonate ion, and are, therefore, involved in crucial physiological processes related to pH homeostasis. These processes include CO_2 and ion transport, respiration, bone resorption, biosynthetic reactions (e.g., gluconeogenesis, lipogenesis, and

ureagenesis), the production of body fluids, fertilization, tumorigenesis, and many other physiological or pathological processes (Sly and Hu 1995, Parkkila 2000, Supuran 2008). Each α-CA isozyme has a characteristic distribution in mammalian tissues; certain isozymes are expressed in certain cell types of nearly all tissues, whereas others are expressed only in a small number of tissues. Furthermore, each of these isozymes has a unique enzymatic activity and affinity for inhibitors. The features of these isozymes are summarized in Table 1.

Table 1. Catalytic activities, inhibition constants of acetazolamide (AZA) and subcellular localizations of all human CAs (hCAs) and mouse CA XV (mCA XV). The table is modified from (Hilvo et al. 2008b).

Isozyme	k_{cat} (s^{-1})	k_{cat}/k_M ($M^{-1}s^{-1}$)	K_I AZA (nM)	Subcellular localization
hCA I	2.0×10^5	5.0×10^7	250	cytosol
hCA II	1.4×10^6	1.5×10^8	12	cytosol
hCA III	1.3×10^4	2.5×10^5	240000	cytosol
hCA IV	1.1×10^6	5.1×10^7	74	GPI-anchored
hCA VA	2.9×10^5	2.9×10^7	63	mitochondria
hCA VB	9.5×10^5	9.8×10^7	54	mitochondria
hCA VI	3.4×10^5	4.9×10^7	11	secreted
hCA VII	9.5×10^5	8.3×10^7	2.5	cytosol
hCA IX	1.1×10^6	1.5×10^8	16	transmembrane
hCA XII	4.2×10^5	3.5×10^7	5.7	transmembrane
hCA XIII	1.5×10^5	1.1×10^7	16	cytosol
hCA XIV	3.1×10^5	3.9×10^7	41	transmembrane
mCA XV	4.7×10^5	3.3×10^7	72	GPI-anchored

2.2.2 Catalytic mechanism

The α-CAs are globular proteins that exhibit a considerable degree of three-dimensional similarity and a typical folding structure characterized by a central antiparallel β-sheet (Di Fiore et al. 2009). The active site is located in a large, cone-shaped cavity that reaches the center of the protein molecule. The metal ion, which is Zn^{2+} in all α-CAs examined to date, is essential for its catalytic mechanism (Lindskog and Silverman 2000, Supuran 2004). The Zn^{2+} ion is coordinated by three histidine residues (His94, His96 and His119 in CA II) and a water molecule or hydroxide ion (Stams and Christianson 2000). The active form of the enzyme is

basic with a hydroxide ion bound to Zn^{2+} (Lindskog and Silverman 2000). This strong nucleophile attacks the CO_2 molecule that binds in a nearby hydrophobic pocket, leading to the formation of bicarbonate coordinated to Zn^{2+}. The bicarbonate ion is subsequently displaced by a water molecule and liberated into solution. This results in the enzyme being in the acidic, catalytically inactive form with a water molecule coordinated to Zn^{2+}. This reaction is shown in Equation 1 (Lindskog and Silverman 2000, Supuran 2004). To regenerate the basic form, a proton transfer reaction from the active site to the environment takes place, which may be assisted either by active-site residues or by buffers present in the medium. This reaction is represented in Equation 2 (Lindskog and Silverman 2000, Supuran 2004).

(1) $EZn^{2+} - OH^- + CO_2 \longleftrightarrow EZn^{2+} - HCO_3^- \overset{H_2O}{\longleftrightarrow} EZn^{2+} - OH_2 + HCO_3^-$

(2) $EZn^{2+} - OH_2 \longleftrightarrow EZn^{2+} - HO^- + H^+$

The rate-limiting step in the catalysis is the proton transfer reaction (Equation 2). In isozymes with high catalytic activity, this step is assisted by a histidine residue (His64), which is termed a proton-shuttle residue and is located at the opening of the active site (Tu et al. 1989). In addition to His64, a unique cluster of histidines is thought to be important for the high catalytic activity of the CA II isozyme, ensuring an efficient proton transfer process (Di Fiore et al. 2009). This property also explains the fact that CA II is one of the most active enzymes known, approaching the limit of diffusion control. Interestingly, in addition to its catalytic function, the intramolecular proton shuttle supports a non-catalytic function of CA II by enhancing the activity of acid- or base-transporting proteins in a direct, non-catalytic manner (Becker et al. 2011).

In addition to the reversible hydration of carbon dioxide, α-CAs can catalyze a variety of other reactions, such as the hydration of cyanate to carbamic acid, the hydration of cyanamide to urea, and other less-investigated processes. It is still unclear whether CA-catalyzed reactions other than CO_2 hydration have physiological significance. (Supuran 2004)

Because CAs are involved in numerous physiological and pathological processes, their inhibition has long been considered an important area of research. There are two primary classes of CA inhibitors: the unsubstituted sulfonamides, including

their bioisosteres (e.g., sulfamates and sulfamides) and metal-complexing anions. Sulfonamide inhibitors bind to the Zn^{2+} ion via a substitution mechanism where the sulfonamide is exchanged for the water molecule (Equation 3), whereas the anionic inhibitors become a portion of the metal coordination sphere (Equation 4). (Supuran 2004)

(3) $EZn^{2+} - OH_2 + I \quad \longleftrightarrow \quad EZn^{2+} - I + H_2O$ (substitution)

(4) $EZn^{2+} - OH_2 + I \quad \longleftrightarrow \quad EZn^{2+} - OH_2(I)$ (addition)

Coumarins are a recently discovered class of CA inhibitors (Vu et al. 2008, Maresca et al. 2009). They do not directly interact with the metal ion in the enzyme active site, which is an interaction that is critical for the inhibition of CAs by other classes of compounds, including sulfonamides and metal-complexing anions. In fact, as shown by kinetic and X-ray crystallographic studies, coumarins are mechanism-based inhibitors; they undergo hydrolysis under the influence of the zinc-hydroxide in the nucleophilically active species of the enzyme, thereby generating substituted-2-hydroxycinnamic acids. These acids bind at the entrance of the active site cavity and block the entire entrance to it, thereby inhibiting the catalytic activity of the enzyme (Maresca et al. 2010). Sulfonamides incorporating coumarin rings have also been examined and were shown to possess a distinct inhibition mechanism compared to the coumarins (Wagner et al. 2010). Thus, the discovery of these compounds may further broaden the repertoire of CA inhibitors against various enzymes of mammalian or parasitic origin.

CA inhibitors have been primarily used as diuretics and to treat glaucoma, epilepsy and acute mountain sickness. A crucial problem in CA inhibitor design is related to the high number of isoenzymes and their scattered localization in several tissues and organs. Moreover, the use of presently available inhibitors is hampered by their lack of isozyme selectivity. However, progress has recently been made in the generation of CA-selective and isozyme-specific inhibitors; it is now possible to design membrane-impermeant CA inhibitors, which may specifically inhibit membrane-associated CAs without interacting with the cytosolic mitochondrial isoforms. A further approach for selectively inhibiting the tumor-associated

isoforms (CAs IX and XII) that are present in hypoxic tumor tissues makes use of bioreductive prodrugs that are activated by hypoxia. (Supuran 2008)

Although CA inhibitors have been extensively examined, the subject of CA activators has remained largely unexplored. However, over the past decade, activators have been demonstrated to bind within the CA active cavity at a site distinct from the inhibitor or substrate-binding sites. These activators facilitate the proton-transfer step. Several physiologically relevant compounds, such as biogenic amines (histamine, serotonin and catecholamines), amino acids, oligopeptides or small proteins, act as efficient CA activators. It has been suggested that CA activators may be used for treating Alzheimer's disease and other conditions in which the improvement of spatial learning and memory is necessary. (Supuran 2008)

2.2.3 Carbonic anhydrase-related proteins

Members of the α-CA family encode not only proteins that possess the catalytic activity of CA but also carbonic anhydrase-related proteins (CA-RPs). Members of this latter group are devoid of CA catalytic activity, due to the absence of one or more of the zinc-binding histidine residues. The CA-RPs that are found in mammals include CA-RP VIII, X, and XI (Kato 1990, Hewett-Emmett and Tashian 1996, Lovejoy et al. 1998). In addition, the receptor-type protein tyrosine phosphatases β and γ (RPTPβ and RPTPγ) contain 'CA-like' domains in their N-termini (Tashian et al. 2000).

Studies on the distribution of CA-RPs have demonstrated wide expression profiles in all parts of the human and mouse brain (Fujikawa-Adachi et al. 1999c, Okamoto et al. 2001, Taniuchi et al. 2002). CA-RP VIII is predominantly expressed in the human and mouse cerebellum, especially in Purkinje cells. However, weaker expression has been detected in several other mouse tissues, including the liver, submandibular gland, stomach, and lung (Aspatwar et al. 2010). In the same study, CA-RP XI was shown to exhibit a similar expression pattern as CA-RP VIII, although the staining intensity was clearly less intense. Moreover, CA-RP X expression was only observed in a small number of tissues, including the brain. The presence of CA-RPs in the human and mouse brain implies important roles for these

proteins in brain development and/or neural function. Furthermore, CAs VIII and XI appear to have a role in cancer development in the gastrointestinal tract and the lungs (Akisawa et al. 2003, Miyaji et al. 2003, Morimoto et al. 2005, Ishihara et al. 2006, Nishikata et al. 2007).

Both RPTPβ and RPTPγ are expressed in specific areas of the developing and adult central nervous system (CNS). In addition to their CA domain, their extracellular portion consists of a fibronectin III (FN III) repeat domain and a Cys-free domain. The long extracellular region is joined by a transmembrane region to the intracellular catalytic D1 and D2 phosphatase domains. The exact roles of RPTPβ and RPTPγ have not been fully elucidated. (Tashian et al. 2000)

2.3 Expression and function of carbonic anhydrase isozymes

2.3.1 Cytosolic isozymes (I, II, III, VII, XIII)

CA I is highly expressed in human erythrocytes (Tashian 1989) but appears to contribute only 50% of the total CA activity in these cells (Dodgson et al. 1988). However, the presence of CA I may explain why no abnormal phenotype has been detected in the erythrocytes of individuals with CA II deficiency syndrome (Sly and Hu 1995). Alternatively, there is no clear abnormal phenotype in CA I-deficient individuals, suggesting that other CA isozymes may complement the function of CA I (Tashian 1992). In effect, the functional importance of CA I remains unclear. In addition to erythrocytes, CA I is expressed in several other tissues, including the epithelia of the esophagus, small intestine and colon and the α-cells of the islets of Langerhans (Lonnerholm et al. 1985, Parkkila et al. 1994, Christie et al. 1997). Furthermore, CA I is expressed in the placenta and fetal membranes, the corneal endothelium, the lens of the eye, sweat glands, adipose tissue, neutrophils and the zona glomerulosa of the adrenal glands (Venta et al. 1987, Parkkila et al. 1993, Campbell et al. 1994, Muhlhauser et al. 1994, Sly and Hu 1995). The gene encoding CA I has two tissue type-specific promoters, which are separated by a large 35-36 kb intron (Fraser et al. 1989, Brady et al. 1991). One of these promoters is

functional in erythrocytes, whereas the other produces a transcript in non-erythroid tissues.

CA II is a highly active enzyme and has the widest expression pattern of all CA isozymes. Accordingly, CA II is considered to play an important role in various physiological reactions. CA II was first discovered in erythrocytes where it catalyzes the reversible hydration of carbon dioxide (Meldrum and Roughton 1932, Meldrum and Roughton 1933). In the human alimentary tract, CA II is thought to participate in many processes. CA II is expressed in serous acinar cells of the parotid and submandibular glands and is thought to supply the saliva with bicarbonate (Parkkila et al. 1990). Similarly, CA II may contribute to the bicarbonate production in the esophagus where it is expressed by the stratified squamous epithelium (Parkkila et al. 1994). In the stomach, both surface epithelial cells and parietal cells express high levels of CA II. In parietal cells, CA II produces protons for gastric acid and further provides bicarbonate in the surface epithelial cells to protect these cells from acid digestion (Davenport 1939, Parkkila et al. 1994). CA II is also expressed in the duodenum, colon, liver, gallbladder, pancreas and brain (Maren 1967, Kumpulainen and Korhonen 1982, Parkkila et al. 1994). Furthermore, CA II is expressed in renal tissues where it participates in the acidification of urine (Parkkila 2000). In bones, CA II is expressed in osteoclasts where it provides the protons required for bone resorption, and it has also been proposed to contribute to osteoclast differentiation (Vaananen 1984, Lehenkari et al. 1998).

In addition to various normal tissues, CA II expression has been detected in neoplastic tissues, including malignant brain tumors (Parkkila et al. 1995a, Haapasalo et al. 2007, Korhonen et al. 2009), leukemia (Leppilampi et al. 2002), lung cancer (Chiang et al. 2002), pancreatic cancer (Parkkila et al. 1995b), colorectal cancer (Bekku et al. 2000), and gastrointestinal stromal tumors (GISTs) (Parkkila et al. 2010). In some tumor types, such as astrocytomas, CA II expression is associated with a poor prognosis (Haapasalo et al. 2007). In contrast, CA II expression indicates a favorable prognosis in GISTs (Parkkila et al. 2010). Moreover, CA II expression has been observed in tumor vessel endothelia, suggesting that CA II may play a role in tumor angiogenesis (Yoshiura et al. 2005).

A deficiency of human CA II produces a syndrome that is characterized by osteopetrosis, renal tubular acidosis, cerebral calcification, mental retardation, and

impaired growth (Sly et al. 1983, Sly et al. 1985). Surprisingly, no gastrointestinal symptoms have been described in CA II-deficient patients, despite the fact that CA II is highly expressed in various tissues of the gastrointestinal tract. However, a study of *Car2* knockout mice demonstrated an abnormal histological phenotype with impaired prostaglandin E_2-mediated bicarbonate secretion in the duodenum (Leppilampi et al. 2005b). This finding implies that there may be an abnormal gastrointestinal phenotype in CA II-deficient patients.

CA III has unique properties among the CA isozymes, including low catalytic activity, a resistance to sulfonamide inhibitors and an unusual tissue distribution. The primary reasons for the low activity of CA III are the absence of the proton shuttle residue His64 and the presence of Phe198 in place of Leu198 (Tu et al. 1989, Chen et al. 1993, LoGrasso et al. 1993). CA III is primarily concentrated in skeletal muscle type I fibers but is also present in other fiber types at lower levels (Vaananen et al. 1985, Laurila et al. 1991). Additionally, CA III is highly expressed in adipose cells (Stanton et al. 1991). Serum CA III is a potential marker of myocardial infarction because these patients show a significantly increased serum myoglobin/CA III ratio (Vaananen et al. 1990, Beuerle et al. 2000). The same ratio may be useful in evaluating the success of reperfusion following acute myocardial infarction (Vuotikka et al. 2003).

Given that CA III has a notably low catalytic activity, it is plausible that pH regulation is not the primary function of this isozyme. In fact, several studies have suggested that CA III may be an antioxidative agent. In NIH/3T3 cells, the expression of CA III was demonstrated to protect the cells from hydrogen peroxide-induced apoptosis (Raisanen et al. 1999). CA III expression is also increased in experimentally-induced alcoholic liver disease (Parkkila et al. 1999). Furthermore, it has been shown that CA III has two sulfhydryl groups that can conjugate to glutathione (GSH) in a process termed S-glutathiolation (Mallis et al. 2000). This process is important for protecting cells from reactive oxygen and nitrogen species (Klatt and Lamas 2000). It is, therefore, somewhat surprising that CA III knockout mice exhibit no apparent abnormal phenotype (Kim et al. 2004). However, it was later found that CA III deficiency may impair mitochondrial ATP synthesis (Liu et al. 2007).

CA VII is one of the least-examined and understood cytosolic CA isoforms, even though it was identified and characterized 20 years ago (Montgomery et al. 1991).

With respect to its amino acid sequence, CA VII appears to be the most highly conserved CA isozyme in mammals (Earnhardt et al. 1998). CA VII is expressed in the human salivary gland and in the mouse cerebrum and cerebellum (Montgomery et al. 1991, Lakkis et al. 1997). In the brain, CA VII contributes to gamma-aminobutyric acid (GABA)-mediated signaling by enabling the synchronous firing of CA1 pyramidal neurons (Ruusuvuori et al. 2004). It was recently demonstrated that there are two isoforms of CA VII of which the full-length form appears to be the primary isoform expressed *in vivo* (Bootorabi et al. 2010). The same study also demonstrated that in addition to the brain, CA VII is also expressed in several other organs, including the stomach, duodenum, colon, liver, and skeletal muscle, suggesting that this isozyme may play multiple roles in different organs.

CA XIII was first characterized in 2004 and was shown to be phylogenetically most closely related to the cytosolic isozymes I, II, and III (Lehtonen et al. 2004). CA XIII expression has been examined in human and mouse tissues by immunohistochemistry. CA XIII is widely expressed in the gastrointestinal tract of both species; however, the expression pattern is somewhat different between the two species (Lehtonen et al. 2004, Pan et al. 2007). Moreover, both human and mouse kidneys express CA XIII in the renal cortex and medulla with the strongest expression detected in the collecting ducts (Lehtonen et al. 2004). In mice, CA XIII is also expressed in the brain and lungs. Interestingly, CA XIII appears to be abundant in reproductive tissues. In humans, different stages of developing sperm cells express CA XIII, but the enzyme is not present in mouse testis. In the human female reproductive tract, CA XIII is expressed in the uterine cervix, and certain endometrial glands are also positive. In addition, CA XIII is expressed in the mouse uterine epithelial cells. CA XIII expression in the reproductive tract indicates that CA XIII may contribute to the fertilization process. Accordingly, it has been observed that the inhibition constant of bicarbonate for mouse CA XIII is exceptionally high (Innocenti et al. 2004). Therefore, it is plausible that this isozyme is active in physiological environments characterized by high bicarbonate concentration, such as reproductive tissues.

In neoplastic tissues, CA XIII has been investigated only in colorectal tumors (Kummola et al. 2005). The results indicated that the expression pattern of CA XIII is a similar to CAs I and II, i.e., expression becomes weaker with increasing dysplasia and malignancy grades. It was suggested that this downregulation may

result from reduced levels of a common transcription factor or the loss of the closely linked *CA1*, *CA2* and *CA13* alleles on chromosome 8.

2.3.2 Mitochondrial isozymes (VA and VB)

Mitochondrial CA activity was originally observed several decades ago (Dodgson et al. 1980), yet this enzyme was only later named CA V (Dodgson and Forster 1986). It was not until 1999 that two nuclear-encoded mitochondrial CAs were described in mammals (Fujikawa-Adachi et al. 1999b). Consequently, CA V was designated **CA VA**, and the newly discovered enzyme was named **CA VB**. CA VA is abundantly expressed in the liver and, to a lesser degree, in the skeletal muscle and kidney. CA VB is ubiquitously expressed in several tissues, excluding the liver in humans; it is, however, expressed in the mouse liver (Fujikawa-Adachi et al. 1999b, Shah et al. 2000). Mitochondrial CAs have been suggested to contribute to several metabolic processes, such as gluconeogenesis, lipogenesis and ureagenesis, by providing bicarbonate for the early carboxylation reaction (Chegwidden et al. 2000).

2.3.3 Secretory isozyme (VI)

CA VI is the only secreted member of the CA family (Fernley et al. 1979). CA VI is secreted into the saliva by the serous acinar cells of the parotid, submandibular (Parkkila et al. 1990), and lingual von Ebner's glands (Leinonen et al. 2001). It has been shown that salivary CA VI concentrations follow a circadian periodicity with low levels observed during the sleeping period (Parkkila et al. 1995c). CA VI is also secreted into milk by the mammary glands (Karhumaa et al. 2001b). Furthermore, CA VI has been detected in the lacrimal (Ogawa et al. 2002), nasal, septal, and lateral glands (Kimoto et al. 2004), the esophagus (Kasuya et al. 2007), the tracheobronchial glands, epithelial serous cells (Leinonen et al. 2004), and the alimentary canal (Kaseda et al. 2006). Low concentrations of CA VI have also been observed in human serum because small amounts leak from the salivary glands or are absorbed from the alimentary canal (Kivela et al. 1997).

Even though CA VI has been studied for 30 years, its physiological role is still uncertain. It has been suggested that salivary CA VI may protect teeth from caries

(Kivela et al. 1999, Kimoto et al. 2006). It is also thought that CA VI may protect the esophageal and gastric epithelium from acid injury, given that low CA VI concentrations are linked to the appearance of acid-peptic diseases in many patients suffering from gastrointestinal (GI) disorders (Parkkila et al. 1997). CA VI has also been proposed to be an essential factor in normal growth and development of the infant alimentary tract, given that it is found in both human and rat milk with particularly high concentrations in the colostrum (Karhumaa et al. 2001b). Furthermore, it has been suggested that CA VI contributes to the growth and development of taste buds (Henkin et al. 1999). A stress-inducible form of CA VI has also been described (Sok et al. 1999). This form is expressed from an internal promoter and encodes an intracellular form of the protein. However, the physiological significance of the stress-inducible form is unknown.

A recent study reported the generation and phenotype of CA VI-deficient mice, which were viable and fertile and had a normal life span (Pan et al. 2011a). No morphological differences were observed between knockout and wild-type mice in the salivary, lacrimal, or mammary glands, all of which are known to secrete CA VI. The only histological difference between the knockout and control mice was that the number of lymphoid follicles in small intestinal Peyer's patches was substantially higher in adult knockout mice than in wild-type mice. Analysis of the transcriptomic differences between *Car6*$^{-/-}$ and wild-type mice revealed that genes important in catabolic processes were downregulated in both the submandibular gland and stomach, although they were upregulated in the duodenum. This finding may suggest a functional role for CA VI in catabolic processes.

2.3.4 Membrane-bound isozymes (IV, XIV, XV)

CA IV is attached to the cell membrane with a glycosylphosphatidylinositol (GPI)-anchor and was originally observed in the lung and kidney (Whitney and Briggle 1982, Wistrand and Knuuttila 1989). CA IV is expressed in multiple tissues and has been shown to perform important functions. The presumed function of CA IV in the lung is to catalyze the dehydration of plasma HCO_3^- to CO_2, which can readily diffuse across the capillary endothelial surface and pass out of the lungs through expiration (Zhu and Sly 1990). CA IV has been found in the thick ascending limb

and S2 segments of the proximal tubules in the rat kidney (Brown et al. 1990) and in the intercalated cells of the rabbit collecting duct (Schwartz et al. 2000), suggesting that this isozyme contributes to HCO_3^- reabsorption. CA IV has been principally observed in the luminal membranes of the kidney, and some expression has been reported in the basolateral membranes (Brown et al. 1990, Purkerson et al. 2007). In the gastrointestinal tract, CA IV was detected in the submucosal capillary endothelium of all gastrointestinal regions and in the apical plasma membranes of the epithelial cells in the small and large intestine, where it is proposed to participate in ion and water transport (Fleming et al. 1995). CA IV is also expressed in the apical plasma membrane of gallbladder epithelial cells and in the endothelium of the subepithelial capillaries, suggesting that it may participate with CA II and ion transporters in the acidification of bile via bicarbonate reabsorption (Parkkila et al. 1996). Furthermore, CA IV is expressed in several other tissues, including skeletal and heart muscle (Sender et al. 1994, Sender et al. 1998), the brain (Ghandour et al. 1992) and the eye (Hageman et al. 1991).

It has been suggested that CA IV may form a metabolon with CA II and several other anion exchange proteins because CA II and CA IV have been experimentally shown to interact with several anion exchange proteins, including Cl^-/HCO_3^- exchangers, Na^+/HCO_3^- cotransporters and Na^+/H^+ exchangers. Therefore, it has been proposed that CA II and CA IV may facilitate the rate of anion exchange across the plasma membrane in physiologically relevant tissues, such as renal tubules (Purkerson and Schwartz 2007).

CA XIV was originally characterized by two independent research groups from the mouse kidney (Mori et al. 1999) and human spinal cord (Fujikawa-Adachi et al. 1999a). In terms of amino acid similarity, CA XIV is most closely related to CA XII. CA XIV is expressed in various human and mouse tissues, including the kidney, heart, brain, skeletal muscle, and liver (Fujikawa-Adachi et al. 1999a, Mori et al. 1999). In the mouse kidney, CA XIV is abundantly expressed in the apical plasma membranes of the S1 and S2 segments of the proximal tubules and, more weakly, in the basolateral membranes (Kaunisto et al. 2002). It is also present in the initial portion of the thin descending limbs of Henle. These results indicate that CA XIV is likely to contribute to the acidification of urine in cooperation with CA IV. In the mouse liver, CA XIV is also expressed on both the apical and basolateral plasma membranes of hepatocytes (Parkkila et al. 2002). Moreover, CA XIV has

been observed on neuronal membranes and axons in the human and mouse brain (Parkkila et al. 2001). The highest degree of expression is observed on the large neuronal bodies and axons in the anterolateral portion of pons and medulla oblongata. Furthermore, it has been demonstrated that both CA XIV and CA IV contribute to extracellular buffering in the central nervous system (CNS) (Shah et al. 2005). Interestingly, CA XIV has been shown to interact with the AE3 Cl^-/HCO_3^- exchanger in the CNS, indicating that the AE3/CA XIV metabolon constitutes a system to dispose of high CO_2 and H^+ production and to regulate pH in the brain and retina (Casey et al. 2009).

CA XV is the most recently identified member of the mammalian CA family and was characterized in 2005. CA XV appears to be a unique member of the CA family because the gene encoding this isozyme is a non-processed pseudogene in humans and chimpanzees. In contrast, several other species appear to possess an active gene coding for CA XV. According to sequence analysis, this isozyme is evolutionarily conserved from fish to mammals but has become an inactive gene recently in the evolutionary timescale. Phylogenetic analyses have indicated that CA XV is most closely related to CA IV. In fact, the biochemical properties of CA XV are similar to those of CA IV; both isozymes are attached to the cell membrane by a GPI anchor and are N-glycosylated. The activity of mouse CA XV has been shown to be comparable to that of human CA XII and XIV, placing CA XV within the group of CAs with moderate levels of catalytic activity. (Hilvo et al. 2005)

The distribution of *Car15* in different mouse tissues is quite limited with expression being observed predominantly in the kidney. Within this organ, the highest signal is observed in the renal cortex and lower expression is seen in the medulla (Hilvo et al. 2005). In a recent study, the localization of CA XV in the kidney was confirmed at the protein level (Saari et al. 2010). Moreover, a systematic study of CA mRNA expression in the mouse digestive system showed that *Car15* expression is extremely low in the gastrointestinal tract (Pan et al. 2007). The absence of CA XV in some species raises the questions of why it was lost during evolution and why it is not required in humans. It is possible that CA IV and CA XV are functionally redundant and that a highly active human CA IV may compensate for the loss of CA XV.

2.3.5 Membrane-bound isozyme IX

2.3.5.1 General aspects

CA IX was originally named MN protein and was identified as a cell density-regulated plasma membrane antigen in the HeLa human cervical carcinoma cell line using the monoclonal antibody M75 (Pastorekova et al. 1992). The MN antigen was detected in several tumor cell lines and surgical tumor specimens but not in corresponding normal tissues (Zavada et al. 1993). These two pioneering studies revealed the connection between the MN protein and cancer. Later, the full-length cDNA for the MN protein was cloned and was found to contain a large CA domain in the extracellular portion of the encoded protein (Pastorek et al. 1994, Opavsky et al. 1996). Sequence analysis revealed that the MN gene encodes a 459-amino acid protein. The protein consists of a 414-amino acid N-terminal extracellular portion followed by 20-amino acid hydrophobic transmembrane region and a 25-amino acid C-terminal intracellular tail. The extracellular portion of the protein is composed of a 37-amino acid signal peptide, a 59-amino acid proteoglycan (PG) domain with similarity to the keratan sulfate-binding domain of the large proteoglycan aggrecan, and a 257-amino acid CA domain. Because the CA domain was found to be well-conserved, exhibiting significant identity with CA VI, II, and other CA isozymes, the MN protein was renamed carbonic anhydrase IX as the ninth mammalian CA identified (Hewett-Emmett and Tashian 1996). Moreover, CA IX is the only member of the CA isozyme family with both PG and CA domains.

In an independent line of research, the monoclonal antibody G250 was reported to recognize a specific antigen in renal cell carcinomas (RCCs) (Oosterwijk et al. 1986). Much later, this antigen was shown to be identical to CA IX (Oosterwijk 2008).

CA IX is a dimeric enzyme, and the dimerization is suggested to be mediated by the formation of an intermolecular disulfide bond between the same Cys residue on the CA catalytic domain of the two monomers (Hilvo et al. 2008a, Alterio et al. 2009). According to crystallographic data, both active sites of the dimer are exposed to the extracellular medium for efficient CO_2 hydration (Alterio et al. 2009). The catalytic activity of the entire extracellular portion of CA IX (composed of the PG and CA domains) that is expressed in the baculovirus system is high and is in the

same range as CA II (Hilvo et al. 2008a). Furthermore, the addition of $ZnCl_2$ increased the catalytic activity of the insect-cell derived human enzyme by approximately 10-fold. Thus, CA IX appears to possess the highest catalytic activity that has ever been measured for a human CA enzyme. The three-dimensional structure of the dimeric CA IX catalytic domain is presented in Figure 1.

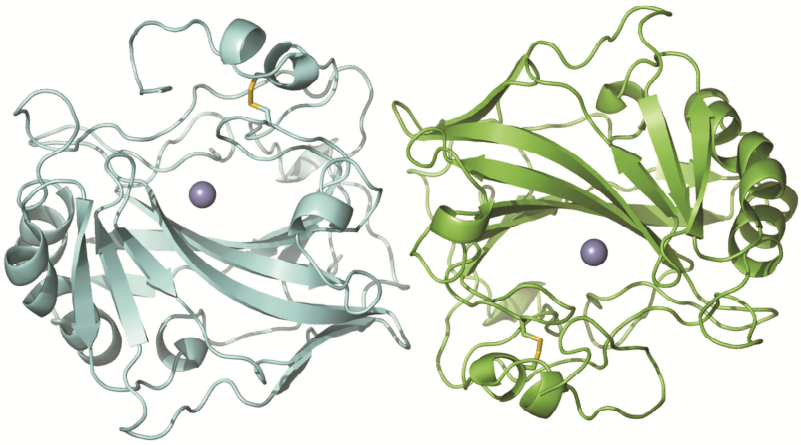

Figure 1. The X-ray structure of the dimeric CA IX catalytic domain. This figure was generated from X-ray coordinates as reported previously (Alterio et al. 2009). The PDB ID for the structure is 3IAI, and the figure was generated using the PyMOL Molecular Graphics System, Version 1.3 (Schrödinger, LLC). The Zn^{2+} ion and intramolecular disulfide bond are shown in purple and yellow, respectively.

2.3.5.2 Expression in normal tissues

CA IX has an exceptional expression pattern, as it is only expressed in a small number of normal tissues; however, its ectopic expression is induced in a wide spectrum of human tumors. CA IX expression has been reported in human, rat, and mouse tissues.

In humans, CA IX expression has been examined thoroughly in the alimentary tract (Pastorekova et al. 1997). The strongest expression is detected in the gastric mucosa from the gastric pits to the deep gastric glands and is confined to the basolateral surface of the epithelial cells. Staining is observed in all of the major cell

types of the gastric epithelium, including the surface epithelial cells, parietal cells and glandular chief cells. In the human intestine, the most intense CA IX expression is observed in the crypt enterocytes of the duodenum and jejunum (Saarnio et al. 1998b). Moderate staining is detected in the crypts of the ileum, cecum, and ascending colon. Expression becomes weaker toward the rectum. In addition to the gastric and intestinal epithelium, the gallbladder epithelium also shows abundant expression of CA IX (Pastorekova et al. 1997). Furthermore, CA IX is expressed moderately in the basolateral membrane of epithelial cells in the bile ducts and faintly in the pancreatic ducts (Pastorekova et al. 1997). Varying expression intensities of CA IX in humans have been observed in the coelomic epithelium of the body cavities, the rete ovarii, the rete testis and efferent ducts, the ventricular linings of the CNS and the choroid plexus (Ivanov et al. 2001, Karhumaa et al. 2001a).

In rats, staining for CA IX is strong in the stomach with the same expression pattern as in humans. In the rat intestine, epithelial staining is present in the duodenum and colon but is absent from sections of the jejunum and ileum. Again, the positive reaction is confined to the basolateral surface of the epithelium. In the rat colon, the distribution of CA IX through the mucosal layer is different from that of humans, as the positive signal is strongest in the surface epithelium. In human colon, however, expression is highest at the base of the crypts. CA IX is also present at the basolateral plasma membrane of rat bile ducts but is absent from the pancreatic ducts. (Pastorekova et al. 1997)

In mice, the highest expression of CA IX has been observed in the stomach, where it is confined to the basolateral plasma membrane of the surface epithelial cells, chief cells and parietal cells, similar to humans and rats. Moderate expression has been observed in the colon with the strongest reaction in the surface epithelial cuff region. In the mouse small intestine, CA IX expression is generally weak. A moderate level of expression has been detected in the pancreas, brain, and cerebellum. Lower levels of CA IX are expressed in the mouse liver, spleen, thymus, epididymis, testis, and kidney. (Hilvo et al. 2004)

2.3.5.3 Expression in neoplastic tissues

CA IX is ectopically expressed at relatively high levels and with a high prevalence in different tumor tissues with normal counterparts that show low levels of this protein or none at all. These include carcinomas of the brain, lung, esophagus, colon, pancreas, liver, breast, endometrium, ovary, skin, and kidney (Liao et al. 1997, McKiernan et al. 1997, Turner et al. 1997, Saarnio et al. 1998a, Vermylen et al. 1999, Kivela et al. 2000b, Ivanov et al. 2001, Saarnio et al. 2001, Bartosova et al. 2002). In contrast, tissues with high natural CA IX expression, such as the stomach and gallbladder, have been shown to lose a portion of or all CA IX expression upon conversion to carcinoma (Saarnio et al. 2001, Leppilampi et al. 2003). In the colonic epithelium, CA IX is normally expressed in the deep crypts and abnormally in superficial adenomas and carcinomas; the most intense staining is detected in tumors with a mucinous component (Saarnio et al. 1998a). For unknown reasons, CA IX is generally absent from normal prostate tissues and from prostate carcinomas. CA IX overexpression has correlated with poor prognosis in a broad spectrum of tumor types (Chia et al. 2001, Giatromanolaki et al. 2001, Loncaster et al. 2001, Haapasalo et al. 2006).

Cancers that contain a high proportion of CA IX-positive specimens include carcinomas of the cervix, lung, and kidney. CA IX is expressed in virtually all cervical carcinomas and the majority of cervical intraepithelial neoplasias (Liao et al. 1994). In lung cancer, CA IX is not found in preneoplastic lesions but is present in malignant tumors with expression being associated with tumor aggressiveness, hypoxia, and necrosis (Vermylen et al. 1999, Giatromanolaki et al. 2001, Swinson et al. 2003). In renal cell carcinomas (RCCs), CA IX is most strongly expressed in clear cell RCCs (ccRCC), the most common form of RCC, and is expressed in virtually all cases (Uemura et al. 1999). High levels of CA IX protein and/or mRNA are detected in primary, cystic, and metastatic ccRCCs but not in benign lesions (Liao et al. 1997, McKiernan et al. 1997). However, in contrast to several other cancers, it appears that decreased CA IX expression levels predict a poor prognosis for RCC patients (Bui et al. 2003, Sandlund et al. 2007).

Because there is a clear division between tissues with normal and ectopic expression, CA IX has been proposed to be a promising tumor biomarker and a potential therapeutic target. In fact, the anti-CA IX antibody Rencarex® is currently

being investigated in a phase III clinical trial (www.wilex.de) as a treatment for non-metastatic ccRCC. In phase I and II studies, Rencarex® was demonstrated to be safe and well-tolerated and exhibited a promising efficacy profile.

2.3.5.4 Knockout mouse model

The generation of *Car9* knockout mice revealed that CA IX is required for normal gastric morphogenesis, as these mice exhibit gastric hyperplasia of the glandular epithelium and numerous cysts (Ortova Gut et al. 2002). The most pronounced hyperplasia was in the stomach corpus region. No changes were visible in CA IX-deficient mice during embryonic development, but an increase in mucosal thickness was detected in newborn animals. The hyperplasia became prominent at the end of gastric morphogenesis in four-week-old mice but did not progress with age. The loss of CA IX led to an overproduction of mucus-secreting pit cells and a depletion of pepsinogen-positive chief cells. The absolute number of parietal cells was increased in the *Car9* knockout mice, but the proportion of these cells was significantly reduced when compared to the gastric epithelium of wild-type mice. These alterations suggest that CA IX may contribute to the balance between differentiation and proliferation in the gastric mucosa.

Based on the available evidence, CA IX-deficiency does not appear to have serious physiological consequences; *Car9*$^{-/-}$ mice showed normal gastric pH, gastric acid secretion, and gastrin serum levels. In addition, systemic acid-base balance and plasma electrolyte values were normal in CA IX-deficient mice. These mice showed no deviations from their wild-type controls in terms of growth, behavior, reproductive potential, health, or life span. Moreover, CA-deficiency had no effect on the morphology or histology of other tissues, including the lung, spleen, liver, kidney, jejunum, ileum, and colon.

Given that hyperplasia can lead to dysplasia or malignancy in the presence of carcinogenic factors, it has been studied whether the effects of CA IX deficiency may be modified by a high-salt diet, which is a known co-factor of carcinogenesis (Leppilampi et al. 2005a). Two strains of CA IX-deficient mice, C57BL/6 and BALB/c, were fed either a standard or high-salt diet for 20 weeks. Excess dietary salt did not significantly affect the severity of pit cell hyperplasia, and dysplasia was

not observed in any of the groups. In C57BL/6 mice, however, CA IX-deficiency was associated with gastric submucosal inflammation. Thus, these results indicate that CA IX deficiency alone may not be a significant carcinogenic factor but may initiate a carcinogenic process by affecting cell proliferation and/or differentiation in the gastric mucosa.

The brain phenotype of CA IX-deficient mice was published recently (Pan et al. 2011b). In a one-year study, the brain histology and behavior of *Car9*$^{-/-}$ and wild-type mice were monitored. Morphological analyses revealed vacuolar degenerative changes in the brains of *Car9*$^{-/-}$ mice. These changes became visible at the age of eight to ten months. Behavioral tests indicated that *Car9*$^{-/-}$ mice exhibited abnormal locomotor activity and poor performance in a memory test. Furthermore, the transcriptomic responses to CA IX deficiency in the brain were examined using genome-wide cDNA microarray analyses. Thirty-one and 37 genes were significantly up- or downregulated, respectively, in the brains of CA IX-deficient mice compared to wild-type animals. Functional annotation showed that the genes with increased expression were involved in several processes, such as RNA metabolism, whereas the genes with reduced expression were implicated in other important processes, such as the regulation of cellular ion homeostasis. Consistent with the behavioral phenotype, the biological processes ‘‘behavior’’ and ‘‘locomotory behavior’’ were the two prominent terms overrepresented among the down-regulated genes. Based on these observations, the authors concluded that CA IX may directly or indirectly have novel functions in the brain.

2.3.5.5 Functional role

There is emerging evidence that the roles of CA IX extend far beyond the basic pH regulation function of CAs. For example, CA IX is the only member of the CA isozyme family with both the CA catalytic domain and the PG domain. Accordingly, CA IX was suggested to participate in cell adhesion processes (Pastorekova and Zavada 2004).

In normal tissues, the distribution pattern of CA IX is relatively limited. It has been proposed to participate in the regulation of the acid-base balance on the basolateral surfaces of the gastrointestinal tract epithelia. In addition to the other

major cell types of gastric mucosa, CA IX is highly expressed in the parietal cells, suggesting a role in acid secretion. In fact, CA IX has been shown to interact functionally and physically with the SLC4 family of Cl^-/HCO_3^- anion exchange proteins, including AE1, AE2, and AE3. Moreover, CA IX colocalizes with AE2 at the basolateral plasma membrane of parietal cells. Therefore, it is conceivable that these proteins form a bicarbonate transport metabolon. Upon stimulation, the parietal cells of the gastric mucosa actively secrete H^+ into the gastric lumen, and Cl^- concomitantly moves through Cl^- channels. To sustain acid secretion, parietal cells must replace the HCl lost at the apical surface using two coupled processes. At the parietal cell's basolateral surface, CO_2 diffuses into the cell from adjacent capillaries. CA II catalyzes CO_2 conversion, producing HCO_3^- and H^+ and thus supplying the parietal cells with protons. In the basolateral membrane, Cl^-/HCO_3^- exchangers extrude excess HCO_3^- while importing Cl^-, thereby regulating the intracellular pH. The basolateral localization of CA IX enables it to catalyze the conversion of extruded HCO_3^-, thereby plausibly contributing to gastric acid secretion as part of the AE2-CA II-CA IX bicarbonate transport metabolon. (Morgan et al. 2007)

In tumor tissues, CA IX expression is strongly linked with a hypoxic phenotype, implicating a role for this enzyme in the pH regulation of malignancies. Hypoxia occurs frequently in tumors as a result of aberrant vasculature. Hypoxia triggers the development of acidosis, due to the induction of metabolic shift from oxidative phosphorylation to aerobic glycolysis. While glycolytic metabolism helps tumor cells meet their energy demands in low-oxygen conditions, it also generates an excess of acidic products, such as lactic acid, H^+ and CO_2. These products must subsequently be extruded from the cell.

A proposed involvement of CA IX in the pH regulation of tumors is based on a model that includes a bicarbonate transport metabolon (Pastorekova and Zavada 2004). As an extracellular component of the metabolon, CA IX probably hydrates carbon dioxide, thereby providing bicarbonate for the anion exchanger (AE). Next, the AE transports bicarbonate molecules to the cytoplasm in exchange for chloride. In the cytosol, CA II may convert bicarbonate to carbon dioxide, which would subsequently diffuse out through the plasma membrane, leading to neutralization of the internal pH. At the same time, the protons generated by the activity of CA IX

would contribute to the acidification of the extracellular space. The transport metabolon is illustrated in Figure 2.

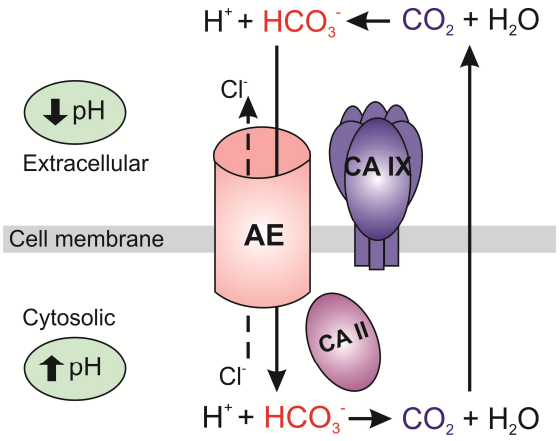

Figure 2. A proposed model of the role of CA IX in the pH regulation of hypoxic tumors. The transport metabolon is composed of an anion exchanger (AE) and CAs II and IX (refer to text for details). The figure is adapted from a prior study (Pastorekova and Zavada 2004).

In fact, there is experimental evidence regarding the functional involvement of CA IX in pH regulation. For example, CA IX was shown to contribute to the acidification of the extracellular microenvironment in hypoxic tumor cells (Svastova et al. 2004). CA IX also minimizes the intracellular pH gradient and increases the extracellular pH gradient in the core of three-dimensional tumor spheroids but not in isolated cells (Swietach et al. 2008). Furthermore, CA IX contributes to extracellular acidification and more alkaline resting intracellular pH in response to CO_2 load, thereby supporting cell survival during acidosis (Chiche et al. 2009). The regulation of CA IX by hypoxia may have a strong effect on cancer progression because an acidic extracellular microenvironment has been shown to contribute to the aggressiveness of tumors by promoting invasion and metastasis (Harris 2002). Accordingly, the silencing of *CA9* mRNA has been demonstrated to lead to a 40% reduction in tumor growth *in vivo*, whereas the silencing of both CA IX and CA XII results in an impressive 85% reduction in tumor growth (Chiche et al. 2009).

Another important function of CA IX is related to cell adhesion and intercellular communication. CA IX was first shown to mediate cell attachment to solid support, and this phenomenon was blocked by an M75 antibody that binds to the CA IX PG domain (Zavada et al. 2000). In addition, experiments with Madin-Darby canine

kidney (MDCK) epithelial cells have shown that CA IX can reduce E-cadherin-mediated cell-cell adhesion by interacting with β-catenin (Svastova et al. 2003). This function of CA IX is in agreement with the proposal that hypoxia can initiate tumor invasion via decreased E-cadherin-mediated cell-cell adhesion and suggests that CA IX may participate in this process.

The third role of CA IX is its contribution to cell proliferation and differentiation, which was revealed by the generation of CA IX knockout mice and is reviewed in detail in a previous section.

Finally, CA IX has been implicated in cell signaling (Dorai et al. 2005). In renal carcinoma cells, the tyrosine residue in the intracellular tail of CA IX can be phosphorylated in an EGF-dependent manner, thereby leading to interaction with the regulatory subunit of phosphatidylinositol 3-kinase (PI3K). This kinase can subsequently contribute to the activation of the serine/threonine protein kinase Akt and, thereby, to cancer progression.

2.3.6 Membrane-bound isozyme XII

2.3.6.1 General aspects

CA XII was identified a few years after CA IX in two independent studies. CA XII was first identified in a human RCC by serological expression screening with autologous antibodies (Tureci et al. 1998). In this study, *CA12* mRNA was shown to be overexpressed in approximately 10% of RCC patients. Nearly simultaneously, CA XII was cloned as a novel target of von Hippel Lindau protein (pVHL) using RNA differential display (Ivanov et al. 1998). It was also demonstrated that *CA12* expression is strongly inhibited by wild-type pVHL in RCC cell lines, suggesting that it is regulated in a similar manner as *CA9*.

CA XII is expressed as a 354-amino acid protein consisting of a 29-amino acid signal peptide, a 261-amino acid CA domain, a 9-amino acid juxtamembrane segment, a 26-amino acid transmembrane domain, and a 29-amino acid cytoplasmic tail. The molecular weight of human CA XII expressed in COS-7 cells is 43-44 kDa and is reduced to 39 kDa following PNGase treatment, indicating that CA XII has two N-linked glycosylations. (Tureci et al. 1998)

The catalytic activity of recombinant human CA XII in Chinese hamster ovary (CHO) cells was shown to be similar to that of the high-activity human membrane-associated CA IV (Ulmasov et al. 2000). The crystal structure of the extracellular domain of CA XII produced in *E. coli* revealed that the active site cavity is similar to those of CA II and IV (Whittington et al. 2001). It was also demonstrated that CA XII contains one intramolecular disulfide bond and forms dimers. Moreover, the transmembrane domain of CA XII was shown to contain GXXXG and GXXXS motifs that are considered to contribute to this dimerization.

2.3.6.2 Expression in normal tissues

In contrast to CA IX, CA XII has been detected in several normal tissues (Ivanov et al. 2001). Initially, *CA9* mRNA was observed to be expressed in the normal adult kidney, pancreas, colon, prostate, ovary, testis, lung, and brain (Ivanov et al. 1998, Tureci et al. 1998). In addition to the human expression pattern, CA XII protein expression has also been examined in rodents.

In humans, CA XII expression is observed on the epithelial cells of the endometrium where it is present on the basolateral membrane (Karhumaa et al. 2000). It is possible that CA XII participates in the reproductive functions of the uterus by contributing to bicarbonate production. Additionally, CA XII may affect the morphological changes in the uterus that occur during the menstrual cycle. CA XII is also expressed on the basolateral membrane of the epithelial cells in the male efferent ducts (Karhumaa et al. 2001a).

In the human gut, CA XII is expressed in all segments of the large intestine but is absent from the small intestine (Kivela et al. 2000a). Staining is detected on the basolateral plasma membrane of the enterocytes with the reaction being most intense in the surface epithelial cuff region. Thus, CA XII may play a role in the net acidification and concentration of the extracellular fluid.

In human renal tissues, CA XII is highly expressed in the basolateral plasma membrane of the epithelial cells in the thick ascending limb of Henle, the distal convoluted tubules, and in the principal cells of the collecting ducts (Parkkila et al. 2000). A weak basolateral signal was also observed in the epithelium of the proximal convoluted tubules. Additionally, CA XII expression has been

demonstrated in the pancreatic epithelium where it is present on the basolateral plasma membrane of acinar and ductal cells (Kivela et al. 2000b). CA XII is also weakly expressed in the gastric mucosa (Leppilampi et al. 2003) and in the eye where the expression has been shown to increase in the non-pigmented ciliary epithelial cells of patients with glaucoma (Liao et al. 2003).

In mice and rats, CA XII is expressed in the kidney (Kyllonen et al. 2003). In the mouse kidney, CA XII is present in the proximal tubules and in the intercalated cells of the collecting ducts. Positive staining for CA XII is restricted to the basolateral plasma membrane, while the luminal brush border membrane remains negative. This staining pattern is echoed in the rat kidney; however, the expression intensity is weaker in the proximal tubules.

CA XII expression has also been demonstrated in other mouse tissues (Halmi et al. 2004). While CA XII is not expressed in the stomach, duodenum or jejunum, there is a faint staining signal in ileal enterocytes. The staining reaction is much more intense in the colon and rectum. Similar to expression in the human large intestine, the strongest expression in mice is observed in the surface epithelial cuff region. In the same study, weak staining was also detected in developing sperm cells. Furthermore, CA XII expression has been observed in the epithelial cells of the mouse endometrium with the deeper endometrial glands stained most intensely (Hynninen et al. 2004). In rats, CA XII was detected in the epididymis (Hermo et al. 2005). The expression is most intense in the corpus and proximal cauda regions where CA XII is observed on the basolateral plasma membranes of the principal cells.

2.3.6.3 Expression in neoplastic tissues

CA XII expression has been observed in various cancers (Ivanov et al. 2001). A characteristic feature of CA XII expression is that it generally becomes stronger or more widespread in tumors compared to the corresponding normal tissue. Moreover, CA XII expression may indicate a poor or favorable prognosis depending on the type of cancer.

In addition to the normal human kidney, CA XII expression has been reported in most clear-cell carcinomas and oncocytomas (Parkkila et al. 2000). In clear-cell

carcinomas, CA XII expression shows a correlational trend with histological grade, being slightly weaker in well-differentiated carcinomas. However, the difference does not reach statistical significance. In colorectal tumors, CA XII expression clearly differs from that of normal tissue (Kivela et al. 2000a). The most obvious change is observed in the deep parts of the adenomatous mucosa where positive staining clearly increases with the grade of dysplasia. Additionally, the staining pattern of CA XII was observed to associate with the malignant behavior of the colorectal tumors. In brain tumors, the overexpression of CA XII has been detected in gliomas, hemangioblastomas and meningiomas (Proescholdt et al. 2005) and in diffuse astrocytomas where its expression is linked to a poorer prognosis (Haapasalo et al. 2008). CA XII is also expressed in pancreatic tumors, but no correlation has been detected between the staining extent or intensity and the differentiation grade (Kivela et al. 2000b). Similarly, CA XII expression is slightly increased in all pathological lesions when compared to staining in non-neoplastic gastric mucosa, but it does not exhibit any prominent changes in different tumor categories (Leppilampi et al. 2003).

CA XII expression has been detected in 75% of invasive breast carcinomas where it is associated with positive estrogen receptor (ER) status, negative epidermal growth factor receptor (EGFR) status, lower grade disease, lower relapse rate, and superior overall patient survival (Watson et al. 2003). Likewise, CA XII expression has been shown to correlate with favorable prognosis in non-small cell lung cancer (Ilie et al. 2011) and cervical cancer (Yoo et al. 2010).

It has been proposed that CA XII has a similar role in tumors as CA IX, i.e., to maintain a neutral intracellular pH and to acidify the extracellular environment. There is also experimental evidence to support this hypothesis because it has been shown that CA XII and CA IX contribute to cell survival in acidosis (Chiche et al. 2009).

2.4 Carbonic anhydrases in embryonic development

2.4.1 Carbonic anhydrases I, II, III and VI

In erythrocytes, human **CA I** is expressed in a developmental stage-specific manner. No CA I protein is detectable in fetal erythrocytes prior to birth; however, at approximately the time of normal delivery (40 weeks gestation), CA I begins to be expressed. (Brady et al. 1990)

CA II expression at both mRNA and protein levels has been examined in cultured mouse brain cells (De Vitry et al. 1989). Hypothalamic cells of embryonic day (ED) 12-14 were cultured for various periods. It was observed that *Car2* transcripts are detectable as early as ED 12-13, although CA II protein is not detectable until ED 17-18. At postnatal stages, the majority of glial cells express both *Car2* mRNA and protein. Additionally, CA II is present in the epithelial cells of the choroid plexus during human development (Catala 1997). It was observed that both CA activity and the isozyme CA II are present as early as the 9th week of gestation. Therefore, it appears that CA II may already contribute to the secretion of cerebrospinal fluid during fetal life. CA II has also been detected in the developing chicken retina at ED 5 when it is expressed in all retinal cells (Linser and Moscona 1981). As differentiation progresses, neurons cease expressing CA II; by ED 13, the isozyme is found only in Müller glia cells. During retinal maturation, CA II accumulates to a new high level that persists in the adult. Moreover, CA II expression has been demonstrated in the developing chicken lens where it appears to peak at ED 4.5 (Buono et al. 1992).

In the mouse embryonic and fetal heart, CA II expression has been observed from ED 13 to ED 16 (Vuillemin and Pexieder 1997). CA II is present in a unique region of the ventricular myocardium: the anterior and left lateral wall of the left ventricle. In addition, CA II expression has been observed in the developing mouse pancreas, kidney, and lung (Inada et al. 2006). In the pancreas, CA II is expressed in glucagon-positive cells at ED 15.5. At ED 18.5, CA II is faintly evident in the larger ducts and more strongly in some of the intercalated ducts. In both the mouse kidney and lung at ED 15.5, CA II is abundantly expressed in tubular or duct-like structures.

CA III has been detected in human fetal muscles at low levels at the 10th week of gestation but is not expressed in significant amounts until the 15th week of gestation (Jeffery et al. 1980). CA III levels gradually rise until the 25th week of gestation. At this point, there is a more dramatic increase in expression levels, which reach approximately half of the adult level by the time of birth. CA III is also expressed in the embryonic mouse skeletal muscle and notochord (Lyons et al. 1991). *Car3* mRNA is first detected in somite myotomes between 9.5 and 10.5 days post coitum (p.c.). At 15.5 days p.c., *Car3* begins to be restricted to developing slow muscle fibers. By two weeks postpartum (p.p.), *Car3* transcripts are detected primarily in slow muscle fibers. In the developing notochord, *Car3* is observed at an earlier stage (7.25 days p.c.). *Car3* is also expressed at a much higher level in the notochord than in the developing skeletal muscle. Furthermore, CA III expression has been observed in the extraocular muscles of human embryos (Carnegie stages 13-23) (Oguni et al. 1992). At Carnegie stage 20, CA III immunoreactivity appears in some fibers of the extraocular muscles. From stage 21 to stage 23, more CA III-immunoreactive fibers are observed.

CA II and III expression has been demonstrated in the rat liver during fetal and postnatal development (Laurila et al. 1989). It was shown that in the 12-day fetus, the early strong expression of CA I in hepatocytes is partially replaced by CA II and CA III during late prenatal development. In the 20-day fetus, CA III staining intensity is equal to that of a mature female rat. In males, the staining intensity in hepatocytes clearly increases during sexual maturation.

The expression of CA II and III has also been detected in bovine parotid glands during fetal development (Asari et al. 1994). In a 3-month-old fetus with a crown-rump length (CRL) of 17 cm, CA II expression in undifferentiated epithelial cells is observed, whereas immunostaining for CA III remains negative. At 26 cm CRL (4-5 months old), weak CA III expression is observed in large ductal epithelial cells. The accumulation of secreted granules in primary acinar cells is initially observed at this stage. In newborn calves, anti-CA II reactivity nearly disappears from most duct segments. It has been suggested that the time-dependent expression and distribution of the isozymes in parotid glands reflects the different biological functions of these closely structurally related isozymes.

CA VI expression has been observed in the ovine parotid and submandibular glands during fetal and postnatal development (Penschow et al. 1997). CA VI is

detectable by immunohistochemistry in parotid excretory ducts from 106 days of gestation (full-term gestation is 145 days), in striated ducts from 138 days and in acinar cells from 1 postnatal day. The duct cell content of CA VI declines as the acinar cell population increases. The production of CA VI by submandibular duct cells is initially detectable at 125 days gestation, and the acinar production is not observed until 29 postnatal days. With the development of the acinar tissues in the postnatal lamb, there is a dramatic increase (approximately 600-fold) in the level of CA VI expression in the parotid gland between days 7 and 59. The distribution of CA VI has also been examined in bovine parotid glands (Asari et al. 2000). In the 26 cm CRL fetus, which is estimated to be 4-5 months of fetal age, a few immature epithelial cells weakly express CA VI. These cells eventually differentiate into ductal and acinous epithelial cells of the ductal and terminal regions. In the 52 cm CRL fetus, which is estimated to be 7 months of fetal age, most acini (matured terminal tubules) and ductal epithelial cells intensely express CA VI. Both acini and ductal cells exhibit CA VI expression throughout prenatal development. Following birth, CA VI expression gradually begins to disappear from all small (intercalated) and large (interlobular) duct segments. Eventually, staining nearly completely disappears from the entire ductal cell region. Instead, there is strong immunoreactivity observed in acinar cells from 1 to 5 months of age, and the expression pattern is nearly indistinguishable from that of the adult.

2.5 Regulation of carbonic anhydrases

2.5.1 Carbonic anhydrase II

An interesting feature of the CA II gene in mammals is that it is expressed in nearly all tissues but only in a limited subset of cells. Thus, it is conceivable that a variety of mechanisms participate in the regulation of CA II expression. Nevertheless, the regulation of *CA2* gene has not been thoroughly described.

One example of where the regulation of CA II expression has been examined is the rodent reproductive system. In the rat prostate, CA II is regulated in a tissue-specific manner by androgens and estrogens (Harkonen and Vaananen 1988, Harkonen et al. 1991). Moreover, CA II is expressed in all regions of the rat

epididymis where it is also under androgen regulation (Kaunisto et al. 1999). In the rat uterus and liver, *CA2* is downregulated by estrogen in a time-dependent manner with the most pronounced effect detectable 72 h following treatment (Caldarelli et al. 2005).

CA II is one of the proteins expressed by hematopoietic precursors upon their differentiation towards an osteoclast phenotype. In fact, 1,25-dihydroxyvitamin D3 ($1,25(OH)_2D3$) has been shown to stimulate CA II expression in cell culture and in avian marrow cultures (Billecocq et al. 1990, Biskobing et al. 1994). Accordingly, a vitamin D response element (VDRE) consensus sequence has been identified in the chicken CA II promoter (Quelo et al. 1994). However, $1,25(OH)_2D3$ is also known to promote osteoclast formation. Thus, the question remains whether stimulation of CA II expression in marrow culture is due to direct upregulation of the CA II gene by $1,25(OH)_2D3$ or whether it arises during the $1,25(OH)_2D3$-induced program of osteoclastogenesis, which requires the presence of accessory stromal cells. Some studies support the first hypothesis (Billecocq et al. 1990, Biskobing et al. 1994), while others suggest that the ability of $1,25(OH)_2D3$ to stimulate early CA II expression depends on the presence of stromal cells (Biskobing et al. 1997). Furthermore, it has been shown in avian macrophage HD11 cells that the *CA2* promoter contains a retinoic acid response element (RARE) (Quelo and Jurdic 2000). This study also demonstrated that CA II expression is stimulated by *all-trans* retinoic acid when retinoic acid receptor α (RARα) is overexpressed. In this context, CA II expression is dependent on a RARE that is located in the distal portion of the promoter and is bound by the RARα homodimer.

Interestingly, CA II was found to be regulated by hypoxia in an *in vitro* angiogenesis model (Yoshiura et al. 2005). In this investigation, CA II expression in normal human vein endothelial cells was significantly upregulated when cells were cultured in acidic and hypoxic conditions, suggesting that CA II may play a role in tumor angiogenesis.

2.5.2 Carbonic anhydrase IX

The *CA9* promoter has been localized to a genomic sequence spanning 173 nucleotides upstream of the transcription initiation site. The promoter possesses five

regulatory regions designated protected regions 1-5 (PR1-5) where cis-acting regulatory proteins can bind (Kaluz et al. 1999). PR1 and PR2 were shown to be important elements for transcriptional activation, whereas PR4 functions as a silencer. PR5 has a high sequence identity to PR1 and also contributes to the transcriptional activity of *CA9*; however, its activation effect is not as strong (Kaluz et al. 2003). The SP1/SP3 (specificity protein 1/3) complex binds to the PR1 and PR5 elements, while the AP1 (activator protein 1) transcription factor binds to the PR2 region. The synergy achieved by the binding of the SP1 and AP1 transcription factors to the PR1 and PR2, respectively, is required for the basic transcriptional activation of *CA9* gene (Kaluzova et al. 2001, Kaluz et al. 2003). However, the most important regulatory element of the *CA9* promoter is between the SP1 binding site and the transcription start site at nucleotide position -10/-3. The nucleotide sequence of this element is 5'-TACGTGCA-3', which corresponds to a hypoxia response element (HRE) (Wykoff et al. 2000).

The HRE is recognized by hypoxia-inducible factor-1 (HIF-1), which is a transcription factor consisting of two subunits. The oxygen-sensitive α-subunit is cytosolic and is stable only in hypoxic conditions, whereas the β-subunit is constitutively expressed and is localized in the nucleus. Under normal oxygenation conditions, HIF prolyl-4-hydroxylases (PHDs) hydroxylate one or two conserved proline residues on HIF-1α. von Hippel-Lindau protein (pVHL) binds hydroxylated HIF-1α and targets it for degradation by the ubiquitin-proteasome system (Ivan et al. 2001, Jaakkola et al. 2001). In contrast, HIF-1α is not hydroxylated under hypoxic conditions because PHDs are inactive in the absence of dioxygen. Non-hydroxylated HIF-1α is not recognized by pVHL; instead, it is stabilized and accumulates in the cell. HIF-1α then translocates to the nucleus and dimerizes with the HIF-1β subunit to form the active transcription factor HIF. This factor subsequently activates the transcription of hypoxia-regulated genes, including those related to angiogenesis, glycolysis, cell proliferation and survival, metabolism and pH regulation (Maxwell et al. 2001, Semenza 2001). The VHL/HIF-pathway is shown in Figure 3.

The fact that CA IX is highly expressed in ccRCCs can be explained by its regulation by the VHL/HIF pathway. Germline mutations of the *VHL* gene in humans cause a hereditary cancer syndrome, termed von Hippel-Lindau disease, and one typical cancer among these patients is ccRCC (Kondo and Kaelin 2001).

Inactivating mutations in the *VHL* gene result in activation of the VHL/HIF pathway, leading to constitutive upregulation of HIF targets, including CA IX.

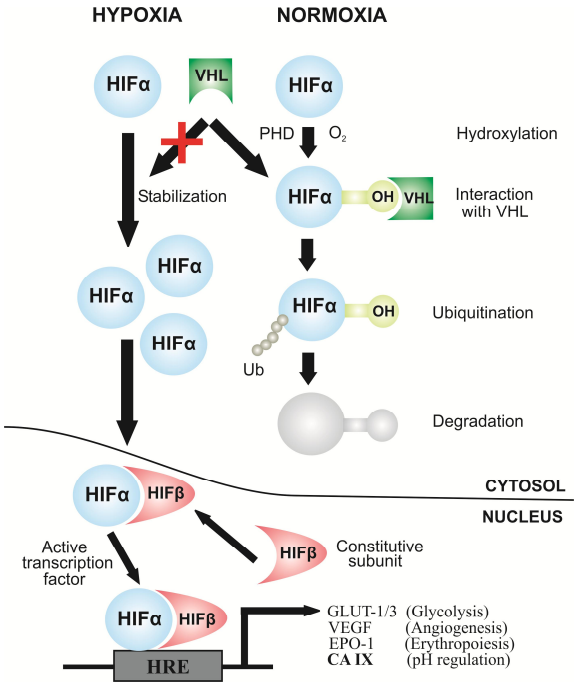

Figure 3. Illustration of the VHL/HIF-pathway. The mechanism is described in detail in the text. The figure is adapted from a prior study (Pastorekova and Pastorek 2004).

Interestingly, CA IX has also been shown to be regulated by a HIF-independent mechanism under hypoxia (van den Beucken et al. 2009). This regulation probably occurs via a PERK/eIF2α/ATF4-dependent pathway, which mediates the unfolded protein response (UPR). In response to stress, such as hypoxia, the UPR is activated in the following way: protein kinase RNA-like endoplasmic reticulum kinase (PERK) phosphorylates eukaryotic translation initiation factor eIF2α, which stimulates the translation of activating transcription factor 4 (ATF4) (Feldman et al. 2005, Koumenis and Wouters 2006). Furthermore, it appears that ATF4 directly binds to the *CA9* promoter and is required for transcriptional induction of *CA9* under hypoxia (van den Beucken et al. 2009). These data, therefore, indicate that the regulation of CA IX is achieved through independent activation of both the HIF and UPR hypoxia response.

In addition, CA IX expression can be modulated by methylation of CpG dinucleotides within the promoter region. Hypomethylation of the promoter has

been shown to induce *CA9* expression in RCC cell lines and in tumors (Cho et al. 2000, Cho et al. 2001). Moreover, it has been demonstrated that in RCCs with *VHL* mutations, hypomethylation of the promoter at CpG sites -74 and -6 relative to the transcriptional start site is required for *CA9* expression (Ashida et al. 2002). Methylation at nucleotide position -74 can also affect *CA9* expression in carcinoma cell lines other than RCCs. In these other cell lines, methylation appears to down-regulate the expression of *CA9* at high cell densities but not under hypoxic conditions or sparse cell densities (Jakubickova et al. 2005). According to a recent study, CA IX expression in gastric cancer is predominantly regulated by methylation of a CpG site at the -74 bp position rather than by hypoxia. Moreover, epigenetic alterations of *CA9* differ with tumor histologic type with the gene being significantly unmethylated in intestinal-type cancers and methylated in diffuse-type cancers (Nakamura et al. 2011).

CA IX expression in tumors is not confined to hypoxic regions, indicating that there may be other pathways that regulate its expression. In fact, it has been shown that CA IX expression is induced under mild hypoxia by high cell density. This regulation is mediated by PI3K signaling; however, minimal HIF-1 activity is also required (Kaluz et al. 2002). Furthermore, the mitogen-activated protein kinase (MAPK) pathway is involved in the regulation of CA IX expression via the control of the *CA9* promoter by both HIF-1-dependent and -independent signals (Kopacek et al. 2005). This pathway is also interconnected with the PI3K pathway and the action of the SP1 transcription factor.

CA IX has also been demonstrated to exist in two splice forms. The short splice variant of *CA9* does not contain exons 8-9 and codes for a truncated protein lacking the C-terminal portion of the catalytic domain (Barathova et al. 2008). This splice variant exhibits diminished catalytic activity and is intracellular or secreted. Its expression level is principally independent of hypoxia and tumor phenotype and can, therefore, give false-positive results in studies designed to assess the prognostic value of hypoxia- and tumor-related *CA9* gene expression. Furthermore, this splice variant can functionally interfere with full-length CA IX, especially under moderate hypoxia.

Finally, CA IX expression has also been examined at the post-translational level. The protein is notably stable with a half-life of approximately 38 h and persists in reoxygenated cells (Rafajova et al. 2004). However, the protein's abundance on the

cell surface is modulated by both constitutive and inducible shedding into the extracellular space, the latter effect being mediated by the metalloproteinase TACE/ADAM17 (Zatovicova et al. 2005). The clinical usefulness of serum CA IX levels in RCCs has also been investigated (Li et al. 2008). Mean serum CA IX levels were observed to be significantly higher in patients with metastatic disease compared to those with localized disease. Levels were also higher in patients with localized disease compared to those of healthy controls. Moreover, higher CA IX levels were significantly associated with postoperative recurrence.

2.5.3 Carbonic anhydrase XII

There is no thorough data concerning the transcriptional regulation of *CA12*. The position and architecture of the promoter and the identity of the critical regulatory factors remain to be elucidated. However, similar to CA IX, CA XII expression is induced by hypoxia (Wykoff et al. 2000, Ivanov et al. 2001). It is not known, however, whether the *CA12* gene is a direct target of HIF or, if so, where the relevant hypoxia-responsive element is located. The induction of CA XII by hypoxia is weaker compared to CA IX, and the region proximal to the transcriptional start site of *CA12* gene does not contain a HRE consensus site. It is, therefore, plausible that hypoxia regulates *CA12* expression via putative HRE elements located in the distant 5' upstream region. Similar to CA IX, CA XII expression is inhibited by wild-type VHL in RCC cell lines (Ivanov et al. 1998). However, the suppression of *CA12* requires both the central VHL domain involved in HIF-1α binding and the C-terminal elongin-binding domain, whereas only the latter is required for the negative regulation of *CA9*.

Furthermore, it has been shown that CA XII expression in breast tumors is associated with positive estrogen receptor α (ERα) status (Wykoff et al. 2001, Watson et al. 2003). It was also demonstrated that the *CA12* gene is regulated by estrogen via ERα binding to a distal, estrogen-responsive enhancer region in breast cancer cells (Barnett et al. 2008). Upon the addition of estradiol, ERα binds directly to the distal enhancer *in vivo*, resulting in the recruitment of RNA polymerase II and the steroid receptor coactivators SRC-2 and SRC-3 and inducing changes in histone acetylation.

A recent paper indicated that gene knockdown of CA XII in the human breast cancer cell line MDA-MB-231 results in decreased invasion and migration by interfering with the p38 MAPK pathway (Hsieh et al. 2010). CA XII knockdown was also shown to decrease the expression of matrix metalloproteinase (MMP)-2, MMP-9 and urokinase-type plasminogen activator (u-PA). CA XII knockdown, however, increased the expression of tissue inhibitor of metalloproteinases (TIMP)-2 and plasminogen activator inhibitor (PAI)-1. However, c-Jun N-terminal kinase (JNK), extracellular signal- regulated kinase (ERK) and the Akt pathways were not affected by CA XII knockdown. Moreover, the invasive and migratory abilities of CA XII-knockdown cells were restored by CA XII overexpression.

Similar to CA IX, CA XII exists in two splice forms. One splice variant of *CA12* mRNA lacks only a short segment coding for 11 amino acids and has been reported to be common in diffuse astrocytomas with poor prognosis (Haapasalo et al. 2008). However, the reasons for the association of this *CA12* splice variant with aggressive brain tumors and the biological role of the variant remain to be elucidated.

3. AIMS OF THE STUDY

The specific aims of this study were to

1) investigate the effects of certain hormones and growth factors on *CA9* and *CA12* transcript levels in human cancer-derived and normal cell lines.

2) examine CA IX and CA XII expression levels during mouse embryonic development.

3) elucidate the whole-genome gene expression changes that occur in response to CA IX deficiency in the murine gastric mucosa.

4) further investigate specific protein(s) that are either up- or downregulated in the stomachs of CA IX-deficient mice.

4. MATERIALS AND METHODS

4.1 Cell lines (**II, IV**)

A total of 16 pancreatic cancer cell lines were used in the study (**IV**). Thirteen of these lines (AsPC-1, BxPC-3, Capan-1, Capan-2, CFPAC-1, HPAC, HPAF-II, Hs 700T, Hs 766T, MIA PaCa-2, PANC-1, Su.86.86, and SW1990) were purchased from the American Type Culture Collection (ATCC, Manassas, VA, USA) and three (DanG, Hup-T3, and Hup-T4) were purchased from the German Collection of Microorganisms and Cell Cultures (Braunschweig, Germany). A panel of 21 breast cancer cell lines (BT-474, CAMA-1, DU4475, HCC38, HCC1419, HCC1954, MCF7, MDA-MB-134-VI, MDA-MB-231, MDA-MB-361, MDA-MB-415, MDA-MB-436, MDA-MB-453, SK-BR-3, T-47D, UACC-732, UACC-812, UACC-893, UACC-3133, ZR-75-1, and ZR-75-30) were obtained from the ATCC (**IV**). The Caki-1 and A-498 human RCC lines and HepG2 human hepatocellular carcinoma cell line were also obtained from the ATCC (**II**). The U373 human glioblastoma astrocytoma cell line (**II**, **IV**) and normal human umbilical vein endothelial cell (HUVEC) line (**II**) were purchased from the European Collection of Cell Cultures. The HeLa human cervical carcinoma cell line (**II**, **IV**) and MCF-7 (**II**) human breast adenocarcinoma cell line were from the laboratory of Professor Jorma Isola (Institute of Biomedical Technology, University of Tampere, Tampere, Finland). All of the cell lines were grown under recommended culture conditions.

4.2 Protein expression analyses

4.2.1 Antibodies (**I, IV**)

The production of polyclonal rabbit antibodies against mouse CA IX and CA XII was previously described by Ortova Gut et al. (Ortova Gut et al. 2002) and Kyllonen

et al. (Kyllonen et al. 2003), respectively (**I**). The M75 monoclonal antibody specific for the PG region of human CA IX has also been previously described (Pastorekova et al. 1992) (**IV**). Rabbit anti-human NCCRP1 serum against the purified full-length NCCRP1 was obtained from Innovagen AB (Lund, Sweden) (**IV**).

4.2.2 Immunohistochemistry (**I**)

CA IX and CA XII expression during mouse embryonic development was examined by immunohistochemical staining. Mouse embryos were obtained by mating male and female NMRI mice. The procedures were approved by the animal care committees of Helsinki University and Tampere University. To determine a time point, noon of the day on which the copulation plug was found was considered to be 0.5 days p.c. Embryos of the following days p.c. were obtained: 7.5 (n=2), 11.5 (n=3), 12.5 (n=4) and 13.5 (n=2). Embryos with or without extraembryonic tissues were briefly washed with PBS, fixed with 4% paraformaldehyde and embedded in paraffin. Sections were cut at 5-8 μm and placed on SuperFrost® Plus microscope slides (Menzel; Braunschweig, Germany). Tissue samples from the stomach, heart, brain, liver, kidney, and pancreas of an adult Balb/c mouse were obtained for control purposes. Immunoperoxidase staining was performed using an automated Lab Vision Autostainer 480 (ImmunoVision Technologies Co., Brisbane, CA, USA). As this automated immunostaining method produced some nonspecific labeling of the nuclei in the embryonic tissues, immunostaining was repeated using a less sensitive but more specific peroxidase-antiperoxidase staining protocol (manual PAP) to confirm the validity of the results.

The automated immunostaining was performed using Power Vision+™ Poly-HRP IHC Kit (ImmunoVision Technologies, Co.) reagents and included the following steps:

1) rinsing in wash buffer
2) treatment in 3% H_2O_2 in ddH_2O for 5 min and rinsing in wash buffer
3) blocking with Universal IHC Blocking/Diluent for 30 min and rinsing in wash buffer

4) incubation with the primary antibody (rabbit anti-mouse CA IX or XII) or normal rabbit serum diluted 1:2000 in Universal IHC Blocking/Diluent for 30 min
5) rinsing in wash buffer for 3 x 5 min
6) incubation in poly-HRP-conjugated anti-rabbit IgG for 30 min and rinsing in wash buffer for 3 x 5 min
7) incubation in DAB (3,3'-diaminobenzidine tetrahydrochloride) solution (one drop of DAB solution A and one drop of DAB solution B in 1 ml) ddH_2O for 6 min
8) rinsing with ddH_2O
9) $CuSO_4$ treatment for 5 min for signal enhancement
10) rinsing with ddH_2O

All the procedures were performed at room temperature. The sections were mounted in Entellan Neu (Merck; Darmstadt, Germany) and examined and photographed with a Zeiss Axioskop 40 microscope (Carl Zeiss; Göttingen, Germany).

Immunostaining using the PAP method included the following steps:

1) treatment with 3% H_2O_2 in methanol for 5 min and washing in PBS for 5 min
2) treatment with undiluted cow colostral whey (Biotop) for 30 min and rinsing in PBS
3) incubation with the primary antibody (rabbit anti-mouse CA IX or XII) diluted 1:100 in 1% bovine serum albumin (BSA) in PBS for 1 h and washing in PBS for 3 x 10 min
4) treatment with undiluted cow colostral whey for 30 min and rinsing in PBS
5) incubation with the secondary antibody (swine anti-rabbit IgG; DAKO, Glostrup, Denmark) diluted 1:100 in 1% BSA in PBS for 1 h and washing in PBS for 3 x 10 min
6) incubation with peroxidase-antiperoxidase complex (PAP-rabbit; DAKO) diluted 1:100 in PBS for 30 min and washing in PBS for 4 x 5 min
7) incubation for 2½ min in DAB solution (6 mg 3,3'-diaminobenzidine tetrahydrochloride; Sigma, St Louis, MO) in 10 ml PBS and 3.3 µl 30% H_2O_2

All incubations and washes were performed at room temperature. The sections were mounted in Entellan Neu (Merck; Darmstadt, Germany) and were examined and photographed using a Zeiss Axioskop 40 microscope.

4.2.3 Immunocytochemistry (**IV**)

Immunocytochemical analysis was used to investigate the subcellular localization of human NCCRP1 in HeLa cells. The HeLa cells were fixed with 4% (vol/vol) neutral-buffered formaldehyde for 30 min. The cells were subsequently rinsed with PBS and were subjected to immunofluorescence staining through the following steps:

1) pretreatment of the cells with 0.1% BSA in PBS (BSA-PBS) for 30 min
2) incubation for 1 h with rabbit NCCRP1 antiserum or normal rabbit serum diluted 1:100 in 0.1% BSA-PBS or mouse CA IX antiserum diluted 1:10 in 0.1% BSA-PBS
3) rinsing for 3 x 5 min with BSA-PBS
4) incubation for 1 h with 1:100 diluted Alexa Fluor 488 goat anti-rabbit IgG antibodies or Alexa Fluor 568 goat anti-mouse IgG antibodies (both of which were obtained from Molecular Probes, Eugene, Oregon, USA) in 0.1% BSA-PBS
5) rinsing twice for 5 min with BSA-PBS and once with PBS

All incubations and washes were performed in the presence of 0.05% saponin. Immunostained cells were analyzed and photographed using a Zeiss LSM 700 confocal laser scanning microscope.

4.3 mRNA expression analyses

4.3.1 Quantitative real-time PCR (QRT-PCR) (**II-IV**)

*4.3.1.1 Human cancer-derived and normal cell lines (**II**)*

The Caki-1, A-498 and HepG2, MCF-7, HeLa, U373, and HUVEC cell lines were used to study whether treatment with certain hormones and growth factors can affect *CA9* and *CA12* mRNA levels. When the cultured cells reached 80-90% confluence, they were trypsinized and plated in 6-well plates (except for the HUVEC cells, which were plated in 59 cm^2 dishes) at appropriate densities. After 24 h, the cells were changed to fresh serum-free medium with the tested hormones and growth factors. Serum-free medium was added to two control wells/dishes. The cells were incubated for 24 h in the presence of different hormones or growth factors. The treatments were performed using recombinant human growth hormone (400 ng/ml), hydrocortisone (10 μM), insulin (30 nM), tri-iodothyronine (T3; 10 nM), estradiol (E2; 2.5 μM), recombinant human insulin-like growth factor 1 (IGF-1; 50 ng/ml), recombinant human transforming growth factor-alpha (TGF-α; 10 ng/ml), recombinant human transforming growth factor-beta 1 (TGF-β1; 10 ng/ml), recombinant human epidermal growth factor (EGF; 10 ng/ml), and deferoxamine mesylate (200 μM), which is an iron chelator commonly used to activate the hypoxia regulatory pathway. Each cell line was treated with the same hormones or growth factors with the exception of the MCF-7 line, which was not treated with insulin because these cells require a high insulin concentration in their culture medium. The growth hormones IGF-1, TGF-β1, and EGF were purchased from ProSpec-Tany TechnoGene Ltd. (Rehovot, Israel). TGF-α was purchased from PromoCell GmbH (Heidelberg, Germany). The other chemicals were obtained from Sigma-Aldrich Finland Oy (Helsinki, Finland) and were diluted when necessary according to the manufacturers' instructions.

*4.3.1.2 Car9$^{-/-}$ mice tissue samples (**III**)*

QRT-PCR was performed to confirm the results of the microarray analysis performed in article **III**. The knockout mouse model for *CA9* used in this work was developed and characterized elsewhere (Ortova Gut et al. 2002). These *Car9*-deficient C57BL/6 mice were produced and maintained in the animal facility of the University of Oulu and then delivered to the animal facility of the University of Tampere. Permission for the use of the experimental mice was obtained from the Animal Care Committees of the Universities of Oulu and Tampere. Six *Car9*$^{-/-}$ mice (3 males and 3 females) and six wild-type control mice (3 males and 3 females) were kept under tightly controlled specific pathogen-free conditions and were fed identical diets. The mice were sacrificed at approximately 11 (SD = ±1.35) months of age. Tissue specimens from the body of the stomach were immediately collected, immersed in RNAlater solution (Ambion, Austin, TX, USA), and frozen at –80 ^{o}C.

*4.3.1.3 Murine tissue samples (**IV**)*

To study *Nccrp1* mRNA expression in mouse tissues, 2-month-old C57BL/6 mice (3 males and 3 females) were used. These mice were maintained in the animal facility of the University of Oulu. Tissue specimens were taken from the following areas: parotid gland, submandibular gland, stomach, duodenum, jejunum, ileum, colon, lung, kidney, prostate, and testis. The tissue samples were immediately immersed in RNAlater solution (Ambion, Austin, TX, USA) and were frozen at –80 ^{o}C.

*4.3.1.4 HeLa cell line samples (**IV**)*

The effects of different treatments on *NCCRP1* transcript levels were examined in HeLa cells. When the cultured cells reached 80-90% confluency, they were trypsinized and plated in 58 cm^2 dishes at a density of 1 million cells per dish. After 24 h, the medium was replaced with fresh medium containing one of the following chemicals: recombinant human transforming growth factor-alpha (TGF-α; 10 ng/ml), recombinant human transforming growth factor-beta 1 (TGF-β1; 10 ng/ml), recombinant human epidermal growth factor (EGF; 10 ng/ml), or deferoxamine

mesylate (200 μM). Untreated medium was added to a control dish. The chemicals were diluted when necessary according to the manufacturers' instructions. The cells were incubated for 72 h after which they were harvested.

*4.3.1.5 Human pancreatic and breast cancer cell line samples (**IV**)*

Human *CA9* and *NCCRP1* mRNA levels were screened in 16 pancreatic cancer cell lines and 21 breast cancer cell lines (see section 4.1).

*4.3.1.6 U373, HeLa and Su.86.86 cell line samples (**IV**)*

The *CA9* and *NCCRP1* genes were silenced using siRNAs in the human U373, HeLa and Su.86.86 cell lines. The efficacy of silencing was verified each time using QRT-PCR.

*4.3.1.7 RNA extraction and cDNA synthesis (**II-IV**)*

Total RNA from the cultured cells (excluding the human pancreatic and breast cancer cell lines) and murine tissue samples was extracted using the RNeasy RNA isolation kit (Qiagen, Valencia, USA) following the manufacturer's instructions. Residual DNA was removed from the samples using RNase-free DNase (Qiagen) (**II-IV**). For the human pancreatic and breast cancer cells, total RNA was isolated using the TRIzol reagent (Invitrogen, Carlsbad, CA) (**IV**). Total RNA was converted into first strand cDNA using a First Strand cDNA synthesis kit (Fermentas, Burlington, Canada) or a SuperScript III First-Strand Synthesis kit (Invitrogen) according to the manufacturer's recommended protocol.

*4.3.1.8 Quantitative real-time PCR (**II-IV**)*

QRT-PCR was performed using the LightCycler detection system (Roche, Rotkreuz, Switzerland). The majority of the primer sets employed in these analyses were designed using Primer3 (http://frodo.wi.mit.edu/primer3/), and primer specificity was verified using NCBI Blast (http://blast.ncbi.nlm.nih.gov/Blast.cgi). To avoid the

amplification of genomic DNA, the primers from each primer pair were targeted to different exons when possible. The human and mouse primer sequences used in these studies are given in Tables 2 and 3, respectively.

Each PCR reaction was performed in a total volume of 20 µl containing 1.0 µl (**II, IV**) or 0.5 µl (**III**) first strand cDNA, QuantiTect SYBR Green PCR Master Mix (Qiagen, Hilden, Germany) and 0.5 µM of each primer. The amplification and detection were performed as follows: following an initial 15 min activation step at 95 °C, amplification was performed using 45 repeats of a three-step cycling procedure of denaturation at 95 °C for 15 s, annealing at a temperature determined according to the T_m for each primer pair for 20 s, and elongation at 72 °C for 15 s (the ramp rate was 20 °C/s for all the steps). A final cooling step was added following the amplification cycles. A melting curve analysis was always performed following the amplification to confirm the specificity of the PCR reaction.

To quantify the target transcript levels, a standard curve was established for each gene using fivefold serial dilutions of known concentrations of purified PCR products generated with the same primer pairs. In most cases, the cDNA sample was tested in triplicate. Using the standard curve method, the crossing point (Cp) values were transformed by the LightCycler software into copy numbers. In the case of triplicate samples, the expression value for each sample was the mean of the copy numbers of the sample's replicates. Expression values were normalized against one (**IV**), two (**II**) or three (**III**) housekeeping genes. When several housekeeping genes were employed, the geometric mean of these genes was used as an accurate normalization factor for gene expression levels.

Table 2. Human primer sequences used for QRT-PCR analyses in original papers **II** and **IV**.

Gene	Direction	Sequence (5'-3')	GenBank number	Original paper
B2M	F	GTATGCCTGCCGTGTGAA	NM_004048	II
	R	CTCCATGATGCTGCTTAC		
CA9[a]	F	GGAAGGCTCAGAGACTCA	NM_001216	II
	R	CTTAGCACTCAGCATCAC		
CA9[b]	F	ATGAGAAGGCAGCACAGAAG	NM_001216	IV
	R	TAATGAGCAGGACAGGACAG		
CA12	F	CTGCCAGCAACAAGTCAG	NM_001218	II
	R	ATATTCAGCGGTCCTCTC		
GAPDH	F	TGCACCACCAACTGCTTAGC	NM_002046	IV
	R	GGCATGGACTGTGGTCATGAG		
HIF-1α	F	TCACCTGAGCCTAATAGTCC	NM_001530	II
	R	GCTAACATCTCCAAGTCTAA		
NCCRP1	F	TTCCGTGGCTGGTACATTAG	NM_001001414	IV
	R	ATGGCTGGTTGTTCGTCATC		
UBC	F	ATTTGGGTCGCGGTTCTTG	NM_021009	II, IV
	R	TGCCTTGACATTCTCGATGGT		

[a]The primers recognize only the full-length splice variant of *CA9*.

[b]The primers recognize both splice variants of *CA9*.

Table 3. Mouse primer sequences used for QRT-PCR analyses in original papers **III** and **IV**.

Gene	Direction	Sequence (5'-3')	GenBank number	Original paper
Actb	F	AGAGGGAAATCGTGCGTGAC	NM_007393	III, IV
	R	CAATAGTGATGACCTGGCCGT		
Adipoq	F	TCCTGCTTTGGTCCCTCCAC	NM_009605	III
	R	TCCTTTCTCTCCCTTCTCTCC		
Car3	F	GCTCTGCTAAGACCATCC	NM_007606	III
	R	ATTGGCGAAGTCGGTAGG		
Cela2a	F	TGATGTGAGCAGGGTAGTTGG	NM_007919	III
	R	CACTCGGTAGGTCTGATAGTTG		
Cela3b	F	TGCCTGTGGTGGACTATGAA	NM_026419	III
	R	CAGCCCAAGGAGGACACAA		
Cfd	F	AACCGGACAACCTGCAATC	NM_013459	III
	R	CCCACGTAACCACACCTTC		
Cpb1	F	GGTTTCCACGCAAGAGAG	NM_029706	III
	R	GTTGACCACAGGCAGAACA		
Cym	F	ATGAGCAGGAATGAGCAG	NM_001111143	III
	R	TGACAAGCCACCACTTCACC		
Dmbt1	F	GCACAAGTCCTCCATCATTC	NM_007769	III
	R	AGACAGAGCAGAGCCACAAC		
Egf	F	GCTCGGTGTTTGTGTCGTG	NM_010113	III
	R	CTGTCCCATCATCGTCTGG		
Hprt	F	AGCTACTGTAATGATCAGTCAACG	NM_013556	III
	R	AGAGGTCCTTTTCACCAGCA		
Il1rl1	F	ATTCTCTCCAGCCCTTCATC	NM_010743	III
	R	AAGCCCAAAGTCCCATTCTC		
Nccrp1	F	GCTGCATGTCTGGCTGTTAG	NM_001081115	IV
	R	ATGCGGTTCTTAGCCTTGTG		
Pkp4	F	GAACATAACCAAAGGCAGAGG	NM_026361	III
	R	GGTGGACAGAGAAGGGTGTG		
Pnlip	F	CCCGCTTTCTCCTCTACACC	NM_026925	III
	R	TCACACTCTCCACTCGGAAC		
Sdha	F	GCTTGCGAGCTGCATTTGG	NM_023281	III
	R	CATCTCCAGTTGTCCTCTTCCA		
Sftpd	F	CCAACAAGGAAGCAATCTGAC	NM_009160	III
	R	TCTCCCATCCCGTCCATCAC		
Slc9a3	F	TGACTGGCGTGGATTGTGTG	NM_001081060	III
	R	ACCAAGGACAGCAGGAAGG		

4.3.2 MediSapiens data (**IV**)

Human *NCCRP1* gene mRNA expression levels across a large number of tissues were retrieved from the IST database system developed by MediSapiens Ltd. The current version of the IST database (4.3) contains 20,218 human tissue or cell line samples analyzed using Affymetrix gene expression microarrays. The database was constructed and validated using methods similar to those described previously (Kilpinen et al. 2008, Autio et al. 2009) for the construction of GeneSapiens database. As the database contains fully integrated expression data both in terms of the annotation and numerical compatibility, it allows for analysis of the expression levels of 19,123 genes across 228 distinct tissues.

4.3.3 cDNA microarray (**III**)

4.3.3.1 Experimental procedure

Microarray analysis was performed to study the effect of CA IX deficiency on whole-genome gene expression in the mouse gastric mucosa. Microarray experiments were performed in the Finnish DNA Microarray Centre at the Turku Centre for Biotechnology. Total RNA was extracted from the stomachs of six C57BL/6 *Car9*$^{-/-}$ mice (3 males and 3 females) and six wild-type mice (3 males and 3 females), which were used as controls. All 12 samples were analyzed individually. Four hundred nanograms of total RNA from each sample was amplified using the Illumina® TotalPrep RNA Amplification kit (Ambion) as recommended by the manufacturer. The *in vitro* transcription reaction, which was conducted for 14.5 h, included labeling of the cRNA by biotinylation.

Labeled and amplified cRNAs (1.5 µg/array) were hybridized to Illumina's Sentrix® Mouse-6 Expression Bead Chips (Illumina, Inc., San Diego, CA) at 58 ºC for 18 h according to the manual for the Illumina® Whole-Genome Gene Expression with IntelliHyb Seal System. The arrays were washed and subsequently stained with 1 µg/ml cyanine3-streptavidin (Amersham Biosciences, Buckinghamshire, UK). The Illumina BeadArray™ Reader was used to scan the arrays according to the manufacturer's instructions. The numerical results were

extracted with Illumina's BeadStudio software without any normalization or background subtraction.

4.3.3.2 Data analysis

The array data were normalized with Chipster (v1.3.0) using the quantile normalization method. The data were filtered according to the SD of the probes. The percentage of data that did not pass through the filter was adjusted to 99.4%, indicating a SD value of nearly 3. Statistical analyses were subsequently performed using the empirical Bayes t-test for the comparison of the two groups. Finally, the probes were further filtered according to fold change with ±1.4 as the cut-off for up- and downregulated expression, respectively. This cut-off value has been proposed as an adequate level above which there is a high correlation between microarray and QRT-PCR data regardless of other factors, such as spot intensity and cycle threshold (Morey et al. 2006).

The functional annotation tool DAVID (Database for Annotation, Visualization and Integrated Discovery, http://david.abcc.ncifcrf.gov/) (Dennis et al. 2003) was used to identify enriched biological categories among the regulated genes when compared to all the genes present on Illumina's Sentrix Mouse-6 Expression Bead Chip. The annotation groupings analyzed were the following: Gene Ontology biological process and molecular functions; SwissProt comments; SwissProt Protein Information Resources Keywords; the Kyoto Encyclopedia of Genes and Genomes pathway; and the Biocarta pathway. Results were filtered to remove categories with EASE (Expression Analysis Systematic Explorer) scores greater than 0.05. Overlapping categories with the same gene members were removed to yield a single representative category.

4.4 siRNA-mediated gene silencing (**IV**)

Gene silencing using gene-specific siRNAs in cancer-derived cell lines was performed to study whether human *CA9* and *NCCRP1* directly regulate each other and to investigate the effect of *NCCRP1* silencing on cell growth. The *NCCRP1* and *CA9* genes were silenced using specific ON-TARGETplus SMARTpool small

interfering RNAs (siRNAs) (Thermo Fisher Scientific, Lafayette, CO). The catalogue numbers for the *NCCRP1* and *CA9* SMARTpools are L-032307-01-0005 and L-005244-00-0005, respectively. The U373 cells, HeLa and Su.86.86 cells were transfected with the siRNAs using INTERFERin™ reagent (PolyPlus-transfection, Illkirch, France) according to the manufacturer's instructions. The transfections were performed on 24-well plates with a desired cell density (25,000 cells per well for U373 and HeLa cells and 50,000 cells per well for Su.86.86 cells). A final siRNA concentration of 10 nM was used for *CA9* siRNA and 30 nM for *NCCRP1* siRNA. Parallel control experiments using a siRNA targeting the firefly *luciferase* (*PPYLUC*) gene were performed in an identical manner. The sequence of the *PPYLUC* siRNA was 5'-GAUUUCGAGUCGUCUUAAUTT-3'. All siRNA experiments were performed with three replicates and were repeated twice. The efficacy of the gene silencing was consistently verified using the QRT-PCR protocol that was described earlier (see section 4.3.1).

4.5 Cell growth analyses (**IV**)

For cell growth analyses, HeLa cells were transfected with *NCCRP1* SMARTpool siRNAs or *luciferase* control siRNA as described in the previous section with the exception that the cell density was 15,000 cells per well. The influence of *NCCRP1* silencing on cell growth was analyzed 48, 96, and 144 h following transfection.

From each well, 4x4 fields were photographed using an Olympus IX71 microscope with 100 x magnification. Quantitative analysis of the captured images was performed using a public domain image processing software, ImageJ (http://rsbweb.nih.gov/ij/), with a custom-made algorithm developed by Dr. Vilppu Tuominen. This algorithm first identifies the cellular area of the sample image at each time point and subsequently measures the relative change of the cellular area as a percentage of the well surface over the sample-specific time course.

4.6 Production of recombinant human NCCRP1 using a bacterial expression system (**IV**)

4.6.1 Construction of recombinant human NCCRP1

The full-length protein coding cDNA sequence for human NCCRP1 was obtained from the Mammalian Gene Collection, and the cDNA clone (IMAGE ID: 30348184) was purchased from Source BioScience LifeSciences (Cambridge, United Kingdom). The plasmid DNA was isolated from an overnight culture using the QIAprep Spin Miniprep Kit (Qiagen, Hilden, Germany). To generate the GST-NCCRP1 construct, the following primers were used: the forward primer sequence was 5´-CCG CGG ATC CAT GGA GGA GGT GCG TGA GGG A-3', and the reverse primer sequence was 5´-CGC CGT CGA CTC ACT CCC GGA GCT GCA CAG-3' with the restriction sites for BamHI and SalI underlined, respectively. The primers were ordered from Biomers (Ulm, Germany). The NCCRP1 cDNA amplification was performed using Phusion™ Hot Start High Fidelity DNA Polymerase (Finnzymes, Espoo, Finland). PCR was performed in a XP Thermal Cycler (Bioer Technology, Hangzhou, China). The program consisted of a single 98 °C denaturation step for 30 s followed by 35 cycles of denaturation at 98 °C for 10 s, annealing at 64 °C for 30 s and extension at 72 °C for 30 s. A final extension was performed at 72 °C for 5 min. The PCR product band was separated from the gel and dissolved using Illustra™ GFX PCR DNA and GEL Band Purification Kit (GE Healthcare Life Sciences, Buckinghamshire, UK). The purified PCR product and pGEX-4T-1 vector (Invitrogen, Carlsbad, CA) were digested at 37 °C for 2 h with BamHI and SalI restriction enzymes (New England Biolabs). The digested plasmid and NCCRP1 construct were purified and ligated overnight at 4 °C using T4 DNA ligase (New England Biolabs). Next, the pGEX-4T-1/GST-NCCRP1 construct was transformed into *E. coli* BL21(DE3)pLysS bacteria (Promega, Madison, WI, USA). Overnight cultures (5 ml) were grown from these colonies, and the plasmids were purified using a QIAprep Spin Miniprep Kit™ (Qiagen). Sequencing was performed to verify the validity of the NCCRP1 construct. The expression of pGEX-4T-1/GST-NCCRP1 constructs in *E. coli* yielded fusion proteins containing a thrombin protease site between the GST tag and NCCRP1. In addition, this vector construct

codes for additional Gly and Ser residues at the N-terminus of the recombinant protein.

4.6.2 Production and purification of recombinant human NCCRP1

A single colony of BL21(DE3)pLysS transformants was amplified through overnight cultivation in 5 ml LB medium containing 50 μg/ml ampicillin. The colonies were grown at room temperature and were shaken (200 rpm). Next, 500 ml of LB/amp medium was inoculated with the resultant growth. This culture was grown until the optical density (OD) at 600 nm reached 0.6. NCCRP1 protein expression was induced using isopropyl β-D-1-thiogalactopyranoside (IPTG) (Fermentas, Ontario, Canada) overnight at room temperature with a final concentration of 0.25 mM.

The cells were harvested by centrifugation (Sorvall RC 28S) at 5000 rpm for 5 min at room temperature. The cell pellet was suspended in 10 ml Tris-buffer containing 0.1M Tris-Cl, pH 8, 0.05% Triton X-100, 200 mg lysozyme, 200 U DNase (Roche, Penzberg, Germany), and the protease inhibitors phenylmethanesulfonylfluoride (0.2 mg; Sigma-Aldrich, Helsinki, Finland) and leupeptin (0.1 mg) (Santa Cruz, Heidelberg, Germany). After 30 min of incubation at room temperature, the cell suspension was kept on ice and was sonicated for 1 min. The suspension was clarified by centrifugation at 10,000 rpm for 30 min at 4 ^{o}C, and the clear supernatant was subsequently subjected to affinity purification using Glutathione Sepharose 4B medium (GE Healthcare, Buckinghamshire, UK). NCCRP1 recombinant protein was isolated under native conditions as described by the manufacturer. A site-specific thrombin (GE Healthcare) was used for specific cleavage of the GST. Cleavage was achieved by shaking the sample at room temperature overnight. Finally, the protein was eluted using the glutathione elution method (GE Healthcare) as recommended by the manufacturer. The size of the expressed NCCRP1 protein was determined under reducing conditions by SDS-PAGE analysis.

4.7 Mass spectrometry (**IV**)

Mass spectrometry analysis of recombinant human NCCRP1 was conducted in Prof. Janne Jänis' laboratory (Department of Chemistry, University of Eastern Finland) using a 4.7-T Fourier transform ion cyclotron resonance (FT-ICR) mass spectrometer (APEX-Qe; Bruker Daltonics, Billerica, MA, USA) equipped with an Apollo-II ion source and a mass-selective quadrupole front-end. This instrument has been described in detail elsewhere (Bootorabi et al. 2008). The protein samples were buffer-exchanged into a 10 mM ammonium acetate pH 6.9 buffer using PD-10 columns (Amersham Biosciences, Billingham, UK) and were directly electrosprayed at a flow rate of 1.5 µL/min. ESI-generated ions were externally accumulated for 1 s in a hexapole ion trap and transmitted to the ICR for trapping, excitation and detection. For each spectrum, one thousand co-added 512-kWord time-domain transients were recorded, zero-filled twice, Gaussian multiplied, and fast Fourier transformed. Magnitude calculations and external mass calibrations with respect to the ions of an ES Tuning Mix (Agilent Technologies, Santa Clara, CA, USA) were then performed. All the data were acquired and processed using Bruker XMASS 6.0.2 software. Mass spectra were further charge-deconvoluted using a standard deconvolution macro implemented in the XMASS software. A tryptic digest was obtained by dissolving a small amount of the protein precipitate in 100 µl of a 10 mM ammonium bicarbonate pH 8.5 buffer to which was added 15 µg of sequencing grade trypsin (Promega GmbH, Mannheim, Germany) in 15 µl of water. The digest sample was incubated at 37 ºC for 1.5 h after which no precipitate was observed, and the sample was directly analyzed without chromatographic separation. The obtained protein or peptide masses were matched against the protein sequence with the use of GPMAW 8.11 software, and tryptic peptide masses were further subjected to a database search using the Mascot search engine (www.matrixscience.com).

4.8 Bioinformatic analyses (**IV**)

Bioinformatic analyses were performed by Dr. Martti Tolvanen. Sequences were retrieved from Ensembl release 62 (www.ensembl.org) (Flicek et al. 2010), UniProt

(www.uniprot.org) (Jain et al. 2009), GenBank (www.ncbi.nlm.nih.gov/genbank/) (Benson et al. 2011) and RefSeq (www.ncbi.nlm.nih.gov/RefSeq/) (Pruitt et al. 2009). BLAST searches were performed via NCBI (blast.ncbi.nlm.nih.gov/Blast.cgi) (Altschul et al. 1997). Multiple sequence alignments were prepared using ClustalW (www.ebi.ac.uk/Tools/msa/clustalw2/) (Thompson et al. 1994) and Mafft (www.ebi.ac.uk/Tools/msa/mafft/) (Katoh et al. 2005) and were visualized with GeneDoc (www.nrbsc.org/gfx/genedoc/). Protein motifs were searched using InterProScan (www.ebi.ac.uk/Tools/pfa/iprscan/) (Hunter et al. 2009), and transmembrane domains were predicted with TMHMM (v. 2.0) (www.cbs.dtu.dk/services/TMHMM/) (Emanuelsson et al. 2007). Signal peptides and other target peptides were predicted using SignalP 3.0 with eukaryotic parameters (www.cbs.dtu.dk/services/SignalP/) (Emanuelsson et al. 2007) and TargetP 1.1. with non-plant parameters (www.cbs.dtu.dk/services/TargetP/) (Emanuelsson et al. 2007), respectively. Intrinsic protein disorder was predicted with DISpro (retire-me.ics.uci.edu/tools/proteomics/psss.html) (Cheng et al. 2005). Phylogenetic trees were prepared using MEGA4 software (www.megasoftware.net/) (Tamura et al. 2007) with maximum parsimony and the complete deletion option for gapped sites with 1000 bootstrap replicates. Molecular images were prepared with PyMol 0.99 (DeLano Scientific, South San Francisco, CA).

4.9 Statistical analyses (**III, IV**)

In article **III**, statistical analyses of the microarray data were performed using the empirical Bayes t-test for comparison of the group values for *Car9*$^{-/-}$ vs. wild-type mice. The p-values are shown in Appendix 1. For the QRT-PCR results in the same study, the Mann-Whitney test was used to evaluate differences between these two groups. For the cell growth analyses in article **IV**, the Mann-Whitney test was used to evaluate differences in growth between the *NCCRP1* SMARTpool siRNA-treated HeLa cells and the *luciferase* control siRNA-treated HeLa cells.

5. RESULTS

5.1 Influence of different treatments on *CA9, CA12* and *NCCRP1* mRNA levels in human cell lines (**II, IV**)

It has long been known that CA IX and CA XII are regulated by the HIF pathway. However, there is a lack of information concerning the other mechanisms through which these isozymes are regulated. Our aim was, therefore, to study other possible regulators of these enzymes in human cancer-derived and normal cell lines. *CA9* expression was detected in only two out of seven cell lines (Table 2 in **II**). The basal level of *CA9* expression was relatively high in the U373 human glioblastoma cell line (Figure 1A in **II**). Compared to the control sample, *CA9* expression increased 4.2-fold following deferoxamine mesylate treatment, which was used as a positive control to induce the hypoxia regulatory pathway (Table 2 and Figure 1A in **II**). Moreover, the IGF-1, TGF-α and EGF treatments markedly elevated *CA9* expression compared to the control sample (fold changes of 2.4, 2.6 and 2.2, respectively). TGF-β1 treatment caused a moderate increase in *CA9* levels (1.7-fold).

In HeLa cells, *CA9* expression was observed only when stimulated with deferoxamine mesylate (Table 2 in **II**). The change in expression was prominent. In the remaining lines, including MCF-7, Caki-1, A-498, HUVEC, and HepG2 cells, the basal *CA9* expression was below the detection limit (copy number <100) of the QRT-PCR analysis (Table 2 in **II**). In addition, none of the treatments induced *CA9* expression in these cell lines.

CA12 had a wider expression pattern compared to *CA9*; it was observed in the U373, MCF-7, Caki-1, A-498, and HUVEC cell lines (Table 3 in **II**). *CA12* was expressed in a similar manner to *CA9* in U373 cells (Table 3 and Figure 1B in **II**). Deferoxamine mesylate treatment notably increased *CA12* expression compared to the control sample (3.8-fold). Additionally, stimulation with TGF-α and EGF both caused a considerable increase in *CA12* expression (fold changes of 3.1 and 2.9,

respectively). Likewise, IGF-1 and TGF-β1 treatments elevated *CA12* levels twofold and 1.6-fold, respectively. Following growth hormone treatment, the levels of *CA12* slightly decreased (fold change of -1.6).

CA12 showed an exceptional expression profile in the human breast adenocarcinoma cell line MCF-7 (Table 3 in **II**). *CA12* transcription was markedly increased following TGF-β1 and EGF treatments (changes of 2.8- and 2.4-fold, respectively). Stimulation with estradiol also elevated *CA12* mRNA levels (1.9-fold). Interestingly, the hypoxia pathway was clearly not induced in this cell line by deferoxamine mesylate treatment. In contrast, deferoxamine mesylate treatment decreased *CA12* levels somewhat.

The Caki-1 and A-498 human renal carcinoma cell lines were selected for this study because the former produces wild-type VHL protein, and the latter represents a VHL-null mutant cell line. In Caki-1 cells, *CA12* expression was highest following deferoxamine mesylate treatment (10.2-fold) as expected (Table 3 in **II**). Additionally, the growth factors IGF-1, TGF-β1, and EGF elevated *CA12* levels moderately (changes of 1.5-, 1.7- and 1.8-fold, respectively). Moreover, estradiol increased *CA12* expression 1.5-fold. Similar to U373 cells, growth hormone treatment caused a decrease in *CA12* levels (change of -1.5-fold). In A-498 cells, *CA12* transcripts were present at high levels, and, as anticipated, deferoxamine mesylate treatment did not affect *CA12* expression (Table 3 in **II**). Again, *CA12* mRNA levels were elevated following growth factor treatments. The highest levels of induction were observed following stimulation with TGF-β1 and EGF (fold changes of 2.5 and 2.6, respectively), whereas TGF-α had a slightly weaker effect (2.2-fold). Furthermore, IGF-1 treatment caused a 1.7-fold increase in *CA12* mRNA levels. The addition of hydrocortisone moderately decreased *CA12* expression (change of -1.6-fold).

In the normal HUVEC cell line, the basal expression level of *CA12* was low. None of the treatments markedly increased *CA12* expression, whereas several treatments reduced its expression (Table 3 in **II**). Hydrocortisone and IGF-1 caused an approximately twofold decrease in *CA12* levels, while TGF-α and TGF-β1 treatments resulted in minor decreases (changes of -1.8- and -1.6-fold, respectively). In HeLa and HepG2 cells, *CA12* expression levels were below the detection limit of the QRT-PCR.

The effects of growth factors and deferoxamine mesylate on *NCCRP1* mRNA levels were examined in HeLa cells where the gene's basal level of expression was relatively high. None of the tested treatments had a notable influence on *NCCRP1* expression (Figure 11 in **IV**). Following deferoxamine mesylate treatment, the expression of *NCCRP1* decreased moderately (-1.4-fold). Likewise, stimulation with EGF modestly decreased *NCCRP1* transcript levels (-1.2-fold).

5.2 Roles of CA IX and CA XII during mouse organogenesis (**I**, **III**)

5.2.1 Expression of CA IX and CA XII during mouse embryonic development (**I**)

Immunochemical staining was used to investigate whether CA IX and CA XII are expressed in mouse embryos of different ages. A relatively wide distribution pattern was observed for both isozymes; however, the signal intensity was quite low or moderate at best.

E7.5 embryos, representing a gastrulation stage, were completely negative for both CA IX and CA XII (Figure 1 in **I**). The expression of both isozymes in the tested tissues during organogenesis is summarized in Tables 1 and 2, respectively, of original publication **I**. Both isozymes were present in the developing brain at all ages examined (Figure 2 in **I**). Moderate CA IX staining was observed in the nerve ganglia and choroid plexus. CA XII staining was most prominent in the choroid plexus at E12.5 and E13.5 when the developing choroid plexus generally becomes visible. CA IX was not detected in the urogenital system at E11.5, whereas a weak positive signal appeared at E12.5 (Figure 3 in **I**). It is notable that although CA XII is highly expressed in the adult mouse kidney, the embryonic kidney showed only a weak signal (Figure 3 in **I**). With respect to CA IX, the developing pancreas showed a moderate positive reaction at E12.5 (Figure 4 in **I**). CA XII showed weak immunostaining in the pancreas where only a few of the developing ducts were positive (Figure 4 in **I**). Weak staining for CA IX was observed in the stomach at all ages examined (Figure 5 in **I**). Additionally, the liver showed positive immunoreactions in scattered cells (Figure 5 in **I**). No CA XII staining was detected

in the stomach or liver at E11.5, while a weakly positive signal appeared at E12.5 (Figure 5 in **I**). The control stainings using normal rabbit serum in place of the anti-CA IX or anti-CA XII serum presented no positive signals.

5.2.2 Genome-wide mRNA expression profiling in the gastric mucosa of *Car9*$^{-/-}$ mice (**III**)

The generation of CA IX-deficient mice has revealed that CA IX contributes to cell proliferation in the gastric mucosa (Ortova Gut et al. 2002); however, the exact molecular mechanisms underlying the hyperplastic phenotype in these mice have not been previously examined. Our aim was, therefore, to investigate the global gene expression changes in the stomach of *Car9*$^{-/-}$ mice. Stomach RNA from 6 *Car9*$^{-/-}$ mice and 6 wild-type mice was subjected to microarray analysis. The results revealed 86 upregulated genes and 46 downregulated genes using a fold change cut-off of ±1.4 for up- and downregulated expression, respectively (Appendix 1). The fold changes ranged from 10.46 to –12.14. When using a cut-off value of ±2.5-fold, all the genes with significantly ($p<0.05$) altered expression are displayed, that is, 14 genes with induced expression and 21 genes with repressed expression (Tables 1 and 2 in **III**). The list of all of the differentially regulated genes was functionally annotated (Appendix 2), showing enrichment for genes related to hydrolase activity, developmental processes, cell differentiation, proteolysis, peptidase activity, structural molecule activity, and immune system process, among others. The functional annotation categories and the number of genes in each category are shown in Table 3 of original publication **III**.

Fourteen genes with notable fold change values were selected from the microarray results for validation. The selected genes contained representatives from different functional categories. The expression levels of these genes were analyzed by QRT-PCR using the same RNA samples as those used for the microarray. Thirteen (92.9%) of the 14 genes showed concordant results between microarray analysis and QRT-PCR, and 9 of these genes displayed statistically significant differences between the knockout and wild-type groups (Tables 1 and 2, Figure 1 in **III**). The sole discrepant result was *Pkp4*, which was upregulated according to the microarray and did not change according to the QRT-PCR (1.09-fold).

5.3 Characterization of recombinant human NCCRP1 (**IV**)

5.3.1 Bioinformatic analyses

One of the upregulated genes in the gastric mucosa of the CA IX-deficient mice was *Nccrp1*, which was selected for further bioinformatic analyses. An ortholog of *NCCRP1* was identified in 35 vertebrate genomes in Ensembl ortholog tables. Two orthologs were identified in fugu (*Takifugu rubripes*). We identified 21 protein sequences from 20 species to be at least 90% complete. Table 1 in **IV** shows the Ensembl gene identifiers for all identified orthologs with boldface font for the 20 species used for additional bioinformatic analyses.

The multiple sequence alignment of the 21 NCCRP1 protein sequences (Figure 1 in **IV)** revealed that the mouse and rat sequences in Ensembl are either 25 residues longer in the N-terminus, or the true start codon actually corresponds to M26. Mammalian sequences are characterized by a proline-rich N-terminal domain of approximately 60 residues, whereas fish sequences show shorter insertions approximately at columns 150 and 190 in the alignment. NCCRP1 from the frog *X. tropicalis* has short insertions similar to fish sequences, but the N-terminus is incomplete such that the presence of the N-terminal domain remains inconclusive.

The major portion of the N-terminal domain in mammals is predicted to be disordered. We ran human, mouse, and wallaby sequences through a prediction server, which predicted disordered domains of 70, 57, and 49 residues in length, respectively. These regions are shown underlined in Figure 1 of original publication **IV**, which displays the endpoint of the disordered regions to be close to the end of the additional sequence observed in mammals. There is an analogous Glu-and-Ala-rich N-terminal domain in the PEST domain of FBXO2 that also appears to be disordered. The N-terminal 47 residues show no electron density in the crystal structures of mouse FBXO2 (2E31, 2E32, 2E33) (Mizushima et al. 2007), and the disorder prediction is consistent with the 41 N-terminal residues predicted to be disordered.

The human paralogs of *NCCRP1*, as shown by the Ensembl comparative genomics tools and Blast searches, include the genes *FBXO2*, *FBXO6*, *FBXO17*, *FBXO27*, and *FBXO44*. The protein products of these five genes are components of

the E3 ubiquitin ligase complex and define a lectin subfamily within the ubiquitin ligases (Glenn et al. 2008). In humans, the genes *FBXO2*, *FBXO6*, and *FBXO44* are contiguous genes on chromosome 1 (at 11.70 to 11.74 Mb), whereas *FBXO17*, *FBXO27* and *NCCRP1* are on chromosome 19 (at 39.4 to 39.7 Mb). The protein sequence identity of NCCRP1 with the other five lectin-type FBXO proteins ranges from 31% to 36% in the last 180 residues, and the Blast E values range from 10^{-27} to 10^{-18}, clearly indicating that these proteins share homology and common ancestry.

In the available fish genomes, we can find orthologs only to *FBXO2*, *FBXO44*, and *NCCRP1*. Interestingly, the zebrafish genome carries a cluster of ten copies of *FBXO44* orthologs on chromosome 23.

By Interpro scan, all 21 protein sequences had domain matches to "Fbox-associated" (FBA, IPR007397) and "galactose-binding domain-like" (IPR008979) patterns in the ~200 C-terminal residues in fish and frog species and ~180 residues in mammalian species. Only the protein products of *NCCRP1* and the above five *FBXO* gene loci are annotated to contain an FBA domain (InterPro entry IPR007397), and no other human proteins were found in Blast searches when NCCRP1 or the FBA domain of FBXO2 were used as queries. The products of these five human *FBXO* genes also contain a cyclin-like F-box domain pattern (InterPro entry IPR001810) in the N-terminal region that spans 50 residues or less, but none of the NCCRP1 proteins matches this pattern.

Figure 2 in **IV** shows the alignment of human NCCRP1 with these five FBXO proteins and their phylogenetic tree. Although there was no match to the cyclin-like F-box domain pattern in the NCCRP1 sequence, 12 residues are conserved between human NCCRP1 and at least three other FBXO proteins within the F-box domain region (lines on top of the alignment in Figure 2 in **IV**). The primary differences in this region are found in three indels in which NCCRP1 has the shorter sequences and lacks many conserved residues, most notably the signature pattern CRxVC.

TMHMM predicts no transmembrane helices in any of the 21 examined NCCRP1 ortholog proteins. SignalP predicts no signal peptides in any of the proteins, and TargetP predicts a non-mitochondrial, non-secreted localization for all of these proteins. The predictions for mouse and rat sequences were run with alternative start sites: residue 1 (as for the Ensembl proteins) and residue 26 in keeping with the translation start site of other mammalian sequences. All of these

results indicate the absence of transmembrane domains and predict a cytoplasmic localization of NCCRP1 in all of the examined species.

5.3.2 Biochemical properties

The human *NCCRP1* cDNA was cloned into the expression vector pGEX-4T-1 and expressed as a fusion protein with GST. The recombinant NCCRP1 protein was first characterized using SDS-PAGE to determine its apparent molecular mass. Following purification by affinity chromatography and digestion with thrombin, NCCRP1 had an apparent mass of approximately 30 kDa in an SDS-PAGE gel (Figure 5, lane 1 in **IV**).

High-resolution ESI FT-ICR mass spectrometry was used to confirm the amino-acid sequence and disulfide arrangements in NCCRP1. Upon buffer exchange, the NCCRP1 protein sample precipitated slightly, and mass analyses, therefore, were conducted from both the precipitate and supernatant. A small amount of the precipitate was dissolved in 100 µl of 10 mM ammonium bicarbonate buffer pH 8.5, further diluted with a acetonitrile/water/acetic acid (49.5:49.5:1.0, v/v) mixture and directly analyzed with ESI FT-ICR mass spectrometry. Based on this analysis, the precipitate was found to contain a 27-kDa protein and a small 3-kDa peptide (Figure 7A in **IV**). A reasonable match was found between most abundant isotopic mass of the protein (27743.57 Da) and the NCCRP1 sequence. The fragment contained residues 31-275 (theoretically 27743.45 Da), indicating the presence of one intra-molecular disulfide bond (Cys158-Cys192) in the protein structure (see inset in Figure 7A in **IV**). The monoisotopic mass of the observed peptide P (3260.51 Da) was also matched against the NCCRP1 sequence and was found to correspond to the first 30 residues of NCCRP1 with an additional Gly-Ser in the N-terminus (theoretically 3260.52 Da). These amino acids are attributable to the pGEX-4T-1 expression vector construct (Figure 7B in **IV**).

To identify the produced protein further, a database search for the trypsin-digested protein was performed. An aliquot of 20 µl of the tryptic digest sample was further diluted with 150 µl of an acetonitrile/water/acetic acid (49.5:49.5:1.0, v/v) mixture and analyzed directly. The digestion resulted in 18 identified tryptic peptides within an average mass error of 6 ppm, covering 75% of the NCCRP1

sequence. A search against the SwissProt database gave an unambiguous hit for human NCCRP1 with a Mowse score of 370 (data not shown).

Mass spectra measured from the supernatant instead revealed the same 3-kDa peptide that was detected in the precipitate and a small amount of the NCCRP1 [31-275] fragment. In addition, small amounts of larger, currently unidentified 7-10 kDa polypeptides were detected (data not shown).

5.3.3 Subcellular localization

Given that NCCRP1 has been predicted to be a type II (Jaso-Friedmann et al. 1997) or type III (Evans et al. 1998) membrane receptor protein and because our bioinformatic analyses strongly contradicted this prediction, we wished to study the subcellular localization of NCCRP1 in HeLa cells using a novel NCCRP1 antibody. NCCRP1 was detected in the cytoplasm as shown in green in Figure 8A and B of original publication **IV**. Predictably, CA IX was expressed on the cell membrane (Figure 8A and C, red color in **IV**). Interestingly, these two proteins were only rarely co-expressed in the same cells (Figure 8A, arrows in **IV**). The control immunostaining using 30 μg of blocking NCCRP1 recombinant protein and anti-NCCRP1 serum together resulted in only faint staining, confirming the specificity of the antiserum (Figure 8D in **IV**). The second control staining using preimmune serum instead of the anti-NCCRP1 serum showed virtually no staining (Figure 8E in **IV**).

5.4 mRNA expression of *NCCRP1* (**IV**)

5.4.1 Expression of *Nccrp1* in mouse tissues

Nccrp1 expression in murine tissues was investigated using QRT-PCR. *Nccrp1* mRNA levels were highest in the kidney and were moderate in the stomach, colon, duodenum, and prostate (Figure 10 in **IV**). Transcripts were also present in other examined tissues, including the parotid and submandibular glands, lung, jejunum, ileum, and testis.

5.4.2 Expression of *NCCRP1* in human normal and cancer-derived tissues

The IST database system developed by MediSapiens Ltd. was used to obtain data regarding *NCCRP1* mRNA expression in human normal and cancer-derived tissues (Figure 9A and B, respectively in **IV**). The normal tissues with the strongest signal included the esophagus, oral cavity, skin, tongue, and male and female reproductive organs. The cancer-derived tissues with high *NCCRP1* expression included squamous cell carcinoma of the skin and cancers of the female reproductive organs.

5.4.3 Expression of *NCCRP1* in human pancreatic and breast cancer cell lines

Sixteen pancreatic cancer cell lines and 21 breast cancer cell lines were screened for *NCCRP1* expression using QRT-PCR. *NCCRP1* expression was highest in the Su.86.86, Hup-T4, and Hs700T pancreatic cancer cell lines and the MDA-MB-415, SK-BR-3, and BT-474 breast cancer cell lines (Figure 12 in **IV**). In other cell lines, *NCCRP1* was expressed at moderate or low levels. In addition, *CA9* expression was examined in the same cell lines and compared to the expression of *NCCRP1*. *CA9* gave the strongest signal in the DU4475 breast cancer cell line and the AsPC-1 pancreatic cancer cell line. Its expression was moderate in a few cell lines and was low in several cell lines. It should be noted that *NCCRP1* and *CA9* showed reciprocal expression patterns in some cell lines; i.e., when *NCCRP1* expression was high *CA9* expression was low or absent and vice versa.

5.5 Silencing of *NCCRP1* and *CA9* (**IV**)

5.5.1 The functional connection between *NCCRP1* and *CA9*

To examine whether *NCCRP1* is directly regulated by *CA9*, siRNA-mediated gene silencing was used. For this purpose, the *CA9* was silenced in the human glioblastoma cell line U373, which has a high basal level of *CA9* expression. Efficient downregulation of mRNA levels (up to 93% reduction compared to

luciferase control siRNA-treated cells) was achieved for the *CA9* gene with siRNA treatment. *CA9* silencing was monitored until 144 h after transfection and remained effective at that time point. *NCCRP1* expression was below the detection limit of QRT-PCR at basal levels in U373 cells and did not change following the silencing of *CA9*.

It was also investigated whether *NCCRP1* silencing has any effect on the expression level of *CA9*. *NCCRP1* mRNA silencing was efficient in both HeLa and Su.86.86 cell lines (up to 91% and 83% reduction when compared to luciferase control siRNA-treated cells, respectively). In HeLa cells, the silencing of *NCCRP1* was monitored until 144 h after transfection and remained effective. *CA9* mRNA levels were not affected by the silencing of *NCCRP1* (Figure 13 in **IV**). *CA9* expression increased until 120 h after transfection after which it decreased dramatically. In Su.86.86 cells, *CA9* expression also remained unchanged following the silencing of *NCCRP1* (data not shown).

5.5.2 Influence of *NCCRP1* silencing on cell growth

The influence of *NCCRP1* silencing on cell growth was examined in HeLa cells at 48, 96, and 144 h after transfection. The data analysis for this experiment was performed using ImageJ. *NCCRP1* silencing resulted in a statistically significant decrease in HeLa cell proliferation at every time point examined (Figure 14 in **IV**).

6. DISCUSSION

6.1 *CA9* and *CA12* are regulated by growth factors in human cell lines

The results of previous studies examining CA IX and CA XII regulation have been primarily confined to these proteins' association with the HIF-regulated hypoxia pathway. Thus, the aim of this study was to identify additional factors that regulate these isozymes. This investigation was performed by stimulating seven human cell lines with several hormones and growth factors.

In untreated cells, high *CA9* expression was detected only in the U373 cell line. Deferoxamine mesylate, which mimics the effect of hypoxia, notably increased *CA9* expression in this line. IGF-1, TGF-α, TGF-β1, and EGF treatments also markedly elevated *CA9* levels. Moreover, *CA9* levels were increased in HeLa cells following deferoxamine mesylate treatment. These results are in accordance with the previous finding that *CA9* is strongly regulated by hypoxia (Wykoff et al. 2000). Furthermore, it appears that *CA9* is under tight regulation of HIF-1α given that additional regulators are not evident. It is noteworthy that basal *CA9* expression was absent in all cell lines in which the treatment failed to induce *CA9* expression, which suggests that the factors necessary to drive *CA9* transcription are missing or non-functional in those cell lines.

Given that CA XII shows more widespread expression than CA IX in non-malignant tissues, it can be presumed that the gene expression of CA XII is regulated differently. In addition, no functional HRE has been reported for the *CA12* gene. These data imply that hypoxia may not be the most important regulator of *CA12* expression. Therefore, it is not surprising that several treatments in our study affected *CA12* expression. In fact, growth factor treatment increased *CA12* transcript levels in four cell lines, all of which were of cancerous origin. In contrast, deferoxamine mesylate treatment elevated *CA12* expression in only two cell lines. Interestingly, in the normal HUVEC cell line, growth factor treatments notably

decreased *CA12* expression levels. Therefore, it may be suggested that the induction of *CA12* expression by growth factors is specific to cancerous cells.

One exceptional line with respect to *CA12* regulation was the MCF-7 line, which is derived from human breast adenocarcinoma. First, deferoxamine mesylate did not elevate *CA12* expression but slightly decreased it. Second, in addition to TGF-β1 and EGF treatments, estradiol increased the levels of *CA12* ≈2-fold. Upregulation by estradiol was not observed in any other cell line except Caki-1, where it increased *CA12* expression 1.5-fold. It has been demonstrated elsewhere that *CA12* is strongly upregulated by estradiol via ERα in MCF-7 cells and that a distal estrogen-responsive enhancer region is involved in this induction (Barnett et al. 2008). In line with these observations, CA XII-positive invasive breast cancer tumors have been shown to be associated with a positive ERα status, low tumor grade and the absence of necrosis (Watson et al. 2003). Because CA XII appears to be a favorable prognostic marker in breast cancer, it could be expected that its expression is not regulated by hypoxia, which has been linked to poor prognosis. Similar to *CA9*, *CA12* expression was not induced in cell lines lacking *CA12* expression in control conditions.

Our data provides no mechanistic explanation regarding how the tested growth factors regulate *CA9* and *CA12*. However, it can be suggested that at least in the case of CA IX, the primary inductive effects observed in this study are mediated via stabilization of HIF-1α protein levels. This effect has been previously demonstrated following treatment with several growth factors under normoxia (Feldser et al. 1999, Zhong et al. 2000). The hypothesis that HIF-1α stabilization drives *CA9* expression may also hold for *CA12*, but it is possible that other unidentified regulatory pathways exist.

6.2 CA IX and CA XII expression during mouse organogenesis

6.2.1 CA IX and CA XII are expressed in several tissues during mouse embryonic development

CA IX and CA XII expression has been previously examined in human and rodent tissues, but no data concerning their expression during embryonic development have been published prior to this study. Therefore, our aim was to investigate whether these enzymes are present in developing mouse embryos.

It was found that both CA IX and CA XII are expressed in several mouse embryonic tissues. CA IX showed a relatively wide distribution pattern; moderate signals were observed in the brain, pancreas, and liver, and weak signals were detected in the urogenital system, lung, and stomach. The fact that CA IX expression was detected in the stomach at all mouse ages examined is in agreement with the discovery that CA IX is required for the normal development of the gastric mucosa (Ortova Gut et al. 2002). The expression pattern of CA XII was also relatively broad, although the staining was weak in most tissues. The positive tissues included the brain (most prominently in the choroid plexus), stomach, pancreas, liver, kidney, and lung.

Interestingly, both isozymes were present in embryonic tissues with adult counterparts that are negative for expression. Positive labeling for CA IX was observed in the heart and lung, which have been shown to be negative in the adult mouse. A weak CA XII signal was detected in several embryonic tissues, including the stomach, pancreas, and liver, which have been previously reported to be negative in adult mice (Halmi et al. 2004), and showed no immunoreaction in the present control stainings with adult tissues. Similar to CA IX, a positive signal was observed for CA XII in the embryonic heart. However, it must be taken into consideration that the adult heart tissue also exhibited a slight positive staining for both CA IX and CA XII based on an automated immunostaining method, even though the expression of both was considered negative (Halmi et al. 2004, Hilvo et al. 2004). Therefore, the signal in the heart is interpreted to be nonspecific.

In a recent study, CA IX and CA XII expression was immunohistochemically examined during human development (Liao et al. 2009). The examined cases

included the embryonic period (4 to 8 weeks), the fetal period (9 weeks to birth) and the postnatal period (one day to 8 years old). The expression pattern of CA IX was considerably extensive, even more so than that of CA XII. CA IX expression was also notably more extensive in comparison to its expression in adult tissues. The expression of these isozymes in mouse and human embryonic tissues is shown in Table 4.

Table 4. CA IX and CA XII expression in mouse and human tissues during embryonic development. Mouse data are from original publication I of this study and human data are derived from (Liao et al. 2009).*

Organ	**CA IX in mouse**	**CA IX in human**	**CA XII in mouse**	**CA XII in human**
Placenta	ND	X	ND	-
Skin	ND	X	ND	-
Body cavity	ND	X	ND	-
Nervous system	X	X	X	X
Nose	ND	X	ND	-
Oral cavity	ND	X	ND	X
Tongue	ND	-	ND	X
Salivary glands	ND	-	ND	X
Thymus	ND	X	ND	-
Heart	X	X	X	-
Lung	X	X	X	X
Esophagus	ND	X	ND	X
Stomach	X	X	X	X
Gastrointestinal canal	X	X	X	X
Pancreas	X	X	X	X
Liver	X	X	X	-
Urogenital system	X	X	X	X
Genital organ system	ND	X	ND	X
Skeletal system	ND	X	ND	-

*Abbreviations: signal is present (X), signal is absent (-), not done (ND).

Transient CA IX expression during human development was limited to immature tissues of mesodermal origin and the skin and ependymal cells (Liao et al. 2009). The only tissues that persistently expressed CA IX were the coelomic epithelium (mesothelium) and its remnants, the epithelium of the stomach and biliary tree, the glands and crypt cells of the duodenum and the more distal small intestine, and the

cells located at sites that were previously identified as harboring adult stem cells in (e.g., in the skin and large intestine). It was noted that during human development, nearly every CA IX-positive cell was derived from the mesoderm and was related to the embryonic coelom and mesenchyme. The only exceptions were the skin, the squamous mucosa, the upper gastrointestinal tract and the efferent ductules. It should also be noted that all of the CA IX positive tissues in our study also showed positive signals in corresponding human tissues.

CA XII expression in human embryonic tissues was restricted to cells involved in secretion and water absorption, such as the parietal cells of the stomach, acinar cells of the salivary glands and pancreas, the epithelium of the large intestine, and the renal tubules (Liao et al. 2009). In contrast to CA IX, nearly every tissue that expressed CA XII during embryonic development retained its expression after birth and throughout adult life. CA XII expression was also rather consistent between mouse and human tissues with the only exceptions being the heart and liver, which were positive for CA XII in our study but lacked this isozyme in human embryonic tissues. These data strongly suggest that both isozymes are required during mouse and human organogenesis. These isozymes probably have a role in the regulation of appropriate pH levels in various embryonic tissues.

It has been demonstrated that the environment of the mammalian embryo and the early fetus is hypoxic (Chen et al. 1999, Ramirez-Bergeron et al. 2004). As vascularization proceeds, hypoxic tissues become progressively normoxic. Thus, the co-localization of CA IX and CA XII with HIF-1α during human development was investigated by a prior study (Liao et al. 2009). The co-localization of CA IX and HIF-1α was limited to certain cell types in embryonic and early fetal tissues. These cells comprised the primitive mesenchyma or were involved in chondrogenesis and skin development. This finding implies that CA IX expression during development is partially regulated by hypoxia but that other mechanisms are also present. Alternatively, co-localization of CA XII with HIF-1α was not observed. Therefore, it appears that CA XII expression is not regulated by hypoxia during human embryonic development.

6.2.2 Transcriptional changes in the mouse gastric mucosa in response to CA IX deficiency

In the present study, we used cDNA microarray technology to identify genes and pathways that are either down- or upregulated in the gastric mucosa of CA IX-deficient mice. This method allows for simultaneous, genome-wide gene expression profiling. The validation of the microarray data was conducted using QRT-PCR. Notably good agreement between the two methods was observed; 13 (92.9%) out of 14 genes showed concordant results between microarray analysis and QRT-PCR. Generally, the fold change values obtained by microarray analysis were smaller than those detected by QRT-PCR. A similar phenomenon has previously been described (DeNardo et al. 2005) and probably reflects the fact that measurement by array analysis is much less quantitative than by QRT-PCR. Therefore, the fold changes observed using the array are likely an underestimation of the true differences in gene expression.

Car9 knockout mice have been previously described (Ortova Gut et al. 2002). These mice were reported to appear healthy and fertile, but closer histopathological analysis of their stomach specimens revealed hyperplastic changes in the gastric mucosa in comparison to their wild-type littermates. These phenotypic changes were accompanied by numerous large cysts. Although it has been observed that CA IX is probably involved in cell proliferation, no detailed data exists to explain this phenomenon. To this end, we performed a genome-wide cDNA microarray analysis to detect the specific transcriptomic responses to CA IX deficiency in the stomach, which is the tissue with the most abundant CA IX expression in normal mice (Hilvo et al. 2004).

According to our analysis, upregulation was more prevalent than downregulation among the differentially expressed genes. The functional categories most overrepresented among the disregulated genes were hydrolase activity, developmental processes, cell differentiation, proteolysis, peptidase activity, structural molecule activity, and immune system process. It should be noted that there was no overrepresented category containing genes involved in the regulation of cellular ion homeostasis. This finding is in agreement with the observation from the original study of *Car9* knockout mice that these mice had a normal gastric pH, systemic acid-base balance, and plasma electrolyte values (Ortova Gut et al. 2002).

However, CA IX has been suggested to participate in gastric acid secretion by contributing to the AE2-CA II-CA IX bicarbonate transport metabolon (Morgan et al. 2007). Based on the accumulated data to date, it appears that CA IX is dispensable in the gastric acid secretion process and is not critical for pH regulation in the stomach. Interestingly, one of the most highly upregulated genes observed in the present study was *SLC9A3/NHE3*, which contributes to the major proton extruding system driven by the inward sodium ion chemical gradient (He and Yun 2010). SLC9A3 is involved in pH regulation and acts by eliminating acids generated by active metabolism or by countering adverse environmental conditions. In the gastrointestinal tract, SLC9A3 is expressed in the apical membrane and recycling endosomes of the ileum, jejunum, colon, and stomach (Hoogerwerf et al. 1996). The strong upregulation of SLC9A3 in response to CA IX deficiency may indicate that CA IX is involved in the regulation of intracellular pH in the stomach. Thus, the high induction of SLC9A3 may be a compensatory mechanism for the lack of CA IX.

As expected, our study revealed that genes associated with developmental processes and cell differentiation were misregulated in the gastric mucosa of CA IX-deficient mice. This supports the previous notion that CA IX has a role in normal gastric morphogenesis and is required for proper cell lineage formation (Ortova Gut et al. 2002). Furthermore, a recent microarray study examining the transcriptomic responses to *Car9* knockout in the brain demonstrated that CA IX deficiency reduced the expression of genes belonging to the functional category "regulation of cell proliferation" (Pan et al. 2011b). These results, therefore, imply that CA IX may contribute to cell proliferation/differentiation in several tissues.

One of the overrepresented functional categories among the misregulated genes in *CA9*-deficient mice was "immune system process." This result is in accordance with the observation from an earlier study that reported gastric submucosal inflammation in the body region in a majority of C57BL/6 *Car9*$^{-/-}$ mice (Leppilampi et al. 2005a). The category "immune system process" included both up- and downregulated genes with several genes being highly induced. Among these were *deleted in malignant brain tumors 1* (*Dmbt1*), *surfactant associated protein D* (*Sftpd/SP-D*), and *interleukin 1 receptor-like 1, transcript variant 2* (*Il1rl1/ST2*). Moreover, CA IX deficiency significantly repressed the *bloom syndrome homolog (human)* gene (*Blm*), which has a role in the proliferation and survival of both

developing and mature T lymphocytes (Babbe et al. 2007). In addition, the conditional knockout of *Blm* has been shown to cause compromised B cell development and maintenance (Babbe et al. 2009). Based on these data, it is plausible that CA IX contributes to immune responses and may have a role in the development of the immune system.

An interesting finding was that several *small proline-rich proteins* (*Sprr*) were markedly upregulated in the *Car9* knockout mice stomach, including *Sprr1a*, *Sprr2d*, *Sprr2e*, *Sprr2i*, and *Sprr3*. It should be noted, however, that only the upregulation of *Sprr1a* was statistically significant. SPRR proteins were originally identified as markers for terminal squamous cell differentiation where they are precursors of the cornified envelope (Baden et al. 1987). It was later shown that SPRR proteins participate in the response to various stresses in many tissues without a stratified epithelium. Therefore, it appears that CA IX deficiency may create a stress condition in the gastric mucosa, requiring the induction of protective factors.

Interestingly, this study revealed several digestive enzymes among the most downregulated genes. Only a portion of these changes were statistically significant. This result may be a direct consequence of the CA IX deficiency or a secondary event in response to a disturbance in cell lineage in the hyperplastic stomach.

To summarize, our microarray analysis indicates that CA IX is indeed a multifunctional enzyme with roles extending far beyond the basic pH regulation function of CAs. In fact, the microarray study of the brain phenotype of *Car9* knockout mice demonstrated that these mice exhibited several abnormal behavioral features and reduced memory capacity (Pan et al. 2011b). Moreover, histological brain samples of old $Car9^{-/-}$ mice revealed vacuolar degeneration in all regions of the brain. According to the results, the functional changes preceded the microscopic alterations in the brain. Thus, it is likely that CA IX also functions in the brain, which would represent yet another role for this enzyme.

6.3 NCCRP1 is the sixth member of the lectin-type FBXO gene family

We took notice of the fact that *Nccrp1* was significantly overexpressed in the gastric mucosa of CA IX-deficient mice. Thus, one of the goals of this study was to

characterize NCCRP1, as it is a strikingly underexamined gene and is studied by only a few publications. Moreover, NCCRP1 has only been examined in fish species, and no information exists regarding its mammalian counterparts. Our bioinformatic analyses clearly showed that the closest human paralogs of *NCCRP1* are the lectin-type F-box-only (FBXO) gene family members *FBXO2*, *FBXO6*, *FBXO17*, *FBXO27*, and *FBXO44*. This result was surprising, given that NCCRP1 has been considered to function as an antigen-binding transmembrane receptor on fish nonspecific cytotoxic cells. For this reason, NCCRP1 was thought to participate in innate immune responses (Evans et al. 1998). Moreover, all of our bioinformatic predictions, which were conducted in several species, showed that NCCRP1 is localized in the cytoplasm. We also experimentally confirmed that human recombinant NCCRP1 indeed is localized in the cytoplasm in HeLa cells.

Given that the protein products of FBXO genes are components of the E3 ubiquitin ligase complex, it is reasonable to believe that NCCRP1 also functions as a protein-binding component in these complexes. The presumed role of FBXO proteins is to bind misfolded and retrotranslocated glycoproteins in the cytoplasm for ubiquitin conjugation. These bound proteins are then degraded in proteasomes (Glenn et al. 2008). Among the dozens of different F-box ubiquitin ligase subunits found in ubiquitin ligase complexes, the ability of the FBXO family members to bind glycoproteins is unique. This is due to the conserved "F-box associated" (FBA) or lectin domain, which is located in the C-terminus of the FBXO proteins and is not found in any other protein in the human proteome. It has been experimentally demonstrated that there are major functional differences among the FBXO proteins (Glenn et al. 2008). It appears that FBXO2 and FBXO6 regulate high mannose glycoproteins while FBXO6 and FBXO17 regulate sulfated glycoproteins. It is also thought that FBXO6, FBXO17, and FBXO27 may regulate certain complex glycoproteins. In a previous study (Glenn et al. 2008), FBXO44 failed to bind glycans. The authors speculated that this may be an actual phenomenom or that the effect was merely due to technical limitations, such as the possibility that their array did not contain the appropriate glycoprotein substrate. Taken together, the glycan-binding ability of NCCRP1 cannot be deduced based on our current studies but remains to be tested experimentally.

We also produced human recombinant NCCRP1 in *E. coli* and analyzed it using mass spectrometry. Surprisingly, mass spectrometry analysis indicated the presence

of a truncated protein in the NCCRP1 sample following purification and buffer exchange. This polypeptide corresponded to residues 31-275 of the full-length protein. However, the peptide corresponding to the first 30 residues was also detected, suggesting that the N-terminal portion had been cleaved following protein production, likely during sample treatment for mass spectrometry. In addition, protein precipitation was observed upon buffer-exchange, but it is not known whether this is related to the observed N-terminal cleavage or to alterations in the buffer conditions. The reason underlying the intrinsic structural weakness of the NCCRP1 protein is also unknown. However, our sequence analyses predict that the N-terminal proline-rich region of mammalian NCCRP1 proteins is disordered. This finding may partially explain the observation of N-terminal truncation. Mass analysis of the NCCRP1 [31-275] fragment also suggested the presence of an intra-molecular disulfide bond between Cys158 and Cys192.

The mRNA expression of *Nccrp1* has previously been examined in different fish species (Ishimoto et al. 2004, Cuesta et al. 2005, Sakata et al. 2005). Prior to the present study, however, there were no data regarding the distribution of *Nccrp1* in human or mouse tissues. In mice, *Nccrp1* showed a broad expression pattern and was detected in each of the eleven tested tissues. The strongest expression was detected in the kidney, and moderate expression was observed in the stomach, colon, duodenum, and prostate. In addition, *Nccrp1* was expressed at a lower level in the lung, jejunum, ileum, testis and in the parotid and submandibular glands. These data would place *Nccrp1* in the group of FBXO6, FBXO27, and FBXO44, which also are expressed relatively ubiquitously (Glenn et al. 2008). In fish, *Nccrp1* also exhibits a similar ubiquitous expression pattern; it is expressed equally in immune and in non-immune tissues, further contradicting the previous consensus that NCCRP1 is a protein involved in immune responses. Interestingly, the *NCCRP1* expression in normal human tissues was primarily detected in tissues consisting of squamous epithelium. These tissues included the esophagus, oral cavity, skin, and tongue. In human cancerous tissues, the *NCCRP1* expression pattern was strikingly similar; the highest expression was observed in squamous cell carcinomas of the skin, cervix, and vagina/vulva. Therefore, it appears that human and mouse *NCCRP1* transcripts are expressed in different sets of tissues, and that the expression pattern of human *NCCRP1* is clearly more restricted. It should be noted, however, that our repertoire of mouse tissues was not as extensive as the database

from which human data were obtained. Thus, it is possible that mouse transcripts are also strongly expressed in tissues with squamous epithelium.

In summary, this study provided a wealth of data suggesting that NCCRP1 is the sixth member of the lectin-type FBXO gene family. Accordingly, we propose that the gene name should be changed to FBXO50 (the number may change based on the decision of the Human Gene Nomenclature Committee).

6.4 *NCCRP1* is not directly regulated by *CA9*

One purpose of this study was to elucidate the possible connections between CA IX and NCCRP1 at both the protein and gene levels. Immunocytochemistry indicated that co-expression of NCCRP1 and CA IX in HeLa cells was rare. A similar phenomenon was observed when the expression levels of these two genes were compared at the mRNA level in an extensive panel of pancreatic and breast cancer cell lines; *NCCRP1* and *CA9* expression exhibited an inverse correlation in certain cell lines. Moreover, it was also revealed that *NCCRP1* transcript levels were moderately decreased following deferoxamine mesylate treatment, which is commonly used to induce a hypoxia-like response and strongly increases *CA9* levels. Based on these preliminary studies, it, therefore, appears that NCCRP1 and CA IX do not share common regulatory mechanisms with respect to their expression.

Interestingly, there are other genes that have been demonstrated to be downregulated by hypoxia. Low oxygen tension has been shown to decrease the levels of the angiogenesis inhibitor thrombospondin-1 in glioblastoma cells, suggesting that hypoxia may promote angiogenesis not only by stimulating the production of angiogenesis inducers but also by reducing the production of angiogenesis inhibitors (Tenan et al. 2000). In addition, hypoxia has been demonstrated to downregulate drug-metabolizing enzymes in human hepatoma cells (Legendre et al. 2009). Furthermore, hypoxia causes a decrease in levels of the CAD enzyme, which catalyzes the first three steps of *de novo* pyrimidine biosynthesis (Chen et al. 2005). DNA synthesis diminishes when cultured cells are exposed to hypoxia (Amellem et al. 1998), leading to cell-cycle arrest at the G1/S-phase. This effect may be due to the decrease in CAD enzyme levels. The exact mechanism by

which hypoxia downregulates *NCCRP1* in HeLa cells remains to be elucidated. However, this downregulation may cause a cell cycle arrest similar to that imparted by CAD. We arrive at this hypothesis because we also observed that silencing *NCCRP1* in the same HeLa cells led to a statistically significant decrease in cell growth. One hypothesis is that NCCRP1 controls the cell cycle by adjusting the degradation of proteins that control the cell cycle, such as cyclins. Cyclins are present only at particular times during the cell cycle; after they are no longer required, they are destroyed through ubiquitination and subsequent digestion by the proteasome (Nandi et al. 2006).

With respect to the regulation of *NCCRP1* and the involvement of *CA9*, it was shown in this research that *NCCRP1* is not directly regulated by *CA9*; when *CA9* was silenced, *NCCRP1* levels remained unaltered. Thus, it appears that the upregulation of *Nccrp1* observed in the stomachs of CA IX-deficient mice is a secondary event. One could speculate that CA IX deficiency leads to an accumulation of misfolded glycoproteins in the gastric mucosa and that NCCRP1 is required to target these proteins for degradation in proteasomes. This hypothesis appears to be reasonable because it is known that CA IX is essential for the development of proper cell lineage architecture in the gastric epithelium.

7. SUMMARY AND CONCLUSIONS

The primary conclusions drawn from this study are the following:

1) Treatment with the growth factors IGF-1, TGF-α, TGF-β1, and EGF increased *CA9* and *CA12* mRNA levels in cancer cell lines. In contrast to *CA9*, *CA12* expression does not appear to be primarily regulated by hypoxia.

2) CA IX and CA XII were present in several tissues of the developing mouse embryo during organogenesis. Both isozymes were expressed in certain embryonic tissues with adult counterparts that are negative for these proteins. Thus, it appears that CA IX and CA XII have important roles in the development of certain tissues.

3) *Car9* gene disruption alters the expression of several genes in the mouse gastric mucosa. The differentially expressed genes include those involved in developmental processes, cell differentiation, and immune responses. Additionally, the downregulation of several digestive enzymes was detected. These data indicate that CA IX is not essential for the pH regulation in the stomach but is required for many other physiological processes.

4) *NCCRP1* was significantly upregulated in the gastric mucosa of CA IX-deficient mice but is not directly regulated by *CA9*. Previously, NCCRP1 has been primarily examined in fish and was thought to be a transmembrane protein responsible for the cytolytic function of nonspecific cytotoxic cells. Our characterization of NCCRP1 demonstrated that it is an intracellular protein and that its mRNA is present in several tissues in human and mouse. These data are incompatible with an immune receptor function. Because the paralogs of NCCRP1 are FBXO proteins with protein products that are components of the E3 ubiquitin ligase complex, it appears evident that

NCCRP1 also functions as a protein-binding component in ubiquitin ligase complexes. Thus, the NCCRP1 gene name should be changed to FBXO50. Additionally, *NCCRP1* silencing led to a statistically significant decrease in the growth of HeLa cells, which is an effect that may be due to the ineffective degradation of misfolded glycoproteins.

ACKNOWLEDGEMENTS

This study was performed at the Institute of Biomedical Technology of the University of Tampere during the years 2007-2011. I thank the Tampere Graduate Program in Biomedicine and Biotechnology (TGPBB) for providing me with the graduate school position to carry out this work.

I owe my deepest gratitude to my supervisor, Professor Seppo Parkkila, for giving me the opportunity to perform my doctoral studies in his research group. I wish to thank Seppo for his impressive expertise and support. Furthermore, his endless optimism has had a great impression on me and played an important role in the completion of this work.

I wish to thank my thesis committee members, Professor Markku Kulomaa and Professor Tapio Visakorpi, for their guidance during my thesis project.

The official reviewers, Docent Peppi Karppinen and Professor Robert McKenna, are acknowledged for their valuable comments regarding this manuscript.

I thank all of my co-authors for their valuable help and contributions: Professor Markku Heikinheimo, Dr. Mika Hilvo, M.Sc. Alise Hyrskyluoto, Professor Jorma Isola, Professor Janne Jänis, Professor Anne Kallioniemi, Dr. Sami Kilpinen, B.Sc. Anna-Maria Lappalainen, B.Sc. Eeva-Helena Lappalainen, M.Sc. Eeva Laurila, Dr. Susanna Mannisto, Dr. Peiwen Pan, Professor Jaromir Pastorek, Professor Silvia Pastoreková, Dr. Alejandra Rodriguez Martinez, Professor William S. Sly, Dr. Martti Tolvanen, M.Sc. Vilppu Tuominen, Assistant Professor Jarkko Valjakka, and Professor Abdul Waheed.

I also wish to thank the Illumina team at the Finnish DNA Microarray Centre at the Turku Centre for Biotechnology, especially Reija Venho, for skillful technical assistance. I am also grateful to Anna-Maija Koivisto for statistical support. Janette Hinkka is acknowledged for her technical support regarding the cell culture experiments and for great discussions conducted while working in the laminar hood.

All of the past and present members of Seppo's lab who have worked with me, including Ale, Alise, Anna, Ashok, Eeva, Henna, Jukka, Leo, Maarit, Marianne,

Marisi, Martti, Mika, Mikaela, Peiwen, and Terhi, are warmly acknowledged for their friendship and support during these years. I give special thanks to Aulikki for her skillful technical assistance, friendship and great discussions on both science and life in general. Moreover, I wish to thank her for introducing me to the world of gluten-free pastry and for baking me her unforgettable delicacy. I also wish to thank the numerous people at IBT who have helped me with my work in any way.

I haven't forgotten how everything began. Therefore, thank you, "Lauma", Katri, Maria, Mika, Milla, Sanna, and Tiia. It was a great pleasure to learn science with you and to begin growing to be who we are today.

Olen kiitollinen vanhemmilleni heidän antamastaan mittaamattoman arvokkaasta tuesta; teihin olen voinut aina luottaa. I also wish to thank my relatives for their genuine interest in my work.

I wish to express my gratitude to my friends; some of you I have known since childhood. Thank you for cheering me up and for entertaining me during these years: Anu, Niia, Paula, Tanja H, and Tanja M. Your love and support have meant everything to me.

This work was financially supported by the TGPBB, DeZnIT EU project, Academy of Finland, Sigrid Juselius Foundation and Pirkanmaa Hospital District.

Tampere, August 2011

Heini Kallio

REFERENCES

Akisawa Y, Nishimori I, Taniuchi K, Okamoto N, Takeuchi T, Sonobe H, Ohtsuki Y and Onishi S (2003): Expression of carbonic anhydrase-related protein CA-RP VIII in non-small cell lung cancer. Virchows Arch 442:66-70.

Alterio V, Hilvo M, Di Fiore A, Supuran CT, Pan P, Parkkila S, Scaloni A, Pastorek J, Pastorekova S, Pedone C, Scozzafava A, Monti SM and De Simone G (2009): Crystal structure of the catalytic domain of the tumor-associated human carbonic anhydrase IX. Proc Natl Acad Sci U S A 106:16233-16238.

Altschul SF, Madden TL, Schaffer AA, Zhang J, Zhang Z, Miller W and Lipman DJ (1997): Gapped BLAST and PSI-BLAST: a new generation of protein database search programs. Nucleic Acids Res 25:3389-3402.

Amellem O, Sandvik JA, Stokke T and Pettersen EO (1998): The retinoblastoma protein-associated cell cycle arrest in S-phase under moderate hypoxia is disrupted in cells expressing HPV18 E7 oncoprotein. Br J Cancer 77:862-872.

Asari M, Miura K, Ichihara N, Nishita T and Amasaki H (2000): Distribution of carbonic anhydrase isozyme VI in the developing bovine parotid gland. Cells Tissues Organs 167:18-24.

Asari M, Miura K, Sasaki K, Igarashi SI, Kano Y and Nishita T (1994): Expression of carbonic anhydrase isozymes II and III in developing bovine parotid gland. Histochemistry 101:121-125.

Ashida S, Nishimori I, Tanimura M, Onishi S and Shuin T (2002): Effects of von Hippel-Lindau gene mutation and methylation status on expression of transmembrane carbonic anhydrases in renal cell carcinoma. J Cancer Res Clin Oncol 128:561-568.

Aspatwar A, Tolvanen ME and Parkkila S (2010): Phylogeny and expression of carbonic anhydrase-related proteins. BMC Mol Biol 11:25.

Autio R, Kilpinen S, Saarela M, Kallioniemi O, Hautaniemi S and Astola J (2009): Comparison of Affymetrix data normalization methods using 6,926 experiments across five array generations. BMC Bioinformatics 10 Suppl 1:S24.

Babbe H, Chester N, Leder P and Reizis B (2007): The Bloom's syndrome helicase is critical for development and function of the alphabeta T-cell lineage. Mol Cell Biol 27:1947-1959.

Babbe H, McMenamin J, Hobeika E, Wang J, Rodig SJ, Reth M and Leder P (2009): Genomic instability resulting from Blm deficiency compromises development, maintenance, and function of the B cell lineage. J Immunol 182:347-360.

Baden HP, Kubilus J, Phillips SB, Kvedar JC and Tahan SR (1987): A new class of soluble basic protein precursors of the cornified envelope of mammalian epidermis. Biochim Biophys Acta 925:63-73.

Barathova M, Takacova M, Holotnakova T, Gibadulinova A, Ohradanova A, Zatovicova M, Hulikova A, Kopacek J, Parkkila S, Supuran CT, Pastorekova S and Pastorek J (2008): Alternative splicing variant of the hypoxia marker carbonic anhydrase IX expressed independently of hypoxia and tumour phenotype. Br J Cancer 98:129-136.

Barnett DH, Sheng S, Charn TH, Waheed A, Sly WS, Lin CY, Liu ET and Katzenellenbogen BS (2008): Estrogen receptor regulation of carbonic anhydrase XII through a distal enhancer in breast cancer. Cancer Res 68:3505-3515.

Bartosova M, Parkkila S, Pohlodek K, Karttunen TJ, Galbavy S, Mucha V, Harris AL, Pastorek J and Pastorekova S (2002): Expression of carbonic anhydrase IX in breast is associated with malignant tissues and is related to overexpression of c-erbB2. J Pathol 197:314-321.

Becker HM, Klier M, Schuler C, McKenna R and Deitmer JW (2011): Intramolecular proton shuttle supports not only catalytic but also noncatalytic function of carbonic anhydrase II. Proc Natl Acad Sci U S A 108:3071-3076.

Bekku S, Mochizuki H, Yamamoto T, Ueno H, Takayama E and Tadakuma T (2000): Expression of carbonic anhydrase I or II and correlation to clinical aspects of colorectal cancer. Hepatogastroenterology 47:998-1001.

Benson DA, Karsch-Mizrachi I, Lipman DJ, Ostell J and Sayers EW (2011): GenBank. Nucleic Acids Res 39:D32-37.

Beuerle JR, Azzazy HM, Styba G, Duh SH and Christenson RH (2000): Characteristics of myoglobin, carbonic anhydrase III and the myoglobin/carbonic anhydrase III ratio in trauma, exercise, and myocardial infarction patients. Clin Chim Acta 294:115-128.

Billecocq A, Emanuel JR, Levenson R and Baron R (1990): 1 alpha,25-dihydroxyvitamin D3 regulates the expression of carbonic anhydrase II in nonerythroid avian bone marrow cells. Proc Natl Acad Sci U S A 87:6470-6474.

Biskobing DM, Fan D, Fan X and Rubin J (1997): Induction of carbonic anhydrase II expression in osteoclast progenitors requires physical contact with stromal cells. Endocrinology 138:4852-4857.

Biskobing DM, Nanes MS and Rubin J (1994): 1,25-Dihydroxyvitamin D3 and phorbol myristate acetate synergistically increase carbonic anhydrase-II expression in a human myelomonocytic cell line. Endocrinology 134:1493-1498.

Bootorabi F, Janis J, Smith E, Waheed A, Kukkurainen S, Hytonen V, Valjakka J, Supuran CT, Vullo D, Sly WS and Parkkila S (2010): Analysis of a shortened form of human carbonic anhydrase VII expressed in vitro compared to the full-length enzyme. Biochimie 92:1072-1080.

Bootorabi F, Janis J, Valjakka J, Isoniemi S, Vainiotalo P, Vullo D, Supuran CT, Waheed A, Sly WS, Niemela O and Parkkila S (2008): Modification of carbonic anhydrase II with acetaldehyde, the first metabolite of ethanol, leads to decreased enzyme activity. BMC Biochem 9:32.

Brady HJ, Edwards M, Linch DC, Knott L, Barlow JH and Butterworth PH (1990): Expression of the human carbonic anhydrase I gene is activated late in fetal erythroid development and regulated by stage-specific trans-acting factors. Br J Haematol 76:135-142.

Brady HJ, Lowe N, Sowden JC, Edwards M and Butterworth PH (1991): The human carbonic anhydrase I gene has two promoters with different tissue specificities. Biochem J 277 (Pt 3):903-905.

Brown D, Zhu XL and Sly WS (1990): Localization of membrane-associated carbonic anhydrase type IV in kidney epithelial cells. Proc Natl Acad Sci U S A 87:7457-7461.

Bui MH, Seligson D, Han KR, Pantuck AJ, Dorey FJ, Huang Y, Horvath S, Leibovich BC, Chopra S, Liao SY, Stanbridge E, Lerman MI, Palotie A, Figlin RA and Belldegrun AS (2003): Carbonic anhydrase IX is an independent predictor of survival in advanced renal clear cell carcinoma: implications for prognosis and therapy. Clin Cancer Res 9:802-811.

Buono RJ, Linser PJ, Cuthbertson RA and Piatigorsky J (1992): Molecular analyses of carbonic anhydrase-II expression and regulation in the developing chicken lens. Dev Dyn 194:33-42.

Caldarelli A, Diel P and Vollmer G (2005): Effect of phytoestrogens on gene expression of carbonic anhydrase II in rat uterus and liver. J Steroid Biochem Mol Biol 97:251-256.

Campbell AR, Andress DL and Swenson ER (1994): Identification and characterization of human neutrophil carbonic anhydrase. J Leukoc Biol 55:343-348.

Casey JR, Sly WS, Shah GN and Alvarez BV (2009): Bicarbonate homeostasis in excitable tissues: role of AE3 Cl-/HCO3- exchanger and carbonic anhydrase XIV interaction. Am J Physiol Cell Physiol 297:C1091-1102.

Catala M (1997): Carbonic anhydrase activity during development of the choroid plexus in the human fetus. Childs Nerv Syst 13:364-368.

Chegwidden WR and Carter ND (2000): Introduction to the carbonic anhydrases. In: The Carbonic Anhydrases: New Horizons, pp. 13-28. Eds. Chegwidden WR, Carter ND and Edwards YH, Birkhäuser Verlag, Basel.

Chegwidden WR, Dodgson SJ and Spencer IM (2000): The roles of carbonic anhydrase in metabolism, cell growth and cancer in animals. In: The Carbonic Anhydrases: New Horizons, pp. 343-363. Eds. Chegwidden WR, Carter ND and Edwards YH, Birkhäuser Verlag, Basel.

Chen EY, Fujinaga M and Giaccia AJ (1999): Hypoxic microenvironment within an embryo induces apoptosis and is essential for proper morphological development. Teratology 60:215-225.

Chen KF, Lai YY, Sun HS and Tsai SJ (2005): Transcriptional repression of human cad gene by hypoxia inducible factor-1alpha. Nucleic Acids Res 33:5190-5198.

Chen X, Tu C, LoGrasso PV, Laipis PJ and Silverman DN (1993): Interaction and influence of phenylalanine-198 and threonine-199 on catalysis by human carbonic anhydrase III. Biochemistry 32:7861-7865.

Cheng J, Sweredoski M and Baldi P (2005): Accurate Prediction of Protein Disordered Regions by Mining Protein Structure Data. Data Mining and Knowledge Discovery 11:213-222.

Chia SK, Wykoff CC, Watson PH, Han C, Leek RD, Pastorek J, Gatter KC, Ratcliffe P and Harris AL (2001): Prognostic significance of a novel hypoxia-regulated marker, carbonic anhydrase IX, in invasive breast carcinoma. J Clin Oncol 19:3660-3668.

Chiang WL, Chu SC, Yang SS, Li MC, Lai JC, Yang SF, Chiou HL and Hsieh YS (2002): The aberrant expression of cytosolic carbonic anhydrase and its clinical significance in human non-small cell lung cancer. Cancer Lett 188:199-205.

Chiche J, Ilc K, Laferriere J, Trottier E, Dayan F, Mazure NM, Brahimi-Horn MC and Pouyssegur J (2009): Hypoxia-inducible carbonic anhydrase IX and XII promote tumor cell growth by counteracting acidosis through the regulation of the intracellular pH. Cancer Res 69:358-368.

Cho M, Grabmaier K, Kitahori Y, Hiasa Y, Nakagawa Y, Uemura H, Hirao Y, Ohnishi T, Yoshikawa K and Ooesterwijk E (2000): Activation of the MN/CA9 gene is associated with hypomethylation in human renal cell carcinoma cell lines. Mol Carcinog 27:184-189.

Cho M, Uemura H, Kim SC, Kawada Y, Yoshida K, Hirao Y, Konishi N, Saga S and Yoshikawa K (2001): Hypomethylation of the MN/CA9 promoter and upregulated MN/CA9 expression in human renal cell carcinoma. Br J Cancer 85:563-567.

Christie KN, Thomson C, Xue L, Lucocq JM and Hopwood D (1997): Carbonic anhydrase isoenzymes I, II, III, and IV are present in human esophageal epithelium. J Histochem Cytochem 45:35-40.

Cox EH, McLendon GL, Morel FM, Lane TW, Prince RC, Pickering IJ and George GN (2000): The active site structure of Thalassiosira weissflogii carbonic anhydrase 1. Biochemistry 39:12128-12130.

Cuesta A, Esteban MA and Meseguer J (2005): Molecular characterization of the nonspecific cytotoxic cell receptor (NCCRP-1) demonstrates gilthead seabream NCC heterogeneity. Dev Comp Immunol 29:637-650.

Davenport HW (1939): Gastric carbonic anhydrase. J Physiol 97:32-43.

Davenport HW (1984): The early days of research on carbonic anhydrase. Ann N Y Acad Sci 429:4-9.

De Vitry F, Gomes D, Rataboul P, Dumas S, Hillion J, Catelon J, Delaunoy JP, Tixier-Vidal A and Dupouey P (1989): Expression of carbonic anhydrase II gene in early brain cells as revealed by in situ hybridization and immunohistochemistry. J Neurosci Res 22:120-129.

DeNardo DG, Kim HT, Hilsenbeck S, Cuba V, Tsimelzon A and Brown PH (2005): Global gene expression analysis of estrogen receptor transcription factor cross talk in breast cancer: identification of estrogen-induced/activator protein-1-dependent genes. Mol Endocrinol 19:362-378.

Dennis G, Jr., Sherman BT, Hosack DA, Yang J, Gao W, Lane HC and Lempicki RA (2003): DAVID: Database for Annotation, Visualization, and Integrated Discovery. Genome Biol 4:P3.

Di Fiore A, Monti SM, Hilvo M, Parkkila S, Romano V, Scaloni A, Pedone C, Scozzafava A, Supuran CT and De Simone G (2009): Crystal structure of human carbonic anhydrase XIII and its complex with the inhibitor acetazolamide. Proteins 74:164-175.

Dodgson SJ and Forster RE, 2nd (1986): Inhibition of CA V decreases glucose synthesis from pyruvate. Arch Biochem Biophys 251:198-204.

Dodgson SJ, Forster RE, 2nd, Sly WS and Tashian RE (1988): Carbonic anhydrase activity of intact carbonic anhydrase II-deficient human erythrocytes. J Appl Physiol 65:1472-1480.

Dodgson SJ, Forster RE, 2nd, Storey BT and Mela L (1980): Mitochondrial carbonic anhydrase. Proc Natl Acad Sci U S A 77:5562-5566.

Dorai T, Sawczuk IS, Pastorek J, Wiernik PH and Dutcher JP (2005): The role of carbonic anhydrase IX overexpression in kidney cancer. Eur J Cancer 41:2935-2947.

Earnhardt JN, Qian M, Tu C, Lakkis MM, Bergenhem NC, Laipis PJ, Tashian RE and Silverman DN (1998): The catalytic properties of murine carbonic anhydrase VII. Biochemistry 37:10837-10845.

Emanuelsson O, Brunak S, von Heijne G and Nielsen H (2007): Locating proteins in the cell using TargetP, SignalP and related tools. Nat Protoc 2:953-971.

Evans DL, Leary JH, 3rd and Jaso-Friedmann L (1998): Nonspecific cytotoxic cell receptor protein-1: a novel (predicted) type III membrane receptor on the teleost equivalent of natural killer cells recognizes conventional antigen. Cell Immunol 187:19-26.

Feldman DE, Chauhan V and Koong AC (2005): The unfolded protein response: a novel component of the hypoxic stress response in tumors. Mol Cancer Res 3:597-605.

Feldser D, Agani F, Iyer NV, Pak B, Ferreira G and Semenza GL (1999): Reciprocal positive regulation of hypoxia-inducible factor 1alpha and insulin-like growth factor 2. Cancer Res 59:3915-3918.

Fernley RT, Wright RD and Coghlan JP (1979): A novel carbonic anhydrase from the ovine parotid gland. FEBS Lett 105:299-302.

Fleming RE, Parkkila S, Parkkila AK, Rajaniemi H, Waheed A and Sly WS (1995): Carbonic anhydrase IV expression in rat and human gastrointestinal tract regional, cellular, and subcellular localization. J Clin Invest 96:2907-2913.

Flicek P, Aken BL, Ballester B, Beal K, Bragin E, Brent S, Chen Y, Clapham P, Coates G, Fairley S, Fitzgerald S, Fernandez-Banet J, Gordon L, Graf S, Haider S, Hammond M, Howe K, Jenkinson A, Johnson N, Kahari A, Keefe D, Keenan S, Kinsella R, Kokocinski F, Koscielny G, Kulesha E, Lawson D, Longden I, Massingham T, McLaren W, Megy K, Overduin B, Pritchard B, Rios D, Ruffier M, Schuster M, Slater G, Smedley D, Spudich G, Tang YA, Trevanion S, Vilella A, Vogel J, White S, Wilder SP, Zadissa A, Birney E, Cunningham F, Dunham I, Durbin R, Fernandez-Suarez XM, Herrero J, Hubbard TJ, Parker A, Proctor G, Smith J and Searle SM (2010): Ensembl's 10th year. Nucleic Acids Res 38:D557-562.

Fraser P, Cummings P and Curtis P (1989): The mouse carbonic anhydrase I gene contains two tissue-specific promoters. Mol Cell Biol 9:3308-3313.

Fujikawa-Adachi K, Nishimori I, Taguchi T and Onishi S (1999a): Human carbonic anhydrase XIV (CA14): cDNA cloning, mRNA expression, and mapping to chromosome 1. Genomics 61:74-81.

Fujikawa-Adachi K, Nishimori I, Taguchi T and Onishi S (1999b): Human mitochondrial carbonic anhydrase VB. cDNA cloning, mRNA expression, subcellular localization, and mapping to chromosome x. J Biol Chem 274:21228-21233.

Fujikawa-Adachi K, Nishimori I, Taguchi T, Yuri K and Onishi S (1999c): cDNA sequence, mRNA expression, and chromosomal localization of human carbonic anhydrase-related protein, CA-RP XI. Biochim Biophys Acta 1431:518-524.

Ghandour MS, Langley OK, Zhu XL, Waheed A and Sly WS (1992): Carbonic anhydrase IV on brain capillary endothelial cells: a marker associated with the blood-brain barrier. Proc Natl Acad Sci U S A 89:6823-6827.

Giatromanolaki A, Koukourakis MI, Sivridis E, Pastorek J, Wykoff CC, Gatter KC and Harris AL (2001): Expression of hypoxia-inducible carbonic anhydrase-9 relates to angiogenic pathways and independently to poor outcome in non-small cell lung cancer. Cancer Res 61:7992-7998.

Glenn KA, Nelson RF, Wen HM, Mallinger AJ and Paulson HL (2008): Diversity in tissue expression, substrate binding, and SCF complex formation for a lectin family of ubiquitin ligases. J Biol Chem 283:12717-12729.

Haapasalo J, Hilvo M, Nordfors K, Haapasalo H, Parkkila S, Hyrskyluoto A, Rantala I, Waheed A, Sly WS, Pastorekova S, Pastorek J and Parkkila AK (2008): Identification of an alternatively spliced isoform of carbonic anhydrase XII in diffusely infiltrating astrocytic gliomas. Neuro Oncol 10:131-138.

Haapasalo J, Nordfors K, Jarvela S, Bragge H, Rantala I, Parkkila AK, Haapasalo H and Parkkila S (2007): Carbonic anhydrase II in the endothelium of glial tumors: a potential target for therapy. Neuro Oncol 9:308-313.

Haapasalo JA, Nordfors KM, Hilvo M, Rantala IJ, Soini Y, Parkkila AK, Pastorekova S, Pastorek J, Parkkila SM and Haapasalo HK (2006): Expression of carbonic anhydrase IX in astrocytic tumors predicts poor prognosis. Clin Cancer Res 12:473-477.

Hageman GS, Zhu XL, Waheed A and Sly WS (1991): Localization of carbonic anhydrase IV in a specific capillary bed of the human eye. Proc Natl Acad Sci U S A 88:2716-2720.

Halmi P, Lehtonen J, Waheed A, Sly WS and Parkkila S (2004): Expression of hypoxia-inducible, membrane-bound carbonic anhydrase isozyme XII in mouse tissues. Anat Rec A Discov Mol Cell Evol Biol 277:171-177.

Harkonen PL, Makela SI, Valve EM, Karhukorpi EK and Vaananen HK (1991): Differential regulation of carbonic anhydrase II by androgen and estrogen in dorsal and lateral prostate of the rat. Endocrinology 128:3219-3227.

Harkonen PL and Vaananen HK (1988): Androgen regulation of carbonic anhydrase II, a major soluble protein in rat lateral prostate tissue. Biol Reprod 38:377-384.

Harris AL (2002): Hypoxia--a key regulatory factor in tumour growth. Nat Rev Cancer 2:38-47.

He P and Yun CC (2010): Mechanisms of the regulation of the intestinal Na+/H+ exchanger NHE3. J Biomed Biotechnol 2010:238080.

Henkin RI, Martin BM and Agarwal RP (1999): Efficacy of exogenous oral zinc in treatment of patients with carbonic anhydrase VI deficiency. Am J Med Sci 318:392-405.

Henriques O (1928): Die Bindungsweise des Kohlendioxyds im Blute. Biochem Ztschrft 200:1-24.

Hermo L, Chong DL, Moffatt P, Sly WS, Waheed A and Smith CE (2005): Region- and cell-specific differences in the distribution of carbonic anhydrases II, III, XII, and XIV in the adult rat epididymis. J Histochem Cytochem 53:699-713.

Hewett-Emmett D (2000): Evolution and distribution of the carbonic anhydrase gene families. In: The Carbonic Anhydrases: New Horizons, pp. 29-76. Eds. Chegwidden WR, Carter ND and Edwards YH, Birkhäuser Verlag, Basel.

Hewett-Emmett D and Tashian RE (1996): Functional diversity, conservation, and convergence in the evolution of the alpha-, beta-, and gamma-carbonic anhydrase gene families. Mol Phylogenet Evol 5:50-77.

Hilvo M, Baranauskiene L, Salzano AM, Scaloni A, Matulis D, Innocenti A, Scozzafava A, Monti SM, Di Fiore A, De Simone G, Lindfors M, Janis J, Valjakka J, Pastorekova S, Pastorek J, Kulomaa MS, Nordlund HR, Supuran CT and Parkkila S (2008a): Biochemical characterization of CA IX, one of the most active carbonic anhydrase isozymes. J Biol Chem 283:27799-27809.

Hilvo M, Innocenti A, Monti SM, De Simone G, Supuran CT and Parkkila S (2008b): Recent advances in research on the most novel carbonic anhydrases, CA XIII and XV. Curr Pharm Des 14:672-678.

Hilvo M, Rafajova M, Pastorekova S, Pastorek J and Parkkila S (2004): Expression of carbonic anhydrase IX in mouse tissues. J Histochem Cytochem 52:1313-1322.

Hilvo M, Tolvanen M, Clark A, Shen B, Shah GN, Waheed A, Halmi P, Hanninen M, Hamalainen JM, Vihinen M, Sly WS and Parkkila S (2005): Characterization of CA XV, a new GPI-anchored form of carbonic anhydrase. Biochem J 392:83-92.

Hoogerwerf WA, Tsao SC, Devuyst O, Levine SA, Yun CH, Yip JW, Cohen ME, Wilson PD, Lazenby AJ, Tse CM and Donowitz M (1996): NHE2 and NHE3 are human and rabbit intestinal brush-border proteins. Am J Physiol 270:G29-41.

Hsieh MJ, Chen KS, Chiou HL and Hsieh YS (2010): Carbonic anhydrase XII promotes invasion and migration ability of MDA-MB-231 breast cancer cells through the p38 MAPK signaling pathway. Eur J Cell Biol 89:598-606.

Hunter S, Apweiler R, Attwood TK, Bairoch A, Bateman A, Binns D, Bork P, Das U, Daugherty L, Duquenne L, Finn RD, Gough J, Haft D, Hulo N, Kahn D, Kelly E, Laugraud A, Letunic I, Lonsdale D, Lopez R, Madera M, Maslen J, McAnulla C,

McDowall J, Mistry J, Mitchell A, Mulder N, Natale D, Orengo C, Quinn AF, Selengut JD, Sigrist CJ, Thimma M, Thomas PD, Valentin F, Wilson D, Wu CH and Yeats C (2009): InterPro: the integrative protein signature database. Nucleic Acids Res 37:D211-215.

Hynninen P, Hamalainen JM, Pastorekova S, Pastorek J, Waheed A, Sly WS, Tomas E, Kirkinen P and Parkkila S (2004): Transmembrane carbonic anhydrase isozymes IX and XII in the female mouse reproductive organs. Reprod Biol Endocrinol 2:73.

Ilie MI, Hofman V, Ortholan C, Ammadi RE, Bonnetaud C, Havet K, Venissac N, Mouroux J, Mazure NM, Pouyssegur J and Hofman P (2011): Overexpression of carbonic anhydrase XII in tissues from resectable non-small cell lung cancers is a biomarker of good prognosis. Int J Cancer 128:1614-1623.

Inada A, Nienaber C, Fonseca S and Bonner-Weir S (2006): Timing and expression pattern of carbonic anhydrase II in pancreas. Dev Dyn 235:1571-1577.

Innocenti A, Lehtonen JM, Parkkila S, Scozzafava A and Supuran CT (2004): Carbonic anhydrase inhibitors. Inhibition of the newly isolated murine isozyme XIII with anions. Bioorg Med Chem Lett 14:5435-5439.

Ishihara T, Takeuchi T, Nishimori I, Adachi Y, Minakuchi T, Fujita J, Sonobe H, Ohtsuki Y and Onishi S (2006): Carbonic anhydrase-related protein VIII increases invasiveness of non-small cell lung adenocarcinoma. Virchows Arch 448:830-837.

Ishimoto Y, Savan R, Endo M and Sakai M (2004): Non-specific cytotoxic cell receptor (NCCRP)-1 type gene in tilapia (Oreochromis niloticus): its cloning and analysis. Fish Shellfish Immunol 16:163-172.

Ivan M, Kondo K, Yang H, Kim W, Valiando J, Ohh M, Salic A, Asara JM, Lane WS and Kaelin WG, Jr. (2001): HIFalpha targeted for VHL-mediated destruction by proline hydroxylation: implications for O2 sensing. Science 292:464-468.

Ivanov S, Liao SY, Ivanova A, Danilkovitch-Miagkova A, Tarasova N, Weirich G, Merrill MJ, Proescholdt MA, Oldfield EH, Lee J, Zavada J, Waheed A, Sly W, Lerman MI and Stanbridge EJ (2001): Expression of hypoxia-inducible cell-surface transmembrane carbonic anhydrases in human cancer. Am J Pathol 158:905-919.

Ivanov SV, Kuzmin I, Wei MH, Pack S, Geil L, Johnson BE, Stanbridge EJ and Lerman MI (1998): Down-regulation of transmembrane carbonic anhydrases in renal cell carcinoma cell lines by wild-type von Hippel-Lindau transgenes. Proc Natl Acad Sci U S A 95:12596-12601.

Jaakkola P, Mole DR, Tian YM, Wilson MI, Gielbert J, Gaskell SJ, Kriegsheim A, Hebestreit HF, Mukherji M, Schofield CJ, Maxwell PH, Pugh CW and Ratcliffe PJ (2001): Targeting of HIF-alpha to the von Hippel-Lindau ubiquitylation complex by O2-regulated prolyl hydroxylation. Science 292:468-472.

Jain E, Bairoch A, Duvaud S, Phan I, Redaschi N, Suzek BE, Martin MJ, McGarvey P and Gasteiger E (2009): Infrastructure for the life sciences: design and implementation of the UniProt website. BMC Bioinformatics 10:136.

Jakubickova L, Biesova Z, Pastorekova S, Kettmann R and Pastorek J (2005): Methylation of the CA9 promoter can modulate expression of the tumor-associated carbonic anhydrase IX in dense carcinoma cell lines. Int J Oncol 26:1121-1127.

Jaso-Friedmann L, Leary JH, 3rd and Evans DL (1997): NCCRP-1: a novel receptor protein sequenced from teleost nonspecific cytotoxic cells. Mol Immunol 34:955-965.

Jeffery S, Edwards Y and Carter N (1980): Distribution of CAIII in fetal and adult human tissue. Biochem Genet 18:843-849.

Kaluz S, Kaluzova M, Chrastina A, Olive PL, Pastorekova S, Pastorek J, Lerman MI and Stanbridge EJ (2002): Lowered oxygen tension induces expression of the hypoxia marker MN/carbonic anhydrase IX in the absence of hypoxia-inducible factor 1 alpha stabilization: a role for phosphatidylinositol 3'-kinase. Cancer Res 62:4469-4477.

Kaluz S, Kaluzova M, Opavsky R, Pastorekova S, Gibadulinova A, Dequiedt F, Kettmann R and Pastorek J (1999): Transcriptional regulation of the MN/CA 9 gene coding for the tumor-associated carbonic anhydrase IX. Identification and characterization of a proximal silencer element. J Biol Chem 274:32588-32595.

Kaluz S, Kaluzova M and Stanbridge EJ (2003): Expression of the hypoxia marker carbonic anhydrase IX is critically dependent on SP1 activity. Identification of a novel type of hypoxia-responsive enhancer. Cancer Res 63:917-922.

Kaluzova M, Pastorekova S, Svastova E, Pastorek J, Stanbridge EJ and Kaluz S (2001): Characterization of the MN/CA 9 promoter proximal region: a role for specificity protein (SP) and activator protein 1 (AP1) factors. Biochem J 359:669-677.

Karhumaa P, Kaunisto K, Parkkila S, Waheed A, Pastorekova S, Pastorek J, Sly WS and Rajaniemi H (2001a): Expression of the transmembrane carbonic anhydrases, CA IX and CA XII, in the human male excurrent ducts. Mol Hum Reprod 7:611-616.

Karhumaa P, Leinonen J, Parkkila S, Kaunisto K, Tapanainen J and Rajaniemi H (2001b): The identification of secreted carbonic anhydrase VI as a constitutive glycoprotein of human and rat milk. Proc Natl Acad Sci U S A 98:11604-11608.

Karhumaa P, Parkkila S, Tureci O, Waheed A, Grubb JH, Shah G, Parkkila A, Kaunisto K, Tapanainen J, Sly WS and Rajaniemi H (2000): Identification of carbonic anhydrase XII as the membrane isozyme expressed in the normal human endometrial epithelium. Mol Hum Reprod 6:68-74.

Kaseda M, Ichihara N, Nishita T, Amasaki H and Asari M (2006): Immunohistochemistry of the bovine secretory carbonic anhydrase isozyme (CA-VI) in bovine alimentary canal and major salivary glands. J Vet Med Sci 68:131-135.

Kasuya T, Shibata S, Kaseda M, Ichihara N, Nishita T, Murakami M and Asari M (2007): Immunohistolocalization and gene expression of the secretory carbonic anhydrase isozymes (CA-VI) in canine oral mucosa, salivary glands and oesophagus. Anat Histol Embryol 36:53-57.

Kato K (1990): Sequence of a novel carbonic anhydrase-related polypeptide and its exclusive presence in Purkinje cells. FEBS Lett 271:137-140.

Katoh K, Kuma K, Toh H and Miyata T (2005): MAFFT version 5: improvement in accuracy of multiple sequence alignment. Nucleic Acids Res 33:511-518.

Kaunisto K, Fleming RE, Kneer J, Sly WS and Rajaniemi H (1999): Regional expression and androgen regulation of carbonic anhydrase IV and II in the adult rat epididymis. Biol Reprod 61:1521-1526.

Kaunisto K, Parkkila S, Rajaniemi H, Waheed A, Grubb J and Sly WS (2002): Carbonic anhydrase XIV: luminal expression suggests key role in renal acidification. Kidney Int 61:2111-2118.

Kilpinen S, Autio R, Ojala K, Iljin K, Bucher E, Sara H, Pisto T, Saarela M, Skotheim RI, Bjorkman M, Mpindi JP, Haapa-Paananen S, Vainio P, Edgren H, Wolf M, Astola J, Nees M, Hautaniemi S and Kallioniemi O (2008): Systematic bioinformatic analysis of expression levels of 17,330 human genes across 9,783 samples from 175 types of healthy and pathological tissues. Genome Biol 9:R139.

Kim G, Lee TH, Wetzel P, Geers C, Robinson MA, Myers TG, Owens JW, Wehr NB, Eckhaus MW, Gros G, Wynshaw-Boris A and Levine RL (2004): Carbonic anhydrase III is not required in the mouse for normal growth, development, and life span. Mol Cell Biol 24:9942-9947.

Kimoto M, Iwai S, Maeda T, Yura Y, Fernley RT and Ogawa Y (2004): Carbonic anhydrase VI in the mouse nasal gland. J Histochem Cytochem 52:1057-1062.

Kimoto M, Kishino M, Yura Y and Ogawa Y (2006): A role of salivary carbonic anhydrase VI in dental plaque. Arch Oral Biol 51:117-122.

Kivela A, Parkkila S, Saarnio J, Karttunen TJ, Kivela J, Parkkila AK, Waheed A, Sly WS, Grubb JH, Shah G, Tureci O and Rajaniemi H (2000a): Expression of a novel transmembrane carbonic anhydrase isozyme XII in normal human gut and colorectal tumors. Am J Pathol 156:577-584.

Kivela AJ, Parkkila S, Saarnio J, Karttunen TJ, Kivela J, Parkkila AK, Pastorekova S, Pastorek J, Waheed A, Sly WS and Rajaniemi H (2000b): Expression of transmembrane carbonic anhydrase isoenzymes IX and XII in normal human pancreas and pancreatic tumours. Histochem Cell Biol 114:197-204.

Kivela J, Parkkila S, Parkkila AK and Rajaniemi H (1999): A low concentration of carbonic anhydrase isoenzyme VI in whole saliva is associated with caries prevalence. Caries Res 33:178-184.

Kivela J, Parkkila S, Waheed A, Parkkila AK, Sly WS and Rajaniemi H (1997): Secretory carbonic anhydrase isoenzyme (CA VI) in human serum. Clin Chem 43:2318-2322.

Klatt P and Lamas S (2000): Regulation of protein function by S-glutathiolation in response to oxidative and nitrosative stress. Eur J Biochem 267:4928-4944.

Kondo K and Kaelin WG, Jr. (2001): The von Hippel-Lindau tumor suppressor gene. Exp Cell Res 264:117-125.

Kopacek J, Barathova M, Dequiedt F, Sepelakova J, Kettmann R, Pastorek J and Pastorekova S (2005): MAPK pathway contributes to density- and hypoxia-induced expression of the tumor-associated carbonic anhydrase IX. Biochim Biophys Acta 1729:41-49.

Korhonen K, Parkkila AK, Helen P, Valimaki R, Pastorekova S, Pastorek J, Parkkila S and Haapasalo H (2009): Carbonic anhydrases in meningiomas: association of endothelial carbonic anhydrase II with aggressive tumor features. J Neurosurg 111:472-477.

Koumenis C and Wouters BG (2006): "Translating" tumor hypoxia: unfolded protein response (UPR)-dependent and UPR-independent pathways. Mol Cancer Res 4:423-436.

Kummola L, Hamalainen JM, Kivela J, Kivela AJ, Saarnio J, Karttunen T and Parkkila S (2005): Expression of a novel carbonic anhydrase, CA XIII, in normal and neoplastic colorectal mucosa. BMC Cancer 5:41.

Kumpulainen T and Korhonen LK (1982): Immunohistochemical localization of carbonic anhydrase isoenzyme C in the central and peripheral nervous system of the mouse. J Histochem Cytochem 30:283-292.

Kyllonen MS, Parkkila S, Rajaniemi H, Waheed A, Grubb JH, Shah GN, Sly WS and Kaunisto K (2003): Localization of carbonic anhydrase XII to the basolateral membrane of H+-secreting cells of mouse and rat kidney. J Histochem Cytochem 51:1217-1224.

Lakkis MM, O'Shea KS and Tashian RE (1997): Differential expression of the carbonic anhydrase genes for CA VII (Car7) and CA-RP VIII (Car8) in mouse brain. J Histochem Cytochem 45:657-662.

Laurila AL, Jeffery S, Savolainen J, Takala TE, Carter ND and Vaananen HK (1991): Immobilization induces carbonic anhydrase III in type II fibers of rat skeletal muscle. J Histochem Cytochem 39:617-624.

Laurila AL, Parvinen EK, Slot JW and Vaananen HK (1989): Consecutive expression of carbonic anhydrase isoenzymes during development of rat liver and skeletal muscle differentiation. J Histochem Cytochem 37:1375-1382.

Legendre C, Hori T, Loyer P, Aninat C, Ishida S, Glaise D, Lucas-Clerc C, Boudjema K, Guguen-Guillouzo C, Corlu A and Morel F (2009): Drug-metabolising enzymes are down-regulated by hypoxia in differentiated human hepatoma HepaRG cells: HIF-1alpha involvement in CYP3A4 repression. Eur J Cancer 45:2882-2892.

Lehenkari P, Hentunen TA, Laitala-Leinonen T, Tuukkanen J and Vaananen HK (1998): Carbonic anhydrase II plays a major role in osteoclast differentiation and bone resorption by effecting the steady state intracellular pH and Ca2+. Exp Cell Res 242:128-137.

Lehtonen J, Shen B, Vihinen M, Casini A, Scozzafava A, Supuran CT, Parkkila AK, Saarnio J, Kivela AJ, Waheed A, Sly WS and Parkkila S (2004): Characterization of CA XIII, a novel member of the carbonic anhydrase isozyme family. J Biol Chem 279:2719-2727.

Leinonen J, Parkkila S, Kaunisto K, Koivunen P and Rajaniemi H (2001): Secretion of carbonic anhydrase isoenzyme VI (CA VI) from human and rat lingual serous von Ebner's glands. J Histochem Cytochem 49:657-662.

Leinonen JS, Saari KA, Seppanen JM, Myllyla HM and Rajaniemi HJ (2004): Immunohistochemical demonstration of carbonic anhydrase isoenzyme VI (CA VI) expression in rat lower airways and lung. J Histochem Cytochem 52:1107-1112.

Leppilampi M, Karttunen TJ, Kivela J, Gut MO, Pastorekova S, Pastorek J and Parkkila S (2005a): Gastric pit cell hyperplasia and glandular atrophy in carbonic anhydrase IX knockout mice: studies on two strains C57/BL6 and BALB/C. Transgenic Res 14:655-663.

Leppilampi M, Koistinen P, Savolainen ER, Hannuksela J, Parkkila AK, Niemela O, Pastorekova S, Pastorek J, Waheed A, Sly WS, Parkkila S and Rajaniemi H (2002): The expression of carbonic anhydrase II in hematological malignancies. Clin Cancer Res 8:2240-2245.

Leppilampi M, Parkkila S, Karttunen T, Gut MO, Gros G and Sjoblom M (2005b): Carbonic anhydrase isozyme-II-deficient mice lack the duodenal bicarbonate secretory response to prostaglandin E2. Proc Natl Acad Sci U S A 102:15247-15252.

Leppilampi M, Saarnio J, Karttunen TJ, Kivela J, Pastorekova S, Pastorek J, Waheed A, Sly WS and Parkkila S (2003): Carbonic anhydrase isozymes IX and XII in gastric tumors. World J Gastroenterol 9:1398-1403.

Li G, Feng G, Gentil-Perret A, Genin C and Tostain J (2008): Serum carbonic anhydrase 9 level is associated with postoperative recurrence of conventional renal cell cancer. J Urol 180:510-513; discussion 513-514.

Liao SY, Aurelio ON, Jan K, Zavada J and Stanbridge EJ (1997): Identification of the MN/CA9 protein as a reliable diagnostic biomarker of clear cell carcinoma of the kidney. Cancer Res 57:2827-2831.

Liao SY, Brewer C, Zavada J, Pastorek J, Pastorekova S, Manetta A, Berman ML, DiSaia PJ and Stanbridge EJ (1994): Identification of the MN antigen as a diagnostic biomarker of cervical intraepithelial squamous and glandular neoplasia and cervical carcinomas. Am J Pathol 145:598-609.

Liao SY, Ivanov S, Ivanova A, Ghosh S, Cote MA, Keefe K, Coca-Prados M, Stanbridge EJ and Lerman MI (2003): Expression of cell surface transmembrane carbonic anhydrase genes CA9 and CA12 in the human eye: overexpression of CA12 (CAXII) in glaucoma. J Med Genet 40:257-261.

Liao SY, Lerman MI and Stanbridge EJ (2009): Expression of transmembrane carbonic anhydrases, CAIX and CAXII, in human development. BMC Dev Biol 9:22.

Lindskog S (1960): Purification and properties of bovine erythrocyte carbonic anhydrase. Biochim Biophys Acta 39:218-226.

Lindskog S and Silverman DN (2000): The catalytic mechanism of mammalian carbonic anhydrases. In: The Carbonic Anhydrases: New Horizons, pp. 175-195. Eds. Chegwidden WR, Carter ND and Edwards YH, Birkhäuser Verlag, Basel.

Linser P and Moscona AA (1981): Carbonic anhydrase C in the neural retina: transition from generalized to glia-specific cell localization during embryonic development. Proc Natl Acad Sci U S A 78:7190-7194.

Liu M, Walter GA, Pathare NC, Forster RE and Vandenborne K (2007): A quantitative study of bioenergetics in skeletal muscle lacking carbonic anhydrase III using 31P magnetic resonance spectroscopy. Proc Natl Acad Sci U S A 104:371-376.

LoGrasso PV, Tu C, Chen X, Taoka S, Laipis PJ and Silverman DN (1993): Influence of amino acid replacement at position 198 on catalytic properties of zinc-bound water in human carbonic anhydrase III. Biochemistry 32:5786-5791.

Loncaster JA, Harris AL, Davidson SE, Logue JP, Hunter RD, Wycoff CC, Pastorek J, Ratcliffe PJ, Stratford IJ and West CM (2001): Carbonic anhydrase (CA IX) expression, a potential new intrinsic marker of hypoxia: correlations with tumor oxygen measurements and prognosis in locally advanced carcinoma of the cervix. Cancer Res 61:6394-6399.

Lonnerholm G, Selking O and Wistrand PJ (1985): Amount and distribution of carbonic anhydrases CA I and CA II in the gastrointestinal tract. Gastroenterology 88:1151-1161.

Lovejoy DA, Hewett-Emmett D, Porter CA, Cepoi D, Sheffield A, Vale WW and Tashian RE (1998): Evolutionarily conserved, "acatalytic" carbonic anhydrase-related protein XI contains a sequence motif present in the neuropeptide sauvagine: the human CA-RP XI gene (CA11) is embedded between the secretor gene cluster and the DBP gene at 19q13.3. Genomics 54:484-493.

Lyons GE, Buckingham ME, Tweedie S and Edwards YH (1991): Carbonic anhydrase III, an early mesodermal marker, is expressed in embryonic mouse skeletal muscle and notochord. Development 111:233-244.

Mallis RJ, Poland BW, Chatterjee TK, Fisher RA, Darmawan S, Honzatko RB and Thomas JA (2000): Crystal structure of S-glutathiolated carbonic anhydrase III. FEBS Lett 482:237-241.

Maren TH (1967): Carbonic anhydrase: chemistry, physiology, and inhibition. Physiol Rev 47:595-781.

Maresca A, Temperini C, Pochet L, Masereel B, Scozzafava A and Supuran CT (2010): Deciphering the mechanism of carbonic anhydrase inhibition with coumarins and thiocoumarins. J Med Chem 53:335-344.

Maresca A, Temperini C, Vu H, Pham NB, Poulsen SA, Scozzafava A, Quinn RJ and Supuran CT (2009): Non-zinc mediated inhibition of carbonic anhydrases: coumarins are a new class of suicide inhibitors. J Am Chem Soc 131:3057-3062.

Maxwell PH, Pugh CW and Ratcliffe PJ (2001): Activation of the HIF pathway in cancer. Curr Opin Genet Dev 11:293-299.

McKiernan JM, Buttyan R, Bander NH, Stifelman MD, Katz AE, Chen MW, Olsson CA and Sawczuk IS (1997): Expression of the tumor-associated gene MN: a potential biomarker for human renal cell carcinoma. Cancer Res 57:2362-2365.

Meldrum N and Roughton F (1932): Some properties of carbonic anhydrase, the carbon dioxide enzyme present in blood. J Physiol 75:15-16.

Meldrum NU and Roughton FJ (1933): Carbonic anhydrase. Its preparation and properties. J Physiol 80:113-142.

Miyaji E, Nishimori I, Taniuchi K, Takeuchi T, Ohtsuki Y and Onishi S (2003): Overexpression of carbonic anhydrase-related protein VIII in human colorectal cancer. J Pathol 201:37-45.

Mizushima T, Yoshida Y, Kumanomidou T, Hasegawa Y, Suzuki A, Yamane T and Tanaka K (2007): Structural basis for the selection of glycosylated substrates by SCF(Fbs1) ubiquitin ligase. Proc Natl Acad Sci U S A 104:5777-5781.

Montgomery JC, Venta PJ, Eddy RL, Fukushima YS, Shows TB and Tashian RE (1991): Characterization of the human gene for a newly discovered carbonic anhydrase, CA VII, and its localization to chromosome 16. Genomics 11:835-848.

Morey JS, Ryan JC and Van Dolah FM (2006): Microarray validation: factors influencing correlation between oligonucleotide microarrays and real-time PCR. Biol Proced Online 8:175-193.

Morgan PE, Pastorekova S, Stuart-Tilley AK, Alper SL and Casey JR (2007): Interactions of transmembrane carbonic anhydrase, CAIX, with bicarbonate transporters. Am J Physiol Cell Physiol 293:C738-748.

Mori K, Ogawa Y, Ebihara K, Tamura N, Tashiro K, Kuwahara T, Mukoyama M, Sugawara A, Ozaki S, Tanaka I and Nakao K (1999): Isolation and characterization of CA XIV, a novel membrane-bound carbonic anhydrase from mouse kidney. J Biol Chem 274:15701-15705.

Morimoto K, Nishimori I, Takeuchi T, Kohsaki T, Okamoto N, Taguchi T, Yunoki S, Watanabe R, Ohtsuki Y and Onishi S (2005): Overexpression of carbonic anhydrase-related protein XI promotes proliferation and invasion of gastrointestinal stromal tumors. Virchows Arch 447:66-73.

Muhlhauser J, Crescimanno C, Rajaniemi H, Parkkila S, Milovanov AP, Castellucci M and Kaufmann P (1994): Immunohistochemistry of carbonic anhydrase in human placenta and fetal membranes. Histochemistry 101:91-98.

Nakamura J, Kitajima Y, Kai K, Hashiguchi K, Hiraki M, Noshiro H and Miyazaki K (2011): Expression of hypoxic marker CA IX is regulated by site-specific DNA methylation and is associated with the histology of gastric cancer. Am J Pathol 178:515-524.

Nandi D, Tahiliani P, Kumar A and Chandu D (2006): The ubiquitin-proteasome system. J Biosci 31:137-155.

Nelson D and Cox M (2000): Lehninger Principles of Biochemistry. In: Water, pp. 82-111. Eds., Worth Publishers, New York.

Nishikata M, Nishimori I, Taniuchi K, Takeuchi T, Minakuchi T, Kohsaki T, Adachi Y, Ohtsuki Y and Onishi S (2007): Carbonic anhydrase-related protein VIII promotes colon cancer cell growth. Mol Carcinog 46:208-214.

Ogawa Y, Matsumoto K, Maeda T, Tamai R, Suzuki T, Sasano H and Fernley RT (2002): Characterization of lacrimal gland carbonic anhydrase VI. J Histochem Cytochem 50:821-827.

Oguni M, Setogawa T, Tanaka O, Shinohara H and Kato K (1992): Immunohistochemical study of carbonic anhydrase III in the extraocular muscles of human embryos. Acta Anat (Basel) 144:316-319.

Okamoto N, Fujikawa-Adachi K, Nishimori I, Taniuchi K and Onishi S (2001): cDNA sequence of human carbonic anhydrase-related protein, CA-RP X: mRNA expressions of CA-RP X and XI in human brain. Biochim Biophys Acta 1518:311-316.

Oosterwijk E (2008): Carbonic anhydrase IX: historical and future perspectives. BJU Int 101 Suppl 4:2-7.

Oosterwijk E, Ruiter DJ, Hoedemaeker PJ, Pauwels EK, Jonas U, Zwartendijk J and Warnaar SO (1986): Monoclonal antibody G 250 recognizes a determinant present in renal-cell carcinoma and absent from normal kidney. Int J Cancer 38:489-494.

Opavsky R, Pastorekova S, Zelnik V, Gibadulinova A, Stanbridge EJ, Zavada J, Kettmann R and Pastorek J (1996): Human MN/CA9 gene, a novel member of the carbonic anhydrase family: structure and exon to protein domain relationships. Genomics 33:480-487.

Ortova Gut MO, Parkkila S, Vernerova Z, Rohde E, Zavada J, Hocker M, Pastorek J, Karttunen T, Gibadulinova A, Zavadova Z, Knobeloch KP, Wiedenmann B, Svoboda J, Horak I and Pastorekova S (2002): Gastric hyperplasia in mice with targeted disruption of the carbonic anhydrase gene Car9. Gastroenterology 123:1889-1903.

Pan PW, Kayra K, Leinonen J, Nissinen M, Parkkila S and Rajaniemi H (2011a): Gene expression profiling in the submandibular gland, stomach, and duodenum of CAVI-deficient mice. Transgenic Res 20:675-698.

Pan PW, Parkkila AK, Autio S, Hilvo M, Sormunen R, Pastorekova S, Pastorek J, Haapasalo H and Parkkila S (2011b): Brain phenotype of carbonic anhydrase IX-deficient mice. Transgenic Res

Pan PW, Rodriguez A and Parkkila S (2007): A systematic quantification of carbonic anhydrase transcripts in the mouse digestive system. BMC Mol Biol 8:22.

Parkkila AK, Herva R, Parkkila S and Rajaniemi H (1995a): Immunohistochemical demonstration of human carbonic anhydrase isoenzyme II in brain tumours. Histochem J 27:974-982.

Parkkila AK, Parkkila S, Juvonen T and Rajaniemi H (1993): Carbonic anhydrase isoenzymes II and I are present in the zona glomerulosa cells of the human adrenal gland. Histochemistry 99:37-41.

Parkkila S (2000): An overview of the distribution and function of carbonic anhydrase in mammals. In: The Carbonic Anhydrases: New Horizons, pp. 79-93. Eds. Chegwidden WR, Carter ND and Edwards YH, Birkhäuser Verlag, Basel.

Parkkila S, Halsted CH, Villanueva JA, Vaananen HK and Niemela O (1999): Expression of testosterone-dependent enzyme, carbonic anhydrase III, and oxidative stress in experimental alcoholic liver disease. Dig Dis Sci 44:2205-2213.

Parkkila S, Kaunisto K, Rajaniemi L, Kumpulainen T, Jokinen K and Rajaniemi H (1990): Immunohistochemical localization of carbonic anhydrase isoenzymes VI, II, and I in human parotid and submandibular glands. J Histochem Cytochem 38:941-947.

Parkkila S, Kivela AJ, Kaunisto K, Parkkila AK, Hakkola J, Rajaniemi H, Waheed A and Sly WS (2002): The plasma membrane carbonic anhydrase in murine hepatocytes identified as isozyme XIV. BMC Gastroenterol 2:13.

Parkkila S, Lasota J, Fletcher JA, Ou WB, Kivela AJ, Nuorva K, Parkkila AK, Ollikainen J, Sly WS, Waheed A, Pastorekova S, Pastorek J, Isola J and Miettinen M (2010): Carbonic anhydrase II. A novel biomarker for gastrointestinal stromal tumors. Mod Pathol 23:743-750.

Parkkila S, Parkkila AK, Juvonen T, Lehto VP and Rajaniemi H (1995b): Immunohistochemical demonstration of the carbonic anhydrase isoenzymes I and II in pancreatic tumours. Histochem J 27:133-138.

Parkkila S, Parkkila AK, Juvonen T and Rajaniemi H (1994): Distribution of the carbonic anhydrase isoenzymes I, II, and VI in the human alimentary tract. Gut 35:646-650.

Parkkila S, Parkkila AK, Juvonen T, Waheed A, Sly WS, Saarnio J, Kaunisto K, Kellokumpu S and Rajaniemi H (1996): Membrane-bound carbonic anhydrase IV is expressed in the luminal plasma membrane of the human gallbladder epithelium. Hepatology 24:1104-1108.

Parkkila S, Parkkila AK, Lehtola J, Reinila A, Sodervik HJ, Rannisto M and Rajaniemi H (1997): Salivary carbonic anhydrase protects gastroesophageal mucosa from acid injury. Dig Dis Sci 42:1013-1019.

Parkkila S, Parkkila AK and Rajaniemi H (1995c): Circadian periodicity in salivary carbonic anhydrase VI concentration. Acta Physiol Scand 154:205-211.

Parkkila S, Parkkila AK, Rajaniemi H, Shah GN, Grubb JH, Waheed A and Sly WS (2001): Expression of membrane-associated carbonic anhydrase XIV on neurons and axons in mouse and human brain. Proc Natl Acad Sci U S A 98:1918-1923.

Parkkila S, Parkkila AK, Saarnio J, Kivela J, Karttunen TJ, Kaunisto K, Waheed A, Sly WS, Tureci O, Virtanen I and Rajaniemi H (2000): Expression of the membrane-associated carbonic anhydrase isozyme XII in the human kidney and renal tumors. J Histochem Cytochem 48:1601-1608.

Pastorek J, Pastorekova S, Callebaut I, Mornon JP, Zelnik V, Opavsky R, Zat'ovicova M, Liao S, Portetelle D, Stanbridge EJ, Zavada J, Burny A and Kettmann R (1994): Cloning and characterization of MN, a human tumor-associated protein with a domain homologous to carbonic anhydrase and a putative helix-loop-helix DNA binding segment. Oncogene 9:2877-2888.

Pastorekova S, Parkkila S, Parkkila AK, Opavsky R, Zelnik V, Saarnio J and Pastorek J (1997): Carbonic anhydrase IX, MN/CA IX: analysis of stomach complementary DNA sequence and expression in human and rat alimentary tracts. Gastroenterology 112:398-408.

Pastorekova S and Pastorek J (2004): Cancer-related carbonic anhydrase isozymes and their inhibition. In: Carbonic Anhydrase: Its Inhibitors and Activators, pp. 255-281. Eds. Supuran C, Scozzafava A and Conway J, CRC Press LLC, Boca Raton.

Pastorekova S and Zavada J (2004): Carbonic anhydrase IX (CA IX) as a potential target for cancer therapy. Cancer Therapy 2:245-262.

Pastorekova S, Zavadova Z, Kostal M, Babusikova O and Zavada J (1992): A novel quasi-viral agent, MaTu, is a two-component system. Virology 187:620-626.

Penschow JD, Giles ME, Coghlan JP and Fernley RT (1997): Redistribution of carbonic anhydrase VI expression from ducts to acini during development of ovine parotid and submandibular glands. Histochem Cell Biol 107:417-422.

Proescholdt MA, Mayer C, Kubitza M, Schubert T, Liao SY, Stanbridge EJ, Ivanov S, Oldfield EH, Brawanski A and Merrill MJ (2005): Expression of hypoxia-inducible carbonic anhydrases in brain tumors. Neuro Oncol 7:465-475.

Pruitt KD, Tatusova T, Klimke W and Maglott DR (2009): NCBI Reference Sequences: current status, policy and new initiatives. Nucleic Acids Res 37:D32-36.

Purkerson JM, Kittelberger AM and Schwartz GJ (2007): Basolateral carbonic anhydrase IV in the proximal tubule is a glycosylphosphatidylinositol-anchored protein. Kidney Int 71:407-416.

Purkerson JM and Schwartz GJ (2007): The role of carbonic anhydrases in renal physiology. Kidney Int 71:103-115.

Quelo I and Jurdic P (2000): Differential regulation of the carbonic anhydrase II gene expression by hormonal nuclear receptors in monocytic cells: identification of the retinoic acid response element. Biochem Biophys Res Commun 271:481-491.

Quelo I, Kahlen JP, Rascle A, Jurdic P and Carlberg C (1994): Identification and characterization of a vitamin D3 response element of chicken carbonic anhydrase-II. DNA Cell Biol 13:1181-1187.

Rafajova M, Zatovicova M, Kettmann R, Pastorek J and Pastorekova S (2004): Induction by hypoxia combined with low glucose or low bicarbonate and high posttranslational stability upon reoxygenation contribute to carbonic anhydrase IX expression in cancer cells. Int J Oncol 24:995-1004.

Raisanen SR, Lehenkari P, Tasanen M, Rahkila P, Harkonen PL and Vaananen HK (1999): Carbonic anhydrase III protects cells from hydrogen peroxide-induced apoptosis. FASEB J 13:513-522.

Ramirez-Bergeron DL, Runge A, Dahl KD, Fehling HJ, Keller G and Simon MC (2004): Hypoxia affects mesoderm and enhances hemangioblast specification during early development. Development 131:4623-4634.

Ruusuvuori E, Li H, Huttu K, Palva JM, Smirnov S, Rivera C, Kaila K and Voipio J (2004): Carbonic anhydrase isoform VII acts as a molecular switch in the development of synchronous gamma-frequency firing of hippocampal CA1 pyramidal cells. J Neurosci 24:2699-2707.

Saari S, Hilvo M, Pan P, Gros G, Hanke N, Waheed A, Sly WS and Parkkila S (2010): The most recently discovered carbonic anhydrase, CA XV, is expressed in the thick ascending limb of Henle and in the collecting ducts of mouse kidney. PLoS One 5:e9624.

Saarnio J, Parkkila S, Parkkila AK, Haukipuro K, Pastorekova S, Pastorek J, Kairaluoma MI and Karttunen TJ (1998a): Immunohistochemical study of colorectal tumors for expression of a novel transmembrane carbonic anhydrase, MN/CA IX, with potential value as a marker of cell proliferation. Am J Pathol 153:279-285.

Saarnio J, Parkkila S, Parkkila AK, Pastorekova S, Haukipuro K, Pastorek J, Juvonen T and Karttunen TJ (2001): Transmembrane carbonic anhydrase, MN/CA IX, is a potential biomarker for biliary tumours. J Hepatol 35:643-649.

Saarnio J, Parkkila S, Parkkila AK, Waheed A, Casey MC, Zhou XY, Pastorekova S, Pastorek J, Karttunen T, Haukipuro K, Kairaluoma MI and Sly WS (1998b): Immunohistochemistry of carbonic anhydrase isozyme IX (MN/CA IX) in human gut reveals polarized expression in the epithelial cells with the highest proliferative capacity. J Histochem Cytochem 46:497-504.

Sakata H, Savan R, Sogabe R, Kono T, Taniguchi K, Gunimaladevi I, Tassakka AC and Sakai M (2005): Cloning and analysis of non-specific cytotoxic cell receptor (NCCRP)-1 from common carp Cyprinus carpio L. Comp Biochem Physiol C Toxicol Pharmacol 140:287-294.

Sandlund J, Oosterwijk E, Grankvist K, Oosterwijk-Wakka J, Ljungberg B and Rasmuson T (2007): Prognostic impact of carbonic anhydrase IX expression in human renal cell carcinoma. BJU Int 100:556-560.

Schwartz GJ, Kittelberger AM, Barnhart DA and Vijayakumar S (2000): Carbonic anhydrase IV is expressed in H(+)-secreting cells of rabbit kidney. Am J Physiol Renal Physiol 278:F894-904.

Semenza GL (2001): Hypoxia-inducible factor 1: oxygen homeostasis and disease pathophysiology. Trends Mol Med 7:345-350.

Sender S, Decker B, Fenske CD, Sly WS, Carter ND and Gros G (1998): Localization of carbonic anhydrase IV in rat and human heart muscle. J Histochem Cytochem 46:855-861.

Sender S, Gros G, Waheed A, Hageman GS and Sly WS (1994): Immunohistochemical localization of carbonic anhydrase IV in capillaries of rat and human skeletal muscle. J Histochem Cytochem 42:1229-1236.

Shah GN, Hewett-Emmett D, Grubb JH, Migas MC, Fleming RE, Waheed A and Sly WS (2000): Mitochondrial carbonic anhydrase CA VB: differences in tissue distribution and pattern of evolution from those of CA VA suggest distinct physiological roles. Proc Natl Acad Sci U S A 97:1677-1682.

Shah GN, Ulmasov B, Waheed A, Becker T, Makani S, Svichar N, Chesler M and Sly WS (2005): Carbonic anhydrase IV and XIV knockout mice: roles of the respective carbonic anhydrases in buffering the extracellular space in brain. Proc Natl Acad Sci U S A 102:16771-16776.

Sly WS, Hewett-Emmett D, Whyte MP, Yu YS and Tashian RE (1983): Carbonic anhydrase II deficiency identified as the primary defect in the autosomal recessive syndrome of osteopetrosis with renal tubular acidosis and cerebral calcification. Proc Natl Acad Sci U S A 80:2752-2756.

Sly WS and Hu PY (1995): Human carbonic anhydrases and carbonic anhydrase deficiencies. Annu Rev Biochem 64:375-401.

Sly WS, Whyte MP, Sundaram V, Tashian RE, Hewett-Emmett D, Guibaud P, Vainsel M, Baluarte HJ, Gruskin A, Al-Mosawi M, Sakati N and Ohlsson A (1985): Carbonic anhydrase II deficiency in 12 families with the autosomal recessive syndrome of osteopetrosis with renal tubular acidosis and cerebral calcification. N Engl J Med 313:139-145.

Sok J, Wang XZ, Batchvarova N, Kuroda M, Harding H and Ron D (1999): CHOP-Dependent stress-inducible expression of a novel form of carbonic anhydrase VI. Mol Cell Biol 19:495-504.

Stams T and Christianson DW (2000): X-ray crystallographic studies of mammalian carbonic anhydrase isozymes. In: The Carbonic Anhydrases: New Horizons, pp. 159-174. Eds. Chegwidden WR, Carter ND and Edwards YH, Birkhäuser Verlag, Basel.

Stanton LW, Ponte PA, Coleman RT and Snyder MA (1991): Expression of CA III in rodent models of obesity. Mol Endocrinol 5:860-866.

Supuran CT (2004): Carbonic anhydrases: catalytic and inhibition mechanisms, distribution and physiological roles. In: Carbonic Anhydrase: Its Inhibitors and Activators, pp. 1-23. Eds. Supuran CT, Scozzafava, A and Conway, J, CRC Press Boca Raton.

Supuran CT (2008): Carbonic anhydrases: novel therapeutic applications for inhibitors and activators. Nat Rev Drug Discov 7:168-181.

Svastova E, Hulikova A, Rafajova M, Zat'ovicova M, Gibadulinova A, Casini A, Cecchi A, Scozzafava A, Supuran CT, Pastorek J and Pastorekova S (2004): Hypoxia activates the capacity of tumor-associated carbonic anhydrase IX to acidify extracellular pH. FEBS Lett 577:439-445.

Svastova E, Zilka N, Zat'ovicova M, Gibadulinova A, Ciampor F, Pastorek J and Pastorekova S (2003): Carbonic anhydrase IX reduces E-cadherin-mediated adhesion of MDCK cells via interaction with beta-catenin. Exp Cell Res 290:332-345.

Swietach P, Wigfield S, Cobden P, Supuran CT, Harris AL and Vaughan-Jones RD (2008): Tumor-associated carbonic anhydrase 9 spatially coordinates intracellular pH in three-dimensional multicellular growths. J Biol Chem 283:20473-20483.

Swinson DE, Jones JL, Richardson D, Wykoff C, Turley H, Pastorek J, Taub N, Harris AL and O'Byrne KJ (2003): Carbonic anhydrase IX expression, a novel surrogate marker of tumor hypoxia, is associated with a poor prognosis in non-small-cell lung cancer. J Clin Oncol 21:473-482.

Syrjanen L, Tolvanen M, Hilvo M, Olatubosun A, Innocenti A, Scozzafava A, Leppiniemi J, Niederhauser B, Hytonen VP, Gorr TA, Parkkila S and Supuran CT (2010): Characterization of the first beta-class carbonic anhydrase from an arthropod (Drosophila melanogaster) and phylogenetic analysis of beta-class carbonic anhydrases in invertebrates. BMC Biochem 11:28.

Tamura K, Dudley J, Nei M and Kumar S (2007): MEGA4: Molecular Evolutionary Genetics Analysis (MEGA) software version 4.0. Mol Biol Evol 24:1596-1599.

Taniuchi K, Nishimori I, Takeuchi T, Fujikawa-Adachi K, Ohtsuki Y and Onishi S (2002): Developmental expression of carbonic anhydrase-related proteins VIII, X, and XI in the human brain. Neuroscience 112:93-99.

Tashian RE (1989): The carbonic anhydrases: widening perspectives on their evolution, expression and function. Bioessays 10:186-192.

Tashian RE (1992): Genetics of the mammalian carbonic anhydrases. Adv Genet 30:321-356.

Tashian RE, Hewett-Emmett D, Carter ND and Bergenhem NC (2000): Carbonic anhydrase (CA)-related proteins (CA-RPs), and transmembrane proteins with CA or CA-RP domains. In: The Carbonic Anhydrases: New Horizons, pp. 105-120. Eds. Chegwidden WR, Carter ND and Edwards YH, Birkhäuser Verlag, Basel.

Tenan M, Fulci G, Albertoni M, Diserens AC, Hamou MF, El Atifi-Borel M, Feige JJ, Pepper MS and Van Meir EG (2000): Thrombospondin-1 is downregulated by anoxia and suppresses tumorigenicity of human glioblastoma cells. J Exp Med 191:1789-1798.

Thompson JD, Higgins DG and Gibson TJ (1994): CLUSTAL W: improving the sensitivity of progressive multiple sequence alignment through sequence weighting, position-specific gap penalties and weight matrix choice. Nucleic Acids Res 22:4673-4680.

Tu CK, Silverman DN, Forsman C, Jonsson BH and Lindskog S (1989): Role of histidine 64 in the catalytic mechanism of human carbonic anhydrase II studied with a site-specific mutant. Biochemistry 28:7913-7918.

Tureci O, Sahin U, Vollmar E, Siemer S, Gottert E, Seitz G, Parkkila AK, Shah GN, Grubb JH, Pfreundschuh M and Sly WS (1998): Human carbonic anhydrase XII: cDNA cloning, expression, and chromosomal localization of a carbonic anhydrase gene that is overexpressed in some renal cell cancers. Proc Natl Acad Sci U S A 95:7608-7613.

Turner JR, Odze RD, Crum CP and Resnick MB (1997): MN antigen expression in normal, preneoplastic, and neoplastic esophagus: a clinicopathological study of a new cancer-associated biomarker. Hum Pathol 28:740-744.

Uemura H, Nakagawa Y, Yoshida K, Saga S, Yoshikawa K, Hirao Y and Oosterwijk E (1999): MN/CA IX/G250 as a potential target for immunotherapy of renal cell carcinomas. Br J Cancer 81:741-746.

Ulmasov B, Waheed A, Shah GN, Grubb JH, Sly WS, Tu C and Silverman DN (2000): Purification and kinetic analysis of recombinant CA XII, a membrane carbonic anhydrase overexpressed in certain cancers. Proc Natl Acad Sci U S A 97:14212-14217.

Vaananen HK (1984): Immunohistochemical localization of carbonic anhydrase isoenzymes I and II in human bone, cartilage and giant cell tumor. Histochemistry 81:485-487.

Vaananen HK, Paloniemi M and Vuori J (1985): Purification and localization of human carbonic anhydrase. III. Typing of skeletal muscle fibers in paraffin embedded sections. Histochemistry 83:231-235.

Vaananen HK, Syrjala H, Rahkila P, Vuori J, Melamies LM, Myllyla V and Takala TE (1990): Serum carbonic anhydrase III and myoglobin concentrations in acute myocardial infarction. Clin Chem 36:635-638.

Wagner J, Avvaru BS, Robbins AH, Scozzafava A, Supuran CT and McKenna R (2010): Coumarinyl-substituted sulfonamides strongly inhibit several human carbonic anhydrase isoforms: solution and crystallographic investigations. Bioorg Med Chem 18:4873-4878.

van den Beucken T, Koritzinsky M, Niessen H, Dubois L, Savelkouls K, Mujcic H, Jutten B, Kopacek J, Pastorekova S, van der Kogel AJ, Lambin P, Voncken W, Rouschop KM and Wouters BG (2009): Hypoxia-induced expression of carbonic anhydrase 9 is dependent on the unfolded protein response. J Biol Chem 284:24204-24212.

Van Slyke D and Hawkins J (1930): Studies of gas and electrolyte equilibrium in blood. XVI. The evolution of carbon dioxide from blood and buffer solutions. J Biol Chem 87:265-279.

Watson PH, Chia SK, Wykoff CC, Han C, Leek RD, Sly WS, Gatter KC, Ratcliffe P and Harris AL (2003): Carbonic anhydrase XII is a marker of good prognosis in invasive breast carcinoma. Br J Cancer 88:1065-1070.

Venta PJ, Montgomery JC and Tashian RE (1987): Molecular genetics of carbonic anhydrase isozymes. Isozymes Curr Top Biol Med Res 14:59-72.

Vermylen P, Roufosse C, Burny A, Verhest A, Bosschaerts T, Pastorekova S, Ninane V and Sculier JP (1999): Carbonic anhydrase IX antigen differentiates between preneoplastic malignant lesions in non-small cell lung carcinoma. Eur Respir J 14:806-811.

Whitney PL and Briggle TV (1982): Membrane-associated carbonic anhydrase purified from bovine lung. J Biol Chem 257:12056-12059.

Whittington DA, Waheed A, Ulmasov B, Shah GN, Grubb JH, Sly WS and Christianson DW (2001): Crystal structure of the dimeric extracellular domain of human carbonic anhydrase XII, a bitopic membrane protein overexpressed in certain cancer tumor cells. Proc Natl Acad Sci U S A 98:9545-9550.

Wistrand PJ and Knuuttila KG (1989): Renal membrane-bound carbonic anhydrase. Purification and properties. Kidney Int 35:851-859.

Vu H, Pham NB and Quinn RJ (2008): Direct screening of natural product extracts using mass spectrometry. J Biomol Screen 13:265-275.

Vuillemin M and Pexieder T (1997): Carbonic anhydrase II expression pattern in mouse embryonic and fetal heart. Anat Embryol (Berl) 195:267-277.

Vuotikka P, Uusimaa P, Niemela M, Vaananen K, Vuori J and Peuhkurinen K (2003): Serum myoglobin/carbonic anhydrase III ratio as a marker of reperfusion after myocardial infarction. Int J Cardiol 91:137-144.

Wykoff CC, Beasley N, Watson PH, Campo L, Chia SK, English R, Pastorek J, Sly WS, Ratcliffe P and Harris AL (2001): Expression of the hypoxia-inducible and tumor-associated carbonic anhydrases in ductal carcinoma in situ of the breast. Am J Pathol 158:1011-1019.

Wykoff CC, Beasley NJ, Watson PH, Turner KJ, Pastorek J, Sibtain A, Wilson GD, Turley H, Talks KL, Maxwell PH, Pugh CW, Ratcliffe PJ and Harris AL (2000): Hypoxia-inducible expression of tumor-associated carbonic anhydrases. Cancer Res 60:7075-7083.

Xu Y, Feng L, Jeffrey PD, Shi Y and Morel FM (2008): Structure and metal exchange in the cadmium carbonic anhydrase of marine diatoms. Nature 452:56-61.

Yoo CW, Nam BH, Kim JY, Shin HJ, Lim H, Lee S, Lee SK, Lim MC and Song YJ (2010): Carbonic anhydrase XII expression is associated with histologic grade of cervical cancer and superior radiotherapy outcome. Radiat Oncol 5:101.

Yoshiura K, Nakaoka T, Nishishita T, Sato K, Yamamoto A, Shimada S, Saida T, Kawakami Y, Takahashi TA, Fukuda H, Imajoh-Ohmi S, Oyaizu N and Yamashita N (2005): Carbonic anhydrase II is a tumor vessel endothelium-associated antigen targeted by dendritic cell therapy. Clin Cancer Res 11:8201-8207.

Zatovicova M, Sedlakova O, Svastova E, Ohradanova A, Ciampor F, Arribas J, Pastorek J and Pastorekova S (2005): Ectodomain shedding of the hypoxia-induced carbonic anhydrase IX is a metalloprotease-dependent process regulated by TACE/ADAM17. Br J Cancer 93:1267-1276.

Zavada J, Zavadova Z, Pastorek J, Biesova Z, Jezek J and Velek J (2000): Human tumour-associated cell adhesion protein MN/CA IX: identification of M75 epitope and of the region mediating cell adhesion. Br J Cancer 82:1808-1813.

Zavada J, Zavadova Z, Pastorekova S, Ciampor F, Pastorek J and Zelnik V (1993): Expression of MaTu-MN protein in human tumor cultures and in clinical specimens. Int J Cancer 54:268-274.

Zavada J, Zavadova Z, Zat'ovicova M, Hyrsl L and Kawaciuk I (2003): Soluble form of carbonic anhydrase IX (CA IX) in the serum and urine of renal carcinoma patients. Br J Cancer 89:1067-1071.

Zavadova Z and Zavada J (2005): Carbonic anhydrase IX (CA IX) mediates tumor cell interactions with microenvironment. Oncol Rep 13:977-982.

Zhong H, Chiles K, Feldser D, Laughner E, Hanrahan C, Georgescu MM, Simons JW and Semenza GL (2000): Modulation of hypoxia-inducible factor 1alpha expression by the epidermal growth factor/phosphatidylinositol 3-kinase/PTEN/AKT/FRAP pathway in human prostate cancer cells: implications for tumor angiogenesis and therapeutics. Cancer Res 60:1541-1545.

Zhu XL and Sly WS (1990): Carbonic anhydrase IV from human lung. Purification, characterization, and comparison with membrane carbonic anhydrase from human kidney. J Biol Chem 265:8795-8801.

SUPPLEMENTARY DATA

Appendix 1. Genes that display altered mRNA expression in the stomach of *Car9*$^{-/-}$ mice.

FC	P-value	Symbol	Description	GeneBank number	Illumina probe	QRT-PCR
10.46	3.50E-05	Cym	chymosin	NM_001111143	101940433	19.66
8.07	3.10E-05	Slc9a3	solute carrier family 9 (sodium/hydrogen exchanger), member 3	NM_001081060	102760048	10.72
5.95	0.0029	U46068	cDNA sequence U46068, transcript variant 2	NM_153418	2690242	
5.68	8.58E-04	Dmbt1	deleted in malignant brain tumors 1	NM_007769	7050270	5.29
5.38	3.53E-04	Il1rl1	interleukin 1 receptor-like 1, transcript variant 2	NM_010743	6020347	8.95
4.26	0.0010	Tm4sf5	transmembrane 4 superfamily member 5	NM_029360	3120280	
4.19	7.92E-04	9130204L05Rik	RIKEN cDNA 9130204L05 gene	NM_001101461	105360685	
4.11	0.0040	Sftpd	surfactant associated protein D	NM_009160	6510181	3.69
3.81	0.0328	Nccrp1	non-specific cytotoxic cell receptor protein 1 homolog (zebrafish)	NM_001081115	107100301	
3.54	0.0103	Pkp4	plakophilin 4, transcript variant 1	NM_026361	106940451	1.09
3.46	0.1915	Sprr2d	small proline-rich protein 2D	NM_011470	1340458	
3.45	0.0120	Gm14446	predicted gene 14446, transcript variant 2	NM_001101605	103610008	
3.39	0.2717	Sprr3	small proline-rich protein 3	NM_011478	580347	
3.31	0.1199	Sprr2i	small proline-rich protein 2I	NM_011475	6760369	
3.30	0.0238	Sprr1a	small proline-rich protein 1A	NM_009264	3870064	
3.08	0.0482	Ivl	involucrin	NM_008412	105570156	
3.02	0.2987	Serpinb12	serine (or cysteine) peptidase inhibitor, clade B (ovalbumin), member 12	NM_027971	1500671	
3.01	0.2953	Krt10	keratin 10	NM_010660	5340471	
2.94	0.3442	Gm94	predicted gene 94	NM_001033280	102350167	
2.94	0.3850	Krt13	keratin 13	NM_010662	540082	
2.88	0.0188	Gsdmc2	gasdermin C2, transcript variant 2	NM_177912	104730059	
2.84	0.4324	Lor	loricrin	NM_008508	50538	
2.78	0.3322	Dmkn	dermokine, transcript variant 2	NM_172899	3290575	
2.69	0.0319	Ly6d	lymphocyte antigen 6 complex, locus D	NM_010742	4050010	
2.52	0.3413	Krt1	keratin 1	NM_008473	2480050	
2.44	0.0739	Isg15	ISG15 ubiquitin-like modifier	NM_015783	3170093	
2.35	0.1425	Tprg	transformation related protein 63 regulated	NM_175165	6860538	
2.25	0.1958	Mup1	major urinary protein 1	NM_031188	430685	
2.20	0.5002	Asprv1	aspartic peptidase, retroviral-like 1	NM_026414	2650079	
2.16	0.5238	Rptn	repetin	NM_009100	5290605	
2.15	0.1051	Oas1g	2'-5' oligoadenylate synthetase 1G	NM_011852	2450280	
2.15	0.1197	Il33	interleukin 33	NM_133775	6590687	
2.11	0.1306	Trex2	three prime repair exonuclease 2	NM_011907	4920707	
2.11	0.3698	Calm4	calmodulin 4	NM_020036	60026	
2.06	0.2388	Stfa1	stefin A1	NM_001082543	3610451	
2.02	0.5696	Lce3f	late cornified envelope 3F	NM_001018079	540524	
1.99	0.3104	LOC625123	PREDICTED: hypothetical LOC625123	XM_889664	100070280	
1.97	0.1978	Igh-VJ558	PREDICTED: Mus musculus immunoglobulin heavy chain (J558 family)	XM_001472091	1690184	
1.94	0.3578	Hopx	HOP homeobox, transcript variant 1	NM_175606	103850021	
1.92	0.3797	Hrnr	hornerin	NM_133698	780121	
1.90	0.3427	2300005B03Rik	RIKEN cDNA 2300005B03 gene	NM_001081961	3840047	
1.89	0.3648	Klk5	kallikrein related-peptidase 5	NM_026806	102900390	
1.88	0.6306	Flg	PREDICTED: filaggrin	XM_001481265	104760609	
1.84	0.2173	Muc5ac	mucin 5, subtypes A and C, tracheobronchial/gastric	NM_010844	103140592	
1.83	0.4764	Lypd3	Ly6/Plaur domain containing 3	NM_133743	4120288	

1.79	0.3676	9130409I23Rik	RIKEN cDNA 9130409I23 gene	NM_001033819	101660086	
1.79	0.5632	Crct1	cysteine-rich C-terminal 1	NM_028798	2320040	
1.78	0.5372	Lce3c	late cornified envelope 3C	NM_033175	6620451	
1.76	0.3926	Lce3b	late cornified envelope 3B	NM_025501	4810400	
1.76	0.5030	Tacstd2	tumor-associated calcium signal transducer 2	NM_020047	6660341	
1.74	0.3182	Sprr2e	small proline-rich protein 2E	NM_011471	6620100	
1.71	0.3080	S100a8	S100 calcium binding protein A8 (calgranulin A)	NM_013650	70112	
1.70	0.5794	Lce1m	late cornified envelope 1M	NM_025420	5570435	
1.68	0.3971	Cdsn	corneodesmosin	NM_001008424	100510520	
1.67	0.3966	Ephx3	epoxide hydrolase 3	NM_001033163	5270400	
1.66	0.6872	Krt14	keratin 14	NM_016958	2340402	
1.63	0.5522	Lce1f	late cornified envelope 1F	NM_026394	6400593	
1.62	0.4682	LOC620017	PREDICTED: similar to Ig kappa chain V-V region L7 precursor	XM_357633	510347	
1.61	0.3825	Klk10	kallikrein related-peptidase 10	NM_133712	4540050	
1.61	0.4577	Defb4	defensin beta 4	NM_019728	4150600	
1.61	0.4581	LOC677643	PREDICTED: similar to monoclonal antibody BBK-2 heavy chain	XR_031047	6860520	
1.61	0.6711	Lce1b	late cornified envelope 1B	NM_026822	3120619	
1.60	0.4044	Tmem45a	transmembrane protein 45a	NM_019631	100770242	
1.59	0.4663	LOC100047788	PREDICTED: similar to gamma-2a immunoglobulin heavy chain	XR_033948	360113	
1.58	0.3848	Scel	sciellin	NM_022886	3190129	
1.56	0.3694	S100a9	S100 calcium binding protein A9 (calgranulin B)	NM_009114	7050528	
1.55	0.6348	Casp14	caspase 14	NM_009809	6510156	
1.54	0.6474	Mt4	metallothionein 4	NM_008631	4780338	
1.53	0.7142	Lgals7	lectin, galactose binding, soluble 7	NM_008496	100840315	
1.52	0.4422	Klk13	kallikrein related-peptidase 13	NM_001039042	105860372	
1.50	0.5629	2310033E01Rik	RIKEN cDNA 2310033E01 gene	NM_001037143	102630524	
1.49	0.5392	Mlze	melanoma-derived leucine zipper, extra-nuclear factor	NM_031378	106510451	
1.49	0.5536	Klk7	kallikrein related-peptidase 7 (chymotryptic, stratum corneum)	NM_011872	870300	
1.48	0.5780	Lce1i	late cornified envelope 1I	NM_029667	3830348	
1.48	0.6786	Lce1d	late cornified envelope 1D	NM_027137	2350014	
1.47	0.7306	Lce1c	late cornified envelope 1C	NM_028622	1780750	
1.45	0.5631	LOC100047162	PREDICTED: similar to immunoglobulin kappa-chain	XM_001477552	110632	
1.45	0.7460	Kprp	keratinocyte expressed, proline-rich	NM_028629	101980465	
1.44	0.5743	Ighg	PREDICTED: immunoglobulin heavy chain (gamma polypeptide), transcript variant 1	XM_001001076	6040164	
1.44	0.6371	Serpina12	serine (or cysteine) peptidase inhibitor, clade A (alpha-1 antiproteinase, antitrypsin), member 12	NM_026535	1230128	
1.43	0.5255	Ppl	periplakin	NM_008909	2360072	
1.43	0.5562	2310005G13Rik	RIKEN cDNA 2310005G13 gene	NM_183281	3130577	
1.43	0.6134	Stfa2	stefin A2	NM_001082545	104670390	
1.41	0.5788	Pla2g4e	phospholipase A2, group IVE	NM_177845	103610088	
1.41	0.6263	Nmu	neuromedin U	NM_019515	6400025	
1.40	0.5496	Trim29	tripartite motif protein 29	NM_023655	4560369	
-1.53	0.3923	Ins1	insulin I	NM_008386	5220072	
-1.54	0.4151	Hp	haptoglobin	NM_017370	6350068	
-1.66	0.3482	Cxcl13	chemokine (C-X-C motif) ligand 13	NM_018866	6290402	
-1.67	0.3355	Cybrd1	cytochrome b reductase 1	NM_028593	105700114	
-1.76	0.4511	Fbxw5	F-box and WD-40 domain protein 5	NM_013908	4810102	
-1.79	0.3131	Ins2	insulin II	NM_008387	610040	
-1.93	0.1899	Lep	leptin	NM_008493	4010053	
-2.08	0.1208	Dbp	D site albumin promoter binding protein	NM_016974	4200270	
-2.27	0.1201	Gcg	glucagon	NM_008100	6220735	
-2.32	0.1337	Cpa2	carboxypeptidase A2, pancreatic	NM_001024698	100380021	
-2.57	0.3655	Zg16	zymogen granule protein 16	NM_026918	1240338	
-2.65	0.1128	Cyp2e1	cytochrome P450, family 2, subfamily e, polypeptide 1	NM_021282	103290400	
-2.68	0.0501	Slc5a8	solute carrier family 5 (iodide transporter), member 8	NM_145423	6130110	
-2.73	0.1115	Cpb1	carboxypeptidase B1 (tissue)	NM_029706	290600	-18.22
-2.77	0.0270	Bhlha15	basic helix-loop-helix family, member a15	NM_010800	6620020	
-2.91	0.0448	Sycn	syncollin	NM_026716	2570040	
-2.96	0.0180	Gper	G protein-coupled estrogen receptor 1	NM_029771	7570008	
-3.19	0.1251	Ctrl	chymotrypsin-like	NM_023182	2120301	
-3.27	0.0452	Scd1	stearoyl-Coenzyme A desaturase 1	NM_009127	2680441	
-3.32	0.0707	Spink3	serine peptidase inhibitor, Kazal type 3	NM_009258	1580008	

-3.32	0.1116	Cela3b	chymotrypsin-like elastase family, member 3B	NM_026419	4060731	-75.74
-3.36	0.0165	Nrn1	neuritin 1	NM_153529	4230471	
-3.37	0.0137	EG640530	PREDICTED: predicted gene, EG640530	XM_917532	70601	
-3.41	0.0049	LOC100043836	PREDICTED: similar to lacrimal androgen-binding protein delta, transcript variant 1	XM_001481113	2360497	
-3.48	0.1086	LOC638418	PREDICTED: similar to Ela3 protein	XM_914439	3990711	
-3.52	0.0468	Chia	chitinase, acidic	NM_023186	5390131	
-3.64	0.0046	Slc38a5	solute carrier family 38, member 5	NM_172479	540093	
-3.67	0.0037	Abpg	androgen binding protein gamma	NM_178308	1660577	
-3.68	0.0046	Egf	epidermal growth factor	NM_010113	5220154	-3.71
-3.72	0.0519	Car3	carbonic anhydrase 3	NM_007606	870687	-15.39
-3.74	0.0515	Adipoq	adiponectin, C1Q and collagen domain containing	NM_009605	6590519	-20.51
-3.80	0.0048	Slc27a2	solute carrier family 27 (fatty acid transporter), member 2	NM_011978	104480458	
-3.95	0.1154	Cpa1	carboxypeptidase A1	NM_025350	4730022	
-4.07	0.0049	Tmed6	transmembrane emp24 protein transport domain containing 6	NM_025458	6510048	
-4.17	0.0033	Sostdc1	sclerostin domain containing 1	NM_025312	6760017	
-4.30	0.0084	Mug1	murinoglobulin 1	NM_008645	3170497	
-5.00	0.1227	Ctrb1	chymotrypsinogen B1	NM_025583	1050347	
-5.35	0.0451	Cfd	complement factor D (adipsin)	NM_013459	2320736	-27.45
-6.23	0.0192	Pnlip	pancreatic lipase	NM_026925	6450341	-23.88
-6.27	5.80E-04	Blm	bloom syndrome homolog (human), transcript variant 1	NM_007550	520619	
-7.04	0.0011	Gdf9	growth differentiation factor 9	NM_008110	2350181	
-7.12	0.0024	Gm12888	predicted gene 12888	NM_001033791	102060176	
-7.59	0.0153	Cela2a	chymotrypsin-like elastase family, member 2A	NM_007919	5270129	-16.23
-9.85	1.45E-04	Amy2a5	amylase 2a5, pancreatic	NM_001042711	580138	
-10.57	9.60E-05	Prss1	protease, serine, 1 (trypsin 1)	NM_053243	6370400	
-12.14	1.02E-04	Try4	trypsin 4	NM_011646	5860044	

Appendix 2. Functional annotation of genes disregulated in the stomach of *Car9* knockout mice.

Functional category	Gene symbol	Description	GenBank number	FC	P-value
Developmental processes	Dmbt1	deleted in malignant brain tumors 1	NM_007769	5.68	0.0009
	Sftpd	surfactant associated protein d	NM_009160	4.11	0.0040
(Contains the following categories:	Sprr2d	small proline-rich protein 2d	NM_011470	3.46	0.1915
Epidermis morphogenesis	Sprr3	small proline-rich protein 3	NM_011478	3.39	0.2717
Tissue morphogenesis	Sprr2i	small proline-rich protein 2i	NM_011475	3.31	0.1199
Epidermis development	Sprr1a	small proline-rich protein 1a	NM_009264	3.30	0.0238
Ectoderm development	Lor	loricrin	NM_008508	2.84	0.4324
Tissue development	Hopx	HOP homeobox, transcript variant 1	NM_175606	1.94	0.3578
Organ development	Hrnr	hornerin	NM_133698	1.92	0.3797
Anatomical structure development	Sprr2e	small proline-rich protein 2e	NM_011471	1.74	0.3182
Anatomical structure morphogenesis	Krt14	keratin 14	NM_016958	1.66	0.6872
Cellular developmental process	Scel	sciellin	NM_022886	1.58	0.3848
Multicellular organismal	Lgals7	lectin, galactose binding, soluble 7	NM_008496	1.53	0.7142
development	Cxcl13	chemokine (c-x-c motif) ligand 13	NM_018866	-1.66	0.3482
Epidermal cell differentiation)	Lep	leptin	NM_008493	-1.93	0.1899
	Bhlha15	basic helix-loop-helix family, member a15	NM_010800	-2.77	0.0270
	Nrn1	neuritin 1	NM_153529	-3.36	0.0165
	Egf	epidermal growth factor	NM_010113	-3.68	0.0046
	Sostdc1	sclerostin domain containing 1	NM_025312	-4.17	0.0033
	Blm	bloom syndrome homolog (human), transcript variant 1	NM_007550	-6.27	0.0006
Keratinization and keratinocyte	Sprr2d	small proline-rich protein 2d	NM_011470	3.46	0.1915
differentiation	Sprr3	small proline-rich protein 3	NM_011478	3.39	0.2717
	Sprr2i	small proline-rich protein 2i	NM_011475	3.31	0.1199
	Sprr1a	small proline-rich protein 1a	NM_009264	3.30	0.0238
	Lor	loricrin	NM_008508	2.84	0.4324
	Hrnr	hornerin	NM_133698	1.92	0.3797
	Sprr2e	small proline-rich protein 2e	NM_011471	1.74	0.3182
	Scel	sciellin	NM_022886	1.58	0.3848
Structural molecule activity	Pkp4	plakophilin 4, transcript variant 1	NM_026361	3.54	0.0103
	Sprr2d	small proline-rich protein 2d	NM_011470	3.46	0.1915
	Sprr3	small proline-rich protein 3	NM_011478	3.39	0.2717
	Sprr2i	small proline-rich protein 2i	NM_011475	3.31	0.1199
	Sprr1a	small proline-rich protein 1a	NM_009264	3.30	0.0238
	Krt10	keratin 10	NM_010660	3.01	0.2953
	Krt13	keratin 13	NM_010662	2.94	0.3850
	Lor	loricrin	NM_008508	2.84	0.4324
	Krt1	keratin 1	NM_008473	2.52	0.3413
	Hrnr	hornerin	NM_133698	1.92	0.3797
	Rptn	repetin	NM_009100	1.79	0.5020
	Sprr2e	small proline-rich protein 2e	NM_011471	1.74	0.3182
	Krt14	keratin 14	NM_016958	1.66	0.6872
Embryo implantation, female	Sprr2d	small proline-rich protein 2d	NM_011470	3.46	0.1915
pregnancy, and menstrual cycle	Sprr2i	small proline-rich protein 2i	NM_011475	3.31	0.1199
	Sprr2e	small proline-rich protein 2e	NM_011471	1.74	0.3182
Rhythmic process	Sprr2d	small proline-rich protein 2d	NM_011470	3.46	0.1915
	Sprr2i	small proline-rich protein 2i	NM_011475	3.31	0.1199
	Sprr2e	small proline-rich protein 2e	NM_011471	1.74	0.3182
	Dbp	d site albumin promoter binding protein	NM_016974	-2.08	0.1208
Multi-organism process	Sprr2d	small proline-rich protein 2d	NM_011470	3.46	0.1915
	Sprr2i	small proline-rich protein 2i	NM_011475	3.31	0.1199
	Isg15	ISG15 ubiquitin-like modifier	NM_015783	2.44	0.0739
	Sprr2e	small proline-rich protein 2e	NM_011471	1.74	0.3182
	Defb4	defensin beta 4	NM_019728	1.61	0.4577
Cell differentiation	Dmbt1	deleted in malignant brain tumors 1	NM_007769	5.68	0.0009
	Sprr2d	small proline-rich protein 2d	NM_011470	3.46	0.1915

	Sprr3	small proline-rich protein 3	NM_011478	3.39	0.2717
	Sprr2i	small proline-rich protein 2i	NM_011475	3.31	0.1199
	Sprr1a	small proline-rich protein 1a	NM_009264	3.30	0.0238
	Lor	loricrin	NM_008508	2.84	0.4324
	Hopx	HOP homeobox, transcript variant 1	NM_175606	1.94	0.3578
	Hrnr	hornerin	NM_133698	1.92	0.3797
	Sprr2e	small proline-rich protein 2e	NM_011471	1.74	0.3182
	Scel	sciellin	NM_022886	1.58	0.3848
	Casp14	caspase 14	NM_009809	1.55	0.6348
	Lgals7	lectin, galactose binding, soluble 7	NM_008496	1.53	0.7142
	Lep	leptin	NM_008493	-1.93	0.1899
	Bhlha15	basic helix-loop-helix family, member a15	NM_010800	-2.77	0.0270
	Nrn1	neuritin 1	NM_153529	-3.36	0.0165
	Blm	bloom syndrome homolog (human), transcript variant 1	NM_007550	-6.27	0.0006
Serine-type endopeptidase activity, serine hydrolase activity, and serine-type peptidase activity	Klk10	kallikrein related-peptidase 10	NM_133712	1.61	0.3825
	Klk13	kallikrein related-peptidase 13	NM_001039042	1.52	0.4422
	Klk7	kallikrein related-peptidase 7 (chymotryptic, stratum corneum)	NM_011872	1.49	0.5536
	Ctrl	chymotrypsin-like	NM_023182	-3.19	0.1251
	Cela3b	chymotrypsin-like elastase family, member 3B	NM_026419	-3.32	0.1116
	Ctrb1	chymotrypsinogen B1	NM_025583	-5.00	0.1227
	Cfd	complement factor D (adipsin)	NM_013459	-5.35	0.0451
	Cela2a	chymotrypsin-like elastase family, member 2A	NM_007919	-7.59	0.0153
	Try4	trypsin 4	NM_011646	-12.14	0.0001
Proteolysis	Isg15	ISG15 ubiquitin-like modifier	NM_015783	2.44	0.0739
	9130409I23Rik	RIKEN cDNA 9130409I23 gene	NM_001033819	1.79	0.3676
	Klk10	kallikrein related-peptidase 10	NM_133712	1.61	0.3825
	Casp14	caspase 14	NM_009809	1.55	0.6348
	Klk13	kallikrein related-peptidase 13	NM_001039042	1.52	0.4422
	Klk7	kallikrein related-peptidase 7 (chymotryptic, stratum corneum)	NM_011872	1.49	0.5536
	Cpa2	carboxypeptidase A2, pancreatic	NM_001024698	-2.32	0.1337
	Cpb1	carboxypeptidase B1 (tissue)	NM_029706	-2.73	0.1115
	Ctrl	chymotrypsin-like	NM_023182	-3.19	0.1251
	Cela3b	chymotrypsin-like elastase family, member 3B	NM_026419	-3.32	0.1116
	Cpa1	carboxypeptidase A1	NM_025350	-3.95	0.1154
	Ctrb1	chymotrypsinogen B1	NM_025583	-5.00	0.1227
	Cfd	complement factor D (adipsin)	NM_013459	-5.35	0.0451
	Cela2a	chymotrypsin-like elastase family, member 2A	NM_007919	-7.59	0.0153
	Try4	trypsin 4	NM_011646	-12.14	0.0001
Peptidase activity	9130409I23Rik	RIKEN cDNA 9130409I23 gene	NM_001033819	1.79	0.3676
	Klk10	kallikrein related-peptidase 10	NM_133712	1.61	0.3825
	Casp14	caspase 14	NM_009809	1.55	0.6348
	Klk13	kallikrein related-peptidase 13	NM_001039042	1.52	0.4422
	Klk7	kallikrein related-peptidase 7 (chymotryptic, stratum corneum)	NM_011872	1.49	0.5536
	Cpa2	carboxypeptidase A2, pancreatic	NM_001024698	-2.32	0.1337
	Cpb1	carboxypeptidase B1 (tissue)	NM_029706	-2.73	0.1115
	Ctrl	chymotrypsin-like	NM_023182	-3.19	0.1251
	Cela3b	chymotrypsin-like elastase family, member 3B	NM_026419	-3.32	0.1116
	Cpa1	carboxypeptidase A1	NM_025350	-3.95	0.1154
	Ctrb1	chymotrypsinogen B1	NM_025583	-5.00	0.1227
	Cfd	complement factor D (adipsin)	NM_013459	-5.35	0.0451
	Cela2a	chymotrypsin-like elastase family, member 2A	NM_007919	-7.59	0.0153
	Try4	trypsin 4	NM_011646	-12.14	0.0001
Endopeptidase activity	Klk10	kallikrein related-peptidase 10	NM_133712	1.61	0.3825
	Casp14	caspase 14	NM_009809	1.55	0.6348
	Klk13	kallikrein related-peptidase 13	NM_001039042	1.52	0.4422
	Klk7	kallikrein related-peptidase 7 (chymotryptic, stratum corneum)	NM_011872	1.49	0.5536
	Ctrl	chymotrypsin-like	NM_023182	-3.19	0.1251
	Cela3b	chymotrypsin-like elastase family, member 3B	NM_026419	-3.32	0.1116
	Ctrb1	chymotrypsinogen B1	NM_025583	-5.00	0.1227

	Cfd	complement factor D (adipsin)	NM_013459	-5.35	0.0451
	Cela2a	chymotrypsin-like elastase family, member 2A	NM_007919	-7.59	0.0153
	Try4	trypsin 4	NM_011646	-12.14	0.0001
Trypsin and chymotrypsin activity	Klk10	kallikrein related-peptidase 10	NM_133712	1.61	0.3825
	Ctrl	chymotrypsin-like	NM_023182	-3.19	0.1251
	Cela3b	chymotrypsin-like elastase family, member 3B	NM_026419	-3.32	0.1116
	Ctrb1	chymotrypsinogen B1	NM_025583	-5.00	0.1227
Hydrolase activity	Trex2	three prime repair exonuclease 2	NM_011907	2.11	0.1306
	9130409I23Rik	RIKEN cDNA 9130409I23 gene	NM_001033819	1.79	0.3676
	Ephx3	epoxide hydrolase 3	NM_001033163	1.67	0.3966
	Klk10	kallikrein related-peptidase 10	NM_133712	1.61	0.3825
	Casp14	caspase 14	NM_009809	1.55	0.6348
	Klk13	kallikrein related-peptidase 13	NM_001039042	1.52	0.4422
	Klk7	kallikrein related-peptidase 7 (chymotryptic, stratum corneum)	NM_011872	1.49	0.5536
	Pla2g4e	phospholipase A2, group IVE	NM_177845	1.41	0.5788
	Cpa2	carboxypeptidase A2, pancreatic	NM_001024698	-2.32	0.1337
	Cpb1	carboxypeptidase B1 (tissue)	NM_029706	-2.73	0.1115
	Ctrl	chymotrypsin-like	NM_023182	-3.19	0.1251
	Cela3b	chymotrypsin-like elastase family, member 3B	NM_026419	-3.32	0.1116
	Chia	chitinase, acidic	NM_023186	-3.52	0.0468
	Cpa1	carboxypeptidase A1	NM_025350	-3.95	0.1154
	Ctrb1	chymotrypsinogen B1	NM_025583	-5.00	0.1227
	Cfd	complement factor D (adipsin)	NM_013459	-5.35	0.0451
	Pnlip	pancreatic lipase	NM_026925	-6.23	0.0192
	Blm	bloom syndrome homolog (human), transcript variant 1	NM_007550	-6.27	0.0006
	Gm12888	predicted gene 12888	NM_001033791	-7.12	0.0024
	Cela2a	chymotrypsin-like elastase family, member 2A	NM_007919	-7.59	0.0153
	Amy2a5	amylase 2a5, pancreatic	NM_001042711	-9.85	0.0001
	Try4	trypsin 4	NM_011646	-12.14	0.0001
Structural constituent of cytoskeleton	Krt10	keratin 10	NM_010660	3.01	0.2953
	Krt13	keratin 13	NM_010662	2.94	0.3850
	Lor	loricrin	NM_008508	2.84	0.4324
	Krt1	keratin 1	NM_008473	2.52	0.3413
	Krt14	keratin 14	NM_016958	1.66	0.6872
Cell communication	Krt10	keratin 10	NM_010660	3.01	0.2953
	Krt13	keratin 13	NM_010662	2.94	0.3850
	Krt1	keratin 1	NM_008473	2.52	0.3413
	Krt14	keratin 14	NM_016958	1.66	0.6872
Metallocarboxypeptidase activity, carboxypeptidase activity, and metalloexopeptidase activity	Cpa2	carboxypeptidase A2, pancreatic	NM_001024698	-2.32	0.1337
	Cpb1	carboxypeptidase B1 (tissue)	NM_029706	-2.73	0.1115
	Cpa1	carboxypeptidase A1	NM_025350	-3.95	0.1154
Serine-type endopeptidase inhibitor activity, endopeptidase inhibitor activity, and protease inhibitor activity	Serpinb12	serine (or cysteine) peptidase inhibitor, clade B (ovalbumin), member 12	NM_027971	3.02	0.2987
	Serpina12	serine (or cysteine) peptidase inhibitor, clade A (alpha-1 antiproteinase, antitrypsin), member 12	NM_026535	1.44	0.6371
	Spink3	serine peptidase inhibitor, Kazal type 3	NM_009258	-3.32	0.0707
	Mug1	murinoglobulin 1	NM_008645	-4.30	0.0084
Taxis and chemotaxis	Sftpd	surfactant associated protein d	NM_009160	4.11	0.0040
	S100a8	S100 calcium binding protein A8 (calgranulin A)	NM_013650	1.71	0.3080
	S100a9	S100 calcium binding protein A9 (calgranulin B)	NM_009114	1.56	0.3694
	Cxcl13	chemokine (c-x-c motif) ligand 13	NM_018866	-1.66	0.3482
Response to external stimulus	Sftpd	surfactant associated protein d	NM_009160	4.11	0.0040
	Hopx	HOP homeobox, transcript variant 1	NM_175606	1.94	0.3578
	S100a8	S100 calcium binding protein A8 (calgranulin A)	NM_013650	1.71	0.3080
	S100a9	S100 calcium binding protein A9 (calgranulin B)	NM_009114	1.56	0.3694
	Cxcl13	chemokine (c-x-c motif) ligand 13	NM_018866	-1.66	0.3482
	Lep	leptin	NM_008493	-1.93	0.1899
	Cfd	complement factor D (adipsin)	NM_013459	-5.35	0.0451

Immune system process	Il1rl1	interleukin 1 receptor-like 1, transcript variant 2	NM_010743	5.38	0.0004
	Sftpd	surfactant associated protein d	NM_009160	4.11	0.0040
	Isg15	ISG15 ubiquitin-like modifier	NM_015783	2.44	0.0739
	Oas1g	2'-5' oligoadenylate synthetase 1G	NM_011852	2.15	0.1051
	S100a9	S100 calcium binding protein A9 (calgranulin B)	NM_009114	1.56	0.3694
	Cxcl13	chemokine (c-x-c motif) ligand 13	NM_018866	-1.66	0.3482
	Lep	leptin	NM_008493	-1.93	0.1899
	Cfd	complement factor D (adipsin)	NM_013459	-5.35	0.0451
	Blm	bloom syndrome homolog (human), transcript variant 1	NM_007550	-6.27	0.0006
	Cela2a	chymotrypsin-like elastase family, member 2A	NM_007919	-7.59	0.0153
Defense response	Il1rl1	interleukin 1 receptor-like 1, transcript variant 2	NM_010743	5.38	0.0004
	Sftpd	surfactant associated protein d	NM_009160	4.11	0.0040
	Ly6d	lymphocyte antigen 6 complex, locus D	NM_010742	2.69	0.0319
	Tacstd2	tumor-associated calcium signal transducer 2	NM_020047	1.76	0.5030
	Defb4	defensin beta 4	NM_019728	1.61	0.4577
	Cxcl13	chemokine (c-x-c motif) ligand 13	NM_018866	-1.66	0.3482
	Cfd	complement factor D (adipsin)	NM_013459	-5.35	0.0451
Positive regulation of cell differentiation	Dmbt1	deleted in malignant brain tumors 1	NM_007769	5.68	0.0009
	Hopx	HOP homeobox, transcript variant 1	NM_175606	1.94	0.3578
	Lep	leptin	NM_008493	-1.93	0.1899
PPAR signaling pathway	Scd1	stearoyl-Coenzyme A desaturase 1	NM_009127	-3.27	0.0452
	Adipoq	adiponectin, C1Q and collagen domain containing	NM_009605	-3.74	0.0515
	Slc27a2	solute carrier family 27 (fatty acid transporter), member 2	NM_011978	-3.80	0.0048
Leukocyte migration	Sftpd	surfactant associated protein d	NM_009160	4.11	0.0040
	S100a9	S100 calcium binding protein A9 (calgranulin B)	NM_009114	1.56	0.3694
	Cela2a	chymotrypsin-like elastase family, member 2A	NM_007919	-7.59	0.0153

ORIGINAL COMMUNICATIONS

BMC Developmental Biology

BioMed Central

Research article

Expression of carbonic anhydrases IX and XII during mouse embryonic development

Heini Kallio[1], Silvia Pastorekova[2], Jaromir Pastorek[2], Abdul Waheed[3], William S Sly[3], Susanna Mannisto[4], Markku Heikinheimo[4,5] and Seppo Parkkila*[1,6]

Address: [1]Institute of Medical Technology, University of Tampere and Tampere University Hospital, Biokatu 8, FIN-33520 Tampere, Finland, [2]Center of Molecular Medicine, Institute of Virology, Slovak Academy of Sciences, Bratislava, Slovak Republic, [3]Edward A. Doisy Department of Biochemistry and Molecular Biology, Saint Louis University School of Medicine, St. Louis, Missouri, USA, [4]Children's Hospital and Program for Developmental and Reproductive Biology, University of Helsinki, Helsinki, Finland, [5]Department of Pediatrics, Washington University, St. Louis, Missouri, USA and [6]Department of Clinical Chemistry, University of Oulu, Oulu, Finland

Email: Heini Kallio - heini.kallio@uta.fi; Silvia Pastorekova - virusipa@savba.sk; Jaromir Pastorek - virupast@savba.sk; Abdul Waheed - waheeda@slu.edu; William S Sly - slyws@slu.edu; Susanna Mannisto - susanna.mannisto@helsinki.fi; Markku Heikinheimo - markku.heikinheimo@helsinki.fi; Seppo Parkkila* - seppo.parkkila@uta.fi

* Corresponding author

Published: 23 May 2006

BMC Developmental Biology 2006, **6**:22 doi:10.1186/1471-213X-6-22

Received: 14 March 2006
Accepted: 23 May 2006

This article is available from: http://www.biomedcentral.com/1471-213X/6/22

Abstract

Background: Of the thirteen active carbonic anhydrase (CA) isozymes, CA IX and XII have been linked to carcinogenesis. It has been suggested that these membrane-bound CAs participate in cancer cell invasion, which is facilitated by an acidic tumor cell environment. Since active cell migration is a characteristic feature of embryonic development, we set out to explore whether these isozymes are expressed in mouse embryos of different ages. The studies were focused on organogenesis stage.

Results: Immunohistochemistry demonstrated that both CA IX and XII are present in several tissues of the developing mouse embryo during organogenesis. Staining for CA IX revealed a relatively wide distribution pattern with moderate signals in the brain, lung, pancreas and liver and weak signals in the kidney and stomach. The expression pattern of CA XII in the embryonic tissues was also relatively broad, although the intensity of immunostaining was weak in most tissues. The CA XII-positive tissues included the brain, where the most prominent staining was seen in the choroid plexus, and the stomach, pancreas, liver and kidney.

Conclusion: Membrane-bound CA isozymes IX and XII are expressed in various tissues during mouse organogenesis. These enzymes may regulate ion and pH homeostasis within the developing embryo.

Background

The carbonic anhydrases (CAs) are a group of zinc-containing metalloenzymes that catalyse the reversible hydration of carbon dioxide in a reaction $CO_2 + H_2O \leftrightarrow H^+ + HCO_3^-$. They are produced in a variety of tissues, where they play important roles in a number of biological processes such as acid-base balance, respiration, carbon dioxide and ion transport, bone resorption, ureagenesis, gluconeogenesis, lipogenesis

and body fluid generation [1-3]. Thirteen enzymatically active alpha CAs have been reported in mammals so far, of which CA I, II, III, VII, and XIII are cytoplasmic [4], CA IV, IX, XII, XIV, and XV are anchored to plasma membranes [5-8], CA VA and VB are mitochondrial [9], and CA VI is the only secretory form, present in saliva and milk [10,11].

Of the thirteen active isozymes, CA IX and XII have been linked to neoplastic invasion [12,13]. Both are transmembrane proteins. CA IX is composed of four domains: an N-terminal proteoglycan domain, a CA catalytic domain, a transmembrane region and a short cytoplasmic tail [14]. It is a highly active enzyme, and its activity can be efficiently inhibited by sulfonamides [15-19]. In addition to its enzyme activity and role in pH control, CA IX is a cell adhesion molecule and may also contribute to cell proliferation [20-22]. The distribution of CA IX has been studied in adult human, rat and mouse tissues [5,23]. The most abundant expression of CA IX was observed in the human alimentary tract, particularly in the mucosa of the stomach and gallbladder, and it was also detected in the ileum, colon, liver and pancreas. In mouse tissues, the highest immunoreactivity for CA IX was reported in the gastric mucosa, while moderate signals were also seen in the colon and brain and lower expression in some other tissues, including the pancreas and various segments of the small intestine. CA IX is ectopically expressed at relatively high levels and with a high prevalence in some tumor tissues whose normal counterparts do not contain this protein, e.g. carcinomas of the cervix uteri, esophagus, kidney, lung and breast [24-29]. On the other hand, tumors originating from tissues with high natural CA IX expression, such as the stomach and gallbladder, often lose some or all of their CA IX upon conversion to carcinomas [30-32].

CA XII contains an N-terminal extracellular domain, a putative transmembrane α-helix and a small intracellular C-terminal segment with potential phosphorylation sites [6,14,33]. Its expression has been demonstrated by immunohistochemistry in the adult human kidney, colon, prostate, pancreas, ovary, testis, lung and brain [34,35], and the enzyme has been localized to the basolateral plasma membranes of the epithelial cells [36-38]. In the human kidney, CA XII is confined to the proximal and distal tubules and the principal cells of the collecting duct [39]. In mouse tissues it is most abundant in the kidney [40] and the surface epithelial cells of the colon [41]. CA XII expression also shows a clear association with certain tumors, being overexpressed in renal cancer cells, for example [6].

One characteristic feature of embryonic development is active cell migration from one place to another. Although this clearly represents a benign process, it has some mechanistic similarities to cancer cell invasion [42,43], e.g. the fact that the moving cells invade through the extracellular matrix. Since CA IX and XII probably participate in neoplastic invasion, we set out to explore how these isozymes are expressed during embryonic development.

Results and discussion

Immunohistochemical staining of CA IX revealed a relatively wide distribution pattern, although the signal intensity most often remained low or moderate. The E7.5 embryos, representing a gastrulation stage, were completely negative (Figure 1). CA IX expression in the various tissues during organogenesis is summarized in Table 1. The protein was present in the developing brain at all ages

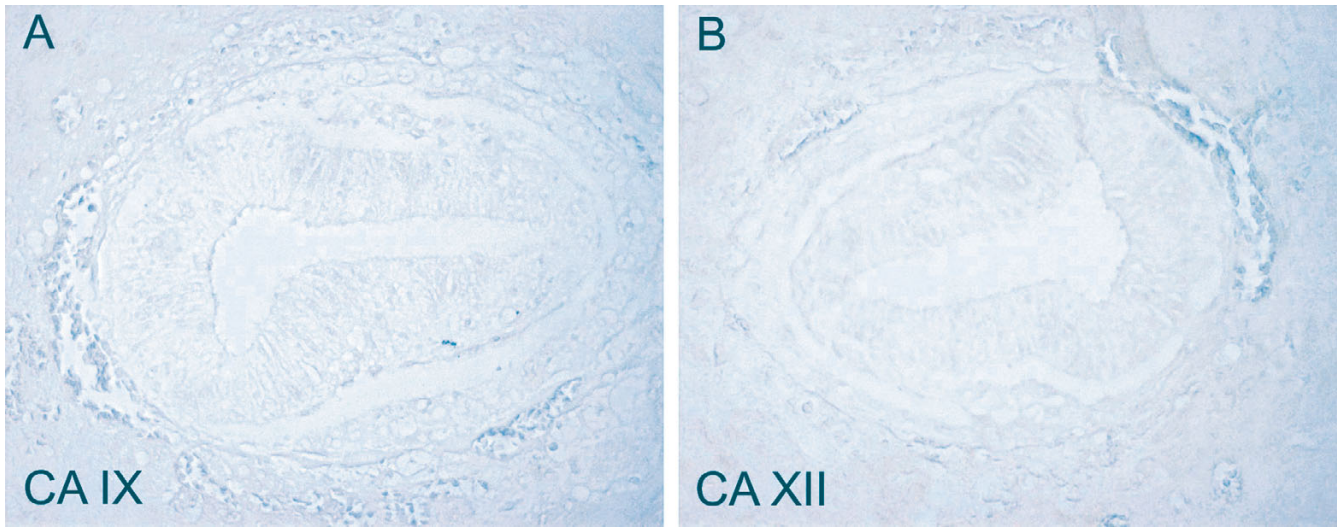

Figure 1
Immunostaining of CA IX and CA XII in the embryos at E7.5. No immunoreaction is detected for either CA IX (A) or CA XII (B). Original magnifications: × 400.

Table 1: Distribution of CA IX in mouse embryonic tissues of different age.*

Organ	E11.5	E12.5	E13.5
Brain	++	++	++
Heart (ventricle/atrium)	+/++	++/++	+/++
Lung	ND	++	+
Kidney	-	+	+
Pancreas	ND	++	ND
Liver	+	++	++
Stomach	+	+	+
Intestine	+	++	+

* Scores in immunohistochemistry: strong reaction (+++), moderate reaction (++), weak reaction (+), no reaction (-), not done (ND).

studied (Figure 2). The brain tissue was stained moderately, and some positivity was occasionally observed in cells present in the mesenchyme beneath the developing brain (data not shown). Moderate staining was also seen in the nerve ganglia and choroid plexus (Figure 2). No immunoreaction for CA IX was detected in the kidney at E11.5, whereas a weak positive signal appeared at E12.5 (Figure 3). The developing pancreas showed a moderate positive reaction at E12.5, which was primarily seen in the basolateral plasma membrane and intracellular compartment of the epithelial cells (Figure 4). Weak staining for CA IX was present in the stomach at all ages studied (Figure 5). This is in accordance with the finding that CA IX is functionally important for a normal gastric histological structure [44]. The liver also showed positive immunostaining in scattered cells (Figure 5). Positive labeling was seen in the lung and heart, tissues not expressing the protein in the adult mouse (data not shown). It is notable, however, that the adult heart tissue also gave a slight positive signal with the automated immunostaining method, even though it has been previously considered negative for CA IX [23].

The expression pattern of CA XII in embryonic tissues was also relatively broad, although the staining intensity was weak in most tissues. The E7.5 embryos showed no immunoreaction (Figure 1). Results at later stages are summarized in Table 2. CA XII protein was expressed in the brain and nerve ganglia at every subsequent age during organogenesis (Figure 2), most prominently in the choroid plexus at E12.5 and E13.5 (Figure 2), i.e. at the time when the developing choroid plexus usually becomes visible. Interestingly, a weak signal for CA XII was detected in several embryonic tissues, including the stomach (Figure 5), pancreas (Figure 4) and liver (Figure 5), which are all negative in adult mice [41]. No staining was detected in the stomach at E11.5, while a weak positive signal appeared there at E12.5. The liver showed weak or moderate staining for CA XII during organogenesis. It is notable that even though CA XII is highly expressed in the adult mouse kidney, the embryonic kidney showed only a weak signal (Figure 3). Weak immunostaining was also seen in the pancreas, where just a few of the developing ducts were positive (Figure 4). In the heart, the staining became stronger during mouse development (data not shown), but as with CA IX, the specificity of CA XII immunostaining is questionable in this particular organ. However, the control stainings using normal rabbit serum instead of the anti-CA IX or anti-CA XII serum gave no positive signals.

CA IX and XII are distinct CA isozymes in that they are overexpressed in certain tumors and subjected to regulation by the von Hippel Lindau tumor suppressor protein/hypoxia pathway [35,45]. In developing embryo, the expression patterns of CA IX and CA XII may also be related to the presence of hypoxia, which is considered essential for proper morphogenesis of various tissues [46]. Hypoxia appears important particularly for development of the brain, myocardial vascularization, lung branching morphogenesis, formation of mesoderm and establishment of various progenitor cells [47-49].

The high catalytic activities of CA IX and XII support their role in acidification of the tumor microenvironment, which in turn facilitates the migration of tumor cells through the extracellular matrix [12,13]. The question is whether CA IX and XII also participate in cell migration during embryonic development. Although the present results provide no functional evidence that CA IX or XII is involved in cell migration during embryogenesis, they do indicate that several cell types in the mouse embryo express these isozymes. Interestingly, both isozymes were present though at quite low level in some embryonic tissues whose adult counterparts do not express these particular proteins or the expression is very low. These findings contrast with prior studies on the developmental regulation of CA IV. This isozyme, like many of the cytosolic isozymes, is expressed at much lower levels in most tissues of the embryo than are found in the adult [50,51].

Conclusion

Membrane-bound CA isozymes IX and XII are expressed in several tissues of developing mouse embryo. As membrane-bound CAs with an extracellular active site, CA IX and XII represent key enzymes in the maintenance of an appropriate pH in the extracellular milieu. Future studies should therefore be focused on exploring how strictly pH homeostasis is regulated in a developing embryo and what are the possible structural or functional consequences if this homeostasis is disrupted.

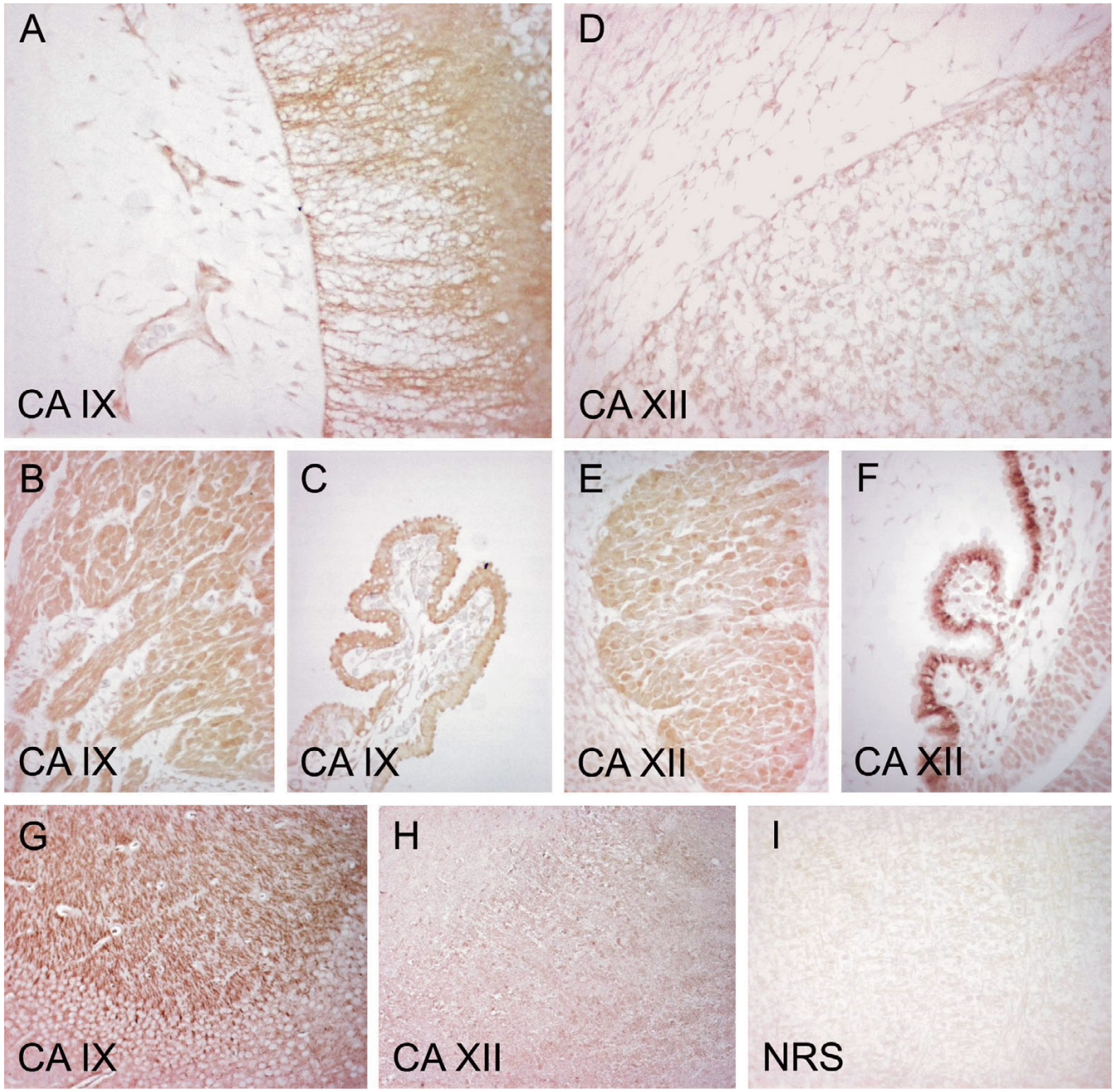

Figure 2
Immunostaining of CA IX and CA XII in embryonic and adult mouse nervous tissues. All embryos are aged E12.5 except the choroid plexus for CA XII, which is aged E13.5. CA IX shows moderate staining in the embryonic brain (A), with the signal mainly located in the neurons. CA IX is also present in the trigeminal ganglion (B) and the choroid plexus (C). Panel G shows strong positive staining for CA IX in the adult brain. CA XII gives weak staining in the embryonic brain (D), but panel E shows moderate staining in the trigeminal ganglion. The strongest immunoreaction is located in the chroid plexus (F). No specific signal for CA XII is detectable in the adult brain (H) except for the choroid plexus (data not shown). Control immunostaining of the embryonic brain with normal rabbit serum is negative (I). Manual PAP staining in panels A-E and I, automated immunostaining in panels F-H. Original magnifications: A-E, I × 400, F × 630, G-H × 200.

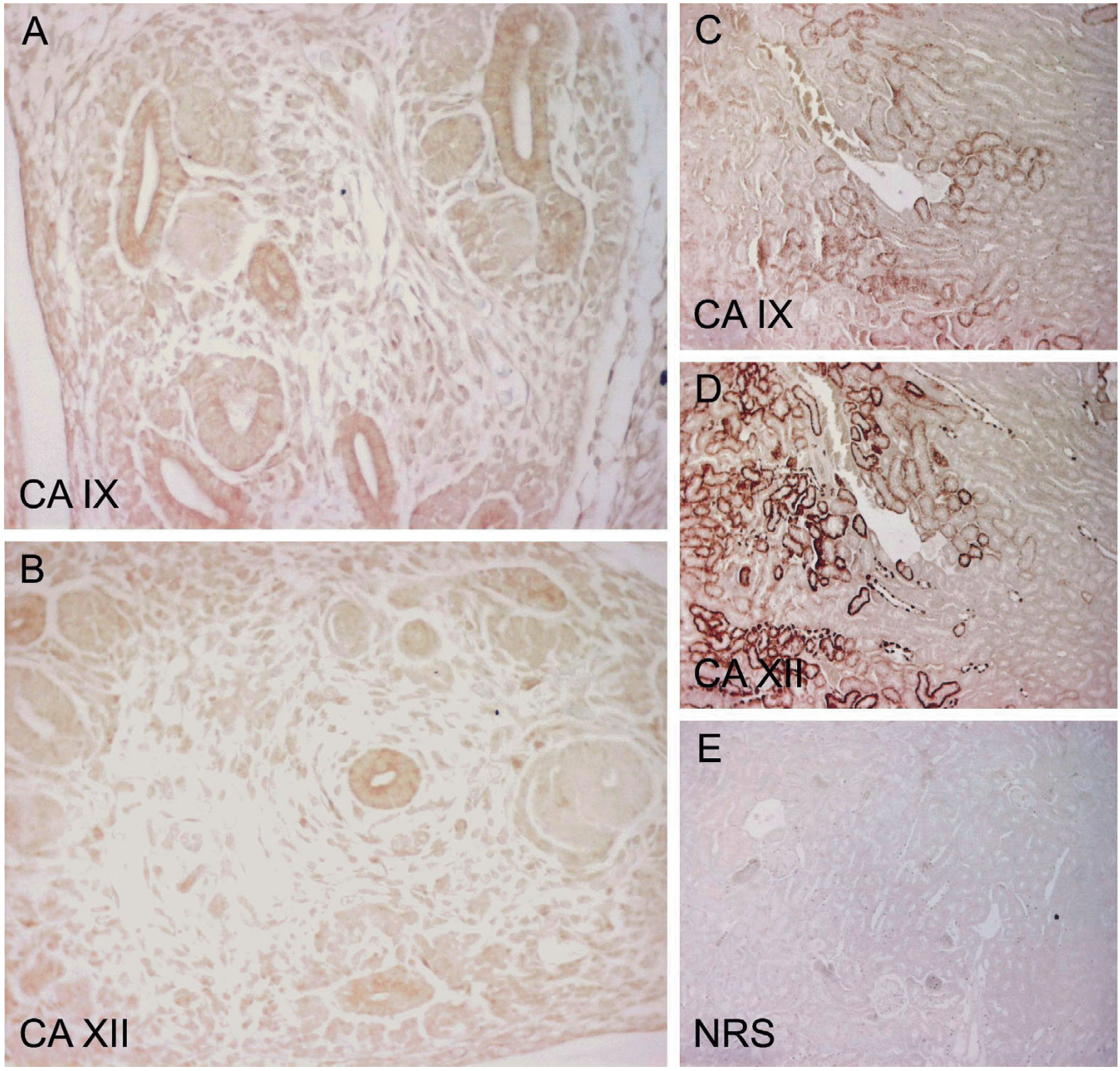

Figure 3
Immunostaining of CA IX and CA XII in the kidney of E12.5 mouse embryos and in the adult mouse kidney. Both CA IX (A) and CA XII (B) show weak staining in the ductal epithelium of the embryonic tissue, and a positive immunoreaction is seen for both isozymes in the adult mouse renal tubules (C, D), with CA XII also located in the collecting ducts. Control immunostaining of an adult mouse kidney with NRS gave no positive signal (E). Manual PAP staining in panels A-B and E, automated immunostaining in panels C-D. Original magnifications: A-B × 400, C-E × 100.

Methods

Antibodies

Polyclonal rabbit antibodies to mouse CA IX and CA XII have been described earlier [40,44]. Non-immune normal rabbit serum (NRS) was used in the control stainings instead of the specific antisera.

Immunohistochemistry

Mouse embryos were obtained by mating male and female NMRI mice. The procedures were approved by the animal care committees of Helsinki University and Tampere University. Noon on the day on which the copulation plug was found was considered to represent 0.5 days

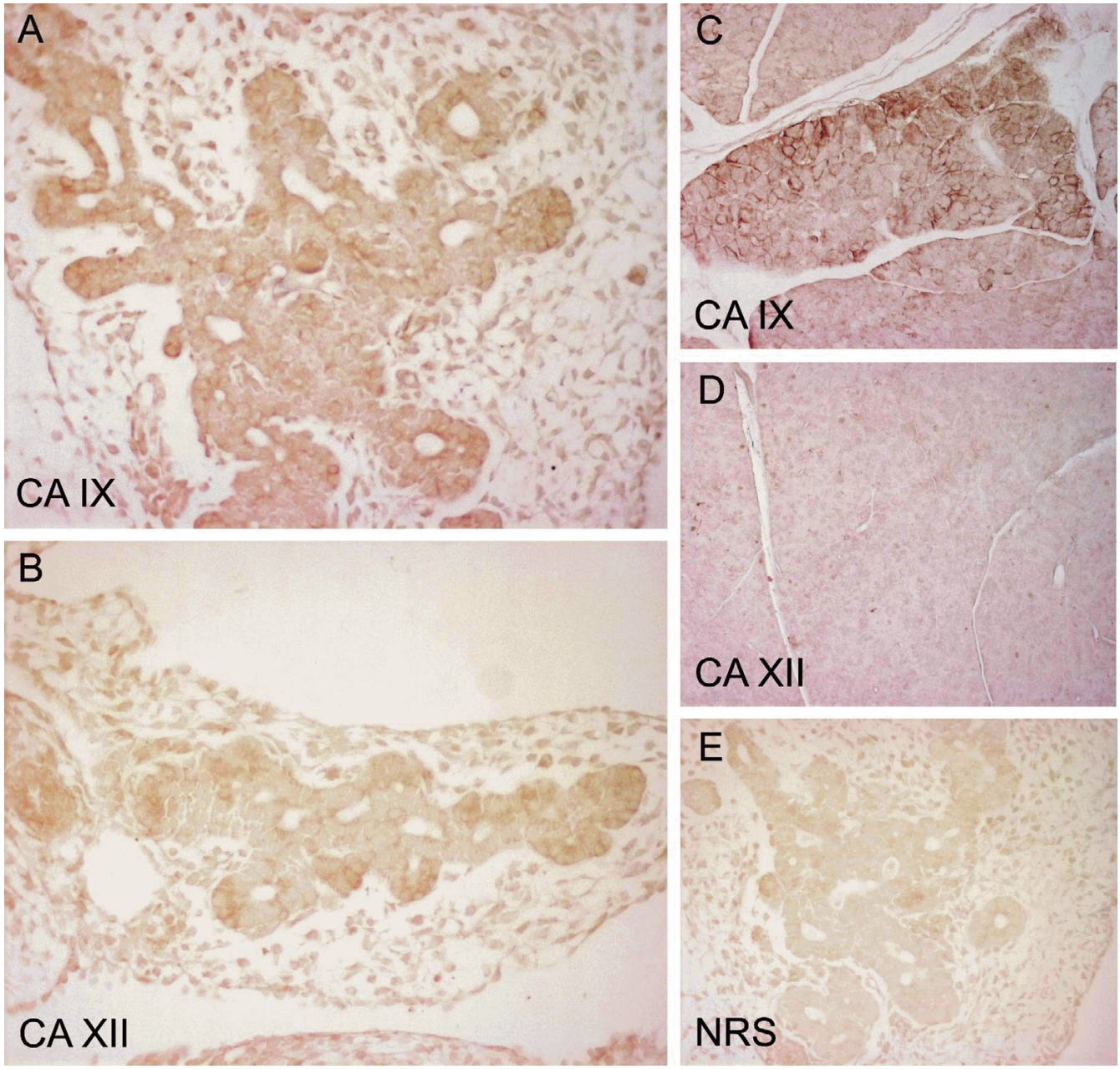

Figure 4
Immunostaining of CA IX and CA XII in the embryonic (E12.5) and adult mouse pancreas. The reaction for CA IX is moderate in the embryonic tissue, with the most intense staining in the epithelial cells (A). CA XII gives weak staining in the epithelium (B). A quite strong but focal signal is seen for CA IX in the acinar cells of the adult pancreas (C), while no immunoreaction is detected for CA XII (D). The control immunostaining of the mouse embryonic pancreas is negative (E). Manual PAP staining in panels A-B and E, automated immunostaining in panels C-D. Original magnifications: A-B, E × 400, C-D × 100.

p.c. 7.5 (n = 2), 11.5 (n = 3), 12.5 (n = 4) and 13.5 (n = 2) p.c. embryos with or without extraembryonic tissues were briefly washed with PBS, fixed with 4% paraformaldehyde and embedded in paraffin. Sections were cut at 5–8 μm and placed on SuperFrost® Plus microscope slides (Menzel; Braunschweig, Germany). Tissue samples from the stomach, heart, brain, liver, kidney and pancreas of an adult NMRI mouse were obtained for control purposes. Immunoperoxidase staining was performed using an automated Lab Vision Autostainer 480 (ImmunoVision Technologies Co., Brisbane, CA, USA). As this automated immunostaining method produced some nonspecific

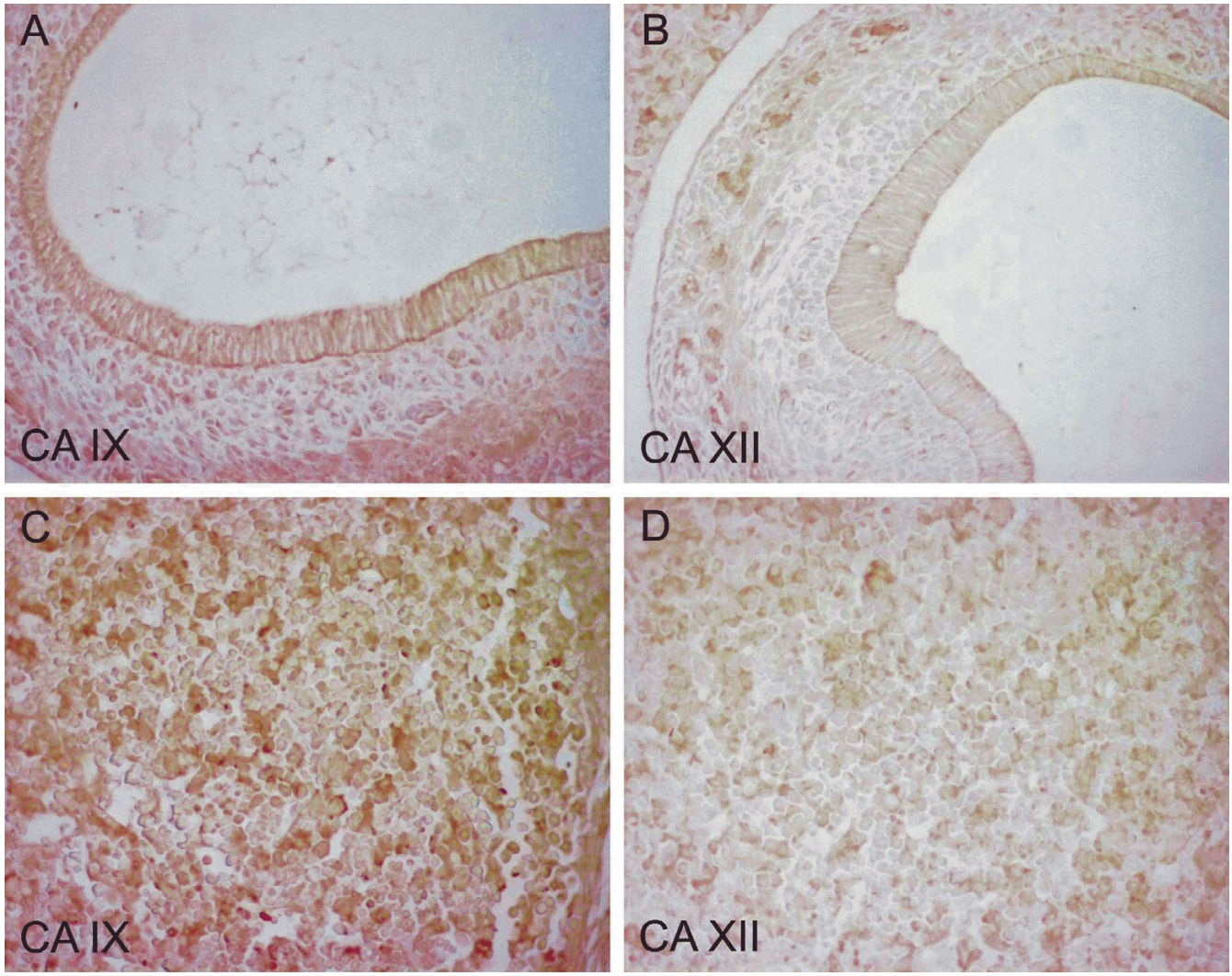

Figure 5
Immunostaining of CA IX and CA XII in the embryonic (E12.5) mouse stomach and liver. Both CA IX (A) and CA XII (B) show weak immunoreaction in the stomach (CA XII barely detectable). CA IX gives moderate staining in the liver, the signal being seen in scattered cells (C). Panel D shows a weak positive signal of CA XII in the liver (D). Manual PAP staining in panels A-D. Original magnifications: × 400.

labeling of the nuclei in the embryonal tissues, immunostaining was repeated using a less sensitive but more specific peroxidase-antiperoxidase complex method (manual PAP) to confirm the validity of the results.

The automated immunostaining, performed using Power Vision+™ Poly-HRP IHC Kit (ImmunoVision Technologies, Co.) reagents, included the following steps: (a) rinsing in wash buffer; (b) treatment in 3% H_2O_2 in ddH_2O for 5 min and rinsing in wash buffer; (c) blocking with Universal IHC Blocking/Diluent for 30 min and rinsing in wash buffer; (d) incubation with the primary antibody (rabbit anti-mouse CA IX or XII) or NRS diluted 1:2000 in Universal IHC Blocking/Diluent for 30 min; (e) rinsing in wash buffer for 3 × 5 min; (f) incubation in poly-HRP-conjugated anti-rabbit IgG for 30 min and rinsing in wash buffer for 3 × 5 min; (g) incubation in DAB (3,3' -diaminobenzidine tetrahydrochloride) solution (one drop of DAB solution A and one drop of DAB solution B in 1 ml) ddH_2O for 6 min; (h) rinsing with ddH_2O ; (i) $CuSO_4$ treatment for 5 min to enhance the signal; and (j) rinsing with ddH_2O. All procedures were carried out at room temperature. The sections were mounted in Entellan Neu (Merck; Darmstadt, Germany) and finally examined and photographed with a Zeiss Axioskop 40 microscope (Carl Zeiss; Göttingen, Germany).

Table 2: Distribution of CA XII in mouse embryonic tissues of different age.*

Organ	E11.5	E12.5	E13.5
Brain	+	+ (CP +++)	++ (CP +++)
Heart (ventricle/atrium)	+/+	++/++	++/++
Lung	ND	+	+
Kidney	ND	+	+
Pancreas	ND	+	+
Liver	+	+	++
Stomach	-	+	+
Intestine	+	+	+

* Scores in immunohistochemistry: strong reaction (+++), moderate reaction (++), weak reaction (+), no reaction (-), choroid plexus (CP), not done (ND).

The immunostaining by the PAP method included the following steps: (a) 3% H_2O_2 in methanol for 5 min and washing in PBS for 5 min; (b) treatment with undiluted cow colostral whey (Biotop) for 30 min and rinsing in PBS; (c) incubation with the primary antibody (rabbit anti-mouse CA IX or XII) diluted 1:100 in 1% bovine serum albumin (BSA) in PBS for 1 hr and washing in PBS 3 times for 10 min; (d) treatment with undiluted cow colostral whey for 30 min and rinsing in PBS; (e) incubation with the secondary antibody (swine anti-rabbit IgG; DAKO, Glostrup, Denmark) diluted 1:100 in 1% BSA in PBS for 1 hr and washing in PBS 3 times for 10 min; (f) incubation with peroxidase-antiperoxidase complex (PAP-rabbit; DAKO) diluted 1:100 in PBS for 30 min and washing in PBS 4 times for 5 min; and (g) incubation for 2 1/2 min in DAB solution (6 mg 3,3' -diaminobenzidine tetrahydrochloride; Sigma, St Louis, MO) in 10 ml PBS plus 3,3 μl 30% H_2O_2. All incubations and washings were carried out at room temperature. The sections were mounted in Entellan Neu (Merck; Darmstadt, Germany) and finally examined and photographed with a Zeiss Axioskop 40 microscope.

Abbreviations

CA, carbonic anhydrase

Authors' contributions

All authors participated in the design of the study. HK, SM, MH and SPar collected the tissue samples. HK and SP drafted the manuscript. JP, SPas, AW and WSS produced and characterized the antibodies. HK performed the immunohistochemical staining. HK, MH and SP analyzed the staining results. All authors read, modified and approved the final manuscript.

Acknowledgements

This work was supported by grants from Sigrid Juselius Foundation, Academy of Finland, Finnish Cancer Foundation, Bayer Corporation, Slovak Grant Agencies VEGA (2/3055) and APVT (51-005802), and National Institutes of Health (DK40163).

References

1. Breton S: **The cellular physiology of carbonic anhydrases.** *Jop* 2001, **2:**159-164.
2. Pastorekova S, Parkkila S, Pastorek J, Supuran CT: **Carbonic anhydrases: current state of the art, therapeutic applications and future prospects.** *J Enzyme Inhib Med Chem* 2004, **19:**199-229.
3. Parkkila S, Parkkila AK: **Carbonic anhydrase in the alimentary tract. Roles of the different isozymes and salivary factors in the maintenance of optimal conditions in the gastrointestinal canal.** *Scand J Gastroenterol* 1996, **31:**305-317.
4. Lehtonen J, Shen B, Vihinen M, Casini A, Scozzafava A, Supuran CT, Parkkila AK, Saarnio J, Kivela AJ, Waheed A, Sly WS, Parkkila S: **Characterization of CA XIII, a novel member of the carbonic anhydrase isozyme family.** *J Biol Chem* 2004, **279:**2719-2727.
5. Pastorekova S, Parkkila S, Parkkila AK, Opavsky R, Zelnik V, Saarnio J, Pastorek J: **Carbonic anhydrase IX, MN/CA IX: analysis of stomach complementary DNA sequence and expression in human and rat alimentary tracts.** *Gastroenterology* 1997, **112:**398-408.
6. Tureci O, Sahin U, Vollmar E, Siemer S, Gottert E, Seitz G, Parkkila AK, Shah GN, Grubb JH, Pfreundschuh M, Sly WS: **Human carbonic anhydrase XII: cDNA cloning, expression, and chromosomal localization of a carbonic anhydrase gene that is overexpressed in some renal cell cancers.** *Proc Natl Acad Sci U S A* 1998, **95:**7608-7613.
7. Parkkila S, Parkkila AK, Rajaniemi H, Shah GN, Grubb JH, Waheed A, Sly WS: **Expression of membrane-associated carbonic anhydrase XIV on neurons and axons in mouse and human brain.** *Proc Natl Acad Sci U S A* 2001, **98:**1918-1923.
8. Hilvo M, Tolvanen M, Clark A, Shen B, Shah GN, Waheed A, Halmi P, Hanninen M, Hamalainen JM, Vihinen M, Sly WS, Parkkila S: **Characterization of CA XV, a new GPI-anchored form of carbonic anhydrase.** *Biochem J* 2005, **392:**83-92.
9. Fujikawa-Adachi K, Nishimori I, Taguchi T, Onishi S: **Human mitochondrial carbonic anhydrase VB. cDNA cloning, mRNA expression, subcellular localization, and mapping to chromosome x.** *J Biol Chem* 1999, **274:**21228-21233.
10. Kivela J, Parkkila S, Parkkila AK, Rajaniemi H: **A low concentration of carbonic anhydrase isoenzyme VI in whole saliva is associated with caries prevalence.** *Caries Res* 1999, **33:**178-184.
11. Karhumaa P, Leinonen J, Parkkila S, Kaunisto K, Tapanainen J, Rajaniemi H: **The identification of secreted carbonic anhydrase VI as a constitutive glycoprotein of human and rat milk.** *Proc Natl Acad Sci U S A* 2001, **98:**11604-11608.
12. Svastova E, Hulikova A, Rafajova M, Zat'ovicova M, Gibadulinova A, Casini A, Cecchi A, Scozzafava A, Supuran CT, Pastorek J, Pastorekova S: **Hypoxia activates the capacity of tumor-associated carbonic anhydrase IX to acidify extracellular pH.** *FEBS Lett* 2004, **577:**439-445.
13. Parkkila S, Rajaniemi H, Parkkila AK, Kivela J, Waheed A, Pastorekova S, Pastorek J, Sly WS: **Carbonic anhydrase inhibitor suppresses invasion of renal cancer cells in vitro.** *Proc Natl Acad Sci U S A* 2000, **97:**2220-2224.
14. Opavsky R, Pastorekova S, Zelnik V, Gibadulinova A, Stanbridge EJ, Zavada J, Kettmann R, Pastorek J: **Human MN/CA9 gene, a novel member of the carbonic anhydrase family: structure and exon to protein domain relationships.** *Genomics* 1996, **33:**480-487.
15. Vullo D, Franchi M, Gallori E, Pastorek J, Scozzafava A, Pastorekova S, Supuran CT: **Carbonic anhydrase inhibitors: inhibition of the tumor-associated isozyme IX with aromatic and heterocyclic sulfonamides.** *Bioorg Med Chem Lett* 2003, **13:**1005-1009.
16. Ilies MA, Vullo D, Pastorek J, Scozzafava A, Ilies M, Caproiu MT, Pastorekova S, Supuran CT: **Carbonic anhydrase inhibitors. Inhibition of tumor-associated isozyme IX by halogenosulfanilamide and halogenophenylaminobenzolamide derivatives.** *J Med Chem* 2003, **46:**2187-2196.
17. Abbate F, Casini A, Owa T, Scozzafava A, Supuran CT: **Carbonic anhydrase inhibitors: E7070, a sulfonamide anticancer agent, potently inhibits cytosolic isozymes I and II, and transmembrane, tumor-associated isozyme IX.** *Bioorg Med Chem Lett* 2004, **14:**217-223.
18. Vullo D, Scozzafava A, Pastorekova S, Pastorek J, Supuran CT: **Carbonic anhydrase inhibitors: inhibition of the tumor-associated isozyme IX with fluorine-containing sulfonamides. The**

first subnanomolar CA IX inhibitor discovered. *Bioorg Med Chem Lett* 2004, **14:**2351-2356.
19. Casey JR, Morgan PE, Vullo D, Scozzafava A, Mastrolorenzo A, Supuran CT: **Carbonic anhydrase inhibitors. Design of selective, membrane-impermeant inhibitors targeting the human tumor-associated isozyme IX.** *J Med Chem* 2004, **47:**2337-2347.
20. Saarnio J, Parkkila S, Parkkila AK, Waheed A, Casey MC, Zhou XY, Pastorekova S, Pastorek J, Karttunen T, Haukipuro K, Kairaluoma MI, Sly WS: **Immunohistochemistry of carbonic anhydrase isozyme IX (MN/CA IX) in human gut reveals polarized expression in the epithelial cells with the highest proliferative capacity.** *J Histochem Cytochem* 1998, **46:**497-504.
21. Zavada J, Zavadova Z, Pastorek J, Biesova Z, Jezek J, Velek J: **Human tumour-associated cell adhesion protein MN/CA IX: identification of M75 epitope and of the region mediating cell adhesion.** *Br J Cancer* 2000, **82:**1808-1813.
22. Svastova E, Zilka N, Zat'ovicova M, Gibadulinova A, Ciampor F, Pastorek J, Pastorekova S: **Carbonic anhydrase IX reduces E-cadherin-mediated adhesion of MDCK cells via interaction with beta-catenin.** *Exp Cell Res* 2003, **290:**332-345.
23. Hilvo M, Rafajova M, Pastorekova S, Pastorek J, Parkkila S: **Expression of carbonic anhydrase IX in mouse tissues.** *J Histochem Cytochem* 2004, **52:**1313-1322.
24. Liao SY, Brewer C, Zavada J, Pastorek J, Pastorekova S, Manetta A, Berman ML, DiSaia PJ, Stanbridge EJ: **Identification of the MN antigen as a diagnostic biomarker of cervical intraepithelial squamous and glandular neoplasia and cervical carcinomas.** *Am J Pathol* 1994, **145:**598-609.
25. Liao SY, Aurelio ON, Jan K, Zavada J, Stanbridge EJ: **Identification of the MN/CA9 protein as a reliable diagnostic biomarker of clear cell carcinoma of the kidney.** *Cancer Res* 1997, **57:**2827-2831.
26. Turner JR, Odze RD, Crum CP, Resnick MB: **MN antigen expression in normal, preneoplastic, and neoplastic esophagus: a clinicopathological study of a new cancer-associated biomarker.** *Hum Pathol* 1997, **28:**740-744.
27. McKiernan JM, Buttyan R, Bander NH, Stifelman MD, Katz AE, Chen MW, Olsson CA, Sawczuk IS: **Expression of the tumor-associated gene MN: a potential biomarker for human renal cell carcinoma.** *Cancer Res* 1997, **57:**2362-2365.
28. Vermylen P, Roufosse C, Burny A, Verhest A, Bosschaerts T, Pastorekova S, Ninane V, Sculier JP: **Carbonic anhydrase IX antigen differentiates between preneoplastic malignant lesions in non-small cell lung carcinoma.** *Eur Respir J* 1999, **14:**806-811.
29. Bartosova M, Parkkila S, Pohlodek K, Karttunen TJ, Galbavy S, Mucha V, Harris AL, Pastorek J, Pastorekova S: **Expression of carbonic anhydrase IX in breast is associated with malignant tissues and is related to overexpression of c-erbB2.** *J Pathol* 2002, **197:**314-321.
30. Saarnio J, Parkkila S, Parkkila AK, Pastorekova S, Haukipuro K, Pastorek J, Juvonen T, Karttunen TJ: **Transmembrane carbonic anhydrase, MN/CA IX, is a potential biomarker for biliary tumours.** *J Hepatol* 2001, **35:**643-649.
31. Leppilampi M, Saarnio J, Karttunen TJ, Kivela J, Pastorekova S, Pastorek J, Waheed A, Sly WS, Parkkila S: **Carbonic anhydrase isozymes IX and XII in gastric tumors.** *World J Gastroenterol* 2003, **9:**1398-1403.
32. Chen J, Rocken C, Hoffmann J, Kruger S, Lendeckel U, Rocco A, Pastorekova S, Malfertheiner P, Ebert MP: **Expression of carbonic anhydrase 9 at the invasion front of gastric cancers.** *Gut* 2005, **54:**920-927.
33. Pastorek J, Pastorekova S, Callebaut I, Mornon JP, Zelnik V, Opavsky R, Zat'ovicova M, Liao S, Portetelle D, Stanbridge EJ, *et al.*: **Cloning and characterization of MN, a human tumor-associated protein with a domain homologous to carbonic anhydrase and a putative helix-loop-helix DNA binding segment.** *Oncogene* 1994, **9:**2877-2888.
34. Ivanov SV, Kuzmin I, Wei MH, Pack S, Geil L, Johnson BE, Stanbridge EJ, Lerman MI: **Down-regulation of transmembrane carbonic anhydrases in renal cell carcinoma cell lines by wild-type von Hippel-Lindau transgenes.** *Proc Natl Acad Sci U S A* 1998, **95:**12596-12601.
35. Ivanov S, Liao SY, Ivanova A, Danilkovitch-Miagkova A, Tarasova N, Weirich G, Merrill MJ, Proescholdt MA, Oldfield EH, Lee J, Zavada J, Waheed A, Sly W, Lerman MI, Stanbridge EJ: **Expression of hypoxia-inducible cell-surface transmembrane carbonic anhydrases in human cancer.** *Am J Pathol* 2001, **158:**905-919.
36. Karhumaa P, Parkkila S, Tureci O, Waheed A, Grubb JH, Shah G, Parkkila A, Kaunisto K, Tapanainen J, Sly WS, Rajaniemi H: **Identification of carbonic anhydrase XII as the membrane isozyme expressed in the normal human endometrial epithelium.** *Mol Hum Reprod* 2000, **6:**68-74.
37. Karhumaa P, Kaunisto K, Parkkila S, Waheed A, Pastorekova S, Pastorek J, Sly WS, Rajaniemi H: **Expression of the transmembrane carbonic anhydrases, CA IX and CA XII, in the human male excurrent ducts.** *Mol Hum Reprod* 2001, **7:**611-616.
38. Kivela A, Parkkila S, Saarnio J, Karttunen TJ, Kivela J, Parkkila AK, Waheed A, Sly WS, Grubb JH, Shah G, Tureci O, Rajaniemi H: **Expression of a novel transmembrane carbonic anhydrase isozyme XII in normal human gut and colorectal tumors.** *Am J Pathol* 2000, **156:**577-584.
39. Parkkila S: **An overview of the distribution and function of carbonic anhydrase in mammals.** *Exs* 2000:79-93.
40. Kyllonen MS, Parkkila S, Rajaniemi H, Waheed A, Grubb JH, Shah GN, Sly WS, Kaunisto K: **Localization of carbonic anhydrase XII to the basolateral membrane of H+-secreting cells of mouse and rat kidney.** *J Histochem Cytochem* 2003, **51:**1217-1224.
41. Halmi P, Lehtonen J, Waheed A, Sly WS, Parkkila S: **Expression of hypoxia-inducible, membrane-bound carbonic anhydrase isozyme XII in mouse tissues.** *Anat Rec A Discov Mol Cell Evol Biol* 2004, **277:**171-177.
42. Derycke LD, Bracke ME: **N-cadherin in the spotlight of cell-cell adhesion, differentiation, embryogenesis, invasion and signalling.** *Int J Dev Biol* 2004, **48:**463-476.
43. Friedl P, Hegerfeldt Y, Tusch M: **Collective cell migration in morphogenesis and cancer.** *Int J Dev Biol* 2004, **48:**441-449.
44. Ortova Gut MO, Parkkila S, Vernerova Z, Rohde E, Zavada J, Hocker M, Pastorek J, Karttunen T, Gibadulinova A, Zavadova Z, Knobeloch KP, Wiedenmann B, Svoboda J, Horak I, Pastorekova S: **Gastric hyperplasia in mice with targeted disruption of the carbonic anhydrase gene Car9.** *Gastroenterology* 2002, **123:**1889-1903.
45. Wykoff CC, Beasley NJ, Watson PH, Turner KJ, Pastorek J, Sibtain A, Wilson GD, Turley H, Talks KL, Maxwell PH, Pugh CW, Ratcliffe PJ, Harris AL: **Hypoxia-inducible expression of tumor-associated carbonic anhydrases.** *Cancer Res* 2000, **60:**7075-7083.
46. Chen EY, Fujinaga M, Giaccia AJ: **Hypoxic microenvironment within an embryo induces apoptosis and is essential for proper morphological development.** *Teratology* 1999, **60:**215-225.
47. Ramirez-Bergeron DL, Runge A, Dahl KD, Fehling HJ, Keller G, Simon MC: **Hypoxia affects mesoderm and enhances hemangioblast specification during early development.** *Development* 2004, **131:**4623-4634.
48. Tomanek RJ, Lund DD, Yue X: **Hypoxic induction of myocardial vascularization during development.** *Adv Exp Med Biol* 2003, **543:**139-149.
49. Gebb SA, Jones PL: **Hypoxia and lung branching morphogenesis.** *Adv Exp Med Biol* 2003, **543:**117-125.
50. Fleming RE, Crouch EC, Ruzicka CA, Sly WS: **Pulmonary carbonic anhydrase IV: developmental regulation and cell-specific expression in the capillary endothelium.** *Am J Physiol* 1993, **265:**L627-35.
51. Schwartz GJ, Olson J, Kittelberger AM, Matsumoto T, Waheed A, Sly WS: **Postnatal development of carbonic anhydrase IV expression in rabbit kidney.** *Am J Physiol* 1999, **276:**F510-20.

Research Paper

Cancer-Associated Carbonic Anhydrases IX and XII: Effect of Growth Factors on Gene Expression in Human Cancer Cell Lines

Heini Kallio[1], Alejandra Rodriguez Martinez, Mika Hilvo, Alise Hyrskyluoto, and Seppo Parkkila

Institute of Medical Technology and School of Medicine, University of Tampere and Tampere University Hospital, Tampere, Finland

AIM: **Carbonic anhydrase IX (CA9) and carbonic anhydrase XII (CA12) are cancer-associated enzymes that are strongly up-regulated by hypoxia via hypoxia-inducible factor HIF-1, but whether these isozymes are regulated by other mechanisms is not well understood. In the present study, we investigated the effects of certain hormones and growth factors on the levels of CA9 and CA12 mRNA expression in human cancer cell lines.**

METHODS: **Seven human cell lines were selected for the study. The cells were treated with several hormones and growth factors for 24 h. Changes in the levels of human CA9 and CA12 transcripts were detected using quantitative real-time PCR.**

RESULTS: **Different growth factors or hormones had different effects on CA9 and CA12 mRNA expression in different cancer cells. The strongest up-regulation of CA9 and CA12 expression was observed after deferoxamine mesylate treatment, which was used to induce a hypoxia-like response. Additionally, CA12 expression could be stimulated by growth factors like IGF-1, TGF-β1 and EGF in U373, MCF-7, Caki-1, and A-498 cells. Induction of CA9 expression was obvious only in U373 cells. Conversely, CA12 expression was reduced in human endothelial cells after growth factor treatments.**

CONCLUSION: **The results suggest that the increase in CA9 and CA12 stimulated by IGF-1, TGF-α, TGF-β1 and EGF is mediated through HIF-1α protein expression, which has been shown to be up-regulated by several growth factors under normal oxygenation conditions in human cell lines. This could represent a novel regulatory mechanism for CA9 and CA12 expression.**

Journal of Cancer Molecules 5(3): 73-78, 2010.

Keywords:

carbonic anhydrase

HIF-1α

deferoxamine mesylate

growth factor

Introduction

Carbonic anhydrases IX (CA9[2]) and XII (CA12) are cancer-associated zinc metalloenzymes belonging to a large enzyme family of mammalian α-carbonic anhydrases that contains 13 active isoforms (i.e., I, II, III, IV, VA, VB, VI, VII, IX, XII, XIII, XIV, and XV). These enzymatically active CAs catalyze the reversible hydration of carbon dioxide in the reaction $CO_2 + H_2O \leftrightarrow H^+ + HCO_3^-$. This reaction affects various biological processes, such as regulation of pH homeostasis, CO_2 and ion transport, respiration, bone resorption, ureagenesis, gluconeogenesis, lipogenesis, production of body fluids, and fertilization [1,2]. Each isozyme has a characteristic subcellular localization, distribution within the body, enzyme activity, and affinity for inhibitors.

Both CA9 and CA12 are transmembrane proteins. CA9 is an unusual isoform because it is present in few normal human tissues, but is ectopically expressed in some tumor cells whose normal counterparts contain none or low levels of this protein. CA9-positive tumors include colon, cervical, breast and renal carcinomas and brain tumors [3]. In addition, the few normal tissues with high natural CA9 expression, such as the stomach and gallbladder, have been demonstrated to lose some, or all, of their CA9 upon conversion to carcinomas [4,5]. The presence of CA9 in various tumor types has been found to correlate with poor prognosis [6-9]. CA9 has also been implicated in the regulation of pH balance during carcinogenesis and tumor progression, but this hypothesis still requires further proof.

In contrast to CA9, CA12 is expressed in a variety of normal human tissues including kidney, colon, prostate, pancreas, ovary, testis, lung, and brain [10,11]. Expression of CA12 usually becomes stronger or more widespread in tumors compared to the corresponding normal tissues [12-15].

Tissue oxygen content has been considered to be the main regulatory mechanism for CA9 and CA12 expression, as both CA9 and CA12 transcript levels are strongly up-regulated via hypoxia-inducible transcription factor 1 (HIF-1). HIF-1 is a heterodimer that consists of an oxygen-sensitive α subunit and a constitutively expressed β subunit. Under normal oxygenation conditions, prolyl-4-hydroxylases (PHDs) hydroxylate two conserved proline residues of HIF-1α. The von Hippel-Lindau protein (pVHL) binds hydroxylated HIF-1α and targets it for degradation by the ubiquitin-proteasome system, and thus abrogates its function in the

Received 2/17/09; Revised 6/3/09; Accepted 6/10/09.

[1]**Correspondence:** Heini Kallio, Institute of Medical Technology, University of Tampere, Biokatu 6, 33520 Tampere, Finland. Phone: 358-3-31175564. Fax: 358-3-35517710. E-mail: heini.kallio@uta.fi

[2]**Abbreviations:** CA, carbonic anhydrase; HIF-1, hypoxia-inducible transcription factor 1; pVHL, von Hippel-Lindau protein; MAPK, mitogen-activated protein kinase; PI3K, phosphatidylinositol 3-kinase.

transcriptional activation of downstream genes [16,17]. In hypoxia, which occurs frequently in tumors as a result of aberrant vasculature, HIF-1α is not hydroxylated, because PHDs are inactive in the absence of oxygen. Non-hydroxylated HIF-1α is not recognized by pVHL; instead, it is stabilized and accumulates in the cell. HIF-1α then translocates to the nucleus and dimerizes with the HIF-1β subunit to form the active transcription factor. The HIF-1 then binds to hypoxia-responsive elements (HREs) within the promoter regions of hypoxia-inducible genes, leading to gene expression. In addition to *CA9* and *CA12*, target genes include glucose transporters (*GLUT-1* and *GLUT-3*), vascular endothelial growth factor (*VEGF*), erythropoietin (*EPO-1*), and a number of other genes with functions in cell survival, proliferation, metabolism, and other cellular processes [18,19]. Thus, activation of the HIF-1 pathway substantially alters the expression profile of pre-malignant lesions by generating tumor cells which either die via apoptosis or adapt to hypoxia. As a result, hypoxia selects more aggressive tumor cells with an increased capability to metastasize, and is therefore often associated with poor prognosis and resistance to anti-cancer therapy [20].

In addition to hypoxia, increased activity of the HIF-1 pathway can result from genetic events such as inactivating mutations in the *VHL* gene or activation of oncogenic pathways, e.g. mitogen-activated protein kinase (MAPK) and/or phosphatidylinositol 3-kinase (PI3K)[20-22]. Notably, suppression of *CA12* expression requires both a central VHL domain involved in the HIF-1α binding and a C-terminal elongin-binding domain, whereas only the latter is needed for the negative regulation of *CA9*. Therefore, CA12 is regulated by hypoxia, in a similar manner to CA9, but using different biochemical pathways [23,24]. Furthermore, CA9 is directly induced by binding of HIF-1 to the HRE within the basal promoter, whereas the *CA12* gene does not contain any HRE that corresponds to the HRE of *CA9*. In fact, the upstream region of the *CA12* gene possesses several putative HREs with a core HIF-binding sequence, but their functionality has not been examined to date. According to tissue distribution analyses and *in vitro* experiments, CA12 does not appear to be as tightly regulated by the hypoxia/pVHL pathway and as strongly linked to cancer as CA9 [11,23].

Apart from hypoxia, very little is known about the mechanisms that regulate CA9 and CA12 expression. It is possible that these cancer-associated enzymes are regulated at higher levels of the biosynthetic pathway in a similar manner to some other hypoxia-induced genes. However, it is also possible that CA12 has an unknown role in cancer progression, which is not directly linked to the hypoxia-associated pathway. In the present study, we examined whether different hormones and growth factors affected the levels of CA9 and CA12 mRNA in human cancer-derived and normal cell lines.

Materials and Methods

Cell lines and treatments

Caki-1 and A-498 human renal carcinoma cell lines and HepG2 human hepatocellular carcinoma cell line were obtained from the American Type Culture Collection (Manassas, VA, USA). HeLa human cervical carcinoma cell line and MCF-7 human breast adenocarcinoma cell line were kindly provided by Professor Jorma Isola (Institute of Medical Technology, University of Tampere, Tampere, Finland). U373 human glioblastoma cell line and HUVEC normal human umbilical vein endothelial cell line were purchased from the European Collection of Cell Cultures (Porton Down, Salisbury, UK).

Caki-1, A-498, and HepG2 cells were cultured in Dulbecco's Modified Eagle's Medium (DMEM; Lonza, Venviers, Belgium) supplemented with 10% (v/v) FBS (Biochrom, Cambridge, UK), 2 mM L-glutamine, 100 unit/ml penicillin, and 100 μg/ml streptomycin (Lonza). MCF-7 cells were cultured in DMEM supplemented with 10% FBS, 1 mM sodium pyruvate (Lonza), 1% (v/v) non-essential amino acids (Lonza), and 10 μg/ml insulin (Sigma-Aldrich Finland Oy, Helsinki, Finland). HeLa cells were maintained in RPMI-1640 medium (Lonza) supplemented with 10% FBS and 2 mM L-glutamine. U373 cells were cultured in Alpha MEM (Lonza) supplemented with 10% FBS, 2 mM L-glutamine, 100 unit/ml penicillin, and 100 μg/ml streptomycin. HUVEC cells were maintained in Endothelial Cell Basal Medium-2 (EBM®-2) supplemented with EGM™-2 SingleQuots® kit (Lonza, Walkersville, MD, USA).

All cell cultures were grown in 75-cm^2 flasks in a 37°C incubator with humidified 5% CO_2/95% air. When the cultured cells reached 80-90% of confluence, they were trypsinized and plated in 6-well plates (except for the HUVEC cells which were plated in 59-cm^2 dishes) at appropriate densities to obtain a sufficient quantity of cells for RNA extraction. After 24 h, the cells were changed to fresh serum-free medium with the tested hormones and growth factors. Only serum-free medium was added to two control wells/dishes. The cells were incubated for 24 h in the presence of different hormones or growth factors. The treatments were performed using recombinant human growth hormone (400 ng/ml), hydrocortisone (10 μM), insulin (30 nM), tri-iodothyronine (T3; 10 nM), estradiol (E2; 2.5 μM), recombinant human insulin-like growth factor-1 (IGF-1; 50 ng/ml), recombinant human transforming growth factor-alpha (TGF-α; 10 ng/ml), recombinant human transforming growth factor-beta 1 (TGF-β1; 10 ng/ml), recombinant human epidermal growth factor (EGF; 10 ng/ml), and deferoxamine mesylate (200 μM), an iron chelator commonly used to induce the hypoxia regulatory pathway. Every cell line was treated with the same hormones or growth factors except for MCF-7, which was not treated with insulin because these cells require a high insulin concentration in their culture medium. The growth hormone, IGF-1, TGF-β1 and EGF were purchased from ProSpec-Tany TechnoGene Ltd. (Rehovot, Israel). TGF-α was purchased from PromoCell GmbH (Heidelberg, Germany). The rest of the chemicals were obtained from Sigma-Aldrich Finland Oy, and diluted when necessary according to the manufacturers' instructions.

RNA extraction and first-strand cDNA synthesis

Total RNA from cultured cells was extracted using the RNeasy RNA isolation kit (Qiagen, Valencia, USA). Residual DNA was removed from samples using RNase-free DNase (Qiagen). The RNA concentration and purity was determined by measurement of the optical density at 260 and 280 nm. Different quantities of RNA (U373, 410 ng; HeLa, 600 ng; A-498, 850 ng; HepG2, 1000 ng; HUVEC and MCF-7, 1100 ng; Caki-1, 1400 ng) were converted into first-strand cDNA using the First Strand cDNA synthesis kit (Fermentas, Burlington, Canada) using random hexamer primers according to the protocol recommended by the manufacturer.

Quantitative real-time PCR

The levels of human *CA9* and *CA12* transcripts in the different cell lines after indicated treatments were assessed by quantitative real-time PCR using the Lightcycler detection system (Roche, Rotkreuz, Switzerland). Real-time PCR primers were designed based on the complete cDNA sequences deposited in GenBank (accession numbers: NM_001216 for *CA9*, NM_001218 for *CA12*, and NM_001530 for *HIF-1α*). The house-keeping genes *ubiquitin C* (*UBC*) and *β-2-microglobulin* (*B2M*) were used as internal controls to normalize the cDNA samples for possible differences in quality and quantity. The *UBC* primers were obtained from RTprimerDB database (under the identification number 8), and the *B2M* primers were designed on the basis of the complete *B2M* cDNA sequences (accession number: NM_004048). In order to avoid amplification of genomic DNA, the primers from each primer pair were located in

Print ISSN 1816-0735; Online ISSN 1817-4256

Table 1: Primer sequences for quantitative real-time PCR used in the study

Gene	Forward primer	Reverse primer	PCR product size	T_a (°C)**
CA9	5'- GGAAGGCTCAGAGACTCA-3'	5'- CTTAGCACTCAGCATCAC-3'	160	53
CA12	5'- CTGCCAGCAACAAGTCAG-3'	5'- ATATTCAGCGGTCCTCTC-3'	179	53
HIF-1α	5'- TCACCTGAGCCTAATAGTCC-3'	5'- GCTAACATCTCCAAGTCTAA-3'	161	52
*UBC**	5'- ATTTGGGTCGCGGTTCTTG-3'	5'- TGCCTTGACATTCTCGATGGT-3'	133	57
B2M	5'- GTATGCCTGCCGTGTGAA-3'	5'- CTCCATGATGCTGCTTAC-3'	84	52

*obtained from RTprimerDB database (http://medgen.ugent.be/rtprimerdb/index.php)
**T_a: annealing temperature

Table 2: *CA9* expression in different cell lines after the treatments (fold change values are shown)**

	U373	HeLa	MCF-7	Caki-1	A-498	HepG2	HUVEC
EGF	2.2	0	0	0	0	0	0
GH	-1.3	0	0	0	0	0	0
HC	1.0	0	0	0	0	0	0
INS	1.4	0	0	0	0	0	0
T3	1.4	0	0	0	0	0	0
DFM	4.2	137.5	0	0	0	0	0
E2	-1.2	0	0	0	0	0	0
IGF-1	2.4	0	0	0	0	0	0
TGF-α	2.6	0	0	0	0	0	0
TGF-β1	1.7	0	0	0	0	0	0

*EGF, epidermal growth factor; GH, growth hormone; HC, hydrocortisone; INS, insulin; T3, tri-iodothyronine; DFM, deferoxamine mesylate; E2, estradiol; IGF-1, insulin-like growth factor-1; TGF-α, transforming growth factor-alpha; TGF-β1, transforming growth factor-beta 1.
**0 = copy number < 100

different exons. The primer sequences used in this study are shown in Table 1.

Each PCR reaction was performed in a total volume of 20 µl containing 1.0 µl of first-strand cDNA, 1× QuantiTect SYBR Green PCR Master Mix (Qiagen, Hilden, Germany), and 0.5 µM of each primer. The amplification and detection were carried out as follows: after an initial 15 min activation step at 95°C, amplification was performed in a three-step cycling procedure for 45 cycles: denaturation at 95°C for 15 sec, annealing at a temperature determined according to the T_m for each primer pair for 20 sec, and elongation at 72°C for 15 sec (the ramp rate was 20°C per sec for all the steps), and a final cooling step. Melting curve analysis was always performed after the amplification to check the specificity of the PCR reaction. To quantify the levels of transcripts in the cell lines studied, a standard curve was established for each gene using five-fold serial dilutions of known concentrations of purified PCR products generated with the same primer pairs. Every cDNA sample was tested in triplicate, and the obtained crossing point (Cp) value permitted the levels of the starting mRNA to be determined using a specific standard curve. The geometric mean of the two internal control genes was used as an accurate normalization factor for gene expression levels [25]. The final relative mRNA expression was indicated as the copy number of the target gene divided by the corresponding normalization factor and multiplied by 10^3.

Statistical analyses

After a statistical consultation, it was decided that the obtained results should be presented using descriptive methods rather than using extensive statistical comparisons. The median values were calculated from the technical triplicates for the quantitative real-time PCR experiments. Subsequently, the median values for treatments were compared to the median values for negative controls.

Results and Discussion

CA9 had a narrow expression profile and was detected in only two out of seven cell lines (Table 2). In a human glioblastoma cell line, U373, the basal level of *CA9* expression was relatively high (Figure 1). This is in accordance with the fact that the strongest CA9 expression among different gliomas has been observed in the most malignant forms, i.e. glioblastomas [26]. Compared to the control sample, *CA9* expression increased 4.2-fold after deferoxamine mesylate treatment, which was used as a positive control to induce a hypoxia-like response (Table 2 and Figure 1). In addition, the IGF-1, TGF-α and EGF treatments notably increased *CA9* expression compared to the control sample (fold changes of 2.4, 2.6 and 2.2, respectively). After TGF-β1 treatment, *CA9* expression was moderately elevated (1.7-fold).

Interestingly, the inhibition of MAPK and PI3K pathways has been shown to result in reduced CA9 expression under both standard and acidic conditions in human glioblastoma 8-MG-BA cells [27]. It is also known that HIF-1α can be up-regulated under normoxic conditions via the MAPK and PI3K/Akt pathways [22]. Furthermore, it has been demonstrated that EGF up-regulates HIF-1α protein expression in several cell lines, including human embryonic kidney 293 cells [28] and human prostate cancer TSU cells [29]. IGF-1, among other growth factors, also increases the levels of HIF-1α protein [28]. The increase in the level of CA9 mRNA induced by EGF and IGF-1 is therefore likely to be mediated through the stabilization of HIF-1α protein rather than via increased mRNA levels. This was supported by our finding, confirming that HIF-1α mRNA expression was not up-regulated after growth factor treatments in U373 cells (data not shown). This result was expected, as HIF-1α regulation mainly involves post-transcriptional changes [30]. One hypothesis is that up-regulation of *CA9* by EGF and IGF-1 treatments is mediated through activation of the MAPK and/or PI3K pathway. In fact, Dorai and co-workers have demonstrated that the tyrosine moiety of CA9 present in its intracellular domain can be phosphorylated in an EGF-dependent manner in the renal cell carcinoma cell line SKRC-01 [31]. Their results also suggested that tyrosine-phosphorylated CA9 interacted with the regulatory subunit of PI3K, leading to Akt activation. Similarly, TGF-α could increase the level of *CA9* expression via these pathways, since TGF-α is one of the ligands of the EGF receptor [32]. It has also been shown that TGF-β1 can contribute to the accumulation of HIF-1α in normoxic conditions. Stimulation with TGF-β1 increased HIF-1α expression levels and DNA

Table 3: ***CA12*** **expression in different cell lines after the treatments (fold change values are shown)****

	U373	HeLa	MCF-7	Caki-1	A-498	HepG2	HUVEC
EGF	2.9	0	2.4	1.8	2.6	0	-1.3
GH	-1.6	0	1.3	-1.5	-1.3	0	-1.2
HC	1.0	0	-1.1	1.4	-1.6	0	-2.0
INS	1.2	0	ND	1.3	-1.3	0	-1.1
T3	-1.3	0	1.3	1.2	-1.4	0	-1.4
DFM	3.8	0	-1.3	10.2	-1.3	0	1.3
E2	1.0	0	1.9	1.5	1.2	0	1.1
IGF-1	2.0	0	1.3	1.5	1.7	0	-2.2
TGF-α	3.1	0	-1.1	1.1	2.2	0	-1.8
TGF-β1	1.6	0	2.8	1.7	2.5	0	-1.6

***EGF, epidermal growth factor; GH, growth hormone; HC, hydrocortisone; INS, insulin; T3, tri-iodothyronine; DFM, deferoxamine mesylate; E2, estradiol; IGF-1, insulin-like growth factor-1; TGF-α, transforming growth factor-alpha; TGF-β1, transforming growth factor-beta 1.**

****0 = copy number < 100, ND = not done**

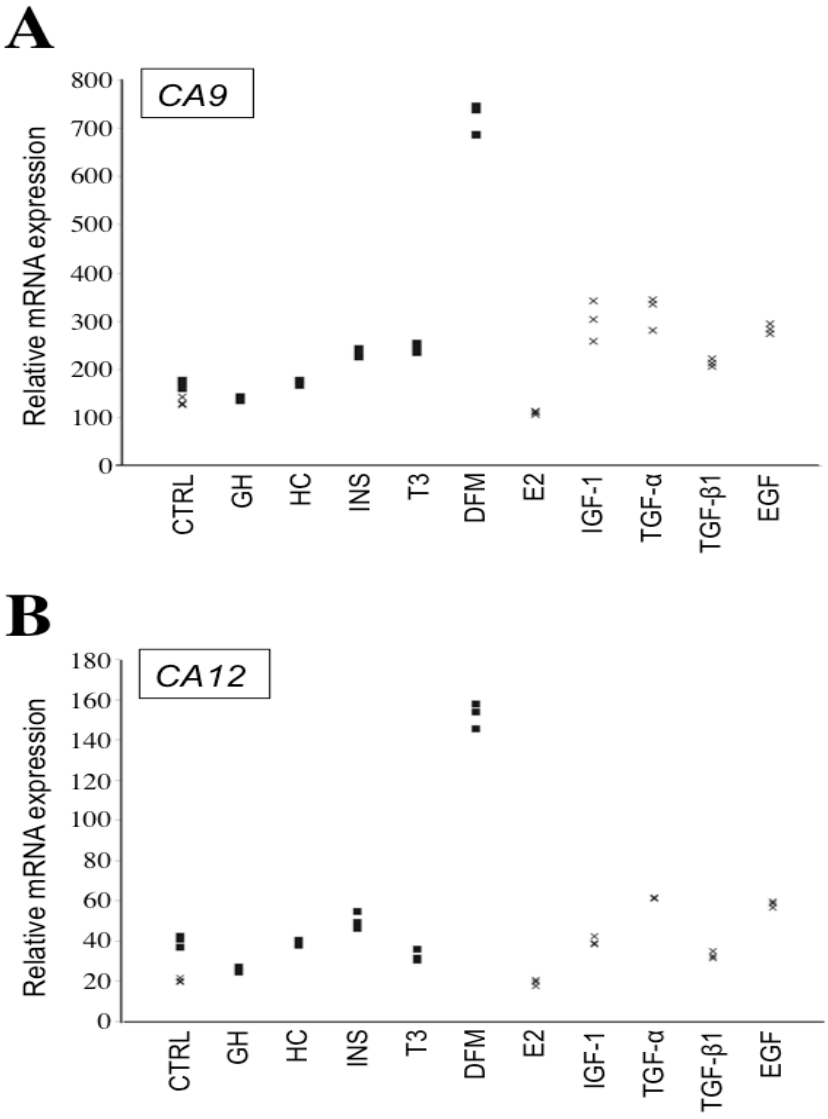

Figure 1: **Effects of different treatments on *CA9* and *CA12* expression in U373 cells, detected by quantitative real-time PCR. The treatments included growth hormone (GH), hydrocortisone (HC), insulin (INS), tri-iodothyronine (T3), deferoxamine mesylate (DFM), estradiol (E2), insulin-like growth factor-1 (IGF-1), transforming growth factor-alpha (TGF-α), transforming growth factor-beta 1 (TGF-β1), and epidermal growth factor (EGF). Both *CA9* (A) and *CA12* (B) expression were maximally induced by DFM treatment. Likewise, growth factor treatments elevated the transcription levels of both isozymes. The normalized values of triplicate experiments are shown. Two control (CTRL) groups were included in the study. The values of the first five treatments are compared to control 1 (squares), and the values of the last five treatments are compared to control 2 (crosses).**

binding activity in human HT-1080 fibrosarcoma cells and in human vascular smooth muscle cells [33,34]. The observed induction of *CA9* by TGF-β1 may also act through accumulation of HIF-1α, but this remains to be tested.

In HeLa cells, *CA9* was expressed only when stimulated with deferoxamine mesylate (Table 2). This change in expression was notable and indicates that hypoxia is an important regulator of *CA9* expression in this cell line, which was already reported [23]. Basal *CA9* expression below the detection limit (copy number < 100) was observed with MCF-7, Caki-1, A-498, HUVEC, and HepG2 cell lines (Table 2). Furthermore, *CA9* expression was not induced by any treatment in these cell lines, suggesting that critical element(s) necessary to drive its transcription could be missing or underrepresented. The fact that *CA9* expression was not induced in Caki-1 cells expressing wild-type pVHL after deferoxamine mesylate treatment is in line with a previous publication showing no *CA9* expression in Caki-1 cells with or without a hypoxic stimulation [23]. It is unclear why the levels of CA9 mRNA were below the detection limit in A-498 cells. It was presumed that there were high basal *CA9* expression levels in these cells due to pVHL inactivation.

Print ISSN 1816-0735; Online ISSN 1817-4256

Furthermore, these cells produced CA9 protein under standard cell culture conditions [35]. The most plausible explanation for this discrepancy is that *CA9* transcription was decreased due to the absence of serum in the cell cultures.

CA12 mRNA expression was detected in U373, MCF-7, Caki-1, A-498 and HUVEC cell lines (Table 3). In U373 cells, the CA12 mRNA levels were not as high as the CA9 levels, but the expression patterns were strikingly similar (Table 3 and Figure 1). Deferoxamine mesylate treatment markedly increased *CA12* expression compared to the control sample (3.8-fold). In addition, stimulation with TGF-α and EGF both caused a notable increase in *CA12* expression (fold changes of 3.1 and 2.9, respectively). Likewise, IGF-1 treatment elevated *CA12* levels two-fold and TGF-β1 treatment increased *CA12* levels 1.6-fold. Addition of growth hormone slightly decreased the levels of *CA12* expression (1.6-fold).

In MCF-7 cells, *CA12* was present at relatively high levels with an unusual expression profile (Table 3). *CA12* transcription was clearly induced after TGF-β1 and EGF treatments (fold changes of 2.8 and 2.4, respectively). Estradiol treatment also increased the CA12 mRNA levels (1.9-fold). A similar effect was demonstrated in MCF-7 cells [36]. The study showed that *CA12* was strongly up-regulated by estradiol via the estrogen receptor α (ERα), and that this regulation involved a distal estrogen-responsive enhancer region. We anticipated that the hypoxia pathway would have been induced in this cell line by deferoxamine mesylate treatment, but this was not the case. In fact, deferoxamine mesylate treatment somewhat decreased the levels of CA12 mRNA, and CA9 mRNA remained completely absent. It is notable that in invasive breast cancer, CA12-positive tumors are associated with positive ERα status, lower grade disease, lower relapse rate, and better overall patient survival [37]. Since hypoxia is usually linked to poor prognosis, it is possible that CA12 is not mainly regulated through the hypoxia-induced pathway in breast cancer, but regulation may involve an alternative pathway triggered by estradiol and certain growth factors.

Caki-1 and A-498 human renal carcinoma cell lines were selected for the study, because the first cell line produces wild-type pVHL and the latter represents a VHL-null cell line. In Caki-1 cells, *CA12* showed the highest signal after deferoxamine mesylate treatment (10.2-fold), as expected (Table 3). Again, IGF-1, TGF-β1 and EGF also induced a moderate increase in CA12 mRNA levels (fold changes of 1.5, 1.7 and 1.8, respectively). Moreover, estradiol induced a 1.5-fold increase in *CA12* expression. Similar to U373 cells, growth hormone treatment caused a decrease in *CA12* expression (1.5-fold). In A-498 cells, *CA12* transcript was present in high levels and, as predicted, deferoxamine mesylate treatment had no effect on gene expression (Table 3). The CA12 mRNA levels were also elevated after growth factor treatments. The highest levels of induction were obtained with TGF-β1 and EGF (fold changes of 2.5 and 2.6, respectively), while TGF-α had a slightly weaker effect (2.2-fold). Moreover, IGF-1 stimulation elicited a 1.7-fold increase in the CA12 mRNA levels. Addition of hydrocortisone moderately decreased the CA12 mRNA levels (1.6-fold). It is worth noticing that the mRNA levels of another hypoxia-induced gene, *VEGF*, have also been demonstrated to be down-regulated in A-498 cells after hydrocortisone treatment [38]. Although this effect was suggested to associate with the glucocorticoid receptor pathway, the exact mechanism for the reduced expression was not reported.

In HUVEC cells, *CA12* was expressed at a low level. None of the treatments markedly increased *CA12* expression (Table 3). Interestingly, several treatments reduced *CA12* expression. Hydrocortisone and IGF-1 caused an approximately two-fold decrease in CA12 mRNA levels whereas TGF-α and TGF-β1 treatments resulted in minor decreases (1.8- and 1.6-fold, respectively). In HeLa and HepG2 cells, the levels of *CA12* expression were below the detection limit of the quantitative PCR.

Like *CA9*, *CA12* expression was also elevated in the cancer-derived cell lines after IGF-1, TGF-α, TGF-β1, and EGF treatments. Since *CA12* is not strongly regulated by hypoxia, it is not surprising that it has additional regulators. It is plausible that the main stimulatory effects observed in this study are mediated through up-regulation of HIF-1α protein, which has been shown to be activated by several growth factors under normoxia. Our data suggests that this effect could be specific to cancerous environments, since it was not observed in normal HUVEC cells. However, in contrast, some inhibition of *CA12* was detectable after growth factor treatment. It is also worth noticing that similar to *CA9*, *CA12* expression could not be induced in cell lines lacking *CA12* expression under control conditions.

In summary, an understanding of *CA9* and *CA12* regulation has been mainly confined to hypoxia. Therefore, the object of the present study was to use several hormones and growth factors in order to find novel potential regulators of *CA9* and *CA12* transcription. In conclusion, we have shown that *CA9* and *CA12* are up-regulated by certain growth factors in human cancer-derived cell lines. For *CA9*, this effect was only observed in one cell line. In contrast, *CA12* expression was elevated in several cancer-derived cell lines after growth factor treatment. This induction may represent a novel regulatory mechanism for *CA12* expression in a cancerous environment and merits further investigation. The regulation of CA isozymes has been generally an understudied research area, and future studies should therefore include investigation of the regulation of other CAs. In the present study, insulin and T3 remained the only representatives of hormones or growth factors which elicited no substantial effects in any of the analyzed cell lines.

Acknowledgments

We gratefully acknowledge Janette Hinkka for technical support, Anna-Maija Koivisto for statistical support and Professor Jorma Isola for providing MCF-7 and HeLa cells.

References

1. Sly WS, Hu PY. Human carbonic anhydrases and carbonic anhydrase deficiencies. *Annu Rev Biochem* 64: 375-401, 1995.
2. Parkkila S. An overview of the distribution and function of carbonic anhydrase in mammals. *EXS* 90: 79-93, 2000.
3. Pastorekova S, Parkkila S, Zavada J. Tumor-associated carbonic anhydrases and their clinical significance. *Adv Clin Chem* 42: 167-216, 2006.
4. Saarnio J, Parkkila S, Parkkila AK, Pastorekova S, Haukipuro K, Pastorek J, Juvonen T, Karttunen TJ. Transmembrane carbonic anhydrase, MN/CA IX, is a potential biomarker for biliary tumours. *J Hepatol* 35: 643-649, 2001.
5. Leppilampi M, Saarnio J, Karttunen TJ, Kivela J, Pastorekova S, Pastorek J, Waheed A, Sly WS, Parkkila S. Carbonic anhydrase isozymes IX and XII in gastric tumors. *World J Gastroenterol* 9: 1398-1403, 2003.
6. Chia SK, Wykoff CC, Watson PH, Han C, Leek RD, Pastorek J, Gatter KC, Ratcliffe P, Harris AL. Prognostic significance of a novel hypoxia-regulated marker, carbonic anhydrase IX, in invasive breast carcinoma. *J Clin Oncol* 19: 3660-3668, 2001.
7. Giatromanolaki A, Koukourakis MI, Sivridis E, Pastorek J, Wykoff CC, Gatter KC, Harris AL. Expression of hypoxia-inducible carbonic anhydrase-9 relates to angiogenic pathways and independently to poor outcome in non-small cell lung cancer. *Cancer Res* 61: 7992-7998, 2001.
8. Haapasalo JA, Nordfors KM, Hilvo M, Rantala IJ, Soini Y, Parkkila AK, Pastorekova S, Pastorek J, Parkkila SM, Haapasalo HK. Expression of carbonic anhydrase IX in astrocytic tumors predicts poor prognosis. *Clin Cancer Res* 12: 473-477, 2006.
9. Loncaster JA, Harris AL, Davidson SE, Logue JP, Hunter RD, Wycoff CC, Pastorek J, Ratcliffe PJ, Stratford IJ, West CM. Carbonic anhydrase (CA IX) expression, a potential new intrinsic marker of hypoxia: correlations with tumor oxygen measure-

ments and prognosis in locally advanced carcinoma of the cervix. *Cancer Res* 61: 6394-6399, 2001.
10. Ivanov SV, Kuzmin I, Wei MH, Pack S, Geil L, Johnson BE, Stanbridge EJ, Lerman MI. Down-regulation of transmembrane carbonic anhydrases in renal cell carcinoma cell lines by wild-type von Hippel-Lindau transgenes. *Proc Natl Acad Sci USA* 95: 12596-12601, 1998.
11. Ivanov S, Liao SY, Ivanova A, Danilkovitch-Miagkova A, Tarasova N, Weirich G, Merrill MJ, Proescholdt MA, Oldfield EH, Lee J, Zavada J, Waheed A, Sly W, Lerman MI, Stanbridge EJ. Expression of hypoxia-inducible cell-surface transmembrane carbonic anhydrases in human cancer. *Am J Pathol* 158: 905-919, 2001.
12. Parkkila S, Parkkila AK, Saarnio J, Kivela J, Karttunen TJ, Kaunisto K, Waheed A, Sly WS, Tureci O, Virtanen I, Rajaniemi H. Expression of the membrane-associated carbonic anhydrase isozyme XII in the human kidney and renal tumors. *J Histochem Cytochem* 48: 1601-1608, 2000.
13. Kivela A, Parkkila S, Saarnio J, Karttunen TJ, Kivela J, Parkkila AK, Waheed A, Sly WS, Grubb JH, Shah G, Tureci O, Rajaniemi H. Expression of a novel transmembrane carbonic anhydrase isozyme XII in normal human gut and colorectal tumors. *Am J Pathol* 156: 577-584, 2000.
14. Kivela AJ, Parkkila S, Saarnio J, Karttunen TJ, Kivela J, Parkkila AK, Bartosova M, Mucha V, Novak M, Waheed A, Sly WS, Rajaniemi H, Pastorekova S, Pastorek J. Expression of von Hippel-Lindau tumor suppressor and tumor-associated carbonic anhydrases IX and XII in normal and neoplastic colorectal mucosa. *World J Gastroenterol* 11: 2616-2625, 2005.
15. Kivela AJ, Parkkila S, Saarnio J, Karttunen TJ, Kivela J, Parkkila AK, Pastorekova S, Pastorek J, Waheed A, Sly WS, Rajaniemi H. Expression of transmembrane carbonic anhydrase isoenzymes IX and XII in normal human pancreas and pancreatic tumours. *Histochem Cell Biol* 114: 197-204, 2000.
16. Ivan M, Kondo K, Yang H, Kim W, Valiando J, Ohh M, Salic A, Asara JM, Lane WS, Kaelin Jr WG. HIFalpha targeted for VHL-mediated destruction by proline hydroxylation: implications for O_2 sensing. *Science* 292: 464-468, 2001.
17. Jaakkola P, Mole DR, Tian YM, Wilson MI, Gielbert J, Gaskell SJ, Kriegsheim A, Hebestreit HF, Mukherji M, Schofield CJ, Maxwell PH, Pugh CW, Ratcliffe PJ. Targeting of HIF-alpha to the von Hippel-Lindau ubiquitylation complex by O_2-regulated prolyl hydroxylation. *Science* 292: 468-472, 2001.
18. Maxwell PH, Pugh CW, Ratcliffe PJ. Activation of the HIF pathway in cancer. *Curr Opin Genet Dev* 11: 293-299, 2001.
19. Semenza GL. Hypoxia-inducible factor 1: oxygen homeostasis and disease pathophysiology. *Trends Mol Med* 7: 345-350, 2001.
20. Harris AL. Hypoxia – a key regulatory factor in tumour growth. *Nat Rev Cancer* 2: 38-47, 2002.
21. Kopacek J, Barathova M, Dequiedt F, Sepelakova J, Kettmann R, Pastorek J, Pastorekova S. MAPK pathway contributes to density- and hypoxia-induced expression of the tumor-associated carbonic anhydrase IX. *Biochim Biophys Acta* 1729: 41-49, 2005.
22. Semenza G. Signal transduction to hypoxia-inducible factor 1. *Biochem Pharmacol* 64: 993-998, 2002.
23. Wykoff CC, Beasley NJ, Watson PH, Turner KJ, Pastorek J, Sibtain A, Wilson GD, Turley H, Talks KL, Maxwell PH, Pugh CW, Ratcliffe PJ, Harris AL. Hypoxia-inducible expression of tumor-associated carbonic anhydrases. *Cancer Res* 60: 7075-7083, 2000.
24. Ashida S, Nishimori I, Tanimura M, Onishi S, Shuin T. Effects of von Hippel-Lindau gene mutation and methylation status on expression of transmembrane carbonic anhydrases in renal cell carcinoma. *J Cancer Res Clin Oncol* 128: 561-568, 2002.
25. Vandesompele J, De Preter K, Pattyn F, Poppe B, Van Roy N, De Paepe A, Speleman F. Accurate normalization of real-time quantitative RT-PCR data by geometric averaging of multiple internal control genes. *Genome Biol* 3: research0034, 2002.
26. Proescholdt MA, Mayer C, Kubitza M, Schubert T, Liao SY, Stanbridge EJ, Ivanov S, Oldfield EH, Brawanski A, Merrill MJ. Expression of hypoxia-inducible carbonic anhydrases in brain tumors. *Neuro Oncol* 7: 465-475, 2005.
27. Ihnatko R, Kubes M, Takacova M, Sedlakova O, Sedlak J, Pastorek J, Kopacek J, Pastorekova S. Extracellular acidosis elevates carbonic anhydrase IX in human glioblastoma cells via transcriptional modulation that does not depend on hypoxia. *Int J Oncol* 29: 1025-1033, 2006.
28. Feldser D, Agani F, Iyer NV, Pak B, Ferreira G, Semenza GL. Reciprocal positive regulation of hypoxia-inducible factor 1alpha and insulin-like growth factor 2. *Cancer Res* 59: 3915-3918, 1999.
29. Zhong H, Chiles K, Feldser D, Laughner E, Hanrahan C, Georgescu MM, Simons JW, Semenza GL. Modulation of hypoxia-inducible factor 1alpha expression by the epidermal growth factor/phosphatidylinositol 3-kinase/PTEN/AKT/FRAP pathway in human prostate cancer cells: implications for tumor angiogenesis and therapeutics. *Cancer Res* 60: 1541-1545, 2000.
30. Maxwell PH. Hypoxia-inducible factor as a physiological regulator. *Exp Physiol* 90: 791-797, 2005.
31. Dorai T, Sawczuk IS, Pastorek J, Wiernik PH, Dutcher JP. The role of carbonic anhydrase IX overexpression in kidney cancer. *Eur J Cancer* 41: 2935-2947, 2005.
32. Lo HW, Hsu SC, Hung MC. EGFR signaling pathway in breast cancers: from traditional signal transduction to direct nuclear translocalization. *Breast Cancer Res Treat* 95: 211-218, 2006.
33. Gorlach A, Diebold I, Schini-Kerth VB, Berchner-Pfannschmidt U, Roth U, Brandes RP, Kietzmann T, Busse R. Thrombin activates the hypoxia-inducible factor-1 signaling pathway in vascular smooth muscle cells: role of the p22(phox)-containing NADPH oxidase. *Circ Res* 89: 47-54, 2001.
34. Shih SC, Claffey KP. Role of AP-1 and HIF-1 transcription factors in TGF-beta activation of VEGF expression. *Growth Factors* 19: 19-34, 2001.
35. Parkkila S, Rajaniemi H, Parkkila AK, Kivela J, Waheed A, Pastorekova S, Pastorek J, Sly WS. Carbonic anhydrase inhibitor suppresses invasion of renal cancer cells *in vitro*. *Proc Natl Acad Sci USA* 97: 2220-2224, 2000.
36. Barnett DH, Sheng S, Charn TH, Waheed A, Sly WS, Lin CY, Liu ET, Katzenellenbogen BS. Estrogen receptor regulation of carbonic anhydrase XII through a distal enhancer in breast cancer. *Cancer Res* 68: 3505-3515, 2008.
37. Watson PH, Chia SK, Wykoff CC, Han C, Leek RD, Sly WS, Gatter KC, Ratcliffe P, Harris AL. Carbonic anhydrase XII is a marker of good prognosis in invasive breast carcinoma. *Br J Cancer* 88: 1065-1070, 2003.
38. Iwai A, Fujii Y, Kawakami S, Takazawa R, Kageyama Y, Yoshida MA, Kihara K. Down-regulation of vascular endothelial growth factor in renal cell carcinoma cells by glucocorticoids. *Mol Cell Endocrinol* 226: 11-17, 2004.

Print ISSN 1816-0735; Online ISSN 1817-4256

BMC Genomics

RESEARCH ARTICLE Open Access

Global transcriptional response to carbonic anhydrase IX deficiency in the mouse stomach

Heini Kallio*[1,2], Mika Hilvo[3], Alejandra Rodriguez[1,2], Eeva-Helena Lappalainen[1,2], Anna-Maria Lappalainen[1,2] and Seppo Parkkila[1,2]

Abstract

Background: Carbonic anhydrases (CAs) are a family of enzymes that regulate pH homeostasis in various tissues. CA IX is an exceptional member of this family because in addition to the basic CA function, it has been implicated in several other physiological and pathological processes. Functions suggested for CA IX include roles in cell adhesion and malignant cell invasion. In addition, CA IX likely regulates cell proliferation and differentiation, which was demonstrated in *Car9*$^{-/-}$ mice. These mice had gastric pit cell hyperplasia and depletion of chief cells; however, the specific molecular mechanisms behind the observed phenotypes remain unknown. Therefore, we wanted to study the effect of CA IX deficiency on whole-genome gene expression in gastric mucosa. This was done using Illumina Sentrix®Mouse-6 Expression BeadChip arrays. The expression of several genes with notable fold change values was confirmed by QRT-PCR.

Results: CA IX deficiency caused the induction of 86 genes and repression of 46 genes in the gastric mucosa. There was 92.9% concordance between the results obtained by microarray analysis and QRT-PCR. The differentially expressed genes included those involved in developmental processes and cell differentiation. In addition, CA IX deficiency altered the expression of genes responsible for immune responses and downregulated the expression of several digestive enzymes.

Conclusions: Microarray analysis identified several potential genes whose altered expression could explain the disturbed cell lineage phenotype in the *Car9*$^{-/-}$ gastric mucosa. The results also indicated a novel role for CA IX in the regulation of immunologic processes and digestion. These findings reinforce the concept that the main role of CA IX is not the regulation of pH in the stomach mucosa. Instead, it is needed for proper function of several physiological processes.

Background

The carbonic anhydrases (CAs) are a family of zinc-containing metalloenzymes that catalyze the reversible hydration of carbon dioxide in the reaction: $CO_2 + H_2O$ $H^+ + HCO_3^-$. They participate in several physiological processes, such as acid-base balance, CO_2 and HCO_3^- transport, respiration, bone resorption, ureagenesis, gluconeogenesis, lipogenesis, production of body fluids, and fertilization [1,2]. The CA family consists of 13 active isozymes in mammals, 12 of which are expressed and function in humans [3]. The CA isozymes have diverse tissue expression patterns, characteristic subcellular localizations, as well as unique kinetic and inhibitory properties.

CA IX is a dimeric protein associated with the cell membrane [4,5]. In its mature form, CA IX is composed of an N-terminal proteoglycan (PG) domain, a CA catalytic domain, a transmembrane region, and a short intracytoplasmic tail at the C-terminus [6]. CA IX is the only member of the CA family containing a PG domain in addition to the CA domain. Consequently, CA IX has been suggested to participate in cell adhesion processes. In fact, using MDCK (Madin-Darby canine kidney) epithelial cells, it was shown that CA IX reduces E-cadherin-mediated cell-cell adhesion by interacting with β-catenin [7].

* Correspondence: heini.kallio@uta.fi
[1] Institute of Medical Technology and School of Medicine, University of Tampere, Biokatu 6, FI-33520 Tampere, Finland
Full list of author information is available at the end of the article

CA IX is expressed in only few normal tissues with the expression being strongest in human, rat, and mouse gastric mucosa, where it is present from the gastric pits to the deep gastric glands [8,9]. CA IX is confined to the basolateral surface of epithelial cells and is produced by all major cell types of the gastric epithelium [8]. CA IX is an exceptional member of the CA family because it is expressed in several cancers that arise from CA IX negative tissues including renal, lung, cervical, ovarian, esophageal, and breast carcinomas [6]. However, gastric cancer and premalignant lesions have shown decreased expression of CA IX [10]. In tumor tissues, CA IX is linked with the hypoxic phenotype mediated by the hypoxia-inducible transcription factor 1 (HIF-1), which binds to the hypoxia responsive element, HRE, of the *CA9* promoter [11]. In hypoxic conditions, cancer cells are dependent mainly on anaerobic metabolism in their energy production. This anaerobic tumor metabolism generates excesses of acidic products, such as lactic acid and H^+ that have to be extruded from the cell interior. It has been shown that CA IX can contribute to the acidification of the hypoxic extracellular milieu, thus helping tumor cells to neutralize the intracellular pH [12]. Accordingly, CA IX overexpression often indicates poor prognosis and resistance to classical radio- and chemotherapies [13]. However, CA IX is not only confined to the hypoxic regions of the tumors, indicating that there might be some other pathways that regulate its expression. In fact, the expression of CA IX can be induced under normoxic conditions by high cell density, and this regulation is mediated by phosphatidylinositol 3-kinase (PI3K) signaling [14]. Moreover, the mitogen-activated protein kinase (MAPK) pathway is involved in the regulation of CA IX expression via control of the *CA9* promoter by both HIF-1-dependent and -independent signals [15]. This pathway is also interrelated with the PI3K pathway and the SP1 (specificity protein 1) transcription factor.

The generation of *Car9*$^{-/-}$ mice has revealed that in addition to pH regulation and cell adhesion, CA IX possesses other functional roles [16]. These *Car9* knockout mice showed no abnormalities in growth, reproductive potential, and life span. However, CA IX deficiency resulted in hyperplasia of the gastric mucosa. The hyperplastic mucosa contained an increased number and proportion of the mucus-producing pit cells whereas the number and proportion of chief cells was reduced. The total number of parietal cells remained unchanged, and accordingly, CA IX-deficient mice had normal gastric pH, acid secretion, and serum gastrin levels. Thus, these findings demonstrate that CA IX contributes to the control of differentiation and proliferation of epithelial cell lineages in the gastric mucosa. A previous study examined whether the effects of CA IX deficiency could be modified by a high-salt diet, a known co-factor of carcinogenesis [17]. These results showed that the high-salt diet slightly increased the glandular atrophy in the body mucosa in *Car9*$^{-/-}$ C57BL/6 mice, whereas this effect was not observed in BALB/c mice. However, no metaplastic or dysplastic abnormalities were seen in the gastrointestinal epithelium of CA IX-deficient C57BL/6 mice. Thus, these observations suggest that CA IX deficiency alone may not be a significant carcinogenic factor but could initiate a carcinogenic process by affecting cell proliferation and/or differentiation in the gastric mucosa.

This study was designed to better understand the hyperplastic phenotype of the stomach mucosa of *Car9*$^{-/-}$ mice because the molecular mechanisms behind it are currently unknown. In addition, we wanted to more specifically elucidate the functional roles of CA IX, as there is a growing body of evidence showing that they extend far beyond pH regulation. For this purpose, a genome-wide expression analysis was performed. Microarray data analysis revealed several genes whose expression was changed due to *Car9* gene disruption in the gastric mucosa.

Results

Transcriptional response to Car9 deficiency in the stomach wall

Stomach RNA from 6 *Car9*$^{-/-}$ mice and 6 wild-type mice was analyzed by microarray. The analysis revealed 86 upregulated genes and 46 downregulated genes, using a fold change cut-off of ± 1.4 for up- and downregulated expression, respectively (See additional file 1: List of genes differentially expressed in the stomach of *Car9*$^{-/-}$ mice). This cut-off value has been proposed as an adequate level above which there is a high correlation between microarray and QRT-PCR data, regardless of other factors such as spot intensity and cycle threshold [18]. The fold changes ranged from 10.46 to -12.14. Herein, a list of genes using a cut-off value of ± 2.5-fold is shown (Tables 1 and 2). When using these criteria, all the genes with significantly ($p < 0.05$) altered expression are displayed, that is, 14 genes with induced expression and 21 genes with repressed expression. The list of all the regulated genes was functionally annotated (see additional file 2: Functional annotation of genes regulated in the stomach of *Car9* knockout mice), showing enrichment of hydrolase activity, developmental processes, cell differentiation, proteolysis, peptidase activity, structural molecule activity, and immune system process, among others. The functional annotation categories and gene numbers in each category are shown in Table 3.

Confirmation of microarray results by QRT-PCR

Changes in the expression levels of selected genes were confirmed, and microarray results were validated by QRT-PCR using the same RNA samples as those used for the microarray. Fourteen genes with notable fold change

Table 1: Genes with upregulated expression using a cut-off value of 2.5-fold.

Gene symbol	Description	GenBank number	FC	QRT-PCR
Cym	chymosin	NM_001111143	10.46	19.66
Slc9a3	solute carrier family 9 (sodium/hydrogen exchanger), member 3	NM_001081060	8.07	10.72
U46068	cDNA sequence U46068, transcript variant 2	NM_153418	5.95	
Dmbt1	deleted in malignant brain tumors 1	NM_007769	5.68	5.29
Il1rl1	interleukin 1 receptor-like 1, transcript variant 2	NM_010743	5.38	8.95
Tm4sf5	transmembrane 4 superfamily member 5	NM_029360	4.26	
9130204L05Rik	RIKEN cDNA 9130204L05 gene	NM_001101461	4.19	
Sftpd	surfactant associated protein D	NM_009160	4.11	3.69
Nccrp1	non-specific cytotoxic cell receptor protein 1 homolog (zebrafish)	NM_001081115	3.81	
Pkp4	plakophilin 4, transcript variant 1	NM_026361	3.54	1.09
Sprr2d	small proline-rich protein 2D	NM_011470	3.46	
Gm14446	predicted gene 14446, transcript variant 2	NM_001101605	3.45	
Sprr3	small proline-rich protein 3	NM_011478	3.39	
Sprr2i	small proline-rich protein 2I	NM_011475	3.31	
Sprr1a	small proline-rich protein 1A	NM_009264	3.30	
Ivl	involucrin	NM_008412	3.08	
Serpinb12	serine (or cysteine) peptidase inhibitor, clade B (ovalbumin), member 12	NM_027971	3.02	
Krt10	keratin 10	NM_010660	3.01	
Gm94	predicted gene 94	NM_001033280	2.94	
Krt13	keratin 13	NM_010662	2.94	
Gsdmc2	gasdermin C2, transcript variant 2	NM_177912	2.88	
Lor	loricrin	NM_008508	2.84	
Dmkn	dermokine, transcript variant 2	NM_172899	2.78	
Ly6d	lymphocyte antigen 6 complex, locus D	NM_010742	2.69	
Krt1	keratin 1	NM_008473	2.52	

Table 2: Genes with downregulated expression using a cut-off value of -2.5-fold.

Gene symbol	Description	GenBank number	FC	QRT-PCR
Try4	trypsin 4	NM_011646	-12.14	
Prss1	protease, serine, 1 (trypsin 1)	NM_053243	-10.57	
Amy2a5	amylase 2a5, pancreatic	NM_001042711	-9.85	
Cela2a	chymotrypsin-like elastase family, member 2A	NM_007919	-7.59	-16.23
Gm12888	predicted gene 12888	NM_001033791	-7.12	
Gdf9	growth differentiation factor 9	NM_008110	-7.04	
Blm	bloom syndrome homolog (human), transcript variant 1	NM_007550	-6.27	
Pnlip	pancreatic lipase	NM_026925	-6.23	-23.88
Cfd	complement factor D (adipsin)	NM_013459	-5.35	-27.45
Ctrb1	chymotrypsinogen B1	NM_025583	-5.00	
Mug1	murinoglobulin 1	NM_008645	-4.30	
Sostdc1	sclerostin domain containing 1	NM_025312	-4.17	
Tmed6	transmembrane emp24 protein transport domain containing 6	NM_025458	-4.07	
Cpa1	carboxypeptidase A1	NM_025350	-3.95	
Slc27a2	solute carrier family 27 (fatty acid transporter), member 2	NM_011978	-3.80	
Adipoq	adiponectin, C1Q and collagen domain containing	NM_009605	-3.74	-20.51
Car3	carbonic anhydrase 3	NM_007606	-3.72	-15.39
Egf	epidermal growth factor	NM_010113	-3.68	-3.71
Abpg	androgen binding protein gamma	NM_178308	-3.67	
Slc38a5	solute carrier family 38, member 5	NM_172479	-3.64	
Chia	chitinase, acidic	NM_023186	-3.52	
LOC638418	PREDICTED: similar to Ela3 protein	XM_914439	-3.48	

Table 2: Genes with downregulated expression using a cut-off value of -2.5-fold. (Continued)

LOC100043836	PREDICTED: similar to lacrimal androgen-binding protein delta, transcript variant 1	XM_001481113	-3.41	
EG640530	PREDICTED: predicted gene, EG640530	XM_917532	-3.37	
Nrn1	neuritin 1	NM_153529	-3.36	
Cela3b	chymotrypsin-like elastase family, member 3B	NM_026419	-3.32	-75.74
Spink3	serine peptidase inhibitor, Kazal type 3	NM_009258	-3.32	
Scd1	stearoyl-Coenzyme A desaturase 1	NM_009127	-3.27	
Ctrl	chymotrypsin-like	NM_023182	-3.19	
Gper	G protein-coupled estrogen receptor 1	NM_029771	-2.96	
Sycn	syncollin	NM_026716	-2.91	
Bhlha15	basic helix-loop-helix family, member a15	NM_010800	-2.77	
Cpb1	carboxypeptidase B1 (tissue)	NM_029706	-2.73	-18.22
Slc5a8	solute carrier family 5 (iodide transporter), member 8	NM_145423	-2.68	
Cyp2e1	cytochrome P450, family 2, subfamily e, polypeptide 1	NM_021282	-2.65	
Zg16	zymogen granule protein 16	NM_026918	-2.57	

values were selected for validation based on the results of functional annotation. The selected genes involved representatives from different functional categories. Thirteen (92.9%) out of 14 genes showed concordant results between microarray analysis and QRT-PCR (Tables 1 and 2, Figure 1). The sole discrepant result was *Pkp4*, which was upregulated according to the microarray and did not change according to the QRT-PCR (1.09-fold).

Discussion

A previous study showed a hyperplastic phenotype of gastric body mucosa in *Car9*$^{-/-}$ mice [16]. CA IX deficiency led to overproduction of gastric pit cells and reduction of chief cells. Quite surprisingly, the gastric pH of CA IX-deficient mice remained unaltered. Based on these observations, it can be concluded that the main role of CA IX in the stomach mucosa is not related to pH regulation but it is required for normal gastric morphogenesis and homeostasis within the gastric mucosa. In this paper, we report alterations in mRNA expression that might contribute to the phenotypic changes reported in the stomach of *Car9*-deficient mice. However, one must take into consideration that some of these changes can merely reflect differences in the relative proportions of various cell types within the gastric mucosa.

As expected, the *Car9*$^{-/-}$ phenotype changed the expression of genes involved in developmental processes and cell differentiation. The depletion of chief cells in *Car9*$^{-/-}$ gastric mucosa may be explained by the significant downregulation of the *basic helix-loop-helix family, member a15/Mist1* (*Bhlha15*) gene, which is a class B basic helix-loop-helix (bHLH) transcription factor that exhibits acinar cell-specific expression [19]. Mist1 gene expression is observed in a wide array of tissues with serous type secretion including the pancreas, salivary glands, chief cells of the stomach, Paneth cells of the small intestine, seminal vesicles, and lacrimal glands [20]. The deletion of *Mist1* blocks normal mucous neck cell redifferentiation into zymogenic chief cells as all basal zymogen-secreting cells in *Mist1*$^{-/-}$ mice show multiple structural defects [21].

Another interesting candidate with regard to cell lineage disturbance in the gastric epithelium of CA IX-defi-

Table 3: The functional annotation categories for the genes regulated by CA IX deficiency.

Functional category	Total regulated genes	Upregulated genes	Downregulated genes
Developmental processes*	20	13	7
Keratinization and keratinocyte differentiation	8	8	0
Structural molecule activity	13	13	0
Embryo implantation, female pregnancy, and menstrual cycle	3	3	0
Rhythmic process	4	3	1
Multi-organism process	5	5	0
Cell differentiation	16	12	4
Serine-type endopeptidase activity, serine hydrolase activity, and serine-type peptidase activity	9	3	6
Proteolysis	15	6	9
Peptidase activity	14	5	9
Endopeptidase activity	10	4	6
Trypsin and chymotrypsin activity	4	1	3
Hydrolase activity	22	8	14
Structural constituent of cytoskeleton	5	5	0
Cell communication	4	4	0
Metallocarboxypeptidase activity, carboxypeptidase activity, and metalloexopeptidase activity	3	0	3
Serine-type endopeptidase inhibitor activity, endopeptidase inhibitor activity, and protease inhibitor activity	4	2	2
Taxis and chemotaxis	4	3	1
Response to external stimulus	7	4	3
Immune system process	10	5	5
Defense response	7	5	2

Table 3: The functional annotation categories for the genes regulated by CA IX deficiency. (Continued)

Positive regulation of cell differentiation	3	2	1
PPAR signaling pathway	3	0	3
Leukocyte migration	3	2	1

*A representative category for the following overlapping categories: epidermis morphogenesis, tissue morphogenesis, epidermis development, ectoderm development, tissue development, organ development, anatomical structure development, anatomical structure morphogenesis, cellular developmental process, multicellular organismal development, and epidermal cell differentiation.

cient mice is *epidermal growth factor* (*Egf*), which has an expression that was significantly decreased when compared to wild-type mice. Among growth factors, the EGF family includes important agents for gastric mucosa. EGF is a single-chain polypeptide of 53 amino acid residues, which is found mainly in the submandibular glands and Brunner's glands of the gastrointestinal tract [22]. EGF binds and activates the epidermal growth factor receptor resulting in cellular proliferation, differentiation, and survival [23]. Interestingly, several investigators have reported that EGF receptors are enriched in rodent chief cells [24,25], suggesting the importance of EGF function in these cells. Therefore alterations in the expression of EGF receptor ligands or, in this case, EGF could contribute to the differentiation and function of chief cells.

One of the most strongly upregulated genes of this study was *deleted in malignant brain tumors 1* (*Dmbt1*), which belongs to the scavenger receptor cysteine-rich (SRCR) superfamily of proteins. This is a superfamily of secreted and membrane-bound proteins with SRCR domains that are highly conserved down to sponges [26,27]. The expression of DMBT1 is the highest in epithelia and is usually observed on the apical cell surface or in luminal exocrine secretions. In mice, DMBT1 is most strongly expressed in the gastrointestinal system [28]. DMBT1 is proposed to be a tumor suppressor [26,29,30] and/or a regulator of epithelial differentiation [31], as well as having roles in innate immune defense and inflammation [32,33]. DMBT1 is located in the crypt cells of the human, mouse, and rabbit small intestine [31,34,35] and the neck region of normal human gastric mucosa [36], which are predominantly composed of stem/progenitor cells. Thus, this gene is potentially involved in the physiological renewing process of gastrointestinal epithelia. A role for DMBT1 in innate immune defense has been demonstrated in various studies. The human DMBT1 glycoprotein, expressed in salivary glands, airways, and genital tract, binds various bacterial pathogens and viruses [37-40]. Additionally, expression of mouse DMBT1 in the gastrointestinal tract is regulated by bacteria [41,42], and its expression is increased during infection [43]. It has also been shown that there is an association of a *Dmbt1* variant allele with Crohn's disease and there is a correlation of expression levels of *Dmbt1* with inflammatory bowel disease severity [44].

Furthermore, DMBT1 binds surfactant proteins SP-D and SP-A. These are collagen- containing, (C-type) calcium-dependent lectins called collectins which interact with glycoconjugates and lipids on the surface of microorganisms mostly through their carbohydrate recognition domains (CRDs) [45]. SP-D and SP-A are involved in a range of immune functions, including viral neutralization, aggregation and killing of bacteria and fungi, and clearance of apoptotic and necrotic cells. In immunologically naïve lungs, they downregulate inflammatory reactions, but when challenged with LPS or apoptotic cells they induce phagocytosis by macrophages, pro-inflammatory cytokine production, and enhancement of adaptive immune responses [46]. It is interesting that in the present study, in addition to *Dmbt1*, the expression of *surfactant associated protein D* (*Sftpd or SP-D*) was highly induced in *Car9*$^{-/-}$ mice. Thus, the upregulation of both *Dmbt1* and *Sftpd* suggest that CA IX deficiency induced an immune process in the gastric mucosa. It should also be noted that CA IX has been suggested to bind to dendritic cells in a receptor-mediated manner and scavenger receptors appear to play an important role in this process [47]. In addition, CA IX seems to activate an immune response by a mechanism characteristic to heat shock proteins. Thus, CA IX could directly interact with DMBT1 via a scavenger receptor.

In fact, the disruption of *Car9* gene caused disregulation of several genes that are involved in immune processes. This corroborates the results from a previous study where gastric submucosal inflammation was detected in the body region in a majority of C57BL/6 *Car9*$^{-/-}$ mice [17]. In the present study, *Il1rl1/ST2* transcript variant 2 mRNA was highly induced due to CA IX deficiency. The *Il1rl1/ST2* gene is a member of the interleukin-1 (IL-1) receptor family and produces a soluble secreted form (sST2) and a transmembrane form (ST2L), coded by transcript variants 2 and 1, respectively. The membrane-bound form is expressed primarily by hematopoietic cells and the soluble form is predominantly expressed by fibroblasts [48]. In particular, ST2L is preferentially expressed in murine and human Th2 cells

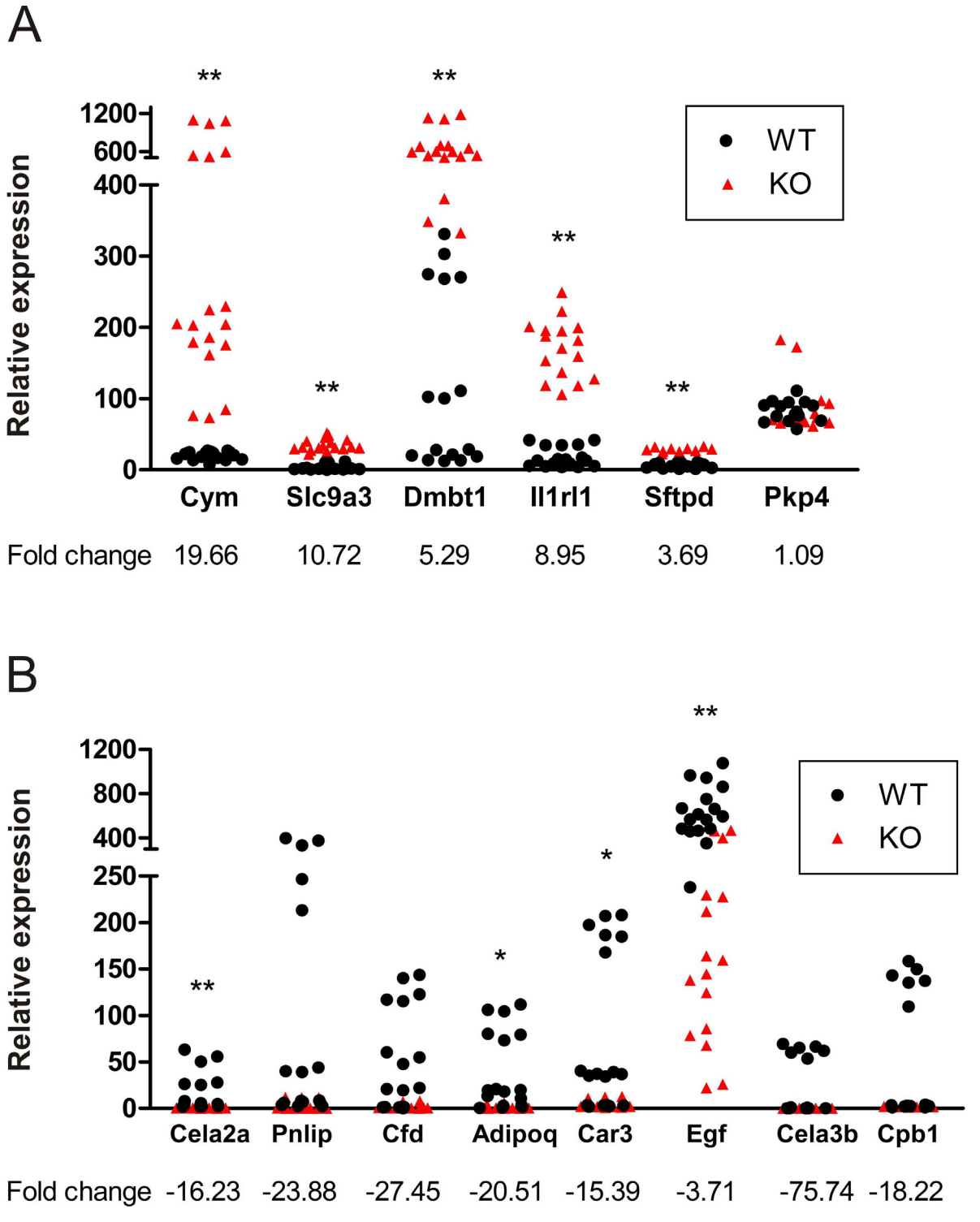

Figure 1 Verification of microarray data from Car9$^{-/-}$ mice by QRT-PCR. The expression of various transcripts in 6 *Car9*$^{-/-}$ mice was compared to that in 6 wild-type controls. The normalized values of triplicate experiments are shown. A, QRT-PCR analysis of 6 genes with induced expression. B, QRT-PCR evaluation of 8 genes with repressed expression. Statistically significant differences relative to wild-type mice were determined. *$p < 0.05$; **$p < 0.01$.

and can be used as a specific marker of Th2 cells in *in vitro* experiments [49-52]. Therefore, the function of ST2L has been suggested to correlate with Th2 cell-mediated immunological responses and IL-33, a newly discovered member of the IL-1 cytokine family, has been reported as a specific ligand for ST2L [53]. Interestingly, several studies have shown that the level of soluble ST2 in sera is elevated in asthmatic disease [54,55]. Therefore, it has been suggested that soluble ST2 may also play a critical role in Th2 cell-mediated diseases. In fact, it has been demonstrated that soluble ST2 acts as an antagonistic decoy receptor for IL-33 using a murine thymoma cell line, EL-4, which stably expresses ST2L, and a murine model of asthma [56]. This suggests that soluble ST2 negatively modulates the production of Th2 cytokines through IL-33 signaling in allergic airway inflammation. It is interesting to note that in the present study, the mRNA level of IL-33 was also elevated ~ 2-fold, although this change was not statistically significant. Thus, it seems plausible that CA IX is somehow involved in regulation of the Th2 response.

CA IX could also contribute to the development of the immune system as CA IX deficiency significantly downregulated the *bloom syndrome homolog (human)* gene (*Blm*), which encodes an ATP-dependent DNA helicase that belongs to an evolutionarily conserved family of RecQ helicases [57]. Mutation of *Blm* causes a rare human autosomal recessive disorder called Bloom's syndrome (BS), which is characterized by marked genomic instability. BS is associated with growth retardation, profound susceptibility to most cancer types, and immunodeficiency [58], with the latter two features accounting for early death [59]. The functions of BLM have been only partially characterized. However, it has been shown that BLM has a role in the proliferation and survival of both developing and mature T lymphocytes, and its deletion leads to defective T-cell immunity [60]. Additionally, the conditional knockout of *Blm* contributed to compromised B cell development and maintenance, strongly impaired T cell-dependent and -independent antibody responses after immunization, and a propensity for developing B cell lymphomas [61]. Therefore, it is conceivable that *Car9*$^{-/-}$ mice have compromised acquired immunity responses.

An unexpected finding was that several *small proline-rich proteins* (*Sprr*) were notably upregulated including *Sprr1a*, *Sprr2d*, *Sprr2e*, *Sprr2i*, and *Sprr3*. However, only the induction of *Sprr1a* was statistically significant. SPRR proteins were originally identified as markers for terminal squamous cell differentiation where they are precursors of the cornified envelope [62]. Additionally, SPRR proteins are expressed in various nonsquamous tissues, and their biological function is not restricted to structural proteins of the cornified envelope [63]. It has been shown that SPRR proteins participate in the response to various stresses in many tissues without a stratified epithelium. In the biliary tract, SPRR2 members appear to contribute to modification of the biliary barrier under conditions of stress [64]. Likewise, SPRR1A has been identified as a novel stress-inducible downstream mediator of gp130 cytokines in cardiomyocytes with a cardioprotective effect against ischemic stress [65]. Furthermore, in mice, SPRR2A protein was reported to be highly induced in gastric mucosa infected by *Helicobacter heilmannii* [66]. In addition, it has been suggested that SPRR1A is a regeneration-associated protein because its induction in neuronal injury correlates with regenerative capacity, with virtually all injured dorsal root ganglion neurons expressing SPRR1A one week after sciatic nerve injury [67]. Therefore, SPRR genes are presumably induced in response to different stress conditions and contribute to cell protection, tissue remodeling, and/or tissue regeneration. In the light of these findings it seems plausible that CA IX deficiency creates a stress condition in the gastric mucosa, which leads to upregulation of some protective factors.

Our analysis identified mRNAs from four members of solute carrier family proteins to be misregulated in the *Car9*$^{-/-}$ mice stomach mucosa. These solute carrier proteins are involved in membrane transport of various molecules. The expression of *Slc9a3* was strongly induced, whereas the expression of *Slc27a2*, *Slc38a5*, and *Slc5a8* was repressed. The basic function of SLC9A3 or NHE3 is the exchange of extracellular Na^+ for intracellular H^+, thus causing either a rise in intracellular pH or, if coupled to the action of other transporters, an increase in cell volume [68]. In the gastrointestinal tract, SLC9A3 is expressed in the apical membrane and recycling endosomes of the ileum, jejunum, colon, and stomach [69]. Further studies are needed to elucidate the possible interplay between CA IX and SLC9A3 in the gastric mucosa.

Surprisingly, among the most downregulated genes we found several genes involved in digestion. These included *trypsin 1*, *amylase 2a5*, *chymotrypsin-like elastase family member 2A*, and *pancreatic lipase* with statistically significant p-values and others, such as *chymotrypsinogen B1*, *carboxypeptidase A1*, and *carboxypeptidase B1* with non-significant p-values. The implication of this finding remains unclear. A possible explanation for this might be that downregulation of these enzymes is a secondary event. If it is assumed that these enzymes are produced by chief cells, the reduced number of chief cells in the *Car9*$^{-/-}$ mice gastric mucosa can also cause a decrease in the amount of the enzymes they produce. However, the exact mechanism behind this phenomenon remains to be elucidated.

Conclusions

In conclusion, CA IX deficiency was shown to alter the expression of various genes in the gastric mucosa. The number of affected genes and the magnitude of changes were relatively high, indicating that CA IX has a remarkable role in gastric functions. Microarray analysis revealed several genes involved in developmental processes and cell differentiation, which could explain the cell lineage disturbance in the gastric epithelium of *Car9*$^{-/-}$ mice. Interestingly, some of the regulated genes identified in this study are involved in digestion as well as functions of the immune and defense responses. This finding suggests that CA IX deficiency compromises the immune system in the gastric epithelium implying yet another role for this multifunctional enzyme.

Methods

Animal model and tissue preparation

Generation of the targeted disruption of the *Car9* gene has been previously described by Ortova Gut et al. [16]. These *Car9*-deficient C57BL/6 mice were produced and maintained in the animal facility of the University of Oulu and then delivered to the animal facility of the University of Tampere. Permissions for use of the experimental mice were obtained from the Animal Care Committees of the Universities of Oulu and Tampere. Six *Car9*$^{-/-}$ mice (3 males and 3 females) and six wild-type control mice (3 males and 3 females) were kept under tightly controlled specific pathogen-free conditions and fed identical diets. The mice were sacrificed at approximately 11 (SD = ± 1.35) months of age. Tissue specimens from the body of the stomach were immediately collected, immersed in RNAlater solution (Ambion, Austin, TX, USA), and frozen at -80°C.

RNA isolation

Total RNA was obtained using the RNeasy RNA isolation kit (Qiagen, Valencia, USA) following the manufacturer's instructions. Residual DNA was removed from the samples using RNase-free DNase (Qiagen). The RNA concentration and purity were determined by measurement of the optical density (OD) at 260 and 280 nm. All samples had an OD260/OD280 ratio of 1.95 or higher.

Microarray analysis

All microarray data reported in the present article are described in accordance with MIAME guidelines, have been deposited in NCBI's Gene Expression Omnibus public repository [70], and are accessible through GEO Series accession number GSE20981 [71]. Microarray experiments were performed in the Finnish DNA Microarray Centre at the Turku Centre for Biotechnology. Stomach RNA samples from 6 *Car9*$^{-/-}$ mice were used. As controls, RNA samples from the stomach of 6 wild-type mice were used. All 12 samples were analyzed individually. 400 ng of total RNA from each sample was amplified using the Illumina® TotalPrep RNA Amplification kit (Ambion) as recommended by the manufacturer. The *in vitro* transcription reaction, which was conducted for 14.5 h, included labeling of the cRNA by biotinylation.

Hybridization and scanning

Labeled and amplified cRNAs (1.5 μg/array) were hybridized to Illumina's Sentrix® Mouse-6 Expression Bead Chips (Illumina, Inc., San Diego, CA) at 58°C for 18 h according to Illumina® Whole-Genome Gene Expression with IntelliHyb Seal System Manual. The arrays were washed and then stained with 1 μg/ml cyanine3-streptavidin (Amersham Biosciences, Buckinghamshire, UK). The Illumina BeadArray™ Reader was used to scan the arrays according the manufacturer's instructions. The numerical results were extracted with the Illumina's BeadStudio software without any normalization or background subtraction.

Data analysis

Array data were normalized with Chipster (v1.3.0) using the quantile normalization method. The data were filtered according to the SD of the probes. The percentage of data that did not pass through the filter was adjusted to 99.4%, implicating a SD value of almost 3. Statistical analysis was next performed using the empirical Bayes t-test for the comparison of two groups. Finally, the probes were further filtered according to fold change with ± 1.4 as the cut-off for up- and downregulated expression, respectively. The functional annotation tool DAVID (Database for Annotation, Visualization and Integrated Discovery) [72,73] was used to identify enriched biological categories among the regulated genes when compared to all the genes present on Illumina's Sentrix Mouse-6 Expression Bead Chip. The annotation groupings analyzed were Gene Ontology biological process and molecular functions, SwissProt comments, SwissProt Protein Information Resources Keywords, Kyoto Encyclopedia of Genes and Genomes pathway, and Biocarta pathway. Results were filtered to remove categories with EASE (Expression Analysis Systematic Explorer) scores greater than 0.05. Overlapping categories with the same gene members were removed to yield a single representative category.

Quantitative real-time PCR

For quantitative real-time PCR (QRT-PCR), the same samples were used as for the microarray analysis. 5 μg of each RNA sample was converted into first strand cDNA using a First Strand cDNA Synthesis Kit (Fermentas, Burlington, Canada) using random hexamer primers following the manufacturer's instructions. The relative

Table 4: Sequences of the QRT-PCR primers used in this study.

Gene symbol	Description	GenBank number	Forward primer (5'-3')	Reverse primer (5'-3')
Adipoq	adiponectin, C1Q and collagen domain containing	NM_009605	TCCTGCTTTGGTCCCTCCAC	TCCTTTCTCTCCCTTCTCTCC
Car3	carbonic anhydrase 3	NM_007606	GCTCTGCTAAGACCATCC	ATTGGCGAAGTCGGTAGG
Cela2a	chymotrypsin-like elastase family, member 2A	NM_007919	TGATGTGAGCAGGGTAGTTGG	CACTCGGTAGGTCTGATAGTTG
Cela3b	chymotrypsin-like elastase family, member 3B	NM_026419	TGCCTGTGGTGGACTATGAA	CAGCCCAAGGAGGACACAA
Cfd	complement factor D (adipsin)	NM_013459	AACCGGACAACCTGCAATC	CCCACGTAACCACACCTTC
Cpb1	carboxypeptidase B1 (tissue)	NM_029706	GGTTTCCACGCAAGAGAG	GTTGACCACAGGCAGAACA
Cym	chymosin	NM_001111143	ATGAGCAGGAATGAGCAG	TGACAAGCCACCACTTCACC
Dmbt1	deleted in malignant brain tumors 1	NM_007769	GCACAAGTCCTCCATCATTC	AGACAGAGCAGAGCCACAAC
Egf	epidermal growth factor	NM_010113	GCTCGGTGTTTGTGTCGTG	CTGTCCCATCATCGTCTGG
Il1rl1	interleukin 1 receptor-like 1, transcript variant 2	NM_010743	ATTCTCTCCAGCCCTTCATC	AAGCCCAAAGTCCCATTCTC
Pkp4	plakophilin 4, transcript variant 1	NM_026361	GAACATAACCAAAGGCAGAGG	GGTGGACAGAGAAGGGTGTG
Pnlip	pancreatic lipase	NM_026925	CCCGCTTTCTCCTCTACACC	TCACACTCTCCACTCGGAAC
Sftpd	surfactant associated protein D	NM_009160	CCAACAAGGAAGCAATCTGAC	TCTCCCATCCCGTCCATCAC
Slc9a3	solute carrier family 9 (sodium/hydrogen exchanger), member 3	NM_001081060	TGACTGGCGTGGATTGTGTG	ACCAAGGACAGCAGGAAGG
Actb	actin, beta	NM_007393	AGAGGGAAATCGTGCGTGAC	CAATAGTGATGACCTGGCCGT
Hprt	hypoxanthine guanine phosphoribosyl transferase	NM_013556	AGCTACTGTAATGATCAGTCAACG	AGAGGTCCTTTTCACCAGCA
Sdha	succinate dehydrogenase complex, subunit A	NM_023281	GCTTGCGAGCTGCATTTGG	CATCTCCAGTTGTCCTCTTCCA

expression levels of the target genes in the stomach wall were assessed by QRT-PCR using the LightCycler detection system (Roche, Rotkreuz, Switzerland). The primer sets for the target genes (Table 4) were designed using Primer3 [74], based on the complete cDNA sequences deposited in GenBank. The specificity of the primers was verified using NCBI Basic Local Alignment Search Tool (BLAST) [20]. The house-keeping genes *β-actin* (*Actb*), *hypoxanthine guanine phosphoribosyl transferase* (*Hprt*), and *succinate dehydrogenase complex, subunit A* (*Sdha*) were used as internal controls to normalize the cDNA samples for possible differences in quality and quantity (Table 4). The *Actb* and *Hprt* primers are available in the public Quantitative PCR Primer Database [75] under the identification numbers 634 and 10050, respectively. The *Sdha* primers were obtained from the public PrimerBank database [76] with the identification number 15030102a2. To avoid amplification of genomic DNA, the primers from each primer pair were located in different exons, when possible.

Each PCR reaction was performed in a total volume of 20 μl containing 0.5 μl of first strand cDNA, 1x of Quanti-Tect SYBR Green PCR Master Mix (Qiagen, Hilden, Germany), and 0.5 μM of each primer. Amplification and detection were carried out as follows: after an initial 15 min activation step at 95°C, amplification was performed in a three-step cycling procedure for 45 cycles: denaturation at 95°C for 15 s, annealing at a temperature determined according to the T_m for each primer pair for 20 s, and elongation at 72°C for 15 s (the ramp rate was 20°C/s for all the steps), followed by a final cooling step. Melting curve analysis was always performed after the amplification to examine the specificity of the PCR. To quantify the levels of the target transcripts, a standard curve was established for each gene using five-fold serial dilutions of known concentrations of purified PCR products generated with the same primer pairs. Every cDNA sample was tested in triplicate. The mean and SD of the 3 crossing point (Cp) values were calculated for each sample and a SD cut-off of 0.2 was set. Accordingly, when the SD of the triplicates of a sample was greater than 0.2, the most outlying replicate was excluded and the analysis was continued with the two remaining replicates. Using a specific standard curve, the Cp values were then transformed by the LightCycler software into copy numbers. The expression value for each sample was the mean of the copy numbers for the sample's replicates. The geometric mean of the three internal control genes was used as an accurate normalization factor for gene expression levels [77]. The final relative mRNA expression was given as the expression value of the sample divided by the corresponding normalization factor and multiplied by 10^3.

Statistical analyses

Statistical analyses of the microarray were performed using the empirical Bayes t-test for comparison of the two groups, and the p-values are shown in Additional file 1. For the QRT-PCR results, the Mann-Whitney test was used to evaluate differences in group values for *Car9*$^{-/-}$ mice vs. wild-type mice.

List of abbreviations used

CA IX: carbonic anhydrase IX; HIF-1: hypoxia-inducible transcription factor 1; HRE: hypoxia responsive element; MAPK: mitogen-activated protein kinase; PI3K: phosphatidylinositol 3-kinase; QRT-PCR: quantitative real-time PCR.

Additional material

Additional file 1 List of genes differentially expressed in the stomach of *Car9*$^{-/-}$ mice. The *Car9*$^{-/-}$ and control groups contained samples from 6 mice. Microarray data were normalized with Chipster (v1.3.0) using the quantile normalization method. Statistical analysis was performed using the empirical Bayes t-test for the comparison of two groups. The probes were filtered according to fold change with cut-off of ± 1.4 for up- and down-regulated expression, respectively.

Additional file 2 Functional annotation of genes regulated in the stomach of *Car9* knockout mice. The functional annotation tool DAVID was used to identify enriched biological categories among the differentially expressed genes as compared to all genes present in Illumina's Sentrix Mouse-6 Expression Bead Chip.

Authors' contributions

HK prepared the samples, participated in the microarray data analysis and QRT-PCR confirmations, and drafted the manuscript. MH participated in the design of the study and microarray data analysis. AR participated in the experimental design of the study and critically reviewed the manuscript. EHL and AML participated in the QRT-PCR confirmations. SP conceived the study, participated in its design and coordination, and critically reviewed the manuscript. All authors read and approved the final manuscript.

Acknowledgements

We thank the Illumina team at the Finnish DNA Microarray Centre at the Turku Centre for Biotechnology, especially Reija Venho for performing the microarray hybridizations and scanning. This study was supported by the Competitive Research Funding of the Tampere University Hospital (9L071), EU FP6 project (DeZnIT), and the Academy of Finland.

Author Details

[1]Institute of Medical Technology and School of Medicine, University of Tampere, Biokatu 6, FI-33520 Tampere, Finland, [2]Center for Laboratory Medicine, Tampere University Hospital, Biokatu 4, FI-33521 Tampere, Finland and [3]VTT Technical Research Centre of Finland, Tietotie 2, P.O. Box 1000, FI-02044 VTT, Espoo, Finland

Received: 11 March 2010 Accepted: 23 June 2010
Published: 23 June 2010

References

1. Sly WS, Hu PY: **Human carbonic anhydrases and carbonic anhydrase deficiencies.** *Annu Rev Biochem* 1995, **64**:375-401.
2. Parkkila S: **An overview of the distribution and function of carbonic anhydrase in mammals.** *Exs* 2000:79-93.
3. Hilvo M, Tolvanen M, Clark A, Shen B, Shah GN, Waheed A, Halmi P, Hanninen M, Hamalainen JM, Vihinen M, Sly WS, Parkkila S:

Characterization of CA XV, a new GPI-anchored form of carbonic anhydrase. *Biochem J* 2005, **392(Pt 1):**83-92.
4. Hilvo M, Baranauskiene L, Salzano AM, Scaloni A, Matulis D, Innocenti A, Scozzafava A, Monti SM, Di Fiore A, De Simone G, Lindfors M, Janis J, Valjakka J, Pastorekova S, Pastorek J, Kulomaa MS, Nordlund HR, Supuran CT, Parkkila S: **Biochemical characterization of CA IX, one of the most active carbonic anhydrase isozymes.** *J Biol Chem* 2008, **283(41):**27799-27809.
5. Alterio V, Hilvo M, Di Fiore A, Supuran CT, Pan P, Parkkila S, Scaloni A, Pastorek J, Pastorekova S, Pedone C, Scozzafava A, Monti SM, De Simone G: **Crystal structure of the catalytic domain of the tumor-associated human carbonic anhydrase IX.** *Proc Natl Acad Sci USA* 2009, **106(38):**16233-16238.
6. Pastorekova S: **Carbonic anhydrase IX (CA IX) as a potential target for cancer therapy.** *Cancer Therapy* 2004, **2:**245-262.
7. Svastova E, Zilka N, Zat'ovicova M, Gibadulinova A, Ciampor F, Pastorek J, Pastorekova S: **Carbonic anhydrase IX reduces E-cadherin-mediated adhesion of MDCK cells via interaction with beta-catenin.** *Exp Cell Res* 2003, **290(2):**332-345.
8. Pastorekova S, Parkkila S, Parkkila AK, Opavsky R, Zelnik V, Saarnio J, Pastorek J: **Carbonic anhydrase IX, MN/CA IX: analysis of stomach complementary DNA sequence and expression in human and rat alimentary tracts.** *Gastroenterology* 1997, **112(2):**398-408.
9. Hilvo M, Rafajova M, Pastorekova S, Pastorek J, Parkkila S: **Expression of carbonic anhydrase IX in mouse tissues.** *J Histochem Cytochem* 2004, **52(10):**1313-1322.
10. Leppilampi M, Saarnio J, Karttunen TJ, Kivela J, Pastorekova S, Pastorek J, Waheed A, Sly WS, Parkkila S: **Carbonic anhydrase isozymes IX and XII in gastric tumors.** *World J Gastroenterol* 2003, **9(7):**1398-1403.
11. Wykoff CC, Beasley NJ, Watson PH, Turner KJ, Pastorek J, Sibtain A, Wilson GD, Turley H, Talks KL, Maxwell PH, Pugh CW, Ratcliffe PJ, Harris AL: **Hypoxia-inducible expression of tumor-associated carbonic anhydrases.** *Cancer Res* 2000, **60(24):**7075-7083.
12. Svastova E, Hulikova A, Rafajova M, Zat'ovicova M, Gibadulinova A, Casini A, Cecchi A, Scozzafava A, Supuran CT, Pastorek J, Pastorekova S: **Hypoxia activates the capacity of tumor-associated carbonic anhydrase IX to acidify extracellular pH.** *FEBS Lett* 2004, **577(3):**439-445.
13. Harris AL: **Hypoxia--a key regulatory factor in tumour growth.** *Nat Rev Cancer* 2002, **2(1):**38-47.
14. Kaluz S, Kaluzova M, Chrastina A, Olive PL, Pastorekova S, Pastorek J, Lerman MI, Stanbridge EJ: **Lowered oxygen tension induces expression of the hypoxia marker MN/carbonic anhydrase IX in the absence of hypoxia-inducible factor 1 alpha stabilization: a role for phosphatidylinositol 3'-kinase.** *Cancer Res* 2002, **62(15):**4469-4477.
15. Kopacek J, Barathova M, Dequiedt F, Sepelakova J, Kettmann R, Pastorek J, Pastorekova S: **MAPK pathway contributes to density- and hypoxia-induced expression of the tumor-associated carbonic anhydrase IX.** *Biochim Biophys Acta* 2005, **1729(1):**41-49.
16. Ortova Gut MO, Parkkila S, Vernerova Z, Rohde E, Zavada J, Hocker M, Pastorek J, Karttunen T, Gibadulinova A, Zavadova Z, Knobeloch KP, Wiedenmann B, Svoboda J, Horak I, Pastorekova S: **Gastric hyperplasia in mice with targeted disruption of the carbonic anhydrase gene Car9.** *Gastroenterology* 2002, **123(6):**1889-1903.
17. Leppilampi M, Karttunen TJ, Kivela J, Gut MO, Pastorekova S, Pastorek J, Parkkila S: **Gastric pit cell hyperplasia and glandular atrophy in carbonic anhydrase IX knockout mice: studies on two strains C57/BL6 and BALB/C.** *Transgenic Res* 2005, **14(5):**655-663.
18. Morey JS, Ryan JC, Van Dolah FM: **Microarray validation: factors influencing correlation between oligonucleotide microarrays and real-time PCR.** *Biol Proced Online* 2006, **8:**175-193.
19. Lemercier C, To RQ, Swanson BJ, Lyons GE, Konieczny SF: **Mist1: a novel basic helix-loop-helix transcription factor exhibits a developmentally regulated expression pattern.** *Dev Biol* 1997, **182(1):**101-113.
20. Pin CL, Bonvissuto AC, Konieczny SF: **Mist1 expression is a common link among serous exocrine cells exhibiting regulated exocytosis.** *Anat Rec* 2000, **259(2):**157-167.
21. Ramsey VG, Doherty JM, Chen CC, Stappenbeck TS, Konieczny SF, Mills JC: **The maturation of mucus-secreting gastric epithelial progenitors into digestive-enzyme secreting zymogenic cells requires Mist1.** *Development* 2007, **134(1):**211-222.
22. Heitz PU, Kasper M, van Noorden S, Polak JM, Gregory H, Pearse AG: **Immunohistochemical localisation of urogastrone to human duodenal and submandibular glands.** *Gut* 1978, **19(5):**408-413.
23. Herbst RS: **Review of epidermal growth factor receptor biology.** *Int J Radiat Oncol Biol Phys* 2004, **59(2 Suppl):**21-26.
24. Fujisawa T, Kamimura H, Hosaka M, Torii S, Izumi T, Kuwano H, Takeuchi T: **Functional localization of proprotein-convertase furin and its substrate TGFbeta in EGF receptor-expressing gastric chief cells.** *Growth Factors* 2004, **22(1):**51-59.
25. Kamimura H, Konda Y, Yokota H, Takenoshita S, Nagamachi Y, Kuwano H, Takeuchi T: **Kex2 family endoprotease furin is expressed specifically in pit-region parietal cells of the rat gastric mucosa.** *Am J Physiol* 1999, **277(1 Pt 1):**G183-190.
26. Mollenhauer J, Wiemann S, Scheurlen W, Korn B, Hayashi Y, Wilgenbus KK, von Deimling A, Poustka A: **DMBT1, a new member of the SRCR superfamily, on chromosome 10q25.3-26.1 is deleted in malignant brain tumours.** *Nat Genet* 1997, **17(1):**32-39.
27. Holmskov U, Mollenhauer J, Madsen J, Vitved L, Gronlund J, Tornoe I, Kliem A, Reid KB, Poustka A, Skjodt K: **Cloning of gp-340, a putative opsonin receptor for lung surfactant protein D.** *Proc Natl Acad Sci USA* 1999, **96(19):**10794-10799.
28. De Lisle RC, Petitt M, Huff J, Isom KS, Agbas A: **MUCLIN expression in the cystic fibrosis transmembrane conductance regulator knockout mouse.** *Gastroenterology* 1997, **113(2):**521-532.
29. Somerville RP, Shoshan Y, Eng C, Barnett G, Miller D, Cowell JK: **Molecular analysis of two putative tumour suppressor genes, PTEN and DMBT, which have been implicated in glioblastoma multiforme disease progression.** *Oncogene* 1998, **17(13):**1755-1757.
30. Mori M, Shiraishi T, Tanaka S, Yamagata M, Mafune K, Tanaka Y, Ueo H, Barnard GF, Sugimachi K: **Lack of DMBT1 expression in oesophageal, gastric and colon cancers.** *Br J Cancer* 1999, **79(2):**211-213.
31. Takito J, Hikita C, Al-Awqati Q: **Hensin, a new collecting duct protein involved in the in vitro plasticity of intercalated cell polarity.** *J Clin Invest* 1996, **98(10):**2324-2331.
32. Rosenstiel P, Sina C, End C, Renner M, Lyer S, Till A, Hellmig S, Nikolaus S, Folsch UR, Helmke B, Autschbach F, Schirmacher P, Kioschis P, Hafner M, Poustka A, Mollenhauer J, Schreiber S: **Regulation of DMBT1 via NOD2 and TLR4 in intestinal epithelial cells modulates bacterial recognition and invasion.** *J Immunol* 2007, **178(12):**8203-8211.
33. Kojouharova MS, Tsacheva IG, Tchorbadjieva MI, Reid KB, Kishore U: **Localization of ligand-binding sites on human C1q globular head region using recombinant globular head fragments and single-chain antibodies.** *Biochim Biophys Acta* 2003, **1652(1):**64-74.
34. Cheng H, Bjerknes M, Chen H: **CRP-ductin: a gene expressed in intestinal crypts and in pancreatic and hepatic ducts.** *Anat Rec* 1996, **244(3):**327-343.
35. Mollenhauer J, Herbertz S, Holmskov U, Tolnay M, Krebs I, Merlo A, Schroder HD, Maier D, Breitling F, Wiemann S, Grone HJ, Poustka A: **DMBT1 encodes a protein involved in the immune defense and in epithelial differentiation and is highly unstable in cancer.** *Cancer Res* 2000, **60(6):**1704-1710.
36. Kang W, Nielsen O, Fenger C, Madsen J, Hansen S, Tornoe I, Eggleton P, Reid KB, Holmskov U: **The scavenger receptor, cysteine-rich domain-containing molecule gp-340 is differentially regulated in epithelial cell lines by phorbol ester.** *Clin Exp Immunol* 2002, **130(3):**449-458.
37. Prakobphol A, Xu F, Hoang VM, Larsson T, Bergstrom J, Johansson I, Frangsmyr L, Holmskov U, Leffler H, Nilsson C, Boren T, Wright JR, Stromberg N, Fisher SJ: **Salivary agglutinin, which binds Streptococcus mutans and Helicobacter pylori, is the lung scavenger receptor cysteine-rich protein gp-340.** *J Biol Chem* 2000, **275(51):**39860-39866.
38. Stoddard E, Cannon G, Ni H, Kariko K, Capodici J, Malamud D, Weissman D: **gp340 expressed on human genital epithelia binds HIV-1 envelope protein and facilitates viral transmission.** *J Immunol* 2007, **179(5):**3126-3132.
39. White MR, Crouch E, van Eijk M, Hartshorn M, Pemberton L, Tornoe I, Holmskov U, Hartshorn KL: **Cooperative anti-influenza activities of respiratory innate immune proteins and neuraminidase inhibitor.** *Am J Physiol Lung Cell Mol Physiol* 2005, **288(5):**L831-840.
40. Wu Z, Van Ryk D, Davis C, Abrams WR, Chaiken I, Magnani J, Malamud D: **Salivary agglutinin inhibits HIV type 1 infectivity through interaction with viral glycoprotein 120.** *AIDS Res Hum Retroviruses* 2003, **19(3):**201-209.

41. Hooper LV, Wong MH, Thelin A, Hansson L, Falk PG, Gordon JI: **Molecular analysis of commensal host-microbial relationships in the intestine.** *Science* 2001, **291(5505):**881-884.
42. Sun FJ, Kaur S, Ziemer D, Banerjee S, Samuelson LC, De Lisle RC: **Decreased gastric bacterial killing and up-regulation of protective genes in small intestine in gastrin-deficient mouse.** *Dig Dis Sci* 2003, **48(5):**976-985.
43. Norkina O, Kaur S, Ziemer D, De Lisle RC: **Inflammation of the cystic fibrosis mouse small intestine.** *Am J Physiol Gastrointest Liver Physiol* 2004, **286(6):**G1032-1041.
44. Renner M, Bergmann G, Krebs I, End C, Lyer S, Hilberg F, Helmke B, Gassler N, Autschbach F, Bikker F, Strobel-Freidekind O, Gronert-Sum S, Benner A, Blaich S, Wittig R, Hudler M, Ligtenberg AJ, Madsen J, Holmskov U, Annese V, Latiano A, Schirmacher P, Amerongen AV, D'Amato M, Kioschis P, Hafner M, Poustka A, Mollenhauer J: **DMBT1 confers mucosal protection in vivo and a deletion variant is associated with Crohn's disease.** *Gastroenterology* 2007, **133(5):**1499-1509.
45. Kishore U, Greenhough TJ, Waters P, Shrive AK, Ghai R, Kamran MF, Bernal AL, Reid KB, Madan T, Chakraborty T: **Surfactant proteins SP-A and SP-D: structure, function and receptors.** *Mol Immunol* 2006, **43(9):**1293-1315.
46. Gardai SJ, Xiao YQ, Dickinson M, Nick JA, Voelker DR, Greene KE, Henson PM: **By binding SIRPalpha or calreticulin/CD91, lung collectins act as dual function surveillance molecules to suppress or enhance inflammation.** *Cell* 2003, **115(1):**13-23.
47. Wang Y, Wang XY, Subjeck JR, Kim HL: **Carbonic anhydrase IX has chaperone-like functions and is an immunoadjuvant.** *Mol Cancer Ther* 2008, **7(12):**3867-3877.
48. Gachter T, Werenskiold AK, Klemenz R: **Transcription of the interleukin-1 receptor-related T1 gene is initiated at different promoters in mast cells and fibroblasts.** *J Biol Chem* 1996, **271(1):**124-129.
49. Yanagisawa K, Naito Y, Kuroiwa K, Arai T, Furukawa Y, Tomizuka H, Miura Y, Kasahara T, Tetsuka T, Tominaga S: **The expression of ST2 gene in helper T cells and the binding of ST2 protein to myeloma-derived RPMI8226 cells.** *J Biochem* 1997, **121(1):**95-103.
50. Xu D, Chan WL, Leung BP, Huang F, Wheeler R, Piedrafita D, Robinson JH, Liew FY: **Selective expression of a stable cell surface molecule on type 2 but not type 1 helper T cells.** *J Exp Med* 1998, **187(5):**787-794.
51. Lohning M, Stroehmann A, Coyle AJ, Grogan JL, Lin S, Gutierrez-Ramos JC, Levinson D, Radbruch A, Kamradt T: **T1/ST2 is preferentially expressed on murine Th2 cells, independent of interleukin 4, interleukin 5, and interleukin 10, and important for Th2 effector function.** *Proc Natl Acad Sci USA* 1998, **95(12):**6930-6935.
52. Lecart S, Lecointe N, Subramaniam A, Alkan S, Ni D, Chen R, Boulay V, Pene J, Kuroiwa K, Tominaga S, Yssel H: **Activated, but not resting human Th2 cells, in contrast to Th1 and T regulatory cells, produce soluble ST2 and express low levels of ST2L at the cell surface.** *Eur J Immunol* 2002, **32(10):**2979-2987.
53. Schmitz J, Owyang A, Oldham E, Song Y, Murphy E, McClanahan TK, Zurawski G, Moshrefi M, Qin J, Li X, Gorman DM, Bazan JF, Kastelein RA: **IL-33, an interleukin-1-like cytokine that signals via the IL-1 receptor-related protein ST2 and induces T helper type 2-associated cytokines.** *Immunity* 2005, **23(5):**479-490.
54. Oshikawa K, Kuroiwa K, Tago K, Iwahana H, Yanagisawa K, Ohno S, Tominaga SI, Sugiyama Y: **Elevated soluble ST2 protein levels in sera of patients with asthma with an acute exacerbation.** *Am J Respir Crit Care Med* 2001, **164(2):**277-281.
55. Oshikawa K, Yanagisawa K, Tominaga S, Sugiyama Y: **Expression and function of the ST2 gene in a murine model of allergic airway inflammation.** *Clin Exp Allergy* 2002, **32(10):**1520-1526.
56. Hayakawa H, Hayakawa M, Kume A, Tominaga S: **Soluble ST2 blocks interleukin-33 signaling in allergic airway inflammation.** *J Biol Chem* 2007, **282(36):**26369-26380.
57. Bachrati CZ, Hickson ID: **RecQ helicases: suppressors of tumorigenesis and premature aging.** *Biochem J* 2003, **374(Pt 3):**577-606.
58. German J: **Bloom syndrome: a mendelian prototype of somatic mutational disease.** *Medicine (Baltimore)* 1993, **72(6):**393-406.
59. German J: **Bloom's syndrome. XX. The first 100 cancers.** *Cancer Genet Cytogenet* 1997, **93(1):**100-106.
60. Babbe H, Chester N, Leder P, Reizis B: **The Bloom's syndrome helicase is critical for development and function of the alphabeta T-cell lineage.** *Mol Cell Biol* 2007, **27(5):**1947-1959.
61. Babbe H, McMenamin J, Hobeika E, Wang J, Rodig SJ, Reth M, Leder P: **Genomic instability resulting from Blm deficiency compromises development, maintenance, and function of the B cell lineage.** *J Immunol* 2009, **182(1):**347-360.
62. Baden HP, Kubilus J, Phillips SB, Kvedar JC, Tahan SR: **A new class of soluble basic protein precursors of the cornified envelope of mammalian epidermis.** *Biochim Biophys Acta* 1987, **925(1):**63-73.
63. Tesfaigzi J, Carlson DM: **Expression, regulation, and function of the SPR family of proteins. A review.** *Cell Biochem Biophys* 1999, **30(2):**243-265.
64. Nozaki I, Lunz JG, Specht S, Stolz DB, Taguchi K, Subbotin VM, Murase N, Demetris AJ: **Small proline-rich proteins 2 are noncoordinately upregulated by IL-6/STAT3 signaling after bile duct ligation.** *Lab Invest* 2005, **85(1):**109-123.
65. Pradervand S, Yasukawa H, Muller OG, Kjekshus H, Nakamura T, St Amand TR, Yajima T, Matsumura K, Duplain H, Iwatate M, Woodard S, Pedrazzini T, Ross J, Firsov D, Rossier BC, Hoshijima M, Chien KR: **Small proline-rich protein 1A is a gp130 pathway- and stress-inducible cardioprotective protein.** *EMBO J* 2004, **23(22):**4517-4525.
66. Mueller A, O'Rourke J, Grimm J, Guillemin K, Dixon MF, Lee A, Falkow S: **Distinct gene expression profiles characterize the histopathological stages of disease in Helicobacter-induced mucosa-associated lymphoid tissue lymphoma.** *Proc Natl Acad Sci USA* 2003, **100(3):**1292-1297.
67. Starkey ML, Davies M, Yip PK, Carter LM, Wong DJ, McMahon SB, Bradbury EJ: **Expression of the regeneration-associated protein SPRR1A in primary sensory neurons and spinal cord of the adult mouse following peripheral and central injury.** *J Comp Neurol* 2009, **513(1):**51-68.
68. He P, Yun CC: **Mechanisms of the regulation of the intestinal Na+/H+ exchanger NHE3.** *J Biomed Biotechnol* 2010:238080.
69. Hoogerwerf WA, Tsao SC, Devuyst O, Levine SA, Yun CH, Yip JW, Cohen ME, Wilson PD, Lazenby AJ, Tse CM, Donowitz M: **NHE2 and NHE3 are human and rabbit intestinal brush-border proteins.** *Am J Physiol* 1996, **270(1 Pt 1):**G29-41.
70. Edgar R, Domrachev M, Lash AE: **Gene Expression Omnibus: NCBI gene expression and hybridization array data repository.** *Nucleic Acids Res* 2002, **30(1):**207-210.
71. **GEO. Gene Expression Omnibus** [http://www.ncbi.nlm.nih.gov/geo/]
72. **DAVID Bioinformatics Resources** [http://david.abcc.ncifcrf.gov/]
73. Dennis G Jr, Sherman BT, Hosack DA, Yang J, Gao W, Lane HC, Lempicki RA: **DAVID: Database for Annotation, Visualization, and Integrated Discovery.** *Genome Biol* 2003, **4(5):**P3..
74. **Primer3** [http://frodo.wi.mit.edu/primer3/]
75. **Quantitative PCR Primer Database** [http://web.ncifcrf.gov/rtp/gel/primerdb/]
76. **PrimerBank database** [http://pga.mgh.harvard.edu/primerbank/]
77. Vandesompele J, De Preter K, Pattyn F, Poppe B, Van Roy N, De Paepe A, Speleman F: **Accurate normalization of real-time quantitative RT-PCR data by geometric averaging of multiple internal control genes.** *Genome Biol* 2002, **3(7):**RESEARCH0034.

doi: 10.1186/1471-2164-11-397
Cite this article as: Kallio *et al.*, Global transcriptional response to carbonic anhydrase IX deficiency in the mouse stomach *BMC Genomics* 2010, **11**:397

OPEN ACCESS Freely available online

PLoS one

Characterization of Non-Specific Cytotoxic Cell Receptor Protein 1: A New Member of the Lectin-Type Subfamily of F-Box Proteins

Heini Kallio[1,3]*, Martti Tolvanen[1], Janne Jänis[4], Pei-wen Pan[1,3], Eeva Laurila[1], Anne Kallioniemi[1,3], Sami Kilpinen[5], Vilppu J. Tuominen[1], Jorma Isola[1], Jarkko Valjakka[1], Silvia Pastorekova[6], Jaromir Pastorek[6], Seppo Parkkila[1,2,3]

1 Institute of Biomedical Technology, University of Tampere, Tampere, Finland, **2** School of Medicine, University of Tampere, Tampere, Finland, **3** Center for Laboratory Medicine, Tampere University Hospital, Tampere, Finland, **4** Department of Chemistry, University of Eastern Finland, Joensuu, Finland, **5** MediSapiens Ltd, Helsinki, Finland, **6** Center of Molecular Medicine, Institute of Virology, Slovak Academy of Sciences, Bratislava, Slovak Republic

Abstract

Our previous microarray study showed that the non-specific cytotoxic cell receptor protein 1 (*Nccrp1*) transcript is significantly upregulated in the gastric mucosa of carbonic anhydrase IX (CA IX)-deficient (*Car9*$^{-/-}$) mice. In this paper, we aimed to characterize human NCCRP1 and to elucidate its relationship to CA IX. Recombinant NCCRP1 protein was expressed in *Escherichia coli*, and a novel polyclonal antiserum was raised against the purified full-length protein. Immunocytochemistry showed that NCCRP1 is expressed intracellularly, even though it has previously been described as a transmembrane protein. Using bioinformatic analyses, we identified orthologs of *NCCRP1* in 35 vertebrate genomes, and up to five paralogs per genome. These paralogs are FBXO genes whose protein products are components of the E3 ubiquitin ligase complexes. NCCRP1 proteins have no signal peptides or transmembrane domains. NCCRP1 has mainly been studied in fish and was thought to be responsible for the cytolytic function of nonspecific cytotoxic cells (NCCs). Our analyses showed that in humans, *NCCRP1* mRNA is expressed in tissues containing squamous epithelium, whereas it shows a more ubiquitous tissue expression pattern in mice. Neither human nor mouse *NCCRP1* expression is specific to immune tissues. Silencing *CA9* using siRNAs did not affect *NCCRP1* levels, indicating that its expression is not directly regulated by *CA9*. Interestingly, silencing *NCCRP1* caused a statistically significant decrease in the growth of HeLa cells. These studies provide ample evidence that the current name, "non-specific cytotoxic cell receptor protein 1," is not appropriate. We therefore propose that the gene name be changed to FBXO50.

Citation: Kallio H, Tolvanen M, Jänis J, Pan P-w, Laurila E, et al. (2011) Characterization of Non-Specific Cytotoxic Cell Receptor Protein 1: A New Member of the Lectin-Type Subfamily of F-Box Proteins. PLoS ONE 6(11): e27152. doi:10.1371/journal.pone.0027152

Editor: Vladimir N. Uversky, University of South Florida College of Medicine, United States of America

Received September 5, 2011; **Accepted** October 11, 2011; **Published** November 7, 2011

Funding: This work was supported by the Competitive Research Funding of the Tampere University Hospital and by grants from the Sigrid Juselius Foundation and the Academy of Finland. The funders had no role in study design, data collection and analysis, decision to publish, or preparation of the manuscript.

Competing Interests: The authors have read the journal's policies and have the following conflict: Sami Kilpinen is an employee of MediSapiens Ltd. This does not alter the authors' adherence to all the PLoS ONE policies on sharing data and materials, and no other authors have any competing interests to declare.

* E-mail: heini.kallio@uta.fi

Introduction

Carbonic anhydrase IX (CA IX) belongs to a family of mammalian α-carbonic anhydrases (CAs), zinc-containing metalloenzymes that catalyze the reversible hydration of carbon dioxide in the reaction $CO_2+H_2O \leftrightarrow H^+ + HCO_3^-$. CA IX is a dimeric transmembrane protein that has many unique features that distinguish it from other CAs [1,2]. First, the expression of CA IX is limited to a few cell types in normal tissues, but it is highly expressed in several tumors, especially under hypoxic conditions. Furthermore, CA IX is involved in the regulation of tumor pH which makes it an attractive antitumor drug target [3]. Second, CA IX is the only member of the CA family that has a proteoglycan (PG) domain, which may contribute to cell adhesion, in addition to a catalytic CA domain [4]. Third, CA IX has a role in cell proliferation; this was demonstrated by the generation of CA IX knockout mice [5]. These mice showed gastric hyperplasia of the glandular epithelium with numerous cysts. In a recent study, we investigated the effect of CA IX deficiency on whole-genome gene expression in gastric mucosa using microarrays [6]. Several candidate genes were identified whose altered expression could explain the abnormal cell lineage phenotype in *Car9*$^{-/-}$ gastric mucosa. In subsequent studies, we focused on three poorly characterized genes that have only been the subject of a few published reports. One of these genes, non-specific cytotoxic cell receptor protein 1 (*Nccrp1*), was significantly overexpressed in *Car9*$^{-/-}$ gastric mucosa compared with wild-type mice.

NCCRP1 has been predicted to be a type II [7] or type III [8] membrane protein and has been cloned from catfish, zebrafish, tilapia, gilthead seabream and carp [7–12]. NCCRP1 is believed to be a receptor expressed in nonspecific cytotoxic cells (NCCs) that is responsible for their cytolytic function and has been suggested to consist of three domains [13].

An interesting feature of the fish NCCRP1 proteins is their homology with the F-box-only proteins. The zebrafish and catfish NCCRP1 proteins share approximately 30% identity with this subset of the F-box superfamily of proteins [12]. The homology is considered to be restricted to an F-box-associated (FBA) domain

located in the C terminus, as fish NCCRP1 proteins are thought to lack the F-box motif in their N-termini. However, our analyses of its sequence and structure indicate the presence of a shorter version of the F-box domain in NCCRP1 proteins in mammals and possibly even in fish. The function of the F-box is to mediate protein-protein interactions, and F-box proteins are known to bind protein substrates for ubiquitin-mediated proteolysis [14]. F-box proteins recognize various substrates, but only members of the FBXO subfamily have the ability to bind glycoproteins [15].

The tissue distribution of *Nccrp1* mRNA has been studied in several fish species, and its expression was found to be ubiquitous. In tilapia, *Nccrp1* is expressed in all immune and non-immune tissues [9]. The relative expression level was highest in the liver, followed by the head, kidney, spleen and intestine. Lower levels were detected in the brain, gill and heart. *Nccrp1* expression was lowest in the skin. Similarly, constitutive expression of *Nccrp1* transcripts was detected in gilthead seabream [10] and carp [11]. *Nccrp1* mRNA expression has also been studied in the tetrapod animal axolotl [16]. *Nccrp1* transcripts were detected in many tissues, including the limb blastema, normal limb, skin, lung and spleen, but not in the brain or liver. High mRNA levels were detected in the spleen and regeneration blastema and in isolated blood cells.

To the best of our knowledge, this is the first study to characterize human NCCRP1. We expressed this gene in *E. coli* and analyzed its structure using biochemical methods. We also examined the expression of *NCCRP1* mRNA in human and mouse tissues. Furthermore, we have investigated the association between NCCRP1 and CA IX using siRNA technology. Our experimental and bioinformatics results contradict the previous prediction that the NCCRP1 protein is localized to the plasma membrane and point unambiguously to its function as a protein-binding F-box component of E3 ubiquitin ligases in the cytoplasm.

Results

Comparison of NCCRP1 and FBXO sequences

An ortholog of *NCCRP1* was identified in 35 vertebrate genomes from Ensembl ortholog tables. In fugu (*Takifugu rubripes*), two orthologs were found. We found 21 protein sequences from 20 species to be at least 90% complete. Table 1 shows the Ensembl gene identifiers for all identified orthologs, with the 20 species used in further bioinformatic analyses in bold.

Multiple sequence alignment of 21 NCCRP1 proteins in Fig. 1 shows that the mouse and rat sequences in Ensembl are either 25 residues longer at the N-terminus, or the real start codon is the one corresponding to M26. Mammalian sequences are characterized by a proline-rich N-terminal domain of approximately 60 residues, whereas fish sequences show shorter insertions around columns 150 and 190 in the alignment. NCCRP1 from the frog *X. tropicalis* has short insertions similar to the fish sequences, but the N-terminus is incomplete, so the presence of the N-terminal domain remains inconclusive.

A major portion of the N-terminal domain in mammals is predicted to be disordered. Prediction analysis of the human, mouse and wallaby sequences yielded disordered domains of 70, 57 and 49 residues, respectively. These regions are underlined in Fig. 1, which shows the end point of the disordered regions to be very close to the end of the additional sequence seen in mammals. There is an analogous Glu- and Ala-rich N-terminal domain in the PEST domain of FBXO2 that also seems to be disordered. The N-terminal 47 residues show no electron density in the crystal structures of mouse FBXO2 (2E31, 2E32, 2E33) [17], and the disorder prediction is consistent with the 41 N-terminal residues predicted to be disordered.

Table 1. NCCRP1 orthologs found in Ensembl genomes.*

Species	Ensembl Gene ID
Anole Lizard (Anolis carolinensis)	ENSACAG00000011950
Armadillo (Dasypus novemcinctus)	ENSDNOG00000018735
Bushbaby (Otolemur garnettii)	ENSOGAG00000012185
Cat (Felis catus)	ENSFCAG00000007425
Chimpanzee (Pan troglodytes)	ENSPTRG00000010953
Cow (Bos taurus)	ENSBTAG00000014296
Dog (Canis familiaris)	ENSCAFG00000005593
Dolphin (Tursiops truncatus)	ENSTTRG00000014969
Elephant (Loxodonta africana)	ENSLAFG00000026532
Fugu (Takifugu rubripes) (1 of 2)	ENSTRUG00000006309
Fugu (Takifugu rubripes) (2 of 2)	ENSTRUG00000013740
Gibbon (Nomascus leucogenys)	ENSNLEG00000014516
Gorilla (Gorilla gorilla)	ENSGGOG00000028030
Guinea Pig (Cavia porcellus)	ENSCPOG00000009451
Hedgehog (Erinaceus europaeus)	ENSEEUG00000015408
Horse (Equus caballus)	ENSECAG00000018954
Human (Homo sapiens)	ENSG00000188505
Hyrax (Procavia capensis)	ENSPCAG00000004015
Kangaroo rat (Dipodomys ordii)	ENSDORG00000001051
Macaque (Macaca mulatta)	ENSMMUG00000013906
Marmoset (Callithrix jacchus)	ENSCJAG00000014055
Medaka (Oryzias latipes)	ENSORLG00000000459
Microbat (Myotis lucifugus)	ENSMLUG00000002162
Mouse (Mus musculus)	ENSMUSG00000047586
Opossum (Monodelphis domestica)	ENSMODG00000013456
Orangutan (Pongo abelii)	ENSPPYG00000009956
Panda (Ailuropoda melanoleuca)	ENSAMEG00000008646
Pika (Ochotona princeps)	ENSOPRG00000006693
Platypus (Ornithorhynchus anatinus)	ENSOANG00000015297
Rabbit (Oryctolagus cuniculus)	ENSOCUG00000011658
Rat (Rattus norvegicus)	ENSRNOG00000026244
Stickleback (Gasterosteus aculeatus)	ENSGACG00000020167
Tetraodon (Tetraodon nigroviridis)	ENSTNIG00000006031
Wallaby (Macropus eugenii)	ENSMEUG00000001939
Xenopus tropicalis	ENSXETG00000005319
Zebrafish (Danio rerio)	ENSDARG00000035326

*Twenty-one genes with at least 90% complete predicted protein products are shown in boldface.

doi:10.1371/journal.pone.0027152.t001

The human paralogs of *NCCRP1*, as shown by the Ensembl comparative genomics tools and Blast searches, are the genes *FBXO2*, *FBXO6*, *FBXO17*, *FBXO27* and *FBXO44*. The protein products of these five genes are components of E3 ubiquitin ligase complexes, and they define a lectin subfamily of ubiquitin ligases [15]. In humans, the genes *FBXO2*, *FBXO6* and *FBXO44* are contiguous genes on chromosome 1 (at 11.70 to 11.74 Mb), and *FBXO17*, *FBXO27* and *NCCRP1* are on chromosome 19 (at 39.4 to 39.7 Mb). The protein sequence identity of NCCRP1 with the other five lectin-type FBXO proteins ranges from 31% to 36% in the last 180 residues, and the Blast E values range from 10^{-27} to 10^{-18}, clearly indicating that these proteins share homology and common ancestry.

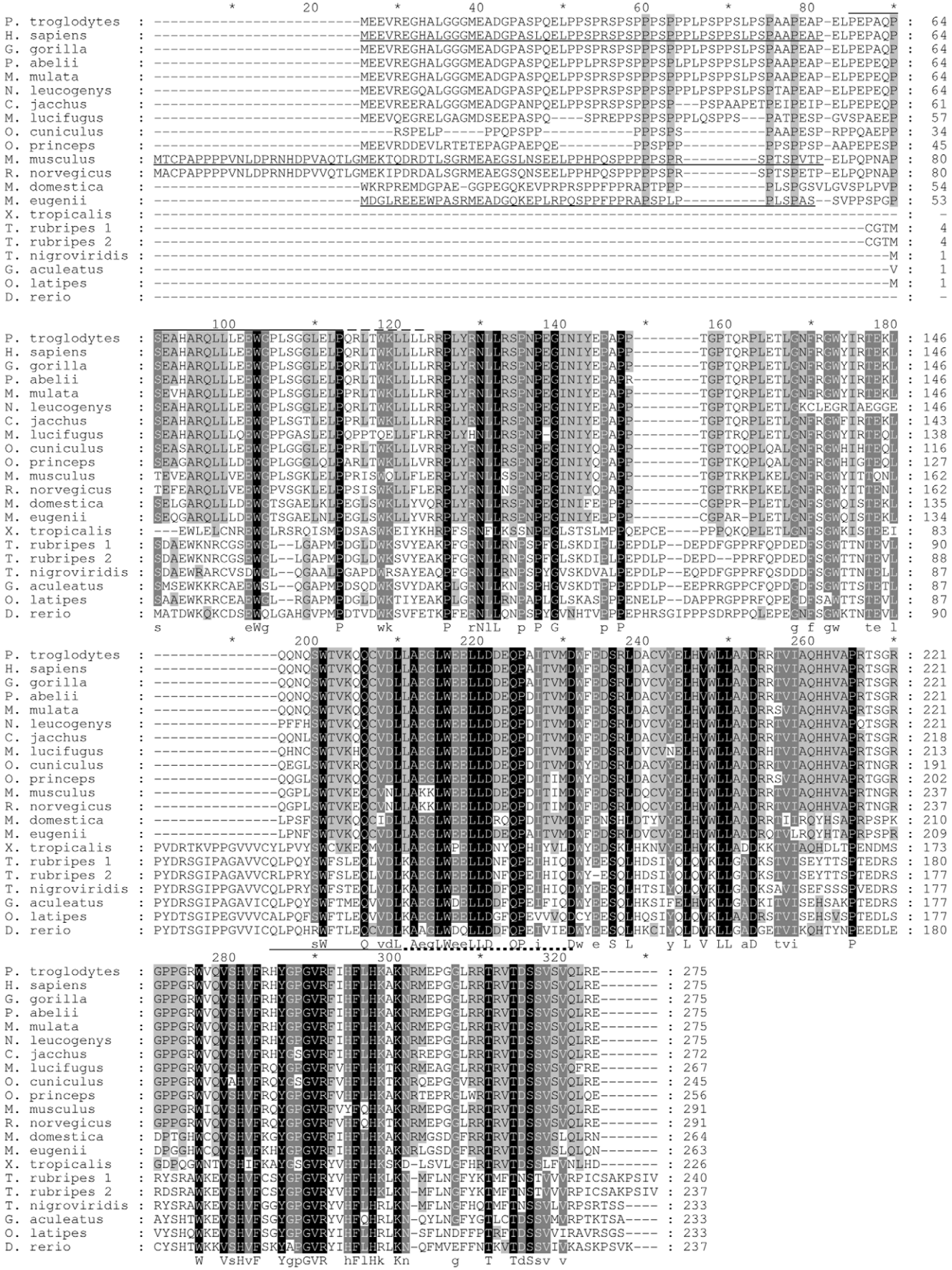
P. troglodytes
H. sapiens
G. gorilla
P. abelii
M. mulata
N. leucogenys
C. jacchus
M. lucifugus
O. cuniculus
O. princeps
M. musculus
R. norvegicus
M. domestica
M. eugenii
X. tropicalis
T. rubripes 1
T. rubripes 2
T. nigroviridis
G. aculeatus
O. latipes
D. rerio

Figure 1. Alignment of 21 NCCRP1 protein sequences from 20 species. Shading indicates conservation, with more strongly conserved positions shaded in darker colors. Uppercase letters under the alignment give the identity of fully conserved residues, and lowercase letters show the consensus residue of partially conserved positions. Underlined sequences in the N-terminal region are predicted to be disordered in the three species studied. The line over the sequence (columns 85 to 123) indicates the predicted F-box domain. The solid line (cols. 85 to 113) indicates an alternative model (see "Analysis of protein domains"). Underlining of the bottom consensus line indicates the location of the peptides discussed in "Modeling of suggested active peptides" and studied in previous work [8]. Solid line: 16-mer peptide; Solid line plus dotted line: 37-mer peptide.
doi:10.1371/journal.pone.0027152.g001

In the available fish genomes, we only found orthologs to *FBXO2*, *FBXO44* and *NCCRP1*. Interestingly, the zebrafish genome carries a cluster of ten copies of *FBXO44* orthologs on chromosome 23.

Analysis of protein domains

By Interpro scan, all 21 protein sequences had domain matches to "Fbox-associated" (FBA, IPR007397) and "galactose-binding domain-like" (IPR008979) patterns in the ~200 C-terminal residues in fish and frog species and ~180 residues in mammalian species. Only the protein products of *NCCRP1* and the above five *FBXO* gene loci are annotated to contain an FBA domain (InterPro entry IPR007397), and no other human proteins were found in Blast searches when NCCRP1 or the FBA domain of FBXO2 were used as queries. The products of these five human *FBXO* genes also contain a cyclin-like F-box domain pattern (InterPro entry IPR001810) in the N-terminal region that spans 50 residues or less, but none of the NCCRP1 proteins match this pattern.

Fig. 2 shows the alignment of human NCCRP1 with these five FBXO proteins and their phylogenetic tree. Although there was no match to the cyclin-like F-box domain pattern in the NCCRP1 sequence, 12 residues are conserved between human NCCRP1 and at least three other FBXO proteins within the F-box domain region (lines on top of the alignment in Fig. 2). The main differences in this region are found in three indels, in which NCCRP1 has shorter sequences and lacks many conserved residues, most notably the signature pattern CRxVC. To test whether these deletions would be compatible with the F-box domain structure, we visualized them in the known 3D structure of mouse FBXO2 [17].

Fig. 3 shows the sequences to be deleted in purple. They constitute one complete helical turn in alpha helix α1 (helices named as described previously [17]), one helix turn in α2 and part of the α2′ loop, the end of helix α4, and the major part of the linker before α5, including the flexible residues 104 to 108 that are missing from the structure between the open ends (purple and cyan). These deletions could be modeled in a shorter version of the F-box fold while retaining the positions of α3 and α4 and the sugar-binding domain (SBD), as in the structure 2E31 in PDB, by linking α5 to the truncated α4 and shifting the right-hand ends of helices α1 and α2 to the left. Alternatively, the SBD could be moved to bring α5 into the position of α4, which would still maintain the relative orientation between the F-box and the SBD. Fig. 1 shows the extent of the F-box domain in these two models. The solid line over the alignment indicates the version in which α4 is truncated, whereas the dotted line indicates the fusion of α5 into the F-box domain. In conclusion, we believe that the region preceding the SBD in human and other mammalian NCCRP1 proteins is indeed folded as an F-box domain.

In fish NCCRP1 sequences, the F-box domain is not detected (by matching to the F-box pattern in InterPro), which is not surprising because the fish sequences start in the middle of the F-box region (Fig. 1). However, because the fish sequences only lack six residues or less from the beginning of the structurally defined F-box domain (see line at the top of the alignment in Fig. 1), a version with a shortened initial helix α1 might exist. This remains speculative because the fish and mammalian sequences are not highly conserved in the putative F-box region.

TMHMM predicted that there are no transmembrane helices in any of the studied 21 NCCRP1 ortholog proteins. SignalP predicted no signal peptides in any of the proteins, and TargetP predicted a non-mitochondrial, non-secreted localization for all proteins. The predictions for the mouse and rat sequences were run with alternative start sites: residue 1, as in Ensembl proteins, and residue 26, consistent with the translation start site of other mammalian sequences. All of these results indicate the absence of transmembrane domains and cytoplasmic localization of NCCRP1 in all of the studied species.

Jaso-Friedmann et al. [12] reported Box-1 motifs in zebrafish and catfish NCCRP1 proteins. We did not detect these motifs in the NCCRP1 proteins we analyzed, and we disagree with their finding because they took the liberty of reversing the sequences, which does not make sense for peptides.

Modelling of suggested active peptides

Because the NCCRP1 proteins could not be located on the cell surface, as would be expected for the proteins to function as antigen receptors [7], we next asked whether there were any structural explanations for the previously reported [8,12] cytotoxicity-inhibiting activity of NCCRP1-derived peptides (a more potent 16-mer and a less potent 37-mer). The location of these two overlapping peptides is shown under the alignment in Fig. 1. Fig. 4 shows the location of the 16-mer in yellow and the 37-mer in yellow plus blue, extrapolated into the structure of mouse FBXO2 based on the sequence alignment. These peptides contain long beta-strand elements coming from the amphiphilic beta sheets, which have one side of mainly hydrophobic residues (facing the protein core). Randomized peptides with same residues would be highly unlikely to have such an organized amphiphilic surface.

Production, purification and characterization of recombinant human NCCRP1

The human *NCCRP1* cDNA was cloned into the expression vector pGEX-4T-1 and expressed as a fusion protein with GST. The recombinant NCCRP1 protein was characterized using SDS-PAGE based on its apparent size. After purification by affinity chromatography and digestion with thrombin, NCCRP1 appeared as polypeptide of approximately 30 kDa after SDS-PAGE (Fig. 5, lane 1). Fig. 5 also shows the 26-kDa GST band (lane 2).

Western blotting was used to confirm the reactivity of the antibody produced against NCCRP1. Fig. 6 shows a single band for NCCRP1 in lane 1, whereas the control blot using normal rabbit serum was negative (Fig. 6, lane 2).

Mass spectrometry

Upon buffer exchange, the NCCRP1 protein sample slightly precipitated, and therefore, mass analyses were conducted from both the precipitate and supernatant. A small amount of the precipitate was dissolved in 100 µl of 10 mM ammonium bicarbonate buffer, pH 8.5, further diluted with acetonitrile/water/acetic acid (49.5:49.5:1.0, v/v) mixture and directly analyzed with ESI FT-ICR mass spectrometry. From this analysis, the

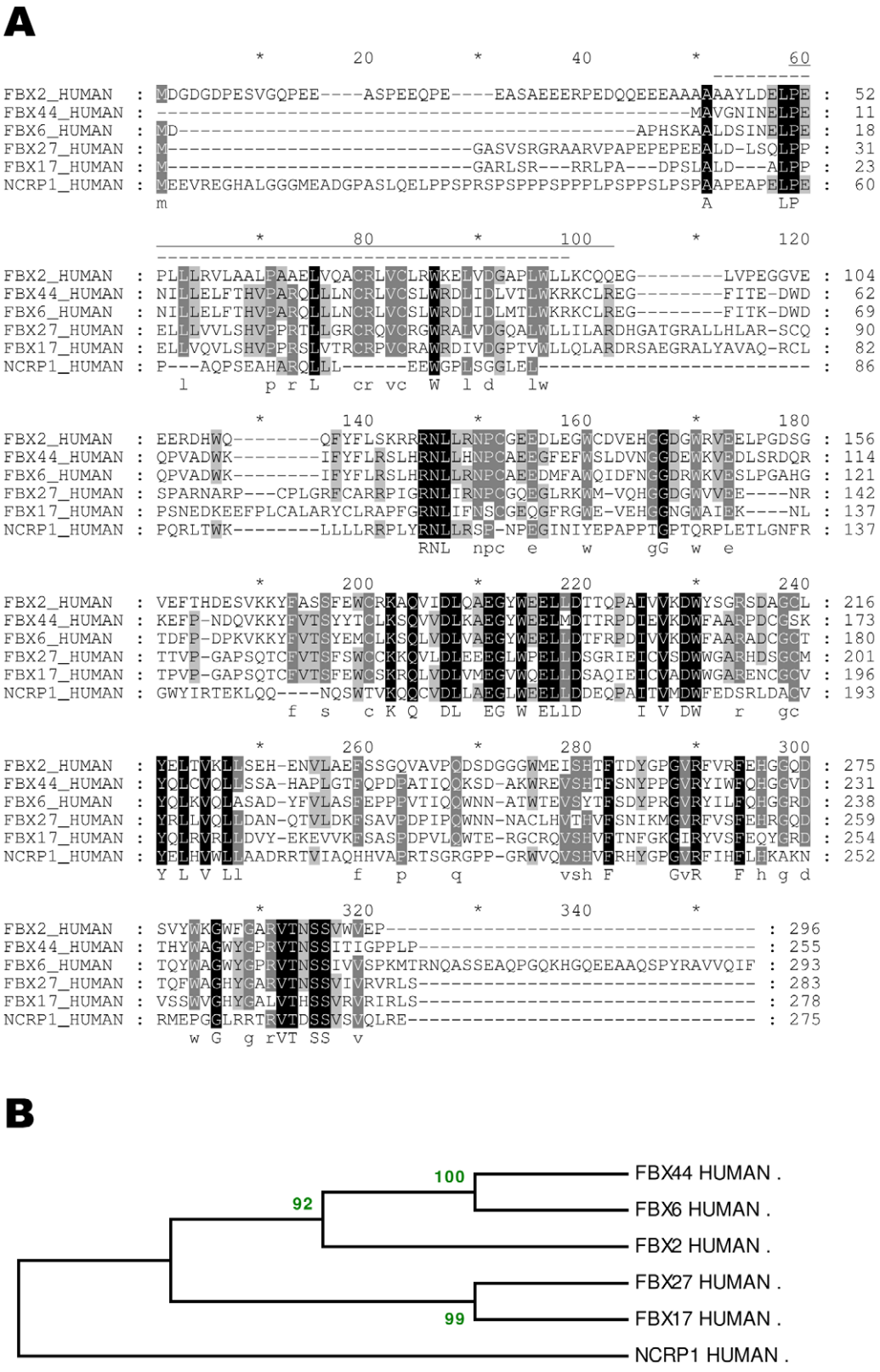

Figure 2. Alignment of human NCCRP1 with its closest five paralogs and their phylogenetic tree. (A) Shading and consensus lettering were used as described in Fig. 1. Dotted line over the sequence: F-box domain, cyclin-like, as defined in human FBXO2 by InterPro. Solid line over the sequence: F-box domain as defined by compact alpha-helical folding in PDB entry 2E31 [17]. Line under the sequence: the sugar-binding domain as defined previously [17]. (B) Phylogenetic tree with bootstrap support percentages for each node.
doi:10.1371/journal.pone.0027152.g002

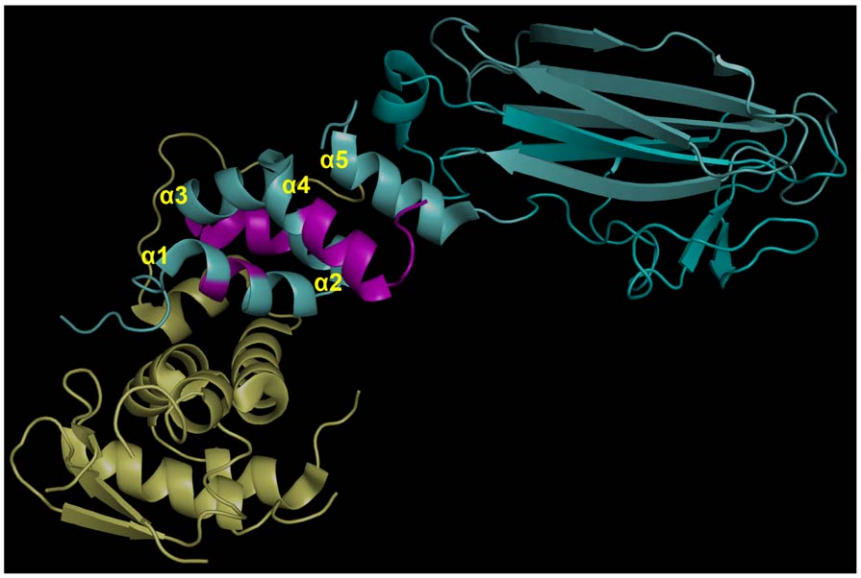

Figure 3. Structure of mouse FBXO2 (cyan) complexed with SKP1 (yellow). PDB entry 2E31 [17]. The regions of FBXO2 shown in purple correspond to parts that would be deleted from a model of the F-box domain of human NCCRP1. The first 46 residues and residues 104–108 of FBXO2 are not resolved in the structure. The sugar-binding site (SBD) is at the extreme right in this image. Alpha helices of FBXO2 are labeled at the N-end of each helix, as described previously [17].
doi:10.1371/journal.pone.0027152.g003

precipitate was found to contain a 27-kDa protein as well as a small 3-kDa peptide (Fig. 7A). The most abundant isotopic mass of the protein (27743.57 Da) was matched against the NCCRP1 sequence and a reasonable match was found with the fragment containing residues 31–275 (theoretically 27743.45 Da), indicating the presence of one intra-molecular disulfide (Cys158-Cys192) in the protein structure (see inset in Figure 7A). The monoisotopic mass of the observed peptide P (3260.51 Da) was also matched against the NCCRP1 sequence, and it was found to correspond to the first 30 residues of NCCRP1 with an additional Gly-Ser in the N-terminus (theoretically 3260.52 Da). These amino acids are attributable to the pGEX-4T-1 expression vector construct (Fig. 7B).

To further identify the produced protein, a database search for the trypsin-digested protein was performed. An aliquot of 20 µl of the tryptic digest sample was further diluted with 150 µl of an acetonitrile/water/acetic acid (49.5:49.5:1.0, v/v) mixture and analyzed directly. The digestion resulted in 18 identified tryptic peptides within an average mass error of 6 ppm, covering 75% of the NCCRP1 sequence. A search against the SwissProt database gave an unambiguous hit for human NCCRP1 (NCRP1_HUMAN) with a Mowse score of 370 (Figure S1).

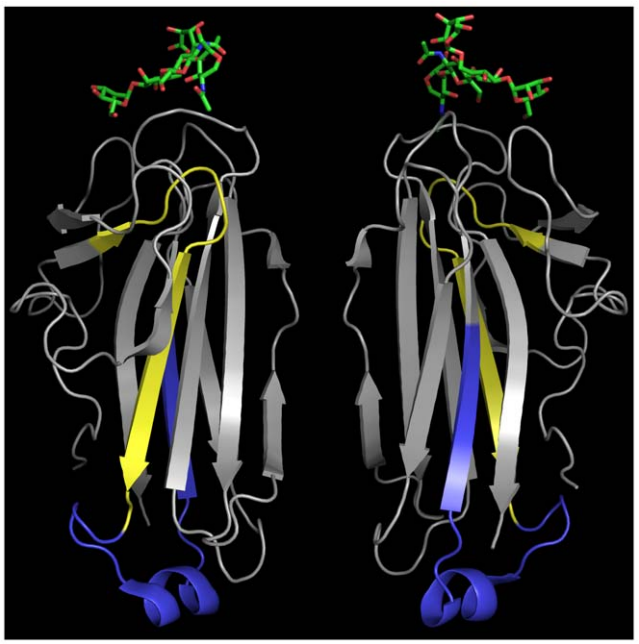

Figure 4. Structure of the sugar-binding domain of mouse FBXO2 complexed with an oligosaccharide of bovine ribonuclease A. PDB entry 2E33 [17]. Two views rotated 180 degrees vertically are shown. The protein part of ribonuclease A is omitted. The coloring indicates the positions homologous to the NCCRP1 peptides discussed in "Modeling of suggested active peptides" and studied in previous work [8,13]. Yellow: 16-mer peptide; yellow plus blue: 37-mer peptide.
doi:10.1371/journal.pone.0027152.g004

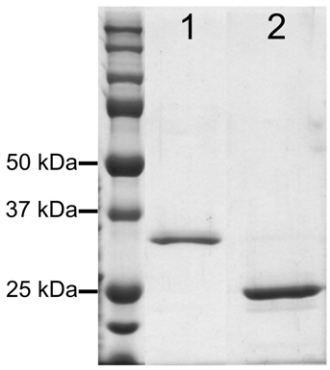

Figure 5. SDS-PAGE of the human recombinant NCCRP1 protein produced in *E. coli*. Lane 1 shows the 30-kDa NCCRP1 eluted from the affinity chromatography column after thrombin treatment. In lane 2, 26-kDa GST is shown.
doi:10.1371/journal.pone.0027152.g005

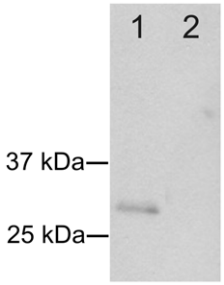

Figure 6. Western blot analysis of the antibody produced against NCCRP1. Lane 1 shows a single band confirming the expected reactivity of the antibody towards NCCRP1 protein. The control experiment using normal rabbit serum is negative (lane 2).
doi:10.1371/journal.pone.0027152.g006

Mass spectra measured from the supernatant instead revealed the same 3-kDa peptide that was detected from the precipitate as well as a small amount of the NCCRP1 [31–275] fragment. In addition, small amounts of some larger, currently unidentified 7–10 kDa polypeptides were detected (data not shown).

Localization of NCCRP1 in HeLa cells

The subcellular localization of NCCRP1 was examined in HeLa cells by immunocytochemistry. The protein was detected in the cytoplasm, as shown in green in Fig. 8. In contrast, CA IX was localized at the cell membrane, as expected (Fig. 8A and C, red). Interestingly, these two proteins were only rarely detected in the same cell (Fig. 8A, arrows). Control immunostaining using 30 μg of blocking NCCRP1 recombinant protein and anti-NCCRP1 serum resulted in only very faint staining, confirming the specificity of the antiserum (Fig. 8D). A second control using pre-immune serum instead of the anti-NCCRP1 serum showed virtually no staining (Fig. 8E).

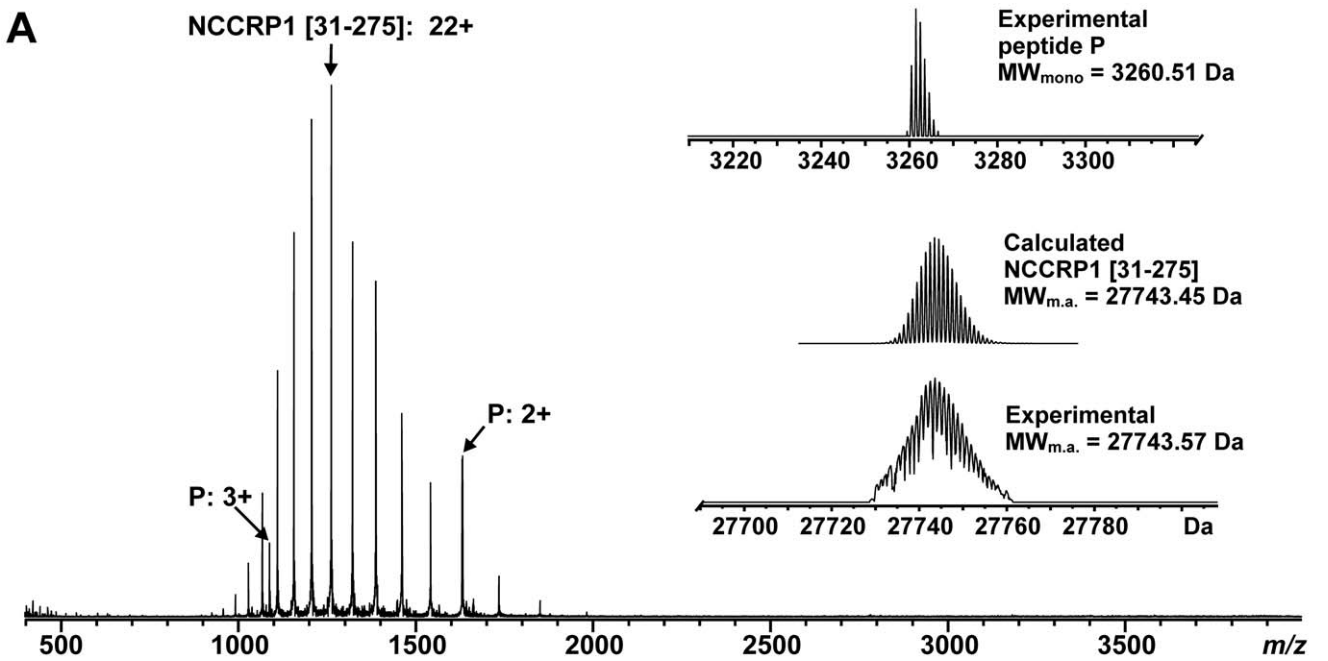

B

```
         10         20         30         40         50         60         70         80
GSMEEVREGHALGGGMEADGPASLQELPPSPRSPSPPPSPPPLPSPPSLPSPAAPEAPELPEPAQPSEAHARQLLLEEWGPL
         90        100        110        120        130        140        150        160
SGGLELPQRLTWKLLLLRRPLYRNLLRSPNPEGINIYEPAPPTGPTQRPLETLGNFRGWYIRTEKLQQNQSWTVKQQCVD
        170        180        190        200        210        220        230        240
LLAEGLWEELLDDEQPAITVMDWFEDSRLDACVYELHVWLLAADRRTVIAQHHVAPRTSGRGPPGRWVQVSHVFRHYGPG
        250        260        270
VRFIHFLHKAKNRMEPGGLRRTRVTDSSVSVQLRE
```

Figure 7. Mass spectrometry analysis of NCCRP1. (A) ESI FT-ICR mass spectrum of NCCRP1 sample measured in an acetonitrile/water/acetic acid (49.5:49.5:1.0, v/v) mixture. The sample contained an NCCPR1 [31–275] fragment (charge state 22+ denoted) and a peptide P (charge states 2+ and 3+ denoted), corresponding to the first 30 residues with an additional Gly-Ser in the N-terminus due to the used expression vector construct. The charge-deconvoluted mass spectrum in the inset shows calculated and experimental isotopic distributions for the NCCRP1 [31–275] fragment (with the most abundant masses indicated), as well as experimental isotopic distribution for the peptide P with a monoisotopic mass of 3260.15 Da. (B) Primary sequence of NCCRP1. The residues corresponding to the peptide P are underlined and cysteines (Cys158, Cys192) are marked with asterisks.
doi:10.1371/journal.pone.0027152.g007

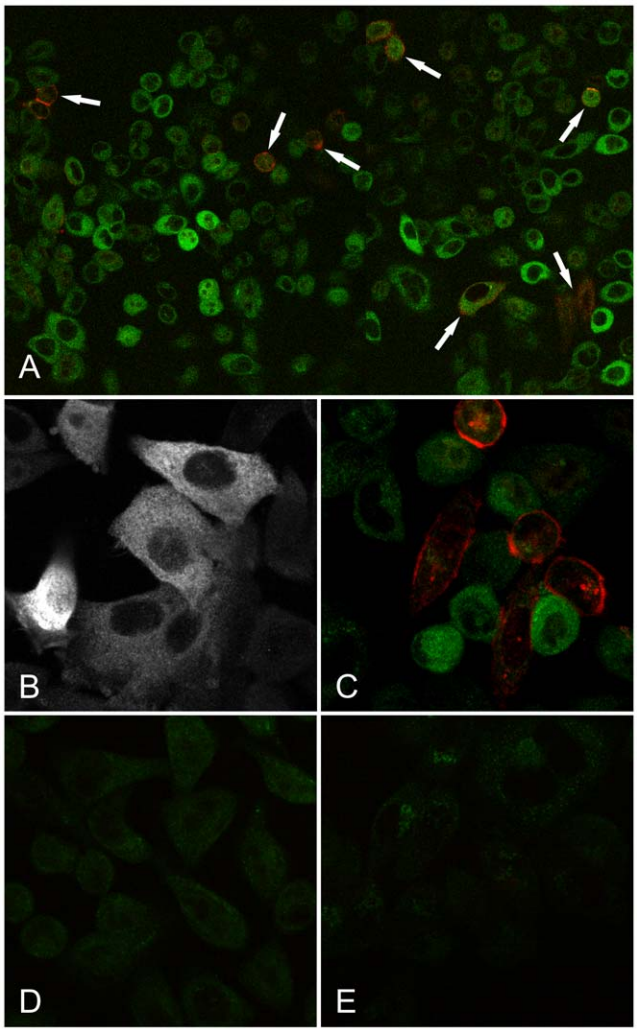

Figure 8. Subcellular localization of NCCRP1 in HeLa cells by immunocytochemistry. (A, B) Staining for NCCRP1 is detected in the cytosol as shown in green. (A, C) CA IX is expressed on the cell membrane as shown in red. (A; arrows) Only a few HeLa cells expressed both proteins at the same time. (D) Control immunostaining using 30 μg of blocking NCCRP1 recombinant protein and anti-NCCRP1 serum together gives only a very faint staining. (E) Other control staining using pre-immune serum instead of the anti-NCCRP1 serum shows a barely detectable signal.
doi:10.1371/journal.pone.0027152.g008

NCCRP1 expression in human tissues

The IST database system developed by MediSapiens Ltd was used to obtain the data for *NCCRP1* mRNA expression in human normal and cancer-derived tissues (Fig. 9A and B). The expression pattern of *NCCRP1* was relatively narrow in both normal and cancerous tissues. The normal tissues with the highest signal were the esophagus, oral cavity, skin, tongue and male and female reproductive organs. The cancer-derived tissues with high *NCCRP1* expression included the squamous cell carcinoma of the skin and cancers of the female reproductive organs.

Nccrp1 expression in mouse tissues

Nccrp1 mRNA expression was studied in several mouse tissues by QRT-PCR. *Nccrp1* transcript was expressed in all tissues studied and the signal was highest in the kidney (Fig. 10). The expression was moderate in the stomach, colon, duodenum and prostate. In other tissues, *Nccrp1* was expressed to a lesser degree but signal was still clearly detectable.

The effect of growth factors and deferoxamine mesylate on *NCCRP1* mRNA expression

The influence of growth factors and deferoxamine mesylate on *NCCRP1* transcript levels was studied in HeLa cells using QRT-PCR. The basal level of *NCCRP1* expression was relatively high in these cells and neither treatment had a major effect on its expression. After treatment with deferoxamine mesylate, which is commonly used to induce a hypoxia-like response, the expression of *NCCRP1* decreased moderately (1.4-fold), as shown in Fig. 11. In contrast, deferoxamine mesylate treatment induced *CA9* expression 4-fold, as expected (data not shown). Stimulation with EGF decreased *NCCRP1* expression levels but the decline was small (1.2-fold). Other treatments did not have any effect on *NCCRP1* mRNA levels.

Expression of *NCCRP1* and *CA9* in human pancreatic and breast cancer cell lines

The expression of *NCCRP1* and *CA9* was measured by QRT-PCR in 16 pancreatic cancer cell lines and 21 breast cancer cell lines. *NCCRP1* showed the highest expression in the Su.86.86, Hup-T4 and Hs700T pancreatic cancer cell lines and the MDA-MB-415, SK-BR-3 and BT-474 breast cancer cell lines (Fig. 12). In other cell lines, *NCCRP1* was expressed at moderate or low levels. In general, the expression of *CA9* was lower than *NCCRP1* in the studied cell lines. *CA9* had the strongest signal in the DU4475 breast cancer and AsPC-1 pancreatic cancer cell lines. Its expression was moderate in a few cell lines and very low in several others. *NCCRP1* and *CA9* showed reciprocal expression patterns in some cell lines; i.e., when *NCCRP1* expression was high *CA9* expression was low or absent, and vice versa.

NCCRP1 and *CA9* silencing

CA9 was silenced in the human glioblastoma cell line, U373, which has a high basal level of *CA9* expression. Efficient downregulation of mRNA expression (up to 93% reduction compared with luciferase control siRNA-treated cells) was detected for the *CA9* gene after siRNA treatment (data not shown). Silencing of *CA9* was monitored until 144 h after transfection and remained efficient at that time point. The mRNA level of *NCCRP1* was studied in U373 cells after *CA9* silencing to examine whether *NCCRP1* was directly regulated by *CA9* expression. The expression of *NCCRP1* was below the detection limit of QRT-PCR at the basal level in U373 cells and did not change after the silencing of *CA9*.

NCCRP1 silencing was performed in two cell lines, HeLa and Su.86.86, and the effect of silencing on the expression level of *CA9* was studied. The silencing of *NCCRP1* was efficient in both cell lines (up to 91% and 83% reduction compared with luciferase control siRNA-treated cells for HeLa and Su.86.86 cells, respectively). In HeLa cells, the silencing of *NCCRP1* was monitored until 144 h after transfection and remained efficient. *CA9* mRNA levels were not affected by *NCCRP1* silencing (Fig. 13). The expression of *CA9* steadily increased until 120 h after transfection, after which it decreased dramatically. In Su.86.86 cells, *CA9* expression was also unaffected by the silencing of *NCCRP1* (data not shown).

Effect of *NCCRP1* silencing on cell growth

The effect of *NCCRP1* silencing on cell growth was studied in HeLa cells at 48, 96 and 144 h after transfection, and the analysis was performed using ImageJ. Silencing of *NCCRP1* led to a

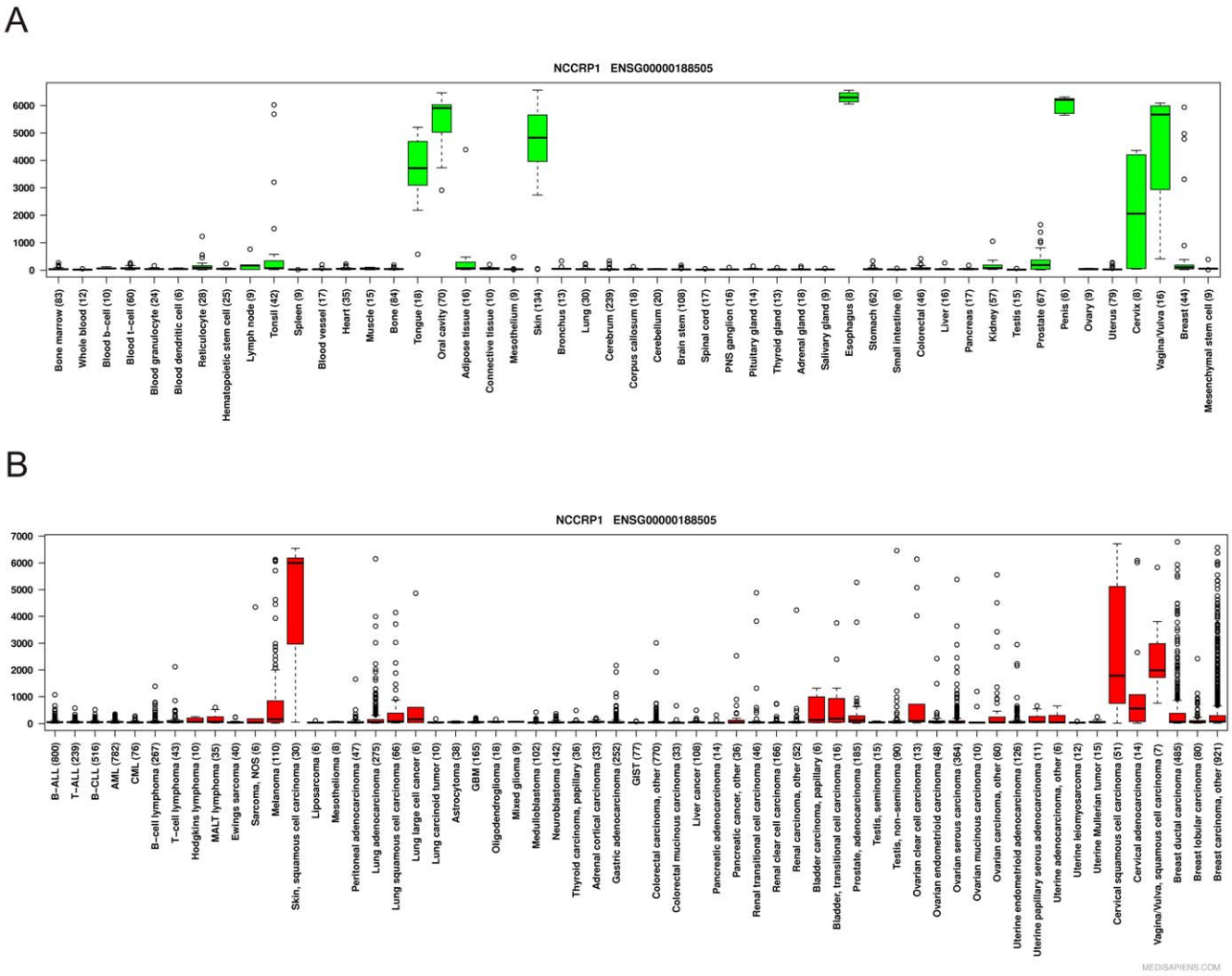

Figure 9. Data for human *NCCRP1* mRNA expression from the MediSapiens database. (A) Boxplot analysis of the *NCCRP1* expression levels across healthy human tissues. (B) Boxplot analysis of the *NCCRP1* expression levels across a large panel of cancer tissues. Among the normal tissues with the highest *NCCRP1* expression are the esophagus, oral cavity, skin, tongue and reproductive organs. In cancerous tissues, the expression profile of *NCCRP1* is relatively narrow, with the highest expression seen in the squamous cell carcinomas of the skin and cancers of the female reproductive organs. The number of samples in each category is shown in parenthesis. The box refers to the quartile distribution (25–75%) range, with the median shown as a black horizontal line. The whiskers extend to 1.5 times the interquartile range from the edges of the box, and any data points beyond this are considered outliers and marked by open circles.
doi:10.1371/journal.pone.0027152.g009

statistically significant decrease in HeLa cell proliferation at every time point (Fig. 14).

Discussion

According to our previous cDNA microarray analysis, carbonic anhydrase IX-deficient mice showed significantly upregulated expression of *Nccrp1* in the stomach, which is the most abundant site of CA IX expression in normal mice. This finding led us to investigate possible connections between these two genes/proteins and to further assess the structure, regulation and function of the NCCRP1 protein. Our bioinformatic analyses clearly linked NCCRP1 protein to the FBXO gene family. The FBA domain in the FBXO2, FBXO6, FBXO17 and FBXO27 proteins is a lectin domain, and these proteins have been experimentally shown to bind various glycans [15]. The presumed role of these proteins is to bind misfolded and retrotranslocated glycoproteins in the cytoplasm for ubiquitin conjugation leading to proteasomal degradation [15]. The fact that this family of lectin-type F-box proteins (among the dozens of different F-box proteins found in ubiquitin ligase complexes) comprises the closest paralogs of NCCRP1 gives us a strong reason to predict that NCCRP1 functions as a protein-binding component in ubiquitin ligase complexes. Whether it actually binds glycans, similar to FBXO2, FBXO6, FBXO17 and FBXO27, or lacks the ability to bind sugar, like FBXO44 [15], remains to be tested experimentally. However, sequence alignments and structural interpretations (Figs. 1, 2, 3) suggest that NCCRP1 is a sixth member of the lectin-type FBXO gene family, and we therefore propose that the gene name be changed to FBXO50 (the number may change based on the decision of the Human Gene Nomenclature Committee, http://www.genenames.org/).

Jaso-Friedmann et al. [12] stated that NCCRP1 does not contain an F-box and is therefore an exception in this subfamily.

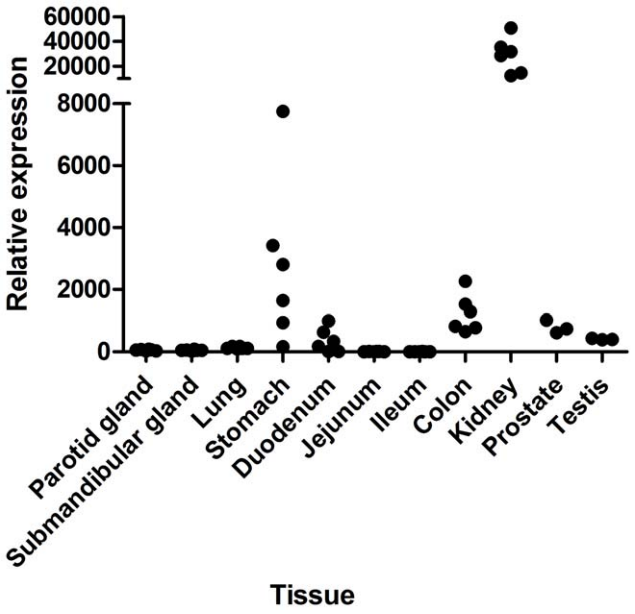

Figure 10. The *Nccrp1* mRNA expression in mouse tissues by QRT-PCR. *Nccrp1* is present in all the tissues studied. The expression of *Nccrp1* is highest in the kidney and moderate in the stomach, colon, duodenum and prostate. In the other tissues *Nccrp1* expression is modest. Normalized median values calculated from the technical triplicates are shown.
doi:10.1371/journal.pone.0027152.g010

However, our analysis points to the existence of an F-box in mammalian NCCRP1 proteins, and at least the remnants of one in the fish sequences, so the name FBXO50 would be appropriate.

The "F-box associated" domain occurs in the human proteome only in the six gene products discussed in this paper. This domain could also be renamed to reflect its known functions, e.g. F-box associated lectin(-like) domain or ubiquitin ligase lectin(-like) domain.

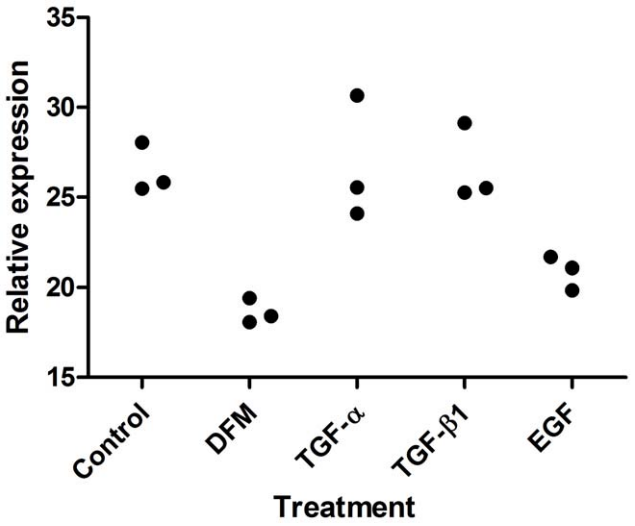

Figure 11. The effect of different treatments on *NCCRP1* levels in HeLa cells. The treatments included deferoxamine mesylate (DFM), transforming growth factor-alpha (TGF-α), transforming growth factor-beta 1 (TGF-β1) and epidermal growth factor (EGF). Deferoxamine mesylate and EGF treatments moderately decreased the expression of *NCCRP1* (1.4-fold and 1.2-fold, respectively). The normalized values of triplicate experiments as detected by QRT-PCR are shown.
doi:10.1371/journal.pone.0027152.g011

To our surprise, mass spectrometry analysis indicated the presence of a truncated protein in the NCCRP1 sample after purification and buffer exchange, which corresponded to the residues 31–275 of the full-length polypeptide. However, the peptide corresponding to the first 30 residues was also detected, which suggests that the N-terminal region had been cleaved after the protein production, probably during purification or desalting steps. Protein precipitation was also observed upon buffer-exchange but it is not known whether this is related to the observed N-terminal cleavage or change in the buffer conditions. The reason for the intrinsically weak N-terminal region of the NCCRP1 protein is unknown and will be investigated further. Based on our sequence analyses, the N-terminal proline-rich region of mammalian NCCRP1 proteins is predicted to be disordered, which might contribute to the N-terminal truncation. Mass analysis of the NCCRP1 [31–275] fragment also indicated that there is an intra-molecular disulfide between Cys158 and Cys192.

None of the NCCRP1 sequences contain any putative signal sequences or transmembrane domains, which rules out a membrane location. Accordingly, we showed using immunocyto-chemistry that recombinant human NCCRP1 is expressed intracellularly. Jaso-Friedmann, Leary and Evans previously reported two contradictory predictions of membrane topology and transmembrane helix location [7,8]. Both papers suggest unrealistically short and fairly hydrophilic transmembrane helices but provide no explanation as to how these predictions were made. Moreover, both predictions locate the transmembrane regions in the middle of what we now know to be the beta sandwich fold of the FBA domain.

We speculate that the initial NCCRP1 research [7] was hampered by an unfortunate incident of purifying and cloning an incorrect protein with approximately the correct molecular weight (27.3 kDa) instead of the real antigen they originally discovered (34 kDa). In any case, our study now clearly demonstrates that NCCRP1 is an intracellular ubiquitin ligase protein, not a cell surface protein.

Previous reports provide some indirect results that have been interpreted as linking fish NCCRP1 proteins with cytotoxicity. First, *NCCRP1* anti-sense oligonucleotides were found to reduce the cytotoxicity of catfish NCC cells [7]. In our study, we have demonstrated the anti-proliferative effect of siRNA-mediated *NCCRP1* knockdown in HeLa cells, which may be due to a failure to degrade misfolded glycoproteins. We hypothesize that similar disturbances in viability or in protein secretion could account for the effect of anti-sense oligonucleotides in catfish NCC cells. Second, peptides derived from catfish and zebrafish NCCRP1 were observed to reduce NCC-mediated cell lysis [8,12]. These peptides (Figs. 1 and 4) come from the most highly conserved region of the lectin domain and contain amphiphilic beta strands. We believe that the hydrophobic patches in these peptides would have a high degree of nonspecific binding and could interfere with various cell surface events. The uniform orientation of hydrophobic residues is sequence-dependent and would be lost in most randomized peptides, which may have been the case in a previous report [12], leading to seemingly specific results for a peptide that is not derived from a cell-surface receptor.

The human lectin-type F-box-only (FBXO) genes are present in two clusters in the genome: *FBXO2*, *FBXO6* and *FBXO44* on chromosome 1, and *FBXO17* and *FBXO27* on chromosome 19. *NCCRP1* is only 150 kb away from *FBXO27*, separated by two other genes. The adjacent gene triplet on human chromosome 1

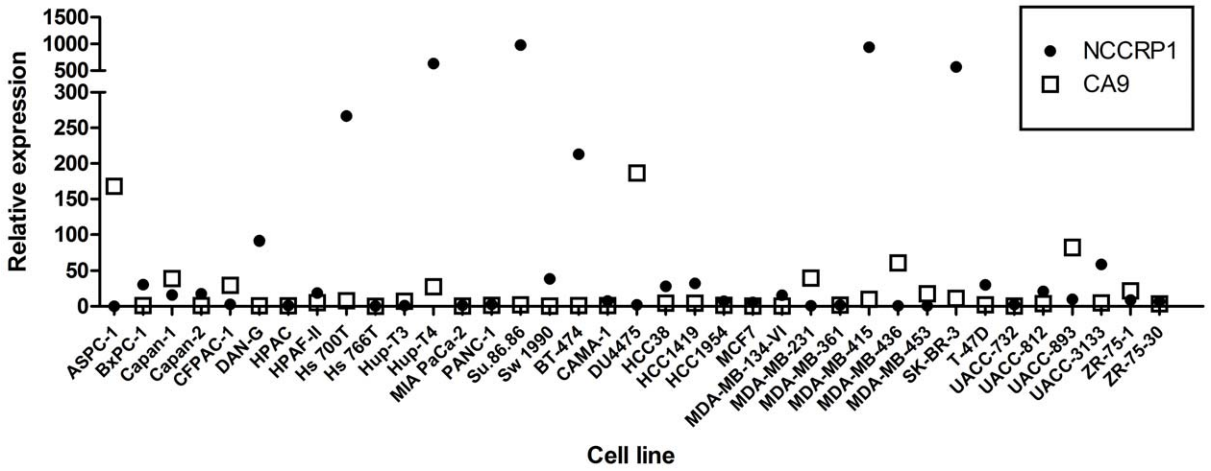

Figure 12. Screening of *NCCRP1* and *CA9* mRNA expression in cancer cell lines. 16 human pancreatic (AsPC-1 to SW 1990) and 21 breast (BT-474 to ZR-75-30) cancer cell lines were screened using QRT-PCR. The expression of *NCCRP1* is highest in the Su.86.86, Hup-T4 and Hs700T pancreatic cancer cell lines and the MDA-MB-415, SK-BR-3 and BT-474 breast cancer cell lines. *CA9* is most highly expressed in the DU4475 breast cancer and AsPC-1 pancreatic cancer cell lines. The expression levels of these genes typically show a reciprocal pattern: high simultaneous expression is observed in none of these cell lines. The normalized values are shown.
doi:10.1371/journal.pone.0027152.g012

and the pair on chromosome 19 are likely due to recent gene duplication events. However, the phylogenetic tree in Fig. 2B indicates that *FBXO17* and *FBXO27* share their latest common ancestor with the triplet of *FBXO* genes on chromosome 1, and therefore, their proximity to *NCCRP1* may be coincidental. A full phylogenetic analysis of FBXO proteins and their emergence in various vertebrate taxa would be an interesting topic for a future study.

Because there have been no previous reports on the expression pattern of *NCCRP1* in mammals, we examined mRNA levels of human and mouse *NCCRP1*. In normal human tissues, *NCCRP1* is strongly confined to the squamous epithelium, mainly being detected in tissues such as the esophagus, oral cavity, skin and tongue. The expression pattern is similar in cancerous tissues; the highest expression was seen in squamous cell carcinomas of the skin, cervix and vagina/vulva. In mice, the expression of *Nccrp1* was highest in the kidney and moderate in the stomach, colon, duodenum and prostate. Lower levels of the transcript were also detectable in the other tissues studied, including the parotid and submandibular glands, lung, jejunum, ileum and testis. These data suggest that NCCRP1 is relatively ubiquitously expressed, similar to FBXO6, FBXO27 and FBXO44 [15]. In contrast, FBXO2 is predominantly expressed in different areas of the brain and only weakly in some other tissues [15,18], and FBXO17 is expressed in only a few tissues [15,18]. It should be noted that many tissues express several FBXO genes. For example, major glycoprotein-producing tissues include the brain, liver and pancreas, all of which express multiple FBXO family members [15]. In this

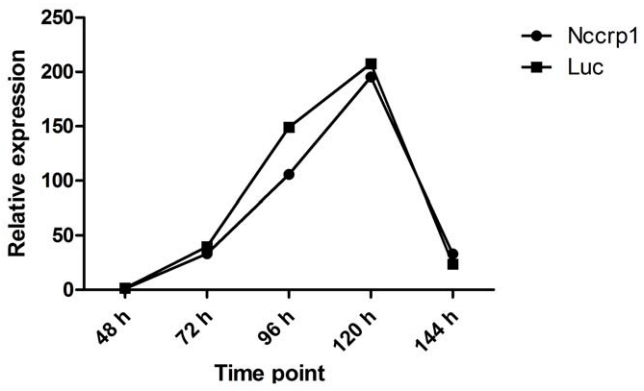

Figure 13. *CA9* expression after silencing of *NCCRP1* in HeLa cells. The mRNA expression of *CA9* was monitored for 144 h after the silencing of *NCCRP1*. No change was observed in *CA9* expression with *NCCRP1* siRNA compared with *luciferase* (Luc) control siRNA. The normalized median values calculated from the three replicates are shown.
doi:10.1371/journal.pone.0027152.g013

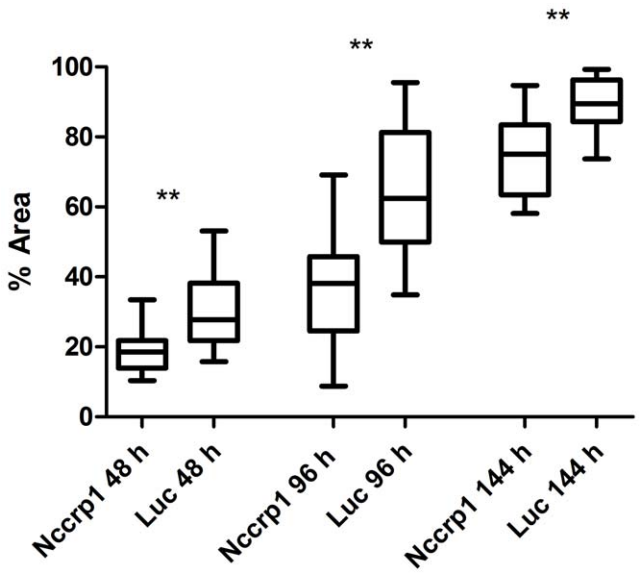

Figure 14. The effect of *NCCRP1* silencing on cell proliferation in HeLa cells as analyzed by ImageJ. Cell growth was studied at 48, 96 and 144 h after transfection. The silencing of *NCCRP1* caused a statistically significant decrease in cell proliferation at every time point. Statistically significant differences relative to luciferase (Luc) control siRNA were determined. ** $p<0.01$.
doi:10.1371/journal.pone.0027152.g014

respect, the expression pattern of *NCCRP1* in human tissues is exceptional because it is almost solely present in tissues containing squamous epithelium. On the other hand, *Nccrp1* is expressed widely in mouse tissues; this pattern resembles the expression of other ubiquitously expressed FBXO genes.

Finally, we examined the connection between *CA9* and *NCCRP1* using several different approaches. *Nccrp1* was originally found to be significantly upregulated in the gastric mucosa of CA IX-deficient mice [6], which prompted us to explore its role more closely, but focusing on the human gene. In HeLa cells, we found that the NCCRP1 and CA IX proteins usually "avoid" each other; that is, they are only rarely expressed in the same cells (Fig. 8A, arrows). Furthermore, in a panel of 16 pancreatic cancer cell lines and 21 breast cancer cell lines, *NCCRP1* and *CA9* expression were inversely correlated in certain cell lines; *NCCRP1* was weakly expressed or absent when *CA9* mRNA was highly expressed, and vice versa. These data support the observation in *Car9* knockout mice in which the expression of *Nccrp1* was increased in the absence of *Car9*. We also determined whether the expression of *NCCRP1* was regulated in a similar manner to *CA9* in HeLa cells. *NCCRP1* expression decreased moderately after stimulation with deferoxamine mesylate, which was used to induce a hypoxia-like response. On the contrary, *CA9* expression increased highly, as expected. Thus, NCCRP1 does not seem to share a main regulatory pathway with CA IX.

siRNA-mediated gene silencing was used to study whether *CA9* expression directly regulates *NCCRP1* expression. Knockdown of *CA9* in U373 cells had no effect on *NCCRP1* expression levels, implying that *NCCRP1* is not directly regulated by *CA9*, at least in this cell line. Likewise, silencing of *NCCRP1* in HeLa and Su.86.86 cells did not affect *CA9* expression. Interestingly, we found that knockdown of *NCCRP1* led to a statistically significant decrease in the growth of HeLa cells, and this effect was still observed at 144 h after transfection. FBXO6 has also been shown to promote growth and proliferation of gastric cancer cells compared with control cells that do not express the protein [19]. One plausible explanation for these observations is that NCCRP1 and FBXO6 are needed to target certain glycoproteins that affect the cell cycle for degradation and that the proliferation of cancer cells is impaired when this function is inhibited. The results of this study indicate that *NCCRP1* is not directly regulated by *CA9*, but there are more complicated regulation events that lead to its upregulation when *CA9* is knocked down.

In conclusion, these studies provide ample evidence that the present name, "non-specific cytotoxic cell receptor protein 1," does not fittingly describe the polypeptide known as NCCRP1. Bioinformatic analyses clearly show that NCCRP1 is a paralog to five other FBXO genes. We have also shown experimentally that the human recombinant NCCRP1 protein is expressed in the cytosol, not on the cell surface. Furthermore, the tissue expression pattern of NCCRP1 in humans and mice is incompatible with an immune receptor function.

Materials and Methods

Bioinformatics

Sequences were retrieved from Ensembl release 62 (www.ensembl.org) [20], UniProt (www.uniprot.org) [21], GenBank (www.ncbi.nlm.nih.gov/genbank/) [22] and RefSeq (www.ncbi.nlm.nih.gov/RefSeq/) [23]. BLAST searches were carried out via NCBI (blast.ncbi.nlm.nih.gov/Blast.cgi) [24]. Multiple sequence alignments were prepared with ClustalW (www.ebi.ac.uk/Tools/msa/clustalw2/) [25] and Mafft (www.ebi.ac.uk/Tools/msa/mafft/) [26] and visualized with GeneDoc (www.nrbsc.org/gfx/genedoc/). Protein motifs were searched using InterProScan (www.ebi.ac.uk/Tools/pfa/iprscan/) [27] and transmembrane domains were predicted with TMHMM v. 2.0 (www.cbs.dtu.dk/services/TMHMM/) [28]. Signal peptides and other target peptides were predicted using SignalP 3.0 with eukaryotic parameters (www.cbs.dtu.dk/services/SignalP/) [28] and TargetP 1.1. with non-plant parameters (www.cbs.dtu.dk/services/TargetP/) [28], respectively. Intrinsic protein disorder was predicted with DISpro (www.ics.uci.edu/~baldig/dispro.html) [29]. Phylogenetic trees were prepared using the MEGA4 software (www.megasoftware.net/) [30] with maximum parsimony and the complete deletion option for gapped sites with 1000 bootstrap replicates. Molecular images were prepared with PyMol 0.99 (DeLano Scientific, South San Francisco, CA).

Construction of recombinant human NCCRP1

The full-length protein-coding cDNA sequence for human NCCRP1 was obtained from the Mammalian Gene Collection, and the cDNA clone (IMAGE ID: 30348184) was purchased from Source BioScience LifeSciences (Cambridge, United Kingdom). Plasmid DNA was isolated from an overnight culture using a QIAprep Spin Miniprep Kit (Qiagen, Hilden, Germany). *NCCRP1* cDNA was amplified by PCR using Phusion™ Hot Start High Fidelity DNA Polymerase (Finnzymes, Espoo, Finland). Primers were ordered from Biomers (Ulm, Germany). The forward primer sequence was 5′-CCG CGG ATC CAT GGA GGA GGT GCG TGA GGG A-3′ and the reverse primer was 5′-CGC CGT CGA CTC ACT CCC GGA GCT GCA CAG-3′, with the restriction sites for BamHI and SalI underlined, respectively. PCR was performed in an XP Thermal Cycler (Bioer Technology, Hangzhou, China) with a program consisting of a single 98°C denaturation step for 30 s followed by 35 cycles of denaturation at 98°C for 10 s, annealing at 64°C for 30 s and extension at 72°C for 30 s, and a final extension at 72°C for 5 min. The PCR product band was separated from agarose gel and dissolved using an Illustra™ GFX PCR DNA and GEL Band Purification Kit (GE Healthcare Life Sciences, Buckinghamshire, UK). The purified PCR product and pGEX-4T-1 vector (Invitrogen, Carlsbad, CA) were digested at 37°C for 2 hours with the BamHI and SalI restriction enzymes (New England Biolabs, Ipswich, MA, USA). The digested plasmid and NCCRP1 construct were purified and ligated overnight at 4°C using T4 DNA ligase (New England Biolabs). The ligated product was transformed into *E. coli* BL21(DE3)pLysS bacteria (Promega, Madison, WI, USA). Overnight cultures (5 ml) were grown from colonies, and plasmids were purified using a QIAprep Spin Miniprep Kit™ (Qiagen). Sequencing was performed to verify the sequence of the NCCRP1 construct. This purification method was based on a glutathione S-transferase (GST) gene fusion system. Expression of pGEX-4T-1 in *E. coli* yielded fusion proteins with the GST moiety at the amino terminus and NCCRP1 recombinant protein at the carboxyl terminus. The construct also contained a thrombin protease site between the GST tag and NCCRP1. This vector construct codes additional Gly and Ser residues to the N-terminus of the recombinant protein.

Production and purification of recombinant human NCCRP1

A single BL21(DE3)pLysS transformant colony was grown in 5 ml LB medium containing 50 μg/ml ampicillin at room temperature with shaking (200 rpm) overnight and used to inoculate 500 ml of LB/amp medium. This culture was grown until the optical density (OD) at 600 nm reached 0.6. Expression of NCCRP1 protein was induced by adding isopropyl β-D-1-

thiogalactopyranoside (IPTG) (Fermentas, Ontario, Canada) at a final concentration of 0.25 mM, and the culture was grown at room temperature overnight. The cells were harvested by centrifugation (Sorvall RC 28S) at 5,000 rpm for 5 min at room temperature. The cell pellet was suspended in 10 ml Tris-buffer containing 0.1 M Tris-Cl, pH 8, 0.05% Triton X-100, 200 mg lysozyme, 200 U DNase (Roche, Penzberg, Germany) and the protease inhibitors phenylmethanesulfonylfluoride (0.2 mg; Sigma-Aldrich, Helsinki, Finland) and leupeptin (0.1 mg) (Santa Cruz, Heidelberg, Germany). After a 30-min incubation at room temperature, the cell suspension was placed on ice and sonicated for 1 min. The suspension was clarified by centrifugation at 10,000 rpm for 30 min at 4°C, and the clear supernatant was affinity purified using Glutathione Sepharose 4B medium (GE Healthcare, Buckinghamshire, UK). Recombinant NCCRP1 protein was isolated under native conditions according to the manufacturer's protocol. A site-specific thrombin (GE Healthcare) was used for specific cleavage of the GST under shaking at room temperature overnight. Finally, the protein was eluted using the glutathione elution method (GE Healthcare) recommended by the manufacturer. The size of the expressed NCCRP1 protein was determined under reducing conditions by sodium dodecyl sulfate-polyacrylamide gel electrophoresis (SDS-PAGE) analysis.

Production of a polyclonal antibody and western blotting

Anti-human NCCRP1 serum was raised in a rabbit against the purified full-length NCCRP1 by Innovagen AB (Lund, Sweden). Western blotting was used to confirm the reactivity of the antibody with NCCRP1.

Recombinant NCCRP1 proteins were subjected to SDS-PAGE under reducing conditions and transferred to polyvinylidene fluoride (PVDF) membranes. The membranes were treated with blocking solution (Santa Cruz, Heidelberg, Germany) for 30 min. After blocking, the membrane was incubated with the primary antibody (rabbit anti-NCCRP1) diluted 1:2,000, or normal rabbit serum as a control, and washed. The membrane was incubated with the secondary antibody diluted 1:25,000 (anti-rabbit Ig, horseradish-peroxidase-linked whole antibody from donkey, Amersham Biosciences, Buckinghamshire, England) and washed, and protein bands were visualized by electrochemiluminescence (ECL) using Amersham ECL™ Western Blotting Detection Reagents (GE Healthcare) according to the manufacturer's instructions.

Mass spectrometry

All experiments were performed on a 4.7-T Fourier transform ion cyclotron resonance (FT-ICR) mass spectrometer (APEX-Qe; Bruker Daltonics, Billerica, MA, USA) equipped with an Apollo-II ion source and a mass-selective quadrupole front-end. This instrument has been described in detail elsewhere [31]. The protein samples were buffer exchanged into 10 mM ammonium acetate buffer, pH 6.9, on PD-10 columns (Amersham Biosciences, Billingham, UK) and directly electrosprayed at a flow rate of 1.5 µL/min. ESI-generated ions were externally accumulated for 1 s in a hexapole ion trap and transmitted to the ICR for trapping, excitation and detection. For each spectrum, 1,000 co-added 512-kWord time-domain transients were recorded, zero-filled twice, Gaussian multiplied and fast Fourier transformed before magnitude calculation and external mass calibration with respect to the ions of an ES Tuning Mix (Agilent Technologies, Santa Clara, CA, USA). All data were acquired and processed using Bruker XMASS 6.0.2 software. Mass spectra were further charge deconvoluted using a standard deconvolution macro implemented in the XMASS software. Tryptic digests were obtained by dissolving a small amount of the protein precipitate in 100 µl of a 10 mM ammonium bicarbonate buffer, pH 8.5, and 15 µg of sequencing grade trypsin (Promega GmbH, Mannheim, Germany) in 15 µl of water was added. The digest sample was incubated at 37°C for 1.5 hours, after which no precipitate was observed, and the sample was directly analyzed without chromatographic separation. The resulting protein or peptide masses were matched against the protein sequence using the GPMAW 8.11 software, and tryptic peptide masses were further subjected to database search using the Mascot search engine (www.matrixscience.com).

Cell lines

A panel of 16 established pancreatic cancer cell lines was used in this study. Thirteen of these (AsPC-1, BxPC-3, Capan-1, Capan-2, CFPAC-1, HPAC, HPAF-II, Hs 700T, Hs 766T, MIA PaCa-2, PANC-1, Su.86.86, and SW 1990) were purchased from the American Type Culture Collection (ATCC, Manassas, VA, USA), and three (DanG, Hup-T3, and Hup-T4) were purchased from the German Collection of Microorganisms and Cell Cultures (Braunschweig, Germany). The 21 breast cancer cell lines used in this study (BT-474, CAMA-1, DU4475, HCC38, HCC1419, HCC1954, MCF7,MDA-MB-134-VI, MDA-MB-231, MDA-MB-361, MDA-MB-415, MDA-MB-436, MDA-MB-453, SK-BR-3, T-47D, UACC-732, UACC-812, UACC-893, UACC-3133, ZR-75-1, and ZR-75-30) were obtained from the ATCC. The U373 human glioblastoma astrocytoma cell line was purchased from the European Collection of Cell Cultures. The HeLa human cervical carcinoma cell line was from the laboratory of Professor Jorma Isola (Institute of Biomedical Technology, University of Tampere, Tampere, Finland). Cells were grown under the recommended culture conditions.

Immunocytochemistry

Rabbit anti-human NCCRP1 serum (Innovagen) and the M75 antibody specific for the PG region of CA IX were used for immunocytochemistry [32]. Non-immune normal rabbit serum was used as a control.

HeLa cells were fixed with 4% (vol/vol) neutral-buffered formaldehyde for 30 min. The cells were then rinsed with PBS and subjected to immunofluorescence staining using the following protocol: (*a*) pre-treatment with 0.1% BSA in PBS (BSA-PBS) for 30 min; (*b*) incubation for 1 h with rabbit NCCRP1 antiserum or normal rabbit serum diluted 1:100 in 0.1% BSA-PBS or mouse CA IX antiserum diluted 1:10 in 0.1% BSA-PBS; (*c*) rinsing three times for 5 min with BSA-PBS; (*d*) incubation for 1 h with 1:100 diluted Alexa Fluor 488 goat anti-rabbit IgG antibodies or Alexa Fluor 568 goat anti-mouse IgG antibodies (both from Molecular Probes, Eugene, Oregon, USA) in 0.1% BSA-PBS; (*e*) rinsing two times for 5 min with BSA-PBS and once with PBS. All incubations and washings were performed in the presence of 0.05% saponin. Immunostained cells were analyzed and photographed using a Zeiss LSM 700 confocal laser scanning microscope.

NCCRP1 expression in human and mouse tissues

NCCRP1 mRNA expression levels across a large number of human tissues were retrieved from the IST database system developed by MediSapiens Ltd. The current version of the IST database (4.3) contains 20,218 human tissue and cell line samples analyzed by Affymetrix gene expression microarrays. The database was constructed and validated using methods similar to those described by Kilpinen et al. [33] and Autio et al. [34] for the construction of the GeneSapiens database. The database contains expression data that is fully integrated in terms of both the

annotation and numerical compatibility, allowing for analysis of the expression levels of 19,123 genes across 228 distinct tissues.

Mouse tissues were obtained from C57BL/6 mice that were maintained in the animal facility of the University of Oulu. A total of six mice (3 males and 3 females) were sacrificed at two months of age. Tissue specimens were taken from the following areas: parotid gland, submandibular gland, stomach, duodenum, jejunum, ileum, colon, lung, kidney, prostate and testis. The tissue samples were immediately immersed in RNAlater solution (Ambion, Austin, TX, USA) and frozen at −80°C.

Total RNA was extracted from the mouse tissues using an RNeasy RNA isolation kit (Qiagen, Valencia, USA) following the manufacturer's instructions. Residual DNA was removed from the samples using RNase-free DNase (Qiagen). The RNA concentration and purity was determined by measuring the optical density at 260 and 280 nm. Different quantities of RNA (lung and prostate: 200 ng, ileum: 900 ng, all other tissues: 2,000 ng) were converted into first strand cDNA using a First Strand cDNA synthesis kit (Fermentas, Burlington, Canada) with random hexamer primers according to the manufacturer's protocol.

The relative expression levels of the mouse *Nccrp1* gene in several tissues were assessed by quantitative real-time PCR (QRT-PCR) using the LightCycler detection system (Roche, Rotkreuz, Switzerland). The primers (Table 2) were designed using Primer3 (http://frodo.wi.mit.edu/primer3/) and based on the complete cDNA sequence deposited in GenBank. The specificity of the primers was verified using NCBI Basic Local Alignment Search Tool (BLAST) (http://blast.ncbi.nlm.nih.gov/Blast.cgi). The housekeeping gene *β-actin* (*Actb*) was used as internal control to normalize the cDNA samples for possible differences in quality and quantity (Table 2).

Each PCR reaction was performed in a total volume of 20 µl containing 1.0 µl of first strand cDNA, 1× QuantiTect SYBR Green PCR Master Mix (Qiagen, Hilden, Germany) and 0.5 µM of each primer. Amplification and detection were conducted as follows: after an initial 15 min activation step at 95°C, amplification was performed in a three-step cycling procedure for 45 cycles consisting of denaturation at 95°C for 15 s, annealing at a temperature determined according to the T_m for each primer pair for 20 s, and elongation at 72°C for 15 s (the ramp rate was 20°C/s for all the steps), and a final cooling step was performed. Melting curve analysis was always performed after the amplification to check the specificity of the PCR reaction. To quantify the levels of transcripts in the cell lines studied, a standard curve was established for each gene using five-fold serial dilutions of known concentrations of purified PCR products generated with the same primer pairs. Each cDNA sample was tested in triplicate, and the crossing point (Cp) value obtained allowed the levels of the starting mRNA to be determined using a specific standard curve. The relative mRNA expression was calculated as the copy number of the target gene divided by the corresponding normalization factor and multiplied by 10^3. Median values were calculated from the technical triplicates.

The effect of growth factors and deferoxamine mesylate on mRNA expression of *NCCRP1*

HeLa cells were grown in 75 cm^2 flasks in a 37°C incubator with humidified 5% CO_2/95% air. When the cultured cells reached 80–90% confluence, they were trypsinized and plated in 58 cm^2 dishes at a density of 1 million cells per dish. After 24 hours, the medium was replaced with fresh medium containing recombinant human transforming growth factor-alpha (TGF-α; 10 ng/ml), recombinant human transforming growth factor-beta 1 (TGF-β1; 10 ng/ml), recombinant human epidermal growth factor (EGF; 10 ng/ml), or deferoxamine mesylate (200 µM), an iron chelator commonly used to induce the hypoxia regulatory pathway. Normal medium was added to control plates. TGF-β1 and EGF were purchased from ProSpec-Tany TechnoGene Ltd. (Rehovot, Israel). TGF-α was purchased from PromoCell GmbH (Heidelberg, Germany). Deferoxamine mesylate was obtained from Sigma-Aldrich Finland Oy (Helsinki, Finland). The chemicals were diluted as necessary according to the manufacturers' instructions. The cells were incubated for 72 hours, after which they were harvested and total RNA was extracted using an RNeasy RNA isolation kit. For each sample, 850 ng of RNA was converted into first strand cDNA by reverse transcription and QRT-PCR was performed as described above. The primers for human *NCCRP1* and *CA9* were designed using Primer3 and the primers for the housekeeping gene ubiquitin C (*UBC*) were obtained from the RTprimerDB database (http://www.rtprimerdb.org/) under the identification number 8 (Table 2). The median values were calculated from the technical triplicates for the QRT-PCR experiments. Subsequently, the median values for treatments were compared to the median values for negative controls.

Table 2. QRT-PCR primer sequences used in this study.

Gene symbol	Description	GenBank number	Forward primer (5′-3′)	Reverse primer (5′-3′)
Nccrp1	Mus musculus non-specific cytotoxic cell receptor protein 1 homolog(zebrafish)	NM_001081115	GCTGCATGTCTGGCTGTTAG	ATGCGGTTCTTAGCCTTGTG
Actb	Mus musculus actin, beta	NM_007393	AGAGGGAAATCGTGCGTGAC	CAATAGTGATGACCTGGCCGT
NCCRP1	Homo sapiens non-specific cytotoxic cell receptor protein 1 homolog(zebrafish)	NM_001001414	TTCCGTGGCTGGTACATTAG	ATGGCTGGTTGTTCGTCATC
CA9	Homo sapiens carbonic anhydrase IX	NM_001216	ATGAGAAGGCAGCACAGAAG	TAATGAGCAGGACAGGACAG
UBC	Homo sapiens ubiquitin C	NM_021009	ATTTGGGTCGCGGTTCTTG	TGCCTTGACATTCTCGATGGT
GAPDH	Homo sapiens glyceraldehyde-3-phosphate dehydrogenase	NM_002046	TGCACCACCAACTGCTTAGC	GGCATGGACTGTGGTCATGAG

doi:10.1371/journal.pone.0027152.t002

Expression of *CA9* and *NCCRP1* in human pancreatic and breast cancer cell lines

To examine the co-expression of human *CA9* and *NCCRP1* in tumor cells, transcript levels were measured in 16 pancreatic and 21 breast cancer cell lines using QRT-PCR. Total RNA was isolated from the cell lines using TRIzol reagent (Invitrogen, Carlsbad, CA), and 5 µg of each RNA sample was converted into first strand cDNA using SuperScript III First-Strand Synthesis kit (Invitrogen) according to the manufacturer's instructions. QRT-PCR reactions were performed as described above, with the exception that each cDNA sample was tested only once. The housekeeping gene glyceraldehyde-3-phosphate dehydrogenase (*GAPDH*) was used as a reference (Table 2). The final relative mRNA expression was calculated as the copy number of the target gene divided by the corresponding normalization factor, multiplied by 10^4.

NCCRP1 and *CA9* silencing

The human *NCCRP1* and *CA9* genes were silenced using specific ON-TARGETplus SMARTpool small interfering RNAs (siRNAs) (Thermo Fisher Scientific, Lafayette, CO). The catalog numbers for *NCCRP1* and *CA9* SMARTpools are L-032307-01-0005 and L-005244-00-0005, respectively. U373 cells, HeLa cells and Su.86.86 cells were transfected with the siRNAs using INTERFERin^{TM} reagent (PolyPlus-transfection, Illkirch, France) according to the manufacturer's instructions. Transfections were performed in 24-well plates with the desired cell density (25,000 cells per well for U373 and HeLa cells and 50,000 cells per well for Su.86.86 cells). Final concentrations of 10 nM for *CA9* siRNA and 30 nM for *NCCRP1* siRNA were used. Parallel control experiments using siRNA targeting the firefly *luciferase* (*PPYLUC*) gene were also performed. The sequence of the *PPYLUC* siRNA was 5′-GAUUUCGAGUCGUCUUAAUTT-3′. All siRNA experiments were performed in triplicate and repeated twice. Gene silencing was verified each time using QRT-PCR as described above. The housekeeping gene glyceraldehyde-3-phosphate dehydrogenase (*GAPDH*) was used as a reference (Table 2). Median values were calculated from the triplicate QRT-PCR experiments, and the median values for *NCCRP1* or *CA9* siRNA-treated cells were compared to the median values for *luciferase* control siRNA-treated cells to estimate the efficacy of silencing.

Cell growth analyses

For cell growth analyses, 15,000 HeLa cells per well were transfected with *NCCRP1* SMARTpool siRNAs or *luciferase* control siRNA as described above. Cell growth was analyzed at 48, 96, and 144 hours after transfection.

From each well, 4×4 fields were photographed using Olympus IX71 microscope with a 100× objective. Quantitative analysis of the captured images was performed using the public domain image processing software ImageJ (http://rsbweb.nih.gov/ij/). A custom-made algorithm was developed for the analysis; it first identified the cellular area of the sample image at each time point and then measured the relative change in the cellular area percentage over the sample-specific time course.

Statistical analyses

For the cell growth analyses, the Mann-Whitney test was used to evaluate differences in group values for *NCCRP1* SMARTpool siRNA-treated HeLa cells vs. *luciferase* control siRNA-treated HeLa cells.

Ethics statement

The animal protocols were approved by the Animal Care and Use Committee of the University of Oulu (Permit Number: 085/07).

Supporting Information

Figure S1 A search result against the SwissProt database for trypsin digestion of recombinant human NCCRP1. A search against the SwissProt database gave an unambiguous hit for human NCCRP1 (NCRP1_HUMAN) with a Mowse score of 370.
(PDF)

Acknowledgments

The authors thank Mrs. Ritva Romppanen for her skillful technical assistance.

Author Contributions

Conceived and designed the experiments: HK PP EL AK JV S. Parkkila. Performed the experiments: HK MT JJ. Analyzed the data: HK MT JJ. Contributed reagents/materials/analysis tools: SK VJT JI S. Pastorekova JP. Wrote the paper: HK MT JJ.

References

1. Hilvo M, Baranauskiene L, Salzano AM, Scaloni A, Matulis D, et al. (2008) Biochemical characterization of CA IX, one of the most active carbonic anhydrase isozymes. J Biol Chem 283: 27799–27809.
2. Alterio V, Hilvo M, Di Fiore A, Supuran CT, Pan P, et al. (2009) Crystal structure of the catalytic domain of the tumor-associated human carbonic anhydrase IX. Proc Natl Acad Sci U S A 106: 16233–16238.
3. Neri D, Supuran CT (2011) Interfering with pH regulation in tumours as a therapeutic strategy. Nat Rev Drug Discov 10: 767–777.
4. Pastorekova S, Zavada J (2004) Carbonic anhydrase IX (CA IX) as a potential target for cancer therapy. Cancer Therapy 2: 245–262.
5. Ortova Gut MO, Parkkila S, Vernerova Z, Rohde E, Zavada J, et al. (2002) Gastric hyperplasia in mice with targeted disruption of the carbonic anhydrase gene Car9. Gastroenterology 123: 1889–1903.
6. Kallio H, Hilvo M, Rodriguez A, Lappalainen EH, Lappalainen AM, et al. (2010) Global transcriptional response to carbonic anhydrase IX deficiency in the mouse stomach. BMC Genomics 11: 397.
7. Jaso-Friedmann L, Leary JH, 3rd, Evans DL (1997) NCCRP-1: a novel receptor protein sequenced from teleost nonspecific cytotoxic cells. Mol Immunol 34: 955–965.
8. Evans DL, Leary JH, 3rd, Jaso-Friedmann L (1998) Nonspecific cytotoxic cell receptor protein-1: a novel (predicted) type III membrane receptor on the teleost equivalent of natural killer cells recognizes conventional antigen. Cell Immunol 187: 19–26.
9. Ishimoto Y, Savan R, Endo M, Sakai M (2004) Non-specific cytotoxic cell receptor (NCCRP)-1 type gene in tilapia (Oreochromis niloticus): its cloning and analysis. Fish Shellfish Immunol 16: 163–172.
10. Cuesta A, Esteban MA, Meseguer J (2005) Molecular characterization of the nonspecific cytotoxic cell receptor (NCCRP-1) demonstrates gilthead seabream NCC heterogeneity. Dev Comp Immunol 29: 637–650.
11. Sakata H, Savan R, Sogabe R, Kono T, Taniguchi K, et al. (2005) Cloning and analysis of non-specific cytotoxic cell receptor (NCCRP)-1 from common carp Cyprinus carpio L. Comp Biochem Physiol C Toxicol Pharmacol 140: 287–294.
12. Jaso-Friedmann L, Peterson DS, Gonzalez DS, Evans DL (2002) The antigen receptor (NCCRP-1) on catfish and zebrafish nonspecific cytotoxic cells belongs to a new gene family characterized by an F-box-associated domain. J Mol Evol 54: 386–395.
13. Jaso-Friedmann L, Leary JH, 3rd, Evans DL (2001) The non-specific cytotoxic cell receptor (NCCRP-1): molecular organization and signaling properties. Dev Comp Immunol 25: 701–711.
14. Kipreos ET, Pagano M (2000) The F-box protein family. Genome Biol 1: REVIEWS3002.
15. Glenn KA, Nelson RF, Wen HM, Mallinger AJ, Paulson HL (2008) Diversity in tissue expression, substrate binding, and SCF complex formation for a lectin family of ubiquitin ligases. J Biol Chem 283: 12717–12729.

16. Reimers K, Abu Qarn M, Allmeling C, Bucan V, Vogt PM (2006) Identification of the non-specific cytotoxic cell receptor protein 1 (NCCRP1) in regenerating axolotl limbs. J Comp Physiol B 176: 599–605.
17. Mizushima T, Yoshida Y, Kumanomidou T, Hasegawa Y, Suzuki A, et al. (2007) Structural basis for the selection of glycosylated substrates by SCF(Fbs1) ubiquitin ligase. Proc Natl Acad Sci U S A 104: 5777–5781.
18. Yoshida Y (2007) F-box proteins that contain sugar-binding domains. Biosci Biotechnol Biochem 71: 2623–2631.
19. Zhang L, Hou Y, Wang M, Wu B, Li N (2009) A study on the functions of ubiquitin metabolic system related gene FBG2 in gastric cancer cell line. J Exp Clin Cancer Res 28: 78.
20. Flicek P, Aken BL, Ballester B, Beal K, Bragin E, et al. (2010) Ensembl's 10th year. Nucleic Acids Res 38: D557–562.
21. Jain E, Bairoch A, Duvaud S, Phan I, Redaschi N, et al. (2009) Infrastructure for the life sciences: design and implementation of the UniProt website. BMC Bioinformatics 10: 136.
22. Benson DA, Karsch-Mizrachi I, Lipman DJ, Ostell J, Sayers EW (2011) GenBank. Nucleic Acids Res 39: D32–37.
23. Pruitt KD, Tatusova T, Klimke W, Maglott DR (2009) NCBI Reference Sequences: current status, policy and new initiatives. Nucleic Acids Res 37: D32–36.
24. Altschul SF, Madden TL, Schaffer AA, Zhang J, Zhang Z, et al. (1997) Gapped BLAST and PSI-BLAST: a new generation of protein database search programs. Nucleic Acids Res 25: 3389–3402.
25. Thompson JD, Higgins DG, Gibson TJ (1994) CLUSTAL W: improving the sensitivity of progressive multiple sequence alignment through sequence weighting, position-specific gap penalties and weight matrix choice. Nucleic Acids Res 22: 4673–4680.
26. Katoh K, Kuma K, Toh H, Miyata T (2005) MAFFT version 5: improvement in accuracy of multiple sequence alignment. Nucleic Acids Res 33: 511–518.
27. Hunter S, Apweiler R, Attwood TK, Bairoch A, Bateman A, et al. (2009) InterPro: the integrative protein signature database. Nucleic Acids Res 37: D211–215.
28. Emanuelsson O, Brunak S, von Heijne G, Nielsen H (2007) Locating proteins in the cell using TargetP, SignalP and related tools. Nat Protoc 2: 953–971.
29. Cheng J, Sweredoski M, Baldi P (2005) Accurate Prediction of Protein Disordered Regions by Mining Protein Structure Data. Data Mining and Knowledge Discovery 11: 213–222.
30. Tamura K, Dudley J, Nei M, Kumar S (2007) MEGA4: Molecular Evolutionary Genetics Analysis (MEGA) software version 4.0. Mol Biol Evol 24: 1596–1599.
31. Bootorabi F, Janis J, Valjakka J, Isoniemi S, Vainiotalo P, et al. (2008) Modification of carbonic anhydrase II with acetaldehyde, the first metabolite of ethanol, leads to decreased enzyme activity. BMC Biochem 9: 32.
32. Pastorekova S, Zavadova Z, Kostal M, Babusikova O, Zavada J (1992) A novel quasi-viral agent, MaTu, is a two-component system. Virology 187: 620–626.
33. Kilpinen S, Autio R, Ojala K, Iljin K, Bucher E, et al. (2008) Systematic bioinformatic analysis of expression levels of 17,330 human genes across 9,783 samples from 175 types of healthy and pathological tissues. Genome Biol 9: R139.
34. Autio R, Kilpinen S, Saarela M, Kallioniemi O, Hautaniemi S, et al. (2009) Comparison of Affymetrix data normalization methods using 6,926 experiments across five array generations. BMC Bioinformatics 10 Suppl 1: S24.